THE UNIVERSITY OF MICHIGAN
JUN - 2 1960
ENGINEERING LIBRARY

JOURNAL OF FLUID MECHANICS

VOLUME 8 PART 1

MAY 1960

PUBLISHED BY

CAMBRIDGE UNIVERSITY PRESS

BENTLEY HOUSE, 200 EUSTON ROAD, LONDON, N.W.1

AMERICAN BRANCH: 32 EAST 57TH STREET, NEW YORK 22, N.Y.

Price 30*s.* (*U.S.A.* $5.00)

The JOURNAL OF FLUID MECHANICS exists for the publication of theoretical and experimental investigations of all aspects of the mechanics of fluids, and is issued in four parts per volume.

EDITOR

DR G. K. BATCHELOR

Department of Applied Mathematics and Theoretical Physics, University of Cambridge, Free School Lane, Cambridge, England

ASSISTANT EDITORS

DR T. B. BENJAMIN, DR I. PROUDMAN, DR P. G. SAFFMAN

Department of Applied Mathematics and Theoretical Physics, University of Cambridge, Free School Lane, Cambridge, England

ASSOCIATE EDITORS

PROF. G. F. CARRIER

Pierce Hall, Harvard University, Cambridge 38, *Massachusetts, U.S.A.*

DR W. C. GRIFFITH

Research and Development Laboratory, Missile Systems Division, Lockheed Aircraft Corporation, Palo Alto, California, U.S.A.

M. J. LIGHTHILL

Royal Aircraft Establishment, Farnborough, Hampshire, England

PROF. R. R. LONG

School of Engineering, The Johns Hopkins University, Baltimore 18, *Maryland, U.S.A.*

Authors wishing to have papers published in the JOURNAL should communicate them to any one of the persons named above, choosing one in their own country where possible.

Authors are urged to ensure that their papers are written clearly and attractively, in order that their work will be readily accessible to readers.

Manuscripts should be typed in double spacing on one side of the paper only, with references listed at the end in alphabetical order of authors. Drawings should be done on a large scale in Indian ink on tracing cloth or drawing paper, the lettering being shown clearly in pencil for reproduction by the printer; the list of captions should be typed at the end of the manuscript. Proofs of papers from overseas will usually be despatched to authors by airmail. There is no charge for publication. Authors are entitled to receive 50 offprints of a paper in the JOURNAL free of charge, and additional offprints can be purchased if ordered in advance.

SUBSCRIPTIONS

The subscription price for a volume of four parts is £5. 10*s*. net, post free, payable in advance; separate parts 30*s*. net, plus postage. Subscriptions may be sent to any bookseller, or to the Cambridge University Press, Bentley House, 200 Euston Road, London, N.W.1.

Subscribers in the United States should send their orders to the Cambridge University Press, American Branch, 32 East 57th Street, New York 22. The subscription price per volume is $18.50, post free, payable in advance; separate parts $5.00, plus postage.

Quotations for available back volumes and parts may be obtained on application to the Cambridge University Press.

Unsteady flow through an underdrained earth dam

By ROGER J. M. DE WIEST
Geological Engineering Department, Princeton University

(Received 24 August 1959)

An analytical treatment is given of the problem of the establishment of the flow through a dam or levee with a horizontal underdrain, when the head behind it is raised and then kept at a constant value. The essential idea employed in the analysis is to consider the unsteady flow as a time-dependent perturbation of the final steady flow. The unsteady potential $\phi(x, y, t)$ is expanded in a power series of $e^{-\lambda t}$, of the form

$$\phi(x, y, t) = \phi_0(x, y) + \phi_1(x, y)\, e^{-\lambda t} + O(e^{-2\lambda t}),$$

where $\phi_0(x, y)$ is the known steady-state potential, $\phi_1(x, y)$ is a perturbation potential and $O(e^{-2\lambda t}) = \phi_2(x, y)\, e^{-2\lambda t} + \phi_3(x, y)\, e^{-3\lambda t} + \ldots$. Each of the terms $\phi_n(x, y)\, e^{-n\lambda t}$ can be thought of as being a perturbation term of its precursor in the series, and the present approach is limited to the computation of the first perturbation term $\phi_1(x, y)\, e^{-\lambda t}$.

It is shown that ϕ_1 satisfies Laplace's equation $\nabla^2\phi_1 = 0$ in a dimensionless hodograph plane. The free-boundary condition is linear but complicated, containing the eigenvalue λ, which is fixed by a determinantal equation. The amplitude of the displacement of the free surface is left undetermined; only the mode of the motion and the eigenvalue are computed. The results of a numerical example are summarized.

1. Introduction

Curle (1956) has obtained a general technique for considering the unsteady development of steady two-dimensional jet and cavity flows. The approach used was that of expanding the velocity potential Φ in ascending powers of $e^{-\lambda t}$, so that

$$\Phi(x, y, t) = \Phi_0(x, y) + \Phi_1(x, y)\, e^{-\lambda t} + O(e^{-2\lambda t}).$$

The unsteady free boundary was determined by normally displacing the steady-state boundary by an amount $\delta(s, t) = \delta_1(s)\, e^{-\lambda t} + O(e^{-2\lambda t})$. In the present paper, the author applies the above technique to a problem of free surface flow in a porous medium. Although the two flows have some essentially different features (gravity is neglected in the jet flow, kinetic energy in the seepage flow), the technique works equally well in both cases. The boundary-value problem arising in the present flow is somewhat more complicated because the trigonometric functions appearing in the free-boundary condition of the jet flow are replaced by algebraic functions, so that no recursion formula is available for the coefficients of the Fourier series solution of $\nabla^2\Phi_1 = 0$. Instead, these coefficients result from the solution of

a system of linear, homogeneous equations. The reader is expected either to be familiar with the flow through porous media or not to be interested in the subject as such, since this paper only emphasizes the extension of Curle's technique and the solution of a special kind of mixed boundary-value problem.

2. Statement of problem and outline of method

The problem considered is that of a homogeneous dam or earth embankment, with a horizontal underdrain and behind which the level of a reservoir is gradually raised to a depth H (figure 1). It is to be expected that some time will elapse before steady flow will be reached after the head H has been kept at a constant value. The purpose of this paper is to analyse the flow when it approaches its final steady state.

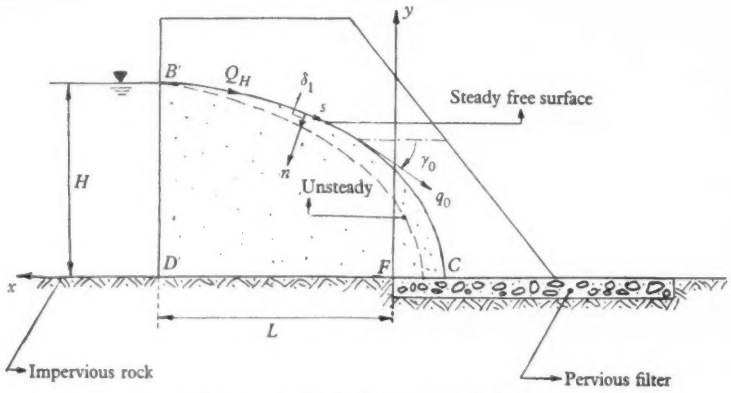

FIGURE 1. Underdrained earth dam.

It is assumed that the porous medium is completely saturated, homogeneous and isotropic, and that the flow is everywhere laminar. If the fluid is restricted to water of constant density and constant viscosity, then all the necessary conditions (Hubbert 1940) for the existence of a velocity potential Φ are satisfied:

$$\Phi = K\phi = K(y + p/\gamma), \tag{2.1}$$

$$K = k\gamma/\mu, \tag{2.2}$$

where the symbols are defined as follows: K, hydraulic conductivity, dimensions $[L/T]$; k, permeability, depending upon the medium alone, dimensions $[L^2]$; μ, viscosity of water; γ, unit weight of water; ϕ, hydraulic head; y, elevation head; p/γ, pressure head. Φ has the dimensions $[L^2/T]$ and can be combined with the stream function Ψ, $[L^2/T]$, to form the complex potential function $W = \Phi + i\Psi$. K is assumed to be constant, and consequently so are k and the porosity ϵ of the medium. Effects of capillarity are neglected and Darcy's law in its simplest form can then be written

$$\mathbf{q} = -K \operatorname{grad} \phi, \tag{2.3}$$

or

$$u = -\frac{\partial \Phi}{\partial x}, \quad v = -\frac{\partial \Phi}{\partial y}. \tag{2.4}$$

The insertion of $\mathbf{q}$ into the continuity equation $\operatorname{div}\mathbf{q} = 0$, leads to

$$\nabla^2\phi = 0. \tag{2.5}$$

Since the compressibility of the medium in unconfined flow can be neglected, (2.1), (2.3), (2.4) and (2.5) are valid as well for $\phi_0(x, y)$ as for $\phi(x, y, t)$. Steady-state values are denoted by the subscript 0, such as q_0; u_0; v_0; p_0; $\gamma_0 = \tan^{-1} v_0/u_0$; ϕ_0; Φ_0; Ψ_0; W_0. The expansion of $\phi(x, y, t)$ in a power series of $e^{-\lambda t}$, of the form

$$\phi(x, y, t) = \phi_0(x, y) + \phi_1(x, y)\, e^{-\lambda t} + O(e^{-2\lambda t}), \tag{2.6}$$

implies that $\phi_1(x, y)$ is a harmonic function, if $\phi_0(x, y)$ represents the known steady potential. In (2.3), λ represents an eigenvalue to be determined. The perturbation potential $\phi_1(x, y)$ remains harmonic under a conformal transformation. Since the steady hodograph can be reduced to a simple configuration, it is quite natural to look for a solution of $\nabla^2\phi_1 = 0$ in such a transformed hodograph plane, provided the basic equation of motion of the unsteady free surface is transferred to the steady boundary. As in the jet flow, the unsteady boundary may be found by normally displacing the steady-state boundary by an amount

$$\delta(x, y, t) = \delta_1(x, y)\, e^{-\lambda t} + O(e^{-2\lambda t}).$$

3. Formulation of the boundary value problem

Consider the dimensionless hodograph plane of figure 2.

$$\chi = \alpha + i\beta = -\frac{K}{\overline{w}_0}, \tag{3.1}$$

where $\overline{w}_0 = u_0 - iv_0$; χ is simply related to W_0 by $W_0 = Q_H\chi$.

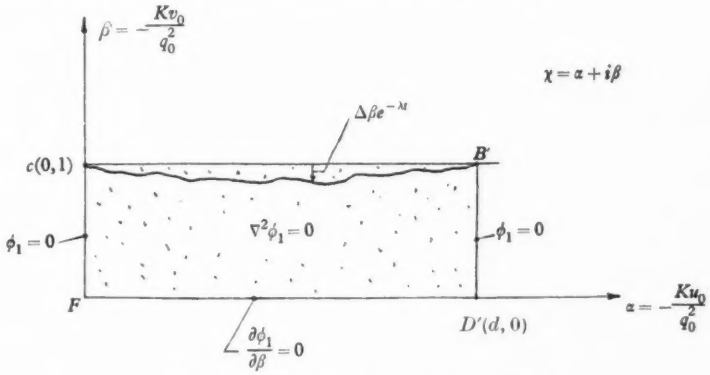

FIGURE 2. Hodograph plane $\chi = -K/\overline{w}_0$.

The abscissa $d = c(KH/Q_H)$, where c is a constant depending upon the ratio H/L of the dam and Q_H is the seepage per unit width for a head H on the dam. Application of the concept of a bounding surface (Lamb 1932, p. 7) leads to the basic equation of motion of the unsteady free surface

$$\frac{\epsilon}{K}\frac{\partial\phi}{\partial t} = \left(\frac{\partial\phi}{\partial x}\right)^2 + \left(\frac{\partial\phi}{\partial y}\right)^2 - \frac{\partial\phi}{\partial y}. \tag{3.2}$$

Let $\phi(x, y, t)$ satisfy (3.2). Then it follows that, at the unsteady free surface,

$$-\frac{\epsilon}{K}\lambda\phi_1 e^{-\lambda t} = \phi_{0x}^2 + \phi_{0y}^2 - \phi_{0y} + (2\phi_{0x}\phi_{1x} + 2\phi_{0y}\phi_{1y} - \phi_{1y})e^{-\lambda t} + O(e^{-2\lambda t}). \quad (3.3)$$

This condition can be transferred to one at the steady free boundary in the hodograph plane. Assume that, corresponding to the displacement $\delta_1(x, y)\, e^{-\lambda t}$ of the boundary in the physical plane, there is a displacement $\Delta\beta\, e^{-\lambda t}$ in the hodograph plane. Under this assumption, (3.3) can be transferred to the steady boundary by addition of a term $-\Delta\beta\, e^{-\lambda t}$. Once at the steady boundary, and only then, $\phi_{0x}^2 + \phi_{0y}^2 - \phi_{0y} = 0$, and, ignoring $O(e^{-2\lambda t})$, (3.3) reduces to

$$-\frac{\epsilon}{K}\lambda\phi_1 = 2\phi_{0x}\phi_{1x} + 2\phi_{0y}\phi_{1y} - \phi_{1y} - \Delta\beta. \quad (3.4)$$

Now,

$$q_0\phi_{1s} = -K(\phi_{1x}\phi_{0x} + \phi_{1y}\phi_{0y}). \quad (3.5)$$

Recall that $W_0 = \Phi_0 + i\Psi_0 = Q_H\alpha + Q_H\beta i$, so that along the steady free surface

$$\left.\begin{aligned} \frac{\partial}{\partial s} &= -q_0\frac{\partial}{\partial\Phi_0} = -\frac{q_0}{Q_H}\frac{\partial}{\partial\alpha}, \\ \frac{\partial}{\partial n} &= -q_0\frac{\partial}{\partial\Psi_0} = -\frac{q_0}{Q_H}\frac{\partial}{\partial\beta}, \\ \frac{\partial}{\partial y} &= \frac{\partial}{\partial\Phi_0}\frac{\partial\Phi_0}{\partial y} = -\frac{v_0}{Q_H}\frac{\partial}{\partial\alpha}. \end{aligned}\right\} \quad (3.6)$$

Then (3.4) reduces via (3.5) and (3.6) to

$$-\frac{\epsilon}{K}\lambda\phi_1 = \frac{2}{K}\frac{q_0^2}{Q_H}\frac{\partial\phi_1}{\partial\alpha} + \frac{v_0}{Q_H}\frac{\partial\phi_1}{\partial\alpha} - \Delta\beta. \quad (3.7)$$

With

$$\Delta\beta = \frac{\partial\beta}{\partial n}\delta_1 = -\frac{q_0}{Q_H}\delta_1 \quad \text{and} \quad q_0^2 = -Kv_0,$$

(3.7) reduces to

$$\frac{\epsilon}{K}\lambda\phi_1 - \frac{v_0}{Q_H}\frac{\partial\phi_1}{\partial\alpha} + \frac{q_0}{Q_H}\delta_1 = 0. \quad (3.8)$$

A second relation between δ_1 and ϕ_1 can be found to hold at the free surface by mathematically expressing that this surface is a material line. The unsteady free surface is not a streamline but has a velocity component normal to the boundary. This component is due:

(*a*) To changes in $\delta_1(x, y)\, e^{-\lambda t}$ because of the exponential decrement with time. These changes, at any (x, y) are expressed as

$$\delta_1(x, y)\, e^{-\lambda(t+\Delta t)} - \delta_1(x, y)\, e^{-\lambda t} \approx -\lambda\Delta t\delta_1 e^{-\lambda t}.$$

The corresponding displacement of the boundary, of order $e^{-\lambda t}$, is equal to

$$-\frac{K}{\epsilon}\frac{\partial\phi_1}{\partial n}e^{-\lambda t}\Delta t.$$

It follows that

$$\frac{K}{\epsilon}\frac{\partial\phi_1}{\partial n} = \lambda\delta_1. \quad (3.9)$$

(*b*) To changes in $\delta_1 e^{-\lambda t}$ because s changes as the fluid particles are convected along the free surface. They can be expressed as

$$\left[\delta_1\left(s+\frac{q_0}{\epsilon}\Delta t\right)-\delta_1(s)\right]e^{-\lambda t}\approx\frac{q_0}{\epsilon}\frac{d\delta_1}{ds}\Delta t\,e^{-\lambda t},$$

so that

$$K\frac{\partial\phi_1}{\partial n}=-q_0\frac{d\delta_1}{ds}. \tag{3.10}$$

It is to be expected that in the case of a slow and gradual rise of the level behind the dam, the component given by (3.10) is small compared to the component of (3.9). The boundary-value problem will be set up and solved under the assumption that component (3.10) can be neglected.

Application of (3.6) to (3.9) leads to

$$\frac{K}{\epsilon}\frac{q_0}{Q_H}\frac{\partial\phi_1}{\partial\beta}=-\lambda\delta_1. \tag{3.11}$$

Elimination of δ_1 from (3.8) and (3.11) gives

$$\frac{\partial\phi_1}{\partial\beta}=\frac{\epsilon^2}{K^2}\frac{Q_H^2}{q_0^2}\lambda^2\phi_1-\frac{\epsilon}{K}\frac{Q_H}{q_0^2}\lambda v_0\frac{\partial\phi_1}{\partial\alpha}. \tag{3.12}$$

Note that

$$\alpha=-\frac{Ku_0}{u_0^2+v_0^2},\quad \beta=-\frac{Kv_0}{u_0^2+v_0^2},\quad q_0^2=\frac{K^2}{\alpha^2+\beta^2}, \tag{3.13}$$

and introduce $a=\epsilon Q_H/K^2$, dimension $[T]$, to find at the free surface ($\beta=1$):

$$\frac{\partial\phi_1}{\partial\beta}=(a\lambda)^2(1+\alpha^2)\phi_1+(a\lambda)\frac{\partial\phi_1}{\partial\alpha}. \tag{3.14}$$

With the free-boundary condition (3.14), the problem is mathematically formulated. It is convenient to consider $a\lambda$ as a dimensionless parameter.

4. The solution

If there is a solution ϕ_1, it must satisfy the condition

$$\int_0^d(-\phi_{1\beta})_{\beta=1}\,d\alpha+\int_0^1(-\phi_{1\alpha})_{\alpha=0}\,d\beta+\int_0^1(\phi_{1\alpha})_{\alpha=d}\,d\beta=0, \tag{4.1}$$

expressing that the perturbation flow must satisfy the continuity requirement that the mass flux of the perturbation flow entering the fluid-filled region through the free surface equals that leaving it through the entrance surface and the drain. This perturbation flow vanishes like $e^{-\lambda t}$ and is superimposed on the steady flow. Separation of variables for $\nabla^2\phi_1=0$ in the strip of figure 2 leads to a solution of the form

$$\phi_1=\sum_{n=1}^{\infty}A_n\cosh\frac{n\pi}{d}\beta\sin\frac{n\pi}{d}\alpha. \tag{4.2}$$

This solution satisfies the boundary conditions along FD', $D'B'$ and FC; A_n is left to be determined by the boundary condition along CB'. It follows from (4.1)

and some integrations that the dimensionless parameter $a\lambda$ now has to satisfy the condition

$$(a\lambda)^2 = \frac{-\sum_1^\infty A_n \sinh\frac{n\pi}{d} + \sum_1^\infty (-1)^n A_n \sinh\frac{n\pi}{d}}{-\sum_1^\infty A_n \frac{d}{n\pi}[1-(-1)^n]\cosh\frac{n\pi}{d} + \sum_1^\infty A_n \left(\frac{d}{n\pi}\right)^3 [(n^2\pi^2-2)(-1)^n+2]\cosh\frac{n\pi}{d}}. \tag{4.3}$$

Although from (4.3), the existence of a solution cannot be guaranteed, the value $a\lambda = 0$ is excluded by consideration of the properties of eigenvalues. In fact, from the nature of the eigenvalue problem and the physics of the flow, we may expect an infinite number of eigenvalues to satisfy (4.3). This result would be analogous to the infinite number of eigenvalues found by Curle in the unsteady jet problem. The smallest of these eigenvalues, $\lambda_{\min}$, will determine the slowest rate of decay. In itself, (4.3) does not determine $a\lambda$, since the A_n are unknown as yet and, moreover, will contain $a\lambda$. It constitutes a check on the computation of the A_n and this has been verified in a numerical example.

The boundary condition of (3.14) can be written as

$$\sum_1^\infty A_n \frac{n\pi}{d}\sinh\frac{n\pi}{d}\sin\frac{n\pi}{d}\alpha = (a\lambda)^2(1+\alpha^2)\sum_1^\infty A_n \cosh\frac{n\pi}{d}\sin\frac{n\pi}{d}\alpha + (a\lambda)\sum_1^\infty A_n \frac{n\pi}{d}\cosh\frac{n\pi}{d}\cos\frac{n\pi}{d}\alpha. \tag{4.4}$$

Multiply each side by $\sin m\pi\alpha/d$ and integrate over the interval $(0, d)$, to obtain

$$\frac{d}{2}A_m\frac{m\pi}{d}\sinh\frac{m\pi}{d} = (a\lambda)^2\sum_1^\infty\left[\int_0^d (1+\alpha^2)\sin\frac{m\pi\alpha}{d}\sin\frac{n\pi\alpha}{d}\,d\alpha\right]A_n\cosh\frac{n\pi}{d} + (a\lambda)\sum_1^\infty\left[\int_0^d \cos\frac{n\pi\alpha}{d}\sin\frac{m\pi\alpha}{d}\,d\alpha\right]A_n\frac{n\pi}{d}\cosh\frac{n\pi}{d}. \tag{4.5}$$

Let

$$b_{m,n} = \int_0^d (1+\alpha^2)\sin\frac{m\pi\alpha}{d}\sin\frac{n\pi\alpha}{d}\,d\alpha. \quad c_{m,n} = \int_0^d \cos\frac{n\pi\alpha}{d}\sin\frac{m\pi\alpha}{d}\,d\alpha. \tag{4.6}$$

Then, (4.5) can be written

$$\frac{d}{2}A_m\frac{m\pi}{d}\sinh\frac{m\pi}{d} = (a\lambda)^2\sum_1^\infty A_n b_{m,n}\cosh\frac{n\pi}{d} + (a\lambda)\sum_1^\infty A_n\frac{n\pi}{d}c_{m,n}\cosh\frac{n\pi}{d}. \tag{4.7}$$

Introduce a new coefficient

$$a_m = \frac{A_m}{2}m\pi\sinh\frac{m\pi}{d}. \tag{4.8}$$

and write (4.7) as

$$a_m = \sum_{n=1}^\infty a_n h_{m,n}(a\lambda) \quad (m = 1, 2, \ldots). \tag{4.9}$$

where

$$h_{m,n}(a\lambda) = (a\lambda)^2\frac{2}{n\pi}b_{m,n}\coth\frac{n\pi}{d} + (a\lambda)\frac{2}{d}c_{m,n}\coth\frac{n\pi}{d}. \tag{4.10}$$

The integrations of (4.6) lead to

$$\left.\begin{aligned} b_{m,n} &= \frac{d^3}{\pi^2(m-n)^2}\cos\pi(m-n) - \frac{d^3}{\pi^2(m+n)^2}\cos\pi(m+n) \quad (m \neq n), \\ c_{m,n} &= -\frac{d}{2(m-n)\pi}[\cos\pi(m-n)-1] - \frac{d}{2(m+n)\pi}[\cos\pi(m+n)-1] \quad (m \neq n), \\ b_{m,m} &= \frac{d}{2} + \frac{d^3}{6} - \frac{d^3}{4m^2\pi^2}, \quad c_{m,m} = 0. \end{aligned}\right\} \tag{4.11}$$

The equations (4.9) represent a system of linear homogeneous equations, infinite in number and with an infinite number of unknowns $a_1, a_2, a_3 \ldots$. This system can be written explicitly as

$$\left.\begin{aligned} &[h_{11}(a\lambda)-1]\,a_1 + h_{12}(a\lambda)\,a_2 + h_{13}(a\lambda)\,a_3 + \ldots = 0, \\ &h_{21}(a\lambda)\,a_1 + [h_{22}(a\lambda)-1]\,a_2 + h_{23}(a\lambda)\,a_3 + \ldots = 0, \\ &h_{31}(a\lambda)\,a_1 + h_{32}(a\lambda)\,a_2 + [h_{33}(a\lambda)-1]\,a_3 + \ldots = 0, \\ &\ldots\ldots\ldots\ldots\ldots\ldots\ldots\ldots\ldots\ldots\ldots\ldots\ldots\ldots\ldots\ldots \end{aligned}\right\} \tag{4.12}$$

In order to have a nontrivial solution of this system of equations, its determinant should vanish. Thus the concept of the infinite determinant as developed by Hill in his Lunar Theory appears in this analysis. Conditions for the convergence of such a determinant are given by Whittaker & Watson (1947, pp. 36, 413–17). The equations (4.12) are similar to Hill's equations except for the range of n in a_n. In Hill's case, n assumes the values $n = \ldots -2, -1, 0, 1, 2, \ldots$, while the parameter $a\lambda$ corresponds to Hill's μ. It was shown by Hill that, for the purposes of his astronomical problem, a remarkably good approximation to the value of μ could be obtained by considering only the three central rows and columns of his determinant. In a numerical example $a\lambda$ has been determined within 2 % by considering only the smallest positive root of the equations $D_4(a\lambda) = 0$, $D_6(a\lambda) = 0$, $D_8(a\lambda) = 0$, where the subscripts 4, 6, 8 denote the degree of the equations in $a\lambda$ which result from the successive consideration of the determinants two by two (rows and columns), three by three, four by four, of the matrix

$$\begin{pmatrix} h_{11}-1 & h_{12} & h_{13} & h_{14} & \ldots \\ h_{21} & h_{22}-1 & h_{23} & h_{24} & \ldots \\ h_{31} & h_{32} & h_{33}-1 & h_{34} & \ldots \\ h_{41} & h_{42} & h_{43} & h_{44}-1 & \ldots \\ \ldots & \ldots & \ldots & \ldots & \ldots \end{pmatrix}. \tag{4.13}$$

A very good approximation to the value of $a\lambda$ is even determined by $D_2(a\lambda) = h_{11}(a\lambda) - 1 = 0$. Once the parameter $a\lambda$ is determined, one can compute the coefficients $h_{m,n}$ from (4.10) and (4.11) and solve the system (4.12) for $a_1, a_2, a_3, \ldots$. Next the coefficients A_n of (4.2) are computed by (4.8) and with this the problem is solved. In particular, the mode of motion of the unsteady free surface can be derived from the equation (3.11), viz.

$$\delta_1 = -\frac{1}{\lambda}\frac{K}{\epsilon}\frac{q_0}{Q_H}\frac{\partial\phi_1}{\partial\beta} = \frac{1}{(\lambda a)}\sin\gamma_0\frac{\partial\phi_1}{\partial\beta}. \tag{4.14}$$

since $q_0 = -K\sin\gamma_0$. In case the component (3.10) cannot be neglected, as in the case of a sudden rise of the water level in the reservoir, then

$$\frac{K}{\epsilon}\frac{\partial\phi_1}{\partial n} = -\frac{q_0}{\epsilon}\frac{d\delta_1}{ds} + \lambda\delta_1, \tag{4.15}$$

or, by the use of (3.6),

$$\frac{K}{\epsilon}\left(-\frac{q_0}{Q_H}\frac{\partial\phi_1}{\partial\beta}\right) = \frac{q_0^2}{\epsilon Q_H}\frac{\partial\delta_1}{\partial\alpha} + \lambda\delta_1. \tag{4.16}$$

Insert the value of δ_1 from (3.8) into (4.16) and use (3.13) to find

$$(\phi_{1\beta})_{\beta=1} = \left[(a\lambda)\frac{\alpha}{1+\alpha^2} + (a\lambda)^2(1+\alpha^2)\right]\phi_1 + \left[2a\lambda - \frac{\alpha}{(1+\alpha^2)^2}\right]\phi_{1\alpha} + \frac{\phi_{1\alpha\alpha}}{1+\alpha^2}. \tag{4.17}$$

The study of the problem with this free-boundary condition can be done exactly in the same way as before although the computations of $h_{m,n}(a\lambda)$ become tedious.

5. A numerical example

The mode of motion of the free surface and the exponential law have been computed for the family of dams for which $d = 3$ (De Wiest 1959). These computations can be simply repeated for any other numerical value of d corresponding to the particular dam that must be investigated. The smallest positive root of $D_2(a\lambda) = 0$ and $D_4(a\lambda) = 0$ has been computed algebraically, whereas the smallest positive root of $D_6(a\lambda) = 0$ and $D_8(a\lambda) = 0$ has been determined graphically on a large-scale plot, a reduced copy of which is given in figure 3. The smallest positive roots of the successive determinants are

Determinant	$D_2(a\lambda)$	$D_4(a\lambda)$	$D_6(a\lambda)$	$D_8(a\lambda)$
$a\lambda$	0·479	0·492	0·480	0·490

(5.1)

From this one may assume that the smallest root of $D_{2n}(a\lambda) = 0$ will converge to the smallest root of $\Delta(a\lambda) = 0$, as $n \to \infty$. The values of $a_1, a_2, a_3, a_4, \ldots$ computed from the system (4.12) will differ if one considers two, three, four, ..., equations and the corresponding value of $a\lambda$ which makes their determinant vanish, because these values of $a\lambda$ vary slightly. However, it is found that the values of the a_n decrease very rapidly, so that it is sufficient to consider only the coefficients A_1 and A_2 in (4.2).

A sketch of the mode of motion of the free surface is given in figure 4, for $d = 3$ and $a\lambda = 0{\cdot}49$. It can be verified that the free surface is no longer a parabola as in the steady state and that component (3.10) is small compared to component (3.9). Also, the value of $a\lambda = 0{\cdot}49$ satisfies the continuity condition (4.3). In figure 4, c^* denotes the undetermined amplitude of the displacement of the free surface.

It is felt that further theoretical investigations or experiments may lead to the relation between the unknown amplitude and the speed at which the water level behind the dam rises.

The present paper is extracted from a doctoral dissertation written in the Civil Engineering Department of Stanford University with Dr Byrne Perry as adviser. The writer also expresses his appreciation for the generous help given by Dr Gordon Latta of the Stanford Mathematics Department. The work was sponsored by the National Science Foundation under Grant NSF-G 4126.

REFERENCES

CURLE, N. 1956 Unsteady two-dimensional flows with free boundaries. *Proc. Roy. Soc.* A, **235**, 375.

DE WIEST, R. J. M. 1959 Unsteady-state phenomena in the flow through porous media. Ph.D. Dissertation. Stanford University. *Technical Report* no. 3, Department of Civil Engineering (or from University Microfilms, Ann Arbor, Michigan).

HUBBERT, K. 1940 The theory of ground-water motion. *J. Geol.* **48**, 785.

LAMB, H. 1932 *Hydrodynamics.* Cambridge University Press.

WHITTAKER, E. T. & WATSON, G. N. 1947 *A Course of Modern Analysis*, pp. 36, 413–17. New York: The Macmillan Co.

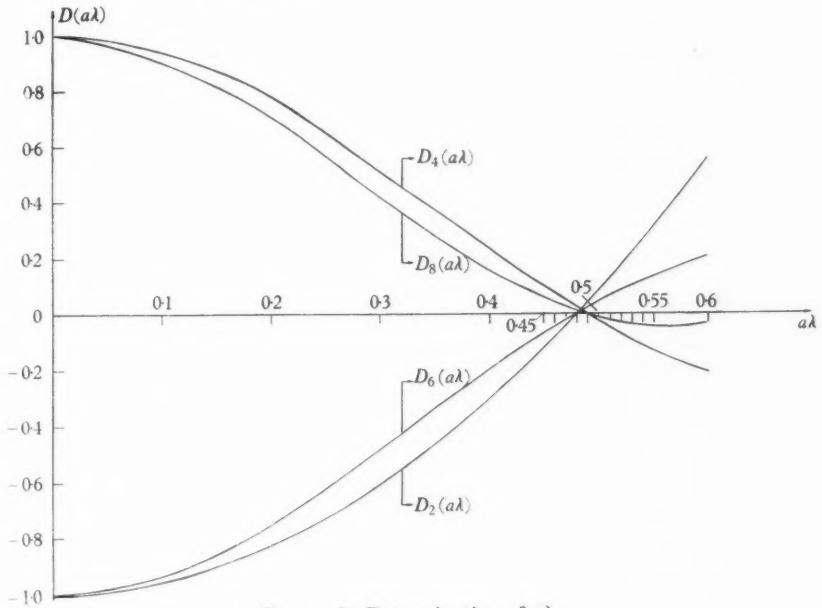

FIGURE 3. Determination of $a\lambda$.

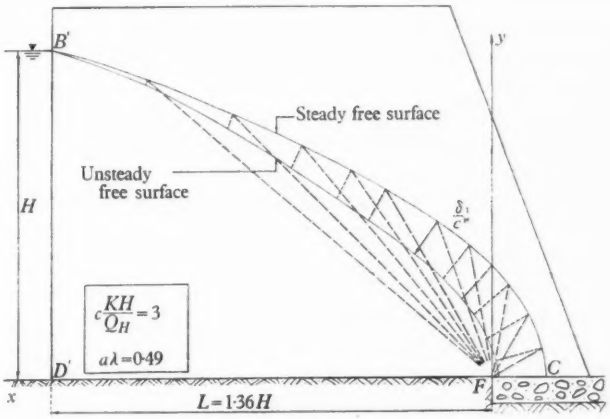

FIGURE 4. Mode of free surface motion.

Forced mixing in boundary layers

By G. B. SCHUBAUER AND W. G. SPANGENBERG
National Bureau of Standards, Washington, D.C.

(Received 16 September 1959)

The effect of increasing the rate of mixing in turbulent boundary layers in a region of adverse pressure gradient has been investigated experimentally. Only the two-dimensional case was considered. The boundary layer was formed on a flat wall in a special wind tunnel in which a variety of adverse pressure gradients could be obtained. Speeds were low enough to justify the neglect of compressibility. The main objective was to compare the effect of increasing the rate of mixing with the effect of reducing the pressure gradient on boundary-layer development and separation. A variety of mixing schemes was tried, all of them involving fixed devices arranged in a row on the surface in the region of rising pressure. While these differed considerably in effectiveness, they had a generally similar effect on the flow; and, except for effects arising from changes in displacement and momentum thickness introduced at the devices, their effect on the layer was basically equivalent to that of a decrease in pressure gradient. Apart from forced mixing, the shape of the pressure distribution was found to have a significant effect on displacement and momentum thickness, these being minimized and the wall distance decreased for a given pressure rise by a distribution with an initially steep and progressively decreasing gradient.

1. Introduction

When the relative motion of a fluid near the surface of a body has been reduced by friction or other momentum-extracting agent, there arises a problem of maintaining flow in regions where the pressure is increasing in the flow direction. The well-known phenomena of excessive boundary-layer thickening and flow separation are manifestations of the reduced ability or inability of the flow to proceed to regions of higher pressure.

These phenomena have been studied very extensively as part of the general boundary-layer problem and are sufficiently well understood to provide some rational rules of design by which unwanted effects may be avoided or reduced. In essence these are rules for exploiting natural turbulence, and in general they amount to giving the body a shape and attitude so that the necessary pressure recovery will occur gradually enough to enable natural turbulent mixing to keep the flow from stagnating under the action of the opposing pressure. The designer can, of course, resort to the expedient of partial removal of the boundary layer by suction or to energizing it by blowing through slots.

While the exploitation of natural turbulent mixing is the basis of most design, the possibility of increasing the rate of mixing by auxiliary devices has been explored in a number of technical applications. The general purpose of this

investigation is to find the effect of augmented mixing on boundary-layer development and flow separation. The major theme is the comparison between pressure gradient and forced mixing as separate controllable parameters. Ultimately we seek the answer to the following question: What difference is there between applying forced mixing to increase the pressure recovery that a boundary layer will withstand before separation occurs, and the alternative of lowering the pressure gradient to permit natural turbulent mixing to delay separation until the same pressure recovery is achieved?

The idea of using mixing devices to assist flow against an opposing pressure gradient and delay or avoid separation is not new. As far as is known to the authors, the first device of this kind was the vortex generator, devised in 1946 by H. D. Taylor and associates of the Research Department of the United Aircraft Corporation. A summary account of this work including references to ten other reports is given by Taylor (1950). Subsequently other devices have been tried by various workers, and a variety of applications of these and vortex generators have been studied, mostly with emphasis on delaying separation and improving performances of airfoils and diffusers. The following references include the known schemes: Grose (1954); McCullough, Nitzberg & Kelly (1951); Pankhurst (1955); Stephens & Collins (1955); Taylor (1948, 1950); Weiberg & McCullough (1952). No reference to the various applications is attempted. The report by Grose (1954) was discovered when the present investigation was about completed. In it we find some parallel between that work and our own, as both deal with the boundary layer on a flat wall and both explore the effectiveness of various types of mixing devices. There seems, however, to have been no study of the problem with the specific aim of the present investigation.

Since this is a boundary-layer study rather than a performance study of some particular body, a two-dimensional turbulent boundary layer on a smooth flat wall was used. The pressure distribution along the wall is independently controlled and is made to rise from a nearly constant level over the fore part of the wall to higher levels at rates (gradients) sufficient to cause flow separation. This produces the pressure-recovery region, which is the only part of a pressure distribution with which this investigation is concerned. The medium is air at speeds low enough to justify the neglect of compressibility effects, but high enough, in conjunction with linear dimensions, to afford Reynolds numbers of technical interest.

Mixing devices presented a special problem. While no moving or running devices were considered, it was realized that an almost endless variety of fixed devices could be conceived. The best hope was that enough schemes could be tried to give a general idea of what could be expected.

An account of this investigation was originally given in *NBS Rep.* 6107 to the Office of Naval Research. In the present paper new data have been added and all results have been re-evaluated in the light of the more complete information. While it is fully realized that this study covers only a limited part of a complex subject, it is hoped that the information will serve to show how forced mixing fits into the pressure-recovery problem and give some idea of its probable significance.

2. Purpose and nature of mixing

A boundary layer comprises fluid that has insufficient momentum to flow as far up a pressure rise as fluid outside the layer. In the limit at the wall the momentum vanishes and with it the ability of the fluid to make any progress against a pressure rise. Thus we see that flow to higher pressure would cease, first at the wall and then farther out, unless maintained by some mechanism that causes the faster moving fluid to render assistance to the slower fluid. Since there is friction, moving fluid tends to drag along fluid that would tend to stop. However, we know that we must look to something other than internal friction between smoothly flowing layers, which is the well-known friction of viscous origin in laminar flow, if we are to meet practical requirements.

Just as we find in many cases that we must resort to stirring when molecular diffusion alone is inadequate to do the desired mixing, so here we find that stirring, which mixes the slower fluid near the wall with faster fluid farther out, greatly facilitates the movement of the less energetic fluid. Just such mixing is provided by nature in turbulent flow. The effect is often expressed as a turbulent shear stress, and by analogy with molecular processes, the agency responsible is likened to a viscosity and is called 'eddy viscosity'. When we consider the fact that eddy viscosity in boundary layers is of the order of 100 times greater than ordinary viscosity, and in jets and wakes is of the order of 1000 times, we see that turbulent flow embodies a relatively powerful self-mixing mechanism. The numbers given are only order-of-magnitude ones, as the actual value of the ratio is proportional to the Reynolds number. This powerful self-mixing makes it possible for turbulent flow to negotiate much steeper and higher pressure rises than can laminar flow. However, even with such capabilities the upper limit is often inconveniently low, and we have reason to expect that we can benefit by a mixing more vigorous than that presented to us naturally, if this is to be had without at the same time introducing other factors that may nullify the possible gain. The benefits consist of delaying or preventing stagnation and the resulting flow separation from a wall and in generally broadening our capabilities for achieving pressure recovery.

We may examine the effect of mixing on the mean flow field without becoming involved with the detailed flow processes by examining the effect on the integral parameters δ^* and θ and the shape parameter H, where

$$\delta^* = \text{displacement thickness} = \int_0^\delta \left(1 - \frac{U}{U_1}\right) dy,$$

$$\theta = \text{momentum thickness} = \int_0^\delta \left(1 - \frac{U}{U_1}\right) \frac{U}{U_1}\, dy,$$

$$H = \delta^*/\theta.$$

Here y is distance from the wall; U is the velocity at any point in the boundary layer; U_1 is the free-stream velocity outside the layer; and δ is the ordinary boundary-layer thickness, taken as the value of y where U is not measurably different from U_1.

A useful relationship in this connexion is the von Kármán momentum integral equation, written as follows for two-dimensional flow

$$\frac{d\theta}{dx} = \frac{\theta}{q}\frac{dp}{dx}\left(\frac{1}{2}\frac{\delta^*}{\theta} + 1\right) + \frac{\tau_w}{2q}, \tag{1}$$

where x is distance along the wall; p is the static pressure, assumed constant across the boundary layer; q is the free-stream dynamic pressure; and τ_w is the shear stress at the wall. As is customary, the term expressing the Reynolds normal stress in turbulent flow has been omitted. The two-dimensional form is used because we are concerned only with a two-dimensional boundary layer in this investigation. While stationary three-dimensional flow patterns will be encountered when forced mixing is applied, it will be assumed that equation (1) is applicable when an average is taken over enough spanwise-distributed patterns to yield representative average values of δ^* and θ.

Our purpose now is to see in terms of δ^* and θ how the boundary layer is affected by mixing. Equation (1) is an expression for the growth of θ with x in terms of the forces exerted on the flow. These forces arise from the pressure gradient and wall friction and are expressed in dimensionless form by the first and second terms, respectively, on the right-hand side of the equation. The retardation of the flow by the forces causes δ^* to increase also. However, the value of δ^* depends on the amount of fluid through which the retardation is distributed, as is perhaps best illustrated by the well-known change in H which occurs with transition from laminar to turbulent flow. With the introduction of turbulence an increase in mixing takes place in a distance so short that θ remains virtually unchanged. For the case of zero pressure gradient, H goes from about 2·6 in the laminar layer to 1·3 in the turbulent layer. This means that δ^* is decreased to half of its original value by the mixing action of turbulence.

It is seen therefore that the more the momentum loss is dispersed throughout the fluid, the less is the flow displacement caused by the retarding forces. Mixing therefore affects δ^* directly. As shown by equation (1), mixing can affect the growth of θ through its explicit effect on the value of δ^*. The effect is to decrease $d\theta/dx$ unless this is offset by an increase in τ_w. Since δ^* occurs in the ratio δ^*/θ, it is customary to discuss its effect in terms of the shape parameter, H. The determination of H is in fact the major task of the several methods that have been proposed for calculating turbulent boundary-layer development.

The quantity τ_w is itself reduced by an adverse pressure gradient, and if the gradient is high enough, the τ_w-term of equation (1) may become negligible compared with the dp/dx-term. The special case where $\tau_w = 0$ and $H = \text{const.}$ is of some interest, and for this case the equation can be integrated directly to give

$$\frac{\theta}{\theta_i} = \left(\frac{q_i}{q}\right)^{(H/2+1)} \begin{Bmatrix} H = \text{const.} \\ \tau_w = 0, \end{Bmatrix} \tag{2}$$

where θ_i and q_i are initial values. The skin friction τ_w will not be zero unless the flow is always in a state of incipient separation, and equation (2) becomes a justifiable approximation only when the τ_w-term is small compared with the dp/dx-term in equation (1). The other condition, $H = \text{const.}$, will not in general

be met, but this will not affect the physical insight afforded by equation (2). Since the skin friction does not enter into the equation, it expresses the growth of θ resulting purely from carrying boundary-layer fluid from a dynamic pressure of q_i to q. This is the only aspect of the growth that mixing can affect favourably, and the effect comes about from a reduction of H. It is known that H is also reduced by reducing the pressure gradient; hence we expect reduced pressure gradient and increased rate of mixing to have similar effects. The similarity may be explained on the grounds that forced mixing and reduced pressure gradient are merely means of assisting mixing to expedite the flow—the one by increasing the rate and the other by increasing the time available. Accordingly, if H is to be held at some fixed value, an increased rate of mixing will make possible a larger pressure gradient. Again, if H is increasing with x, an increase in the rate of mixing will decrease dH/dx, or hold dH/dx the same for some larger value of pressure gradient. Since the separation condition is associated with a particular value of H ($H \simeq 2$), an increase in the rate of mixing can be expected to make the pressure recovery higher before separation occurs, particularly where the pressure gradient is large. Only qualitative estimates of this kind are possible because any reduction of H below its separation value normally brings skin friction into the picture.

We must assume that stirring by any means will increase skin friction by virtue of bringing higher velocities nearer the wall. In this connexion an interesting observation may be made. When mixing takes place by eddy motions comprising bulk movements of fluid, as it does in turbulent mixing, the mixing weakens as the wall is approached and finally disappears leaving only molecular viscosity in a laminar sublayer at the wall. Thus, while the skin friction has been increased, this has come about because of a velocity increase near the wall rather than by a uniform, across-the-layer increase in eddy viscosity. This carries with it a compensating feature, namely, a shaping of the velocity profile toward lower values of H. For this reason values of H in turbulent flow are lower than those in laminar flow. For example, the values of H computed by Clauser (1954) for equilibrium laminar profiles range from 2·592 for constant-pressure flow to 4·031 for a pressure gradient sufficient to maintain a state of incipient separation. For comparison the corresponding values of H for turbulent flow range from about 1·3 to 2. Thus, with turbulence setting the pattern, a good case can be made for mixing, and we are afforded ample justification for attempting to increase it. Care should be exercised that the advantage is not lost through the scheme of mixing adopted. We know, for example, that the advantage would be lost by increasing the rate of mixing by roughening the wall.

When we begin to consider how to go about mixing, we are at once struck by the fact that nature's scheme of turbulent mixing approaches the ideal one. It is simply a self-induced mixing arising out of the velocity differences already existing. The forces are applied by one portion of the fluid on another, and no momentum loss is charged against the mixing process. If we are to match this ideal, we should not consume momentum of mean flow to do the mixing, but should rearrange the velocity field so as to produce steeper gradients within which turbulent mixing motions are generated and across which they transfer

momentum. A pure rearrangement implies guiding the fluid to new positions, leaving no residual motions to require an induced drag from the mixing devices. No fluid-handling device can, however, escape the drag that arises from frictional effects; hence if residual motions contribute enough to the mixing, suppression of them would not be warranted. The well-known vortex generator is an example wherein the derived mixing depends on induced, streamwise vortices. In fact such vortices may be regarded as a rearranging mechanism installed in the flow and persisting for a considerable distance downstream. The study of mixing devices is taken up in § 5.

3. Experimental arrangement

A wind tunnel built specifically for this investigation is shown in figure 1. The boundary-layer studies were conducted on the bottom wall of the test section. This wall was a smooth flat surface 6 ft. wide made of birch plywood. The top wall consisted partly of slatted sections for the purpose of producing a static pressure increase by progressively reducing the volume flow in the duct. By adjusting the slats the boundary layer on the bottom wall could be subjected to various adverse pressure gradients. This type of control was made possible by supplying air from the room to the system under positive pressures by the arrangement shown. The screened diffuser on the outlet of a centrifugal fan and the settling chamber containing a honeycomb and additional screens made the flow entering the test section sufficiently uniform and free from turbulence for the job at hand.

The test section was originally $13\frac{1}{2}$ in. deep and 16 ft. long, but during the course of the investigation it became necessary to extend the length to 24 ft. with the slope of the top adjustable to a final depth of 27 in. The boundary layer was tripped about 1 ft. from the entrance to produce a definite beginning of the turbulent layer. The region of pressure rise was begun after an initial 4 ft. run of constant pressure. All reference quantities pertain to conditions at the 4 ft. position, and this position is taken as the origin of x. Here the boundary layer was about 1 in. thick. The free-stream velocity at the 4 ft. position was maintained at 82 ft./sec, except when altered to investigate scale effects. The corresponding Reynolds number, based on the 4 ft. distance from the approximate beginning of the layer, was $1{\cdot}9 \times 10^6$.

Separate total-head and static-pressure tubes, made from 0·04 in. outside diameter nickel tubing, were used for the measurement of velocities and pressures throughout the boundary layer. Gear for traversing in all directions was provided. By flattening the end of the total head tube to an opening of 0·005 in. it was possible to make reliable measurements sufficiently near the wall. Pressures at the wall were measured by means of $\frac{1}{16}$ in. orifices in the wall itself. To check the spanwise uniformity these were placed in three rows running the full length of the wall, one on the centreline and the other two 15 in. to each side.

A dust method, developed earlier in the laboratory, was used to indicate flow separation. This consisted simply of injecting talc dust into the region downstream of separation and permitting the currents in the wake to carry the dust upstream to the line of separation. A film obtained by wiping the surface with

an oily cloth was sufficient to hold the dust and produce a clearly defined boundary. A typical example showing the region of separation downstream from a row of mixing devices is shown in figure 2. The white line further upstream shows where the line of separation was with devices absent. Since the lines of separation were never straight, an average was taken over the central 45 in. in order to define a mean position. Since the position fluctuates up and downstream, the dust method gives an upstream extreme. Additional examples of the application of this method are given by Smith & Murphy (1955).

An important additional piece of equipment was an especially designed balance installed beneath the test wall for measuring the drag of individual mixing devices when in position in the boundary layer. The mixing device was connected to the balance by a spindle running through a hole in the wall. The balance was sealed to prevent leakage through the hole.

4. Pressure gradients and effect on boundary layer

In order to establish a basis for later investigating the effect of forced mixing, the boundary layer was studied with various adverse pressure distributions which were sufficient in each case to cause eventual separation of the layer. A considerable amount of effort went into attaining a two-dimensional flow. The test for two-dimensionality was the agreement between boundary-layer profiles measured on the centre line and those measured 15 in. to each side. The usual tests were applied to the profiles themselves, namely, agreement with the law of the wall, best agreement being found using the coefficients given by Coles (1956), and agreement with the family of H-parameter profiles given by von Doenhoff & Tetervin (1943). For the lower pressure gradients there were departures from the von Doenhoff–Tetervin set like those found by Clauser (1954) for his equilibrium profiles. Since the form of the profile indicated agreement with the law of the wall, the method suggested by Clauser for obtaining the local skin-friction coefficient from the velocity profile was used.

There was a measureable pressure gradient across the boundary layer, but this was considered to be sufficiently small to permit our taking the pressure at the wall as the pressure applicable to the entire cross-section of the layer. In the determination of velocities, however, the local static pressure was always used.

The several pressure distributions, labelled A to F, are shown in figure 3. In all cases the pressure has been held constant up to the 4 ft. position, where the origin of x is taken, and then made to rise as shown in the figure. The amount of rise is termed the pressure recovery, and this is expressed in terms of a pressure-recovery coefficient $(p-p_0)/q_0$, where p_0 and p are pressures at the wall and q_0 is the free-stream dynamic pressure at the position $x = 0$. Distribution A was set up first in order to provide a condition of early separation and low-pressure recovery to which forced mixing could be applied with some expectation of improvement. Examples of the effect of mixing devices are shown in figure 7. Distribution B and C were next established in order to match as closely as possible the range of pressure recoveries obtained with mixing devices applied to condition A. On the assumption that skin friction would play a minor role in

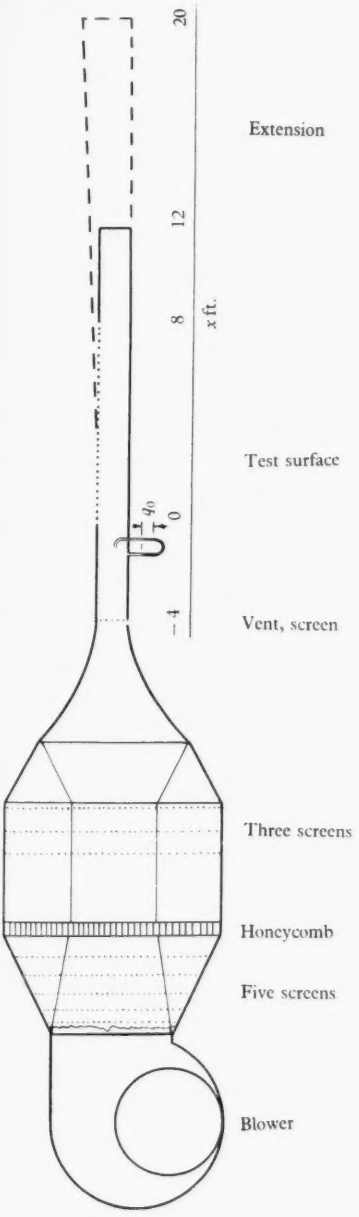

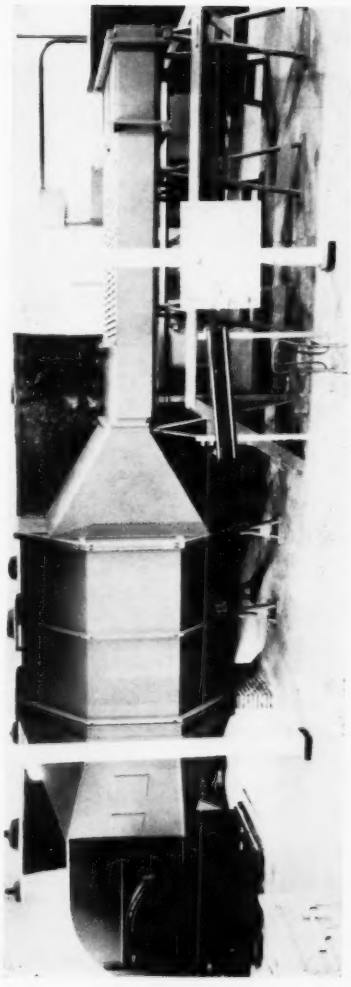

FIGURE 1. Wind tunnel for boundary-layer investigation.

(*Facing p.* 16)

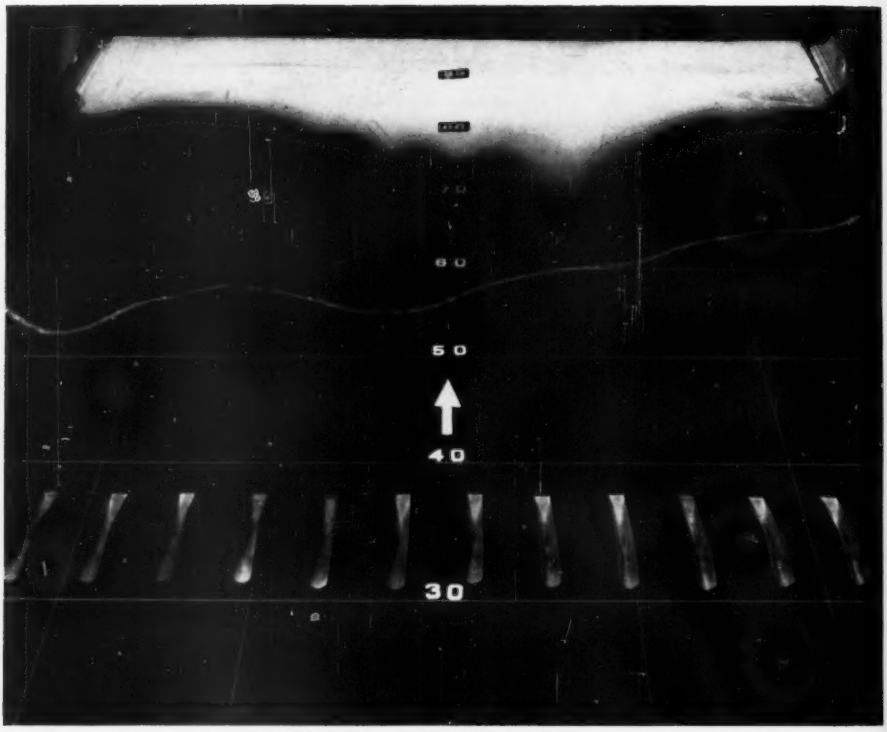

FIGURE 2. Photographs of dust pattern on surface showing separation region (white). The line marks the boundary found in a previous test with mixing devices absent (the dust is now removed). Numbers are distances in inches from the beginning of the pressure rise. The scoop type of mixing device is shown (see figure 6).

boundary-layer development, the idea behind B and C was simply that of promoting flow to higher pressures by reducing the gradient. After the main part of the investigation had been completed, it was suspected that skin friction might be more important than originally supposed, and the investigation was extended to include distributions D, E and F. Forced mixing was applied only in the case of distribution A.

This somewhat elaborate study of naturally turbulent boundary layers was occasioned by the desire to compare the effect of forced mixing to that of the pressure field alone. When the first comparisons were made using only B and C, it was assumed that the shape of the pressure distribution could be ignored and that the rate of pressure rise was the really important quantity. However, the

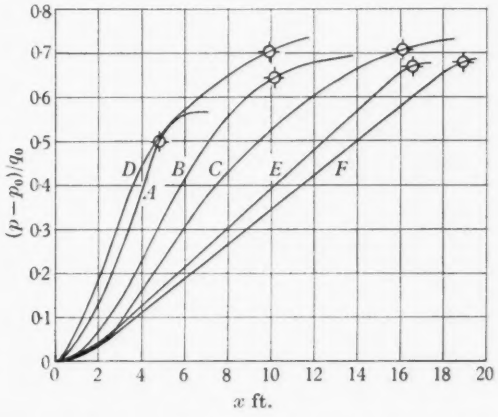

FIGURE 3. Pressure distributions. The origin of x is taken 4 ft. from the leading edge. The pressure is uniform for $-4 \leqslant x \leqslant 0$. ◇, Separation point.

extended study showed a considerable dependence on shape and indicated the necessity for specifying the shape before a firm basis of comparison would be possible. This is apparent in part from the curves of figure 3. Distributions C and D, for example, achieve closely the same pressure recovery, yet C requires an additional 6·3 ft. run of wall.

A more important aspect of the dependence on shape is examined in figure 4. This type of plotting, in which δ^*, θ, and H are plotted against q_0/q, has been found useful for comparing boundary-layer development under different conditions. It amounts to expressing the thickness parameters as functions of pressure rise, now expressed in terms of q_0/q in order to obtain a more open scale than that afforded by $(p-p_0)/q_0$. The connexion is $q/q_0 = 1-(p-p_0)/q_0$. The diagram is most useful in comparing cases where pressure recoveries up to separation are closely the same. Taking C and D as fitting examples, we see that the boundary layer remains thinner for condition D than for C. The curve for condition E has been added to show that the trend is toward greater values of δ^* and θ as the mean pressure gradient is reduced. The opposite trend is exhibited by the H-curves, and the effect of this, as shown by equation (2), is to

oppose the observed trend of θ. In other words, since lowering the pressure gradient reduces H, it should likewise reduce θ and also δ^*. Failure to do so is evidence of an effect of skin friction.

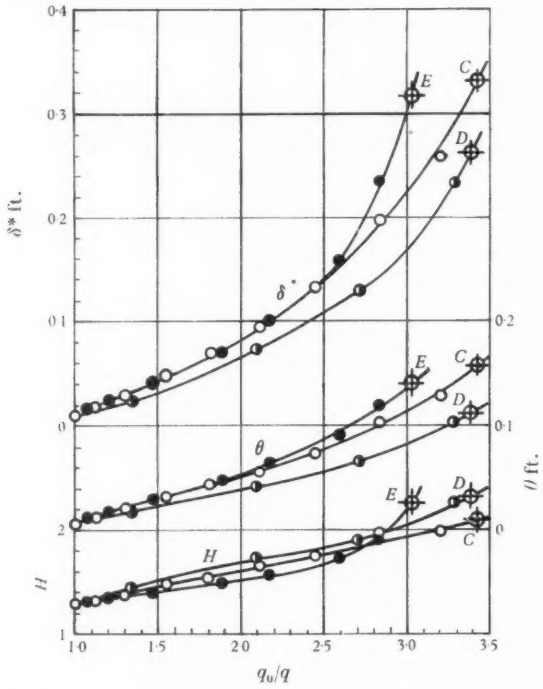

FIGURE 4. The effect of pressure distribution on the relation between δ^*, θ, H. The pressure rise is expressed as q_0/q, where $q/q_0 = 1-(p-p_0)/q_0$. Pressure distribution: C, ○; D, ◑; E, ●. ⊕ Separation point.

The values of the local skin-friction coefficient, τ_w/q, for the naturally turbulent layer were found to decrease monotonically from around 0·0032 at $x = 0$ to around 0·0003 at the indicated separation point. Failure to reach zero is attributed to the fact that the dust method indicates the upstream extreme of a fluctuating separation point. The question of immediate interest is the relative effect of pressure gradient and skin friction on the growth of θ. In this connexion figure 5 has been prepared showing the ratio of the pressure-gradient term to the skin-friction term appearing in equation (1). We see that ultimately the effect of skin friction becomes small by comparison, but when the pressure gradient is low there is a considerable range of x over which it is not negligible. The advantage of distribution D over B, C, E and F arises from the fact that the initially steep pressure gradient of D reduces the skin friction early in the course of the pressure climb and at the same time reduces the length of wall over which the flow proceeds in attaining a given pressure recovery. These effects outweigh the adverse effect arising from the early increase in H shown in figure 4. Comparing

D with A, we find that whereas separation occurs early in A it has been delayed in D by the progressively decreased gradient.

It appears from this that the best form of pressure rise is one that has an initially steep and steadily decreasing gradient. It has been proposed by Stratford (1959) that the optimum pressure curve should be one with gradients such that the flow is on the verge of separation and the skin friction is zero

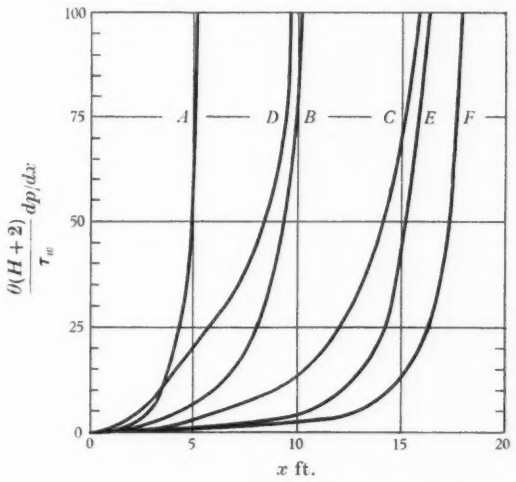

FIGURE 5. Ratio of pressure-gradient term to skin-friction term (1st term to 2nd term on right-hand side of equation (1)) as a function of x for the pressure distributions of figure 3.

throughout. Stratford found the flow to be stable under this condition for his experimental arrangement. In the present investigation, however, it was observed that distribution D was about the limiting high-gradient condition for a stable flow.

5. Mixing devices and effect on separation

While the goal in mixing was reasonably clear, the question of how to accomplish it in a practical manner was quite another matter. The idea, mentioned earlier, of promoting self mixing by simply rearranging the flow was adhered to, but it was found after considerable effort that forms designed to minimize induced drag by cancelling off residual vortex motions generally has as much or more drag than those that produced strong vortex trails. Furthermore, they were always less effective, showing that a vortex with its axis along the stream comprised a sustained rearranging mechanism. It was also learned that mixing on a coarse scale by relatively large, widely spaced devices was far more effective than fine scale mixing; and under these conditions, multiple rows were less effective than a single row of devices properly spaced and properly stationed. Attention was therefore centred on the single-row arrangement as illustrated in figure 2. The devices so studied are shown in figure 6. All except device (B) were

produced in sufficient number to span the 6 ft. width of wall and tested for their effect on separation and pressure recovery with the channel arranged for pressure distribution A. The spacing and position for maximum delay of separation and maximum pressure recovery were found by trial and error. A height of the order of the boundary-layer thickness was adopted, but this was not varied in the process of finding the optimum position. The drag of the device was measured

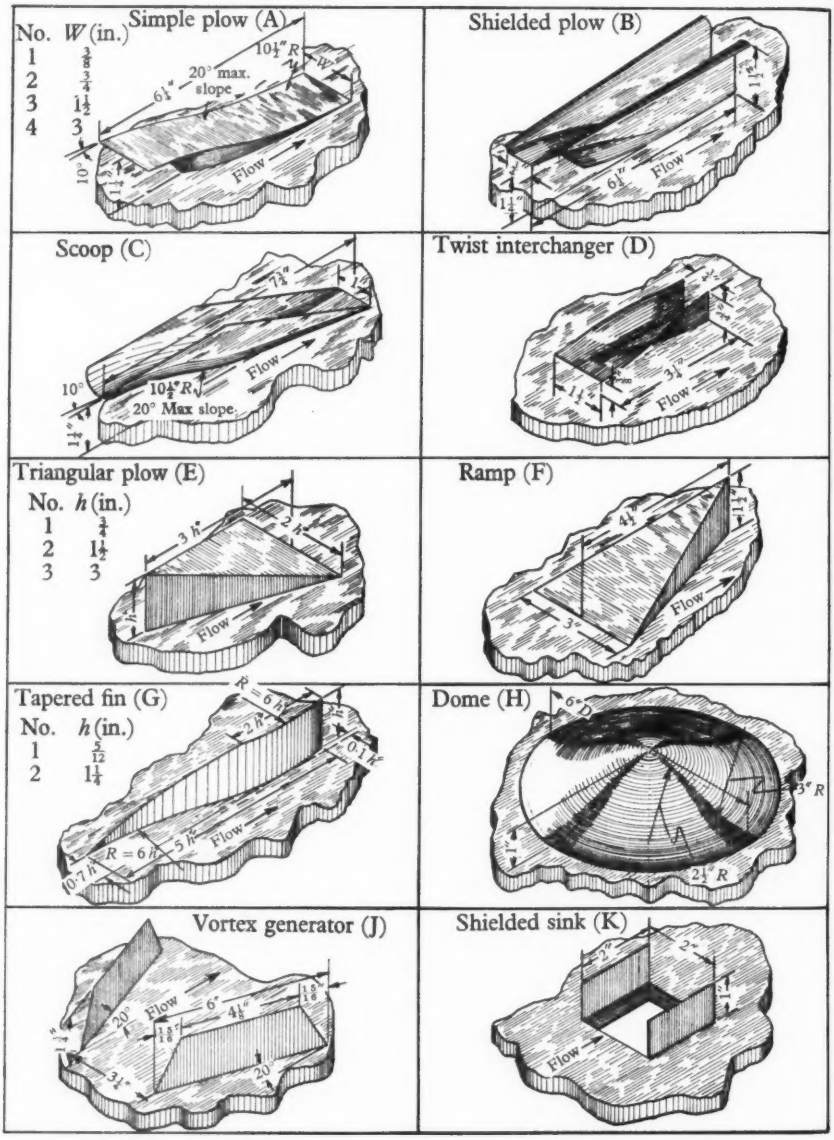

FIGURE 6. Mixing devices.

in its position in a row or with an identical device to each side. No rotating devices or moving agitators were considered.

Before taking up the results, the reasoning behind the devices and their intended action will be discussed. Device (A), called the simple plow, was intended for parting the boundary layer and guiding outer flow toward the wall into the furrow so produced. The motion thus started continued downstream in the form of a pair of trailing vortices. The shielded plow (B) is device (A-2) modified by the addition of enough side shielding to effectively eliminate the vortices. Since the elaborate additions merely increased the drag of the device,

No.	Device Name	L (in.)	x_l (ft.)	x_s (ft.)	$\frac{p_s-p_0}{q_0}$	$\frac{\Delta p_s}{q_0}$	$\frac{D}{q_l}$ (ft.²)	$\Delta\theta_l$ (ft.)	$\frac{\Delta\theta_l}{\theta_l}$
	None	—	—	4·83	0·50	0	0	0	0
A-1	Simple plow	6	0·52	6·33	0·61	0·11	0·0010	0·0010	0·112
A-2	Simple plow	4·5	2·60	7·00	0·71	0·21	0·0015	0·0020	0·126
A-3	Simple plow	8	2·60	7·25	0·71	0·21	0·0045	0·0034	0·214
A-4	Simple plow	8	3·85	6·83	0·71	0·21	0·0100	0·0075	0·274
B	Shielded plow	—	0·52	—	—	—	0·0025	—	—
C	Scoop	6	1·48	6·67	0·65	0·15	0·0023	0·0023	0·200
D	Twist interchanger	3	1·94	5·75	0·58	0·08	0·0016	0·0032	0·242
E-1	Triangular plow	6	1·02	6·42	0·66	0·16	0·0015	0·0015	0·147
E-2	Triangular plow	6	2·87	6·75	0·67	0·17	0·0050	0·0050	0·289
E-3	Triangular plow	6	4·08	7·92	0·75	0·25	0·0240	0·0240	0·780
F	Ramp	6†	2·87	5·75	0·59	0·09	0·0037	0·0037	0·214
G-1	Tapered fin	2	0·17	6·42	0·52	0·02	—	—	—
G-2	Tapered fin	4	0·52	6·00	0·62	0·12	0·0033	0·0050	0·562
H	Dome	6	0·50	5·92	0·60	0·10	0·0032	0·0032	0·364
J	Vortex generator	6·75	3·80	7·17	0·69	0·19	0·0097	0·0086	0·323
K	Shielded sink	6‡	2·67	6·75	0·67	0·17	—	−0·0030	−0·176

L and x_l are optimum spacing and position, respectively.

x_s is the mean position of separation over the central 45 in. of span.

$$\frac{\Delta p_s}{q_0}=\frac{p_s-p_0}{q_0}-0{\cdot}50.$$

† The optimum value of L was 3 in. giving $x_s = 6{\cdot}08$ ft. The value 6 in. was used because of interest in comparing devices (F) and (E-2).

‡ Optimum L and x_l not determined.

TABLE 1. Summary of mixer characteristics

this arrangement was abandoned in favour of (C), called the scoop, which incorporated some shielding and was easier to construct. The twist interchanger (D) and the tapered fin (G) represent other ideas for overturning the flow without intentionally involving residual vortex motions. On the basis of the evidence in table 1 it was concluded that drag reduction by elimination of trailing vortices was not practically possible, and since this amounted to stopping the action started at the device, its effectiveness was reduced without compensating benefits. The triangular plow (E) is a less refined version of (A) having much the same action, and the ramp (F) is simply (E) used in reverse. A device nearly like the triangular plow, called a 'wedge-type vortex generator', was included

among the devices studied by Grose (1954). The ramp, also called a 'wedge' in the literature, has seen use as a boundary-layer control device. The dome (H) was intended as an object that would add little wetted area and at the same time generate vortices by virtue of its being in the non-uniform velocity field of the boundary layer. Device (J) is a conventional vortex generator of the flat-plate type with a trapezoidal shape approximating the taper recommended by

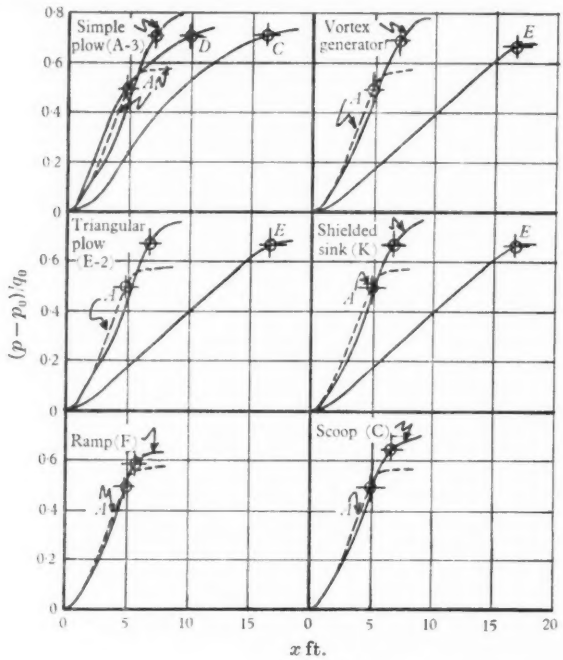

FIGURE 7. Pressure distributions showing typical effect of mixing devices. Distributions A, C, D, E are the same as those given in figure 3. Φ, Separation point.

Taylor (1948). It was arranged in pairs set for producing counter-rotating vortices. The shielded sink (K) falls in a separate category and will be discussed following the discussion of table 1 and figure 7.

The results are summarized in table 1, and selected examples showing the effect in terms of pressure distribution are shown in figure 7. Curve A represents the condition before mixing devices were applied. The devices extend the curve upward and somewhat modify its earlier course, with the result that there is now a new pressure distribution for each type of device. Curves C, D and E show the pressure distributions designed to produce the same pressure recovery as that obtained by means of the mixing device.

The relative performance of the various devices may be judged from table 1. Starting from a separation point at 4·83 ft. and a pressure-recovery coefficient at separation of 0·5 for no mixing devices, the effect of several devices may be judged by running down columns headed x_s, $(p_s-p_0)/q_0$, and $\Delta p_s/q_0$, where

$\Delta p_s/q_0$ is the increase in the coefficient due to the device. From the drag of the individual members of a set of devices the increment in momentum thickness effectively occurring at the trailing edge of a row of devices was calculated according to the formula

$$\Delta\theta_t = \frac{D}{2Lq_t},$$

where D is the drag of one member, L is the cross-stream spacing between devices, and q_t is the free-stream dynamic pressure at the trailing edge of the device. The fractional increase has been expressed by $\Delta\theta_t/\theta_t$, where θ_t is the momentum thickness at the same position in the absence of mixing devices. The quantity $\Delta p_s/q_0$ may be regarded as a measure of accomplishment, while $\Delta\theta_t/\theta_t$ may be regarded as the price paid for the accomplishment. The price has a special significance which will be considered in § 6.

The shielded sink (K) represents a departure from the usual scheme in that suction is employed. It was envisioned that if air was withdrawn through a hole in the wall the air above that entering the hole would be deflected toward the wall producing an effect not unlike that of a plow, where now the boundary-layer flow passes into the hole instead of being pushed aside. The primary aim was to obtain mixing with a decrement in momentum thickness rather than the increment which characterized external devices. Two-inch round holes spaced 6 in. apart were tried, but it turned out that the mixing action was feeble due to the fact that air was drawn off near the wall for a considerable area around the hole without producing steep cross-stream gradients. The shielded arrangement shown in figure 6 was then tried in the location around the optimum for the other devices. Conditions may therefore not have been optimum for this arrangement. The shields were made one-half hole width high to simulate doors which in practice might be closed to return to a plane wall. The suction quantity was fixed at 5·6 % of the boundary-layer flow, producing the decrement, $-\Delta\theta_t$, shown in table 1. It is seen that the effect on separation point and pressure recovery places the shielded sink with the more effective devices. In order to determine how much of the effect was due to boundary-layer removal alone, the same suction quantity was withdrawn through a continuous slot in the same position. The results compare as follows:

	x_s (ft.)	$\frac{p_s-p_0}{q_0}$	$\frac{\Delta p_s}{q_0}$	$\frac{\Delta\theta_t}{\theta_t}$
Shielded sink	6·75	0·67	0·17	−0·176
Continuous slot	5·17	0·57	0·07	−0·183
None (table 1)	4·83	0·50	0	0

While the continuous slot produced the greater reduction in momentum thickness, its effect on the separation point and pressure recovery was small. This shows that the principal effect of the shielded sink was derived from mixing. In this case, furthermore, the mixing involves a negative $\Delta\theta_t$, the decrement of flow of momentum represented by $-\Delta\theta_t$ being contained in the extracted air. Any additional momentum loss resulting from the use of the device will be added

to this, but since it is now internal, it will not result in as great an overall loss as will an equal amount deposited in the boundary layer at the mixer station. The reason for this and the benefits of a $-\Delta\theta_t$ will become apparent in § 6.

6. Effect of mixing on boundary-layer development

Detailed velocity surveys were made throughout the boundary layer with selected sets of mixing devices installed in the positions designated in table 1. Those chosen for this purpose were A-3, C, E-2, F, J and K. The purpose was to find out what was happening to the flow behind such devices and in particular

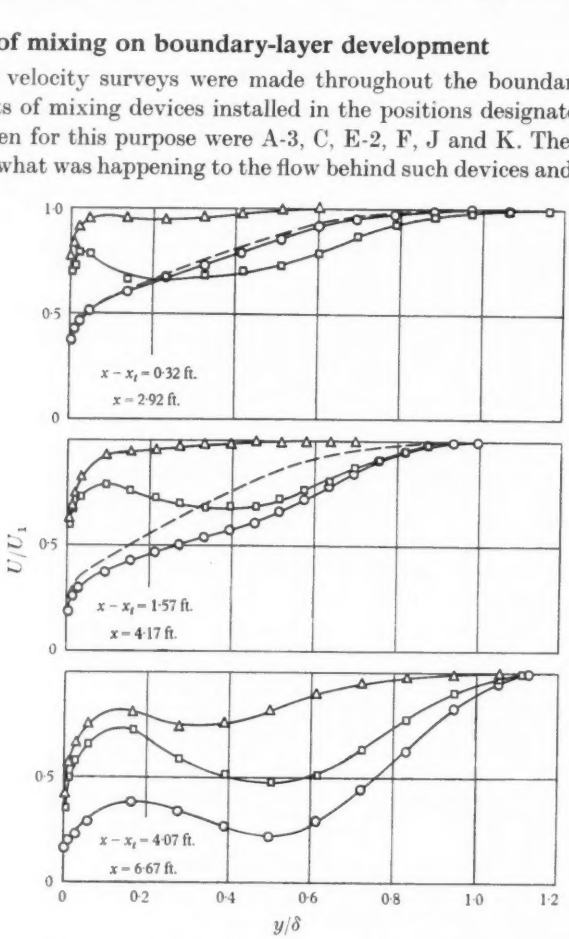

FIGURE 8. Mean-velocity profiles aft of simple plow (A-3) for conditions as given in table 1. Here δ is the boundary-layer thickness at the same station (x) with mixing devices absent. z/L: △, 0·00; □, 0·25; ○, 0·50; – – –, without devices.

to ascertain the average state of the flow in terms of an average δ^* and an average θ, the average being taken across the span. The ultimate purpose was to compare the course of development of such average values of δ^*, θ, and their ratio H with the same quantities in the naturally developing boundary layer. The procedure was to traverse in the y-direction, measuring total head and static pressure, at various cross-stream positions. This was then repeated at various distances downstream, and in this way the flow field was completely mapped out.

There were two sources of error not ordinarily encountered in boundary-layer measurements. One arose from strong vortex motions near the trailing edge of a device, and the other arose from erratic cross-stream movements of the flow pattern. It was the uncertainties introduced by the former that prompted the use of drag measurements for finding the $\Delta\theta_t$'s of table 1. However, values derived from velocity traverses agreed reasonably well with those derived from drag measurements. The second source of error caused uncertainties by introducing a considerable scatter in the data, particularly when the velocity gradients in the z-direction were steep. In general the accuracy approached that ordinarily obtained in boundary-layer measurements with pitot-static tubes uncorrected for the effect of turbulence.

An example of a set of velocity profiles is given in figure 8 at various cross-stream positions and various distances behind the simple plow (A-3). Here δ is the boundary-layer thickness for the same station in the absence of mixing devices, the profiles for this condition being shown by the dashed curves in two cases. This example is typical, with variations in degree, of the velocity patterns of the other devices, with the exception of the ramp (F) which showed a generally similar pattern, but with the higher flow rate displaced to the region between devices. This gave rise to alternate rows of high and low rates of flow in the boundary layer which decreased with distance but generally persisted to the separation point. The effectiveness of a device could be correlated with the intensity of the differences and to their persistence. From profiles like those of figure 8, local values of δ^* and θ were derived, and the average of these was then taken to obtain parameters pertaining to an equivalent two-dimensional boundary layer.

From the results obtained with the six devices certain common behaviour patterns emerged, and we shall here concern ourselves with the generalities derived from them. In all cases the operating conditions were as specified in table 1.

The typical change in boundary-layer development brought about by adding mixing devices is shown in figure 9. Not all devices were as effective as the simple plow (A-3), used here as the sample, but performances were generally similar. The drag of the device results in a step-up in δ^* and θ, placing the curves above the dashed curves pertaining to the boundary layer in its original condition. Subsequent increases are slower, and the solid curves approach or go below the dashed curves and then continue with the characteristic steepening rise to the delayed separation point. In the case of the shielded sink (K), where $\Delta\theta_t$ was negative, the step in δ^* and θ was down, and the curves lay below the dashed curves throughout. The values of H were reduced in the typical fashion shown, but again reached about the same value at separation as that found for the natural layer. On the average this value was 2, although it ranged from 1·75 to 2·3. These somewhat lower values than those usually quoted in the literature are attributed to the fact that they apply to the upstream extreme of a fluctuating separation point.

We next take up the comparisons toward which this investigation has been aimed, namely, comparisons between the boundary-layer development when

forced mixing was used to attain a given pressure recovery and when the recovery was alternately attained by adjusting the pressure distribution alone. Examples of the performance of three of the devices, illustrated by figures 10 and 11, will suffice to show what can be concluded from such comparisons.

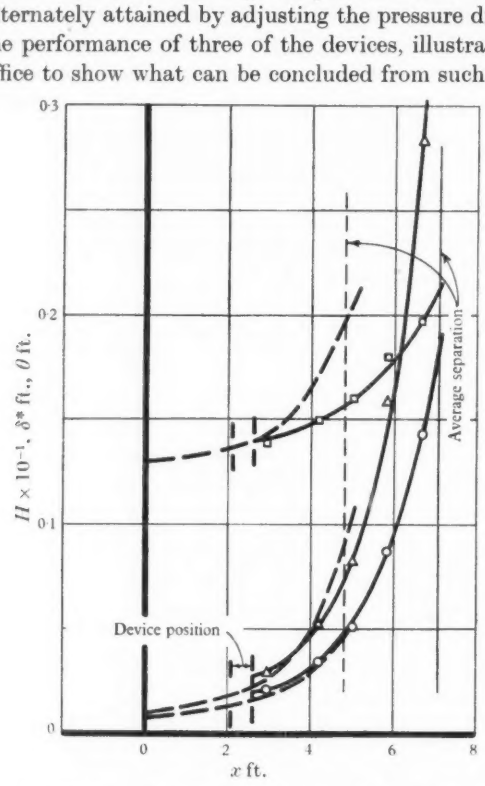

FIGURE 9. Effect of forced mixing on separation and averaged thickness and shape parameters. Here δ^* and θ are mean values derived by averaging local values over a sufficient span to be equivalent to a two-dimensional case. —, Simple plow (A-3): – –, without devices. △, δ^*; ○, θ; □, $H = \delta^*/\theta$.

In figure 10, again illustrating the performance of the simple plow (A-3), the values of δ^*, θ, and H for forced mixing are compared with those for pressure distributions C and D. We observe here a step-up $\Delta\delta_t^*$ and $\Delta\theta_t$, due to the drag of the device, which lifts the curves for δ^* and θ, aft of the 'device position', above the corresponding curves for C and D. Actually none of the curves are quite coincident ahead of this position due to the fact that the boundary layers have different pressure and skin-friction histories. The difference is, however, so small that the curves for the simple plow and distribution C may be regarded as coincident up to the occurrence of the step. The principal feature to be pointed out here is that the θ-curve for forced mixing lies above that for C by an almost constant percentage equal approximately to that given by $\Delta\theta_t/\theta_t$ in table 1. When only data for distributions B and C were available for comparison, this feature was observed to exist more or less in all cases. It was observed also that the H-curves generally lay close together. These tendencies were originally taken

to mean that skin friction was playing a negligible role and that $\Delta\theta_t$ at the devices was affecting the subsequent development of the layer as would be expected from equation (2), namely, by a constant percentage as indicated above. There were, however, obvious discrepancies, and this led to the study of the boundary layer with the additional pressure distributions *D*, *E* and *F*. With the curves for *D* added to figure 10 it became clear at once that the foregoing percentage rule could not be universally applied.

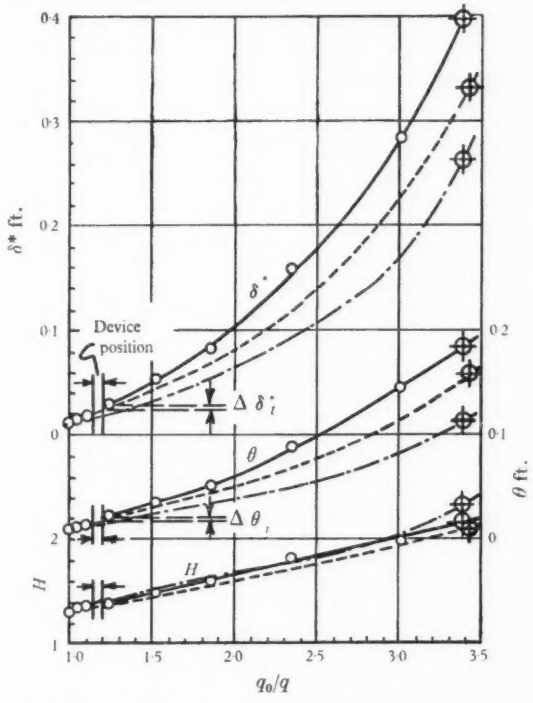

FIGURE 10. Comparison of the effect of forced mixing (conditions as given in table 1) with the effect of pressure distribution alone. δ^*, θ, H are means taken across the span. ⊕, Separation point; ○, simple plow (A-3); - - - -, pressure distribution *C*; —·—, pressure distribution *D*.

It thus became evident that skin friction must still be important and that the end result achieved with a pressure gradient would depend significantly on the shape of the pressure distribution. This raised the very troublesome question about how now to draw a meaningful comparison. It was concluded that a logical scheme would be to compare cases where pressure distributions were similar. Accordingly, distributions *E* and *F* were produced in an attempt to duplicate with a small gradient the nearly linear type of pressure increase existing when forced mixing was applied. Distribution *F* of figure 3 represents the maximum recovery obtainable with a straight-line gradient in the length available, but this was still not sufficient to match the recovery obtained with

device (A-3). Distribution E was planned to match the recovery obtained with the triangular plow (E-2) and the shielded sink (K), making possible the comparisons shown in figure 11. Here again we see no significant differences until the occurrence of the steps $\Delta\delta_t^*$ and $\Delta\theta_t$. Inspection of the θ-curves reveals that the approximate percentage rule has now reappeared. In table 1 $\Delta\theta_t/\theta_t$ for (E-2) is given as 28·9 %; at separation the increase above the dashed curve is 27·2 %. Again in table 1 $\Delta\theta_t/\theta_t$ for (K) is $-17{\cdot}6$ %, while at separation the reduction is $-19{\cdot}4$ %. The rule was previously indicated for δ^* also, but the evidence for it is lacking in figure 11.

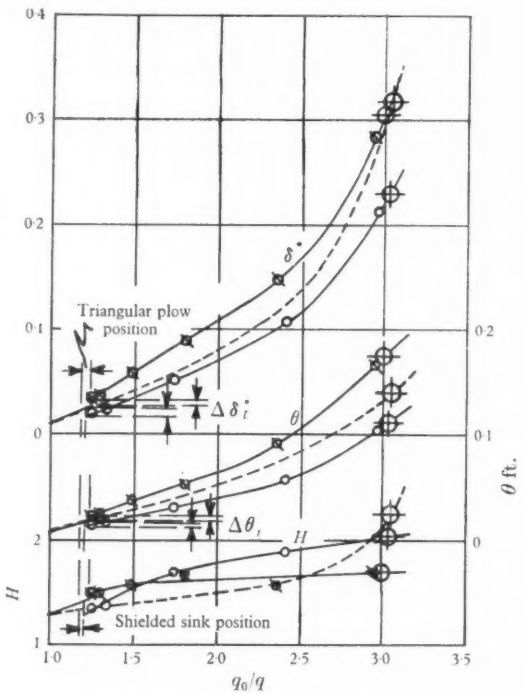

FIGURE 11. Comparison of the effect of forced mixing (conditions as given in table 1) with the effect of reduced pressure gradient. δ^*, θ, H are means taken across the span. ⊕, Separation point; ⊘, triangular plow (E-2); ○, shielded sink (K); – – –, pressure distribution E.

The original purpose of the sink was to provide one case with a negative $\Delta\theta_t$ with which to test the percentage rule. The above numbers indicate close agreement, closer in fact than we would have reason to expect. A firm basis for such a rule exists only when H is always the same function of q_0/q and the skin-friction term in equation (1) is negligible. The approximate conformity to the rule, which has run generally through the cases studied, indicates that the conditions are partially satisfied or that the effect of violations are mitigated by the occurrence of the same deviations in both systems. Evidently the friction avoided by the reduction in wall length with forced mixing is replaced by the greater intensity

of mixing. While skin friction could not be determined from the distorted velocity profiles existing downstream from mixing devices and therefore is not known, we would expect intuitively that it would be increased considerably where high velocities occur near the wall as illustrated in figure 8. Apparently, however, forced mixing does not overemphasize the skin friction on the average, for if it did, the results for the shielded sink with negative $\Delta\theta_t$ would not conform to the rule. The rule can obviously be circumvented by emphasizing the reduction in skin friction in one case and not in another, as, for example, in comparing the performance of the simple plow and pressure distribution D in figure 10.

Mixing devices differ considerably in their effectiveness, as shown by table 1, but they all affect the mechanics of flow to higher pressures in about the same way. Furthermore, on a pressure-recovery basis the increased rate of mixing which they bring about is basically equivalent in its effect to decreased pressure gradient, as anticipated in § 2. Devices differ from one another in the magnitude and sign of $\Delta\delta_t^*$ and $\Delta\theta_t$, and by these quantities they differ in their effect from a decreased pressure gradient. Where the percentage rule can be applied to θ, the difference appears to be solely due to these quantities and presumably would disappear if $\Delta\delta_t^*$ and $\Delta\theta_t$ disappeared. When $\Delta\theta_t$ is positive, a penalty is imposed on forced mixing, not so much because of the force on the devices themselves, but because the resulting percentage momentum loss is magnified by being deposited in a developing boundary layer. When $\Delta\theta_t$ is negative there is a dividend of like kind from the same source. A negative $\Delta\theta_t$ must involve the removal of fluid having a momentum deficiency and involve some additional losses from fluid handling; hence not all of the dividend is clear profit.

The obvious advantage of forced mixing is the saving of wall length made possible by it for a given pressure recovery. For example, with distribution E we require a length of adverse pressure region equal to 16·6 ft. for a pressure-recovery coefficient of 0·67. Using either the triangular plow (E-2) or the shielded sink (K), we obtain the same coefficient in a length of only 6·8 ft.—a saving of 9·8 ft. If we make a similar comparison between distribution C and the simple plow (A-3), where now the pressure-recovery coefficient is 0·71, we find that the length is reduced from 16·1 to 7·3 ft.—a saving of 8·8 ft.

If we now lay aside forced mixing and concentrate on manipulating the pressure distribution into its optimum form (a form approached by distribution D) we may again obtain high pressure recovery in a relatively short distance. Comparing the length for D with that for C, we find a reduction from 16·1 to 9·8 ft.—a saving of 6·3 ft. By making the pressure gradient initially high and then progressively relaxing it just enough to avoid separation we apparently make the useful work load a maximun at all points and in so doing exploit the mixing capabilities of the prevailing turbulence to the fullest. There appears to be little definite information on what this does to the turbulence itself. By observing the action of tufts Stratford (1959) concludes that the level of turbulence increases near the wall for the condition of incipient separation. The measurements of Ruetenik & Corrsin (1955), pertaining to equilibrium flow in a diffuser of 1-degree half angle, show a turbulent kinetic energy 3·1 times that

in a parallel channel. Clauser (1954, 1956), who proposed a concept of equilibrium boundary layers in adverse pressure gradients and made a study of such layers, finds the eddy viscosity, which is effectively a constant for the outer 80–90 % of the layer, to be given by $KU_1\delta^*$, where K is a constant equal to 0·018, independent of pressure gradient and equally applicable to constant pressure flow. This denotes something more than the usual increase of eddy viscosity with thickening of the layer; it denotes an increase caused as well by a change in the form of the profile. There has evidently been an increase in mixing capability brought about by rearrangement of the flow in the y-direction, the 'device' in this case being an adverse pressure gradient applied so as to maintain equilibrium. The only known confirmation of this from turbulence measurements comes from the work of Ruetenik & Corrsin, and this for a condition of small pressure gradient. More turbulence measurements in equilibrium flows would appear to be desirable. We point out in this connexion that flows with zero skin friction represent the high-gradient extreme of an equilibrium flow.

It is not clear how much this depends on an equilibrium condition. Hot-wire data such as those given by Schubauer & Klebanoff (1951), Newman (1951), Sandborn & Slogar (1955), and Robertson & Calehuff (1957), pertaining to non-equilibrium conditions, suggest that there is no marked effect of an adverse pressure gradient on the turbulence, other than to change the distribution across the layer. The principal effect on the mixing is therefore not through a change in rate but through a decrease in the mean velocity, thus increasing the stirring relative to downstream movement. Kline (1958) has observed streaks of backflow even in mild pressure gradients in diffusers, and he infers increasing mixing from this source. However, it is not evident from hot-wire results that there is a significant increase in absolute level of turbulence for the general case of non-equilibrium flow such as that implied for equilibrium flow.

Forced mixing, in the sense of this investigation, obtains rearrangement by involving the third dimension, z, and hence will always increase any pre-existing level of mixing. Thus it would be of considerable interest to apply it under the special conditions just discussed. This would mean, for example, applying forced mixing under conditions such that δ^*, θ, and H could properly be compared with the values in figure 10 for distribution D, or with cases where separation was avoided altogether by a progressive decrease in pressure gradient, allowing a little or a substantial margin as desired. Spatial irregularities which characterize forced mixing may prove to be troublesome in such cases. In application therefore there are certain pitfalls to be recognized. In practice, moreover, it may not be advantageous, and indeed not always possible, to give the pressure curve a special shape for the benefit of the boundary layer.

7. Conclusions

The major conclusions from this investigation are:

1. Forced mixing has basically the same effect on the boundary layer as a general reduction in pressure gradient.

2. Differences in δ^* and θ for forced mixing on the one hand and reduced

pressure gradient on the other arise from increments or decrements in these quantities introduced at the mixing station. These are magnified in the course of development of the layer. In the case of θ, an approximately constant percentage increase or decrease is maintained throughout the subsequent course of the layer. This rule does not apply unless the more gradual pressure rise has essentially the same form as that of the steep rise to which forced mixing was applied.

3. The mechanics of mixing is about the same for all of the devices tried, as well as for those described in the literature, namely, an induction into the boundary layer of currents of higher velocity usually accompanied by streamwise vortices. Devices differ in the manner of accomplishing this and in their effectiveness and drag penalty.

4. Since the mixing potentialities of natural turbulence are best exploited by a pressure distribution with an initially steep and progressively decreasing gradient, it would be of interest to study forced mixing for this condition. Of interest also are those cases where the gradients are regulated to avoid the actual occurrence of separation and yet are kept high enough to reduce skin friction to a negligible magnitude.

The authors wish to acknowledge the assistance of E. Thomas Pierce and William R. Rowland who conducted many of the measurements and contributed generally as members of the research team. This investigation was sponsored by the Office of Naval Research.

REFERENCES

Clauser, Francis H. 1954 Turbulent boundary layers in adverse pressure gradients. *J. Aero. Sci.* **21**, 91–108.

Clauser, Francis H. 1956 The turbulent boundary layer. *Advances in Applied Mechanics*, vol. IV, pp. 1–51. New York: Academic Press Inc.

Coles, Donald 1956 The law of the wake in the turbulent boundary layer. *J. Fluid Mech.* **1**, 191–226.

Grose, R. M. 1954 Theoretical and experimental investigation of various types of vortex generators. *Rep. United Aircraft Corp.* no. R-15362-5.

Kline, Stephen J. 1958 On the nature of stall. *Rep. Mech. Eng. Dep. Stanford University*, no. MD-4.

McCullough, George B., Nitzberg, Gerald E. & Kelly, John A. 1951 Preliminary investigation of the delay of turbulent flow separation by means of wedge-shaped bodies. *NACA Res. Mem.* no. A50 L12.

Newman, B. G. 1951 Some contributions to the study of the turbulent boundary layer near separation. *Rep. Aust. Dep. Supply* no. ACA-53.

Pankhurst, R. C. 1955 Recent British work on methods of boundary-layer control. *Proc. of Symposium on Boundary Layer Effects in Aerodynamics, National Physical Laboratory*, Paper no. 6.

Robertson, J. M. & Calehuff, G. L. 1957 Turbulence in a diffuser boundary layer. *J. of the Hydraul. Div. Amer. Soc. Civil Eng.*, Paper no. 1393.

Ruetenik, J. R. & Corrsin, S. 1955 Equilibrium turbulent flow in a slightly divergent channel. *50 Jahre Grenzschichtforschung* (ed. H. Görtler and W. Tollmien), pp. 446–59. Braunschweig: Freidr. Vieweg und Sohn.

Sandborn, Virgil A. & Slogar, Raymond J. 1955 Study of the momentum distribution of turbulent boundary layers in adverse pressure gradients. *NACA Tech. Note* no. 3264.

SCHUBAUER, G. B. & KLEBANOFF, P. S. 1951 Investigation of separation of the turbulent boundary layer. *Rep. NACA*, no. 1030.

SMITH, A. M. O. & MURPHY, J. S. 1955 A dust method for locating the separation point. *J. Aero. Sci.* **22**, 273.

STEPHENS, A. V. & COLLINS, G. H. 1955 Turbulent boundary layer control by ramps or wedges. *Rep. Aust. Aero. Res. Comm.* no. ACA-55.

STRATFORD, B. S. 1959 An experimental flow with zero skin friction throughout its region of pressure rise. *J. Fluid Mech.* **5**, 17–35.

TAYLOR, H. D. 1948 Design criteria for and application of the vortex generator mixing principle. *Rep. United Aircraft Corp.* no. M-15038-1.

TAYLOR, H. D. 1950 Summary report on vortex generators. *Rep. United Aircraft Corp.* no. R-05280-9.

VON DOENHOFF, ALBERT E. & TETERVIN, NEAL 1943 Determination of general relations for the behavior of turbulent boundary layers. *Rep. NACA* no. 772.

WEIBERG, JAMES A. & MCCULLOUGH, GEORGE B. 1952 Wind-tunnel investigation at low speed of a twisted and cambered wing swept back 63° with vortex generators and fences. *NACA Res. Mem.* no. A 52 A 17.

A note on the velocity profile and longitudinal mixing in a broad open channel

By T. H. ELLISON
Department of the Mechanics of Fluids, University of Manchester

(Received 6 September 1959)

The mean velocity profile near the surface of turbulent flow in a broad open channel is discussed with dimensional arguments, and a new empirical constant m is introduced which is analogous to von Kármán's constant for flow near a rigid boundary. It is shown that, while the velocity profile depends only rather weakly on m, the dependence of the coefficient of apparent longitudinal diffusion is stronger, and measurements of diffusion could, in principle, provide an accurate determination of its value. The new profiles for various values of m are compared with those in current use, and finally the correction for finite Reynolds number is discussed.

1. Introduction

In a recent paper Elder (1959) discussed turbulent mixing in a broad open channel on the basis of Taylor's (1954) theory and calculated a coefficient of apparent longitudinal diffusion in agreement with observation on the assumption of a logarithmic mean velocity profile. This form is not theoretically satisfactory near a free surface, and since the coefficient of apparent longitudinal diffusion depends strongly on the shape of the profile, some further investigation seems desirable.

In this note a more satisfactory form for the profile is sought. It is shown that dimensional reasoning, which in this context is equivalent to mixing-length theory, leads to a new formula containing one unknown constant. This constant plays a role at a free surface analogous to that of von Kármán's constant at a fixed wall, and is named 'the mixing constant at a free surface'. Rather precise measurements of the velocity profile would be needed for a direct determination of the value of the constant, but the more marked dependence of the apparent longitudinal coefficient suggests that it may be found more easily from measurements of diffusion.

There are a large number of complications which may limit the usefulness of the present theory in practical situations. It was first developed some years ago in connexion with the diffusion of salt water in an estuary (Hughes 1958), but it turned out to be irrelevant in that case owing to the large effect of the density difference between the fresh and salt water. In artificial channels the velocity profile is commonly distorted by a secondary flow due to their finite width; and in all cases any relative motion between the water surface and the air

above it may lead to a spurious surface current or even the generation of waves. Nevertheless, it still seems worth while to study the idealized case in which these complications are absent, for until that is understood, there is little hope of deepening our knowledge of real flows no matter how good empirical formulae may be.

2. The velocity profile near a free surface

In a broad open channel containing a steadily flowing fluid of constant density the shear stress varies linearly with height and vanishes at the free surface. So, if z is the height above the bottom, the friction velocity u_* is given by

$$u_*^2 = u_{*0}^2(1-z/h), \tag{1}$$

or

$$u_* = qu_{*0}, \tag{2}$$

where $q = (1-z/h)^{\frac{1}{2}}$. Now if the Froude number $u_{*0}(gh)^{-\frac{1}{2}}$ is so small that the surface remains flat and the Reynolds number $u_{*0}h/\nu$ is so large that molecular viscosity may be neglected, and if it is assumed that the components of the turbulence which contribute to the eddy viscosity near the surface are determined entirely by local quantities without any direct dependence on the total depth of the flow, the usual dimensional arguments assert that the eddy viscosity is given by

$$\begin{aligned} K &= mu_*(h-z) \\ &= mhu_{*0}q^3, \end{aligned} \tag{3}$$

where m is the unknown constant which has already been referred to as 'the mixing constant at a free surface'; the corresponding quantity near a rigid wall is von Kármán's constant k. It follows from (3) that the velocity near the surface must be given by

$$u = u_{\max} - 2m^{-1}u_{*0}(1-z/h)^{\frac{1}{2}}. \tag{4}$$

The logarithmic profile assumed by Elder does not have this form, and seems to lack justification.

There is no difficulty in obtaining a crude estimate of the correction that must be applied to (4) when the Reynolds number is not so large that it can be neglected, and this will be done in §5.

The flow near the free surface differs from that in the constant stress region near the floor in two distinct ways, each of which may cause m to differ from k. First, the stress at the surface is zero so that there is a gradient of turbulent energy and therefore the 'diffusion' and 'pressure flow' terms in the turbulent energy balance may be important. This situation also occurs at a point of separation of a turbulent boundary layer as has been discussed by Stratford† (1959*a*, *b*) who gives a formula equivalent to (3). He has also been able to produce an experimental flow with zero wall stress over a finite distance but which is necessarily complicated by the deceleration produced by a pressure gradient. From his determination of the variation of mixing length *very* near the wall, it would seem

† I am indebted to a referee for calling my attention to this.

that m is greater than k, but it is not possible to obtain accurate numerical values from his paper.†

Secondly, a free surface differs from a rigid wall because tangential movements are not prohibited at the boundary, although it is doubtful whether such movements affect the eddy viscosity appreciably. At first sight it might be thought that all turbulent velocity at the surface was excluded by dimensional reasoning of the same form as that used for the eddy viscosity, but this is not so if the movements extend in scale up to sizes comparable with the depth of the channel, since these scales are not covered by the dimensional argument. The point is quite a subtle one and outside the main theme of this paper; a brief explanation is attempted in the appendix.

3. The velocity profile in an open channel

We know that near the floor of the channel

$$K = ku_{*0}z; \tag{5}$$

so, in order to obtain an approximation to K throughout the depth of the channel, we may conveniently fit a polynomial in q such that (3) is satisfied at the surface and (5) at the floor. Thus

$$\frac{K}{hu_{*0}k} = \frac{m}{k}q^3(1-q^2)\left(1-\frac{m-k}{m}q^2\right)$$

$$= \frac{q^3(1-q^2)(b^2-q^2)}{(b^2-1)}, \tag{6P}$$

where

$$b = \left(\frac{m}{m-k}\right)^{\frac{1}{2}}.$$

This formula may be compared with that resulting from the logarithmic profile

$$\frac{K}{hu_{*0}k} = q^2(1-q^2); \tag{6L}$$

and with that resulting from an application of von Kármán's hypothesis to this flow (see, for example, Hunt 1954):

$$\frac{K}{hu_{*0}k} = 2q^2(1-q). \tag{6K}$$

The velocity profiles corresponding to (6P), (6L) and (6K) may readily be found. They are

$$\frac{k(u-U)}{u_{*0}} = \frac{b^2-1}{b}\ln\frac{b+1}{b-1} - \ln\frac{1+q}{1-q} + b^{-1}\ln\frac{b+q}{b-q}, \tag{7P}$$

$$\frac{k(u-U)}{u_{*0}} = 1+\ln(1-q^2), \tag{7L}$$

$$\frac{k(u-U)}{u_{*0}} = \tfrac{5}{6}+q+\ln(1-q), \tag{7K}$$

† The fact that in contrast to this the quantity β used by Stratford to represent (an average of) m/k in his inner layer is less than unity possibly suggests that in his case the range of validity of (3) is less than his theory implies.

above it may lead to a spurious surface current or even the generation of waves. Nevertheless, it still seems worth while to study the idealized case in which these complications are absent, for until that is understood, there is little hope of deepening our knowledge of real flows no matter how good empirical formulae may be.

2. The velocity profile near a free surface

In a broad open channel containing a steadily flowing fluid of constant density the shear stress varies linearly with height and vanishes at the free surface. So, if z is the height above the bottom, the friction velocity u_* is given by

$$u_*^2 = u_{*0}^2(1-z/h), \tag{1}$$

or

$$u_* = qu_{*0}, \tag{2}$$

where $q = (1-z/h)^{\frac{1}{2}}$. Now if the Froude number $u_{*0}(gh)^{-\frac{1}{2}}$ is so small that the surface remains flat and the Reynolds number $u_{*0}h/\nu$ is so large that molecular viscosity may be neglected, and if it is assumed that the components of the turbulence which contribute to the eddy viscosity near the surface are determined entirely by local quantities without any direct dependence on the total depth of the flow, the usual dimensional arguments assert that the eddy viscosity is given by

$$\begin{aligned} K &= mu_*(h-z) \\ &= mhu_{*0}q^3, \end{aligned} \tag{3}$$

where m is the unknown constant which has already been referred to as 'the mixing constant at a free surface'; the corresponding quantity near a rigid wall is von Kármán's constant k. It follows from (3) that the velocity near the surface must be given by

$$u = u_{\max} - 2m^{-1}u_{*0}(1-z/h)^{\frac{1}{2}}. \tag{4}$$

The logarithmic profile assumed by Elder does not have this form, and seems to lack justification.

There is no difficulty in obtaining a crude estimate of the correction that must be applied to (4) when the Reynolds number is not so large that it can be neglected, and this will be done in § 5.

The flow near the free surface differs from that in the constant stress region near the floor in two distinct ways, each of which may cause m to differ from k. First, the stress at the surface is zero so that there is a gradient of turbulent energy and therefore the 'diffusion' and 'pressure flow' terms in the turbulent energy balance may be important. This situation also occurs at a point of separation of a turbulent boundary layer as has been discussed by Stratford† (1959*a*, *b*) who gives a formula equivalent to (3). He has also been able to produce an experimental flow with zero wall stress over a finite distance but which is necessarily complicated by the deceleration produced by a pressure gradient. From his determination of the variation of mixing length *very* near the wall, it would seem

† I am indebted to a referee for calling my attention to this.

that m is greater than k, but it is not possible to obtain accurate numerical values from his paper.†

Secondly, a free surface differs from a rigid wall because tangential movements are not prohibited at the boundary, although it is doubtful whether such movements affect the eddy viscosity appreciably. At first sight it might be thought that all turbulent velocity at the surface was excluded by dimensional reasoning of the same form as that used for the eddy viscosity, but this is not so if the movements extend in scale up to sizes comparable with the depth of the channel, since these scales are not covered by the dimensional argument. The point is quite a subtle one and outside the main theme of this paper; a brief explanation is attempted in the appendix.

3. The velocity profile in an open channel

We know that near the floor of the channel

$$K = ku_{*0}z; \tag{5}$$

so, in order to obtain an approximation to K throughout the depth of the channel, we may conveniently fit a polynomial in q such that (3) is satisfied at the surface and (5) at the floor. Thus

$$\begin{aligned}\frac{K}{hu_{*0}k} &= \frac{m}{k}q^3(1-q^2)\left(1-\frac{m-k}{m}q^2\right)\\ &= \frac{q^3(1-q^2)(b^2-q^2)}{(b^2-1)},\end{aligned} \tag{6P}$$

where

$$b = \left(\frac{m}{m-k}\right)^{\frac{1}{2}}.$$

This formula may be compared with that resulting from the logarithmic profile

$$\frac{K}{hu_{*0}k} = q^2(1-q^2); \tag{6L}$$

and with that resulting from an application of von Kármán's hypothesis to this flow (see, for example, Hunt 1954):

$$\frac{K}{hu_{*0}k} = 2q^2(1-q). \tag{6K}$$

The velocity profiles corresponding to (6P), (6L) and (6K) may readily be found. They are

$$\frac{k(u-U)}{u_{*0}} = \frac{b^2-1}{b}\ln\frac{b+1}{b-1} - \ln\frac{1+q}{1-q} + b^{-1}\ln\frac{b+q}{b-q}, \tag{7P}$$

$$\frac{k(u-U)}{u_{*0}} = 1+\ln(1-q^2), \tag{7L}$$

$$\frac{k(u-U)}{u_{*0}} = \tfrac{5}{6}+q+\ln(1-q), \tag{7K}$$

† The fact that in contrast to this the quantity β used by Stratford to represent (an average of) m/k in his inner layer is less than unity possibly suggests that in his case the range of validity of (3) is less than his theory implies.

where U is the mean (discharge) velocity. U itself is to be found from the condition that $u = 0$ when $z = z_0$; so, since z_0 is very much smaller than h,

$$\frac{kU}{u_{*0}} = \ln\frac{h}{z_0} + \ln 4 - b\ln\frac{b+1}{b-1}, \tag{8P}$$

$$\frac{kU}{u_{*0}} = \ln\frac{h}{z_0} - 1, \tag{8L}$$

$$\frac{kU}{u_{*0}} = \ln\frac{h}{z_0} - \tfrac{11}{6} + \ln 2$$

$$= \ln\frac{h}{z_0} - 1{\cdot}140. \tag{8K}$$

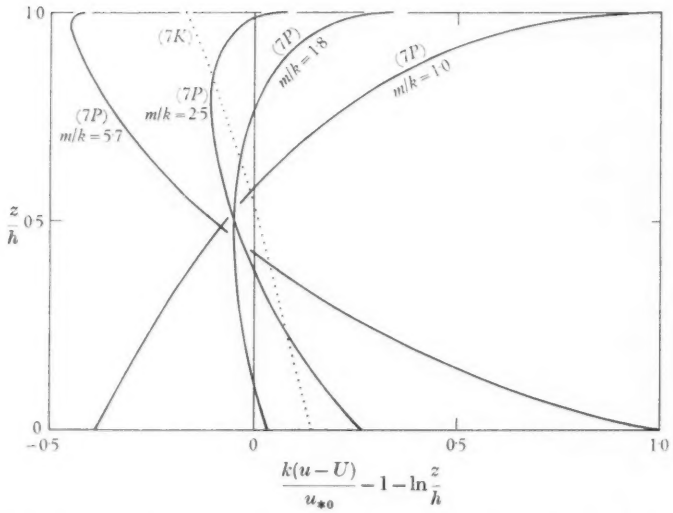

FIGURE 1. Difference between velocity profiles for various values of the mixing constant at the free surface and the logarithmic form. The dotted curve represents the von Kármán profile in the same way.

The fact that $(8L)$ and $(8K)$ are commonly found satisfactory for engineering purposes yields a very crude method of estimating b. If we set

$$\ln 4 - b\ln\frac{b+1}{b-1}$$

equal to $-1{\cdot}07$, so that $(8P)$ coincides with the mean of $(8L)$ and $(8K)$, we find $b = 1{\cdot}45$ and so $m/k = 1{\cdot}91$.

The velocity profiles $(7P)$, $(7L)$ and $(7K)$ are so alike that there is little prospect of deciding between them on the basis of direct measurements of velocity. In order to bring out the small differences most clearly, the difference between $(7L)$ and $(7K)$ and that between $(7L)$ and $(7P)$ for various values of m/k are plotted in figure 1.

4. The apparent longitudinal diffusion coefficient

For a two-dimensional flow it can easily be shown (for example, by integrating equation (9) of Elder's paper by parts) that the coefficient of apparent longitudinal diffusion is given by

$$D = \int_0^1 K^{-1}\left[\int_z^1 (u-U)\,dz\right]^2 dz. \tag{9}$$

From (7*P*), (7*L*) and (7*K*) one finds respectively

$$\int_z^1 (u-U)\,dz = q^2\frac{b^2-1}{b}\ln\frac{b+1}{b-1}+(1-q^2)\ln\frac{1+q}{1-q}-\frac{b^2-q^2}{b}\ln\frac{b+q}{b-q}, \tag{10P}$$

$$\int_z^1 (u-U)\,dz = -(1-q^2)\ln(1-q^2), \tag{10L}$$

$$\int_z^1 (u-U)\,dz = \tfrac{2}{3}q^3+\tfrac{1}{3}q^2-q-(1-q^2)\ln(1-q). \tag{10K}$$

So (9) can readily be calculated numerically in each case. The results are shown in figure 2. Elder's measurements gave a value of $6{\cdot}06u_{*0}h$ for D, which with $k = 0{\cdot}40$ would correspond to $m = 0{\cdot}80$. However, in the present writer's opinion it is unlikely that sufficiently accurate measurements could be taken with the apparatus at Elder's disposal and the resulting value of m should be viewed with caution. It does, nevertheless, confirm the expectation that m is greater than k.

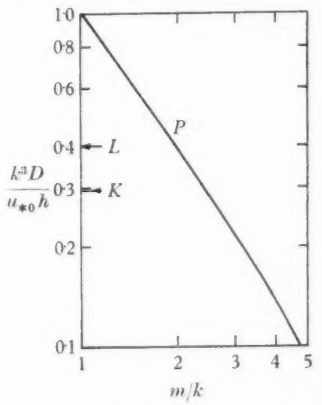

FIGURE 2. The apparent longitudinal diffusion coefficient as a function of the mixing constant at the free surface.

5. The correction for finite Reynolds number

The peaks on the velocity profile at the surface in figure 1 are due to the way in which K falls to zero; and it is important to inquire how they are modified by molecular viscosity, since in reality it is not possible for K to fall below ν. Fortunately the correction which has to be applied is small in most practical cases and can be estimated. The following conventional analysis is certainly not exactly correct but should be adequate for most cases.

Let us write the total effective viscosity K as the sum of a turbulent part K_T and a molecular part ν; and also express the shear stress u_*^2 as the sum of a turbulent part u_{*T}^2 and a molecular part u_{*m}^2. Thus

$$u_*^2 = u_{*T}^2 + u_{*m}^2 = K_T \frac{du}{dz} + \nu \frac{du}{dz} = q^2 u_{*0}^2. \tag{11}$$

If we still use (3) for the turbulent part,

$$K_T' = mhq^2 u_{*T}; \tag{12}$$

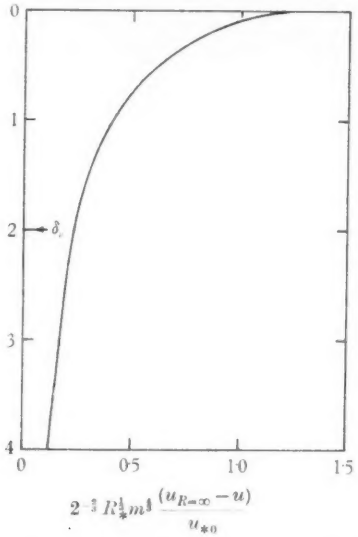

FIGURE 3. Correction to be applied to velocity profiles near the surface to allow for molecular viscosity.

so a little algebra yields

$$\begin{aligned} 2(K_T + \nu) &= \nu + (\nu^2 + 4m^2h^2q^6u_{*0}^2)^{\frac{1}{2}} \\ &= hu_{*0}R_*^{-1}\{1 + (1 + 4m^2R_*^2q^6)^{\frac{1}{2}}\}, \end{aligned} \tag{13}$$

where $R_* = hu_{*0}/\nu$. Hence

$$\begin{aligned} \frac{u_{\max} - u}{u_{*0}} &= \int_0^q \frac{4R_*q'^3\,dq'}{1 + (1 + 4m^2R_*^2q'^6)^{\frac{1}{2}}} \\ &= 2^{\frac{2}{3}}R_*^{-\frac{1}{3}}m^{-\frac{1}{3}} \int_0^x \frac{x'^3\,dx'}{1 + (1 + x'^6)^{\frac{1}{2}}}, \end{aligned} \tag{14}$$

where $x = (2mR_*)^{\frac{1}{4}}q$.

Since (14) must coincide with the high Reynolds number solution (4) at large values of x, the change induced by molecular viscosity can readily be computed. This is shown in figure 3.

Values of R_* encountered in practice may range from very low values in the laboratory to 10^6 or more in geophysical situations. To take two examples, a channel 10 cm deep with $U = 10\,\text{cm sec}^{-1}$ and a drag coefficient of 0·01 gives $R_* = 10^3$, and an estuary 10 m deep with $U = 200\,\text{cm sec}^{-1}$ and a drag coefficient

of 0·0025 gives $R_* = 10^6$. In both these cases it happens (by a coincidence) that with $m = 0{\cdot}8$ the correction to the surface velocity is 0·28 cm sec^{-1} and the depth of the viscous sublayer δ_ν (which may be conveniently defined as the depth where molecular and eddy viscosity are equal) is 0·15 cm. The sublayer is thus of slight significance in the channel, and completely negligible in the estuary.

There would be no difficulty in calculating the correction to the apparent longitudinal diffusion coefficient if one were to assume that in the viscous sublayer the transport of pollutant was by molecular diffusion. However, it is known that the viscous but not laminar motions induced by the turbulence outside are important and these complicate the situation. There is also a further practical reason for not computing these corrections; for them to be valid, experiments would have to be conducted over times long compared with that required for a typical fluid particle to enter or leave the sublayer and that would require channels of immense length.

REFERENCES

Elder, J. 1959 *J. Fluid Mech.* **5**, 544–60.

Hughes, P. 1958 *Geophys. J. Roy. Astr. Soc.* **1**, 271–83.

Hunt, J. N. 1954 *Proc. Roy. Soc.* A, **224**, 322–35.

Stratford, B. S. 1959*a* *J. Fluid Mech.* **5**, 1–16.

Stratford, B. S. 1959*b* *J. Fluid Mech.* **5**, 17–35.

Taylor, G. I. 1954 *Proc. Roy. Soc.* A, **223**, 446–68.

Appendix

The similarity state at the surface

The theoretical idea behind the dimensional argument used in §2 is that there is a region near the surface in which the motion is in a state of dynamical similarity with its length scale proportional to $(h-z)$ and its velocity scale proportional to $u_{*0}(1-z/h)^{\frac{1}{2}}$. If this similarity state applies to the whole of the turbulence, it is clear that the fluctuation in horizontal velocity must be proportional to the velocity scale and so fall to zero at the surface, which should therefore move as a rigid sheet. Such strictly laminar motion of the surface does not accord with observation (though this is confined to channels of finite width) nor physical intuition; it thus seems desirable to modify the theory in such a way that the similarity state applies only to certain aspects of the turbulence, which include the eddy viscosity and the shear stress, but exclude the horizontal velocity.

This modification can readily be made if we suppose that the motion is resolved into elements of different sizes (for example, by Fourier analysis) and admit the possibility that even near the surface there may be components in the horizontal motion with a scale comparable with the depth of the channel; since these extend beyond the region of similarity, it is not reasonable to expect the similarity state to include them and its application may be restricted to smaller eddies. The point may become clearer if we consider specifically the one-dimensional spectrum tensor $\Phi_{ij}(\kappa)$ of the turbulent stress tensor $\overline{u_i u_j}$. The similarity law for small eddies near the surface then asserts that

$$\kappa\Phi_{ij} = (1-z/h)\,u_{*0}^2 F_{ij}(\kappa[h-z]), \quad \text{for} \quad \kappa h \gg 1,$$

where F_{ij} is some unknown function of the dimensionless variable $\kappa(h-z)$. Now, if the shear stress $\overline{u_1 u_3}$ depends only on local quantities, there must be at most a negligible contribution to $\int_0^\infty \Phi_{13} d\kappa$ from values of κ outside the similarity range and $\int_0^\infty \kappa^{-1} F_{13} d\kappa$ must certainly be finite. On the other hand, if there is to be horizontal motion in the surface with a finite amount of energy contained in each part of the spectrum, it is merely necessary that F_{11} should vary as $\kappa^{-1}(h-z)^{-1}$ for small values of $\kappa(h-z)$, since then at $z = h$

$$\kappa\Phi_{11} \propto u_{*0}^2 \kappa^{-1} h^{-1} \quad \text{for} \quad \kappa h \gg 1.$$

Clearly this form for the spectrum does not become small as κ decreases, and indeed would lead to an infinite energy were it not for the cut-off when κ is comparable with h^{-1}. Hence if there are any motions in the surface, they must include some whose scale is comparable with the depth of the channel. Casual observation of natural streams suggests that this is what happens in practice.

The restriction of the similarity state to a limited range of scales is not in any way unusual; a closely analogous situation arises in connexion with the pressure spectrum $\Pi(\kappa)$ at a rigid wall. Close to the wall the stress may be assumed to be approximately constant over a depth δ, and in that case dimensional arguments suggest $\kappa\Pi \propto u_{*0}^4$ and the amplitude of the pressure fluctuations would be infinite if the range of application of the similarity law were not restricted to $z_0^{-1} \gg \kappa \gg \delta^{-1}$.

A line source on an interface between two media

By V. M. PAPADOPOULOS
Division of Engineering, Brown University

(Received 20 August 1959)

The assumption of dynamic similarity is used to determine the velocity potential of an unsteady line source which lies on a plane separating two media of different density and sound velocity. The solution first derived is for a source whose strength varies with time as a step function; the pressure in this case may be identified with Hadamard's elementary solution which in a homogeneous fluid is $(c/2\pi)(c^2t^2-r^2)^{-\frac{1}{2}}$ if $r < ct$, and 0 if $r > ct$. We next derive the solution for a source whose strength has a delta-function time dependence; we then describe the results for a supersonic point source moving on the interface, and finally we transfer the results to solve the corresponding electromagnetic problem.

1. Introduction

In some recent work Craggs (1956, 1957) and Papadopoulos (1959*a*, 1959*b*) have shown the value of the assumption of dynamic similarity in the solution of a number of unsteady two-dimensional problems in various physical situations. In each case the unknown quantity satisfies the wave equation.

In this paper we shall determine the nature of the field of a uniform line source which is suddenly set up at some definite moment on the plane interface between two different homogeneous fluids. We assume a linearized equation of state, and that the source is weak enough for the acoustic approximation to be valid. We take the source to be at the origin $r = 0$, and we take the time $t = 0$ to be the moment at which the source is made active. Under the assumption that the subsequent unsteady motion is irrotational, it is well known (e.g. see Friedlander 1958) that the velocity potential satisfies the wave equation

$$\nabla^2\phi(r,\theta,t) = c^{-2}(\partial^2\phi/\partial t^2),$$

where c is the velocity of sound in the medium at rest, while the pressure change p and the particle velocity $\mathbf{q}$ satisfy the equations

$$p = \partial\phi/\partial t, \quad \rho\mathbf{q} = -\nabla\phi. \tag{1}$$

Here ρ refers to the constant density in an undisturbed medium.

Within a single uniform medium, it is known (e.g. see Lamb 1932) that the potential of a line source of uniform density $U(t)$ ($U(t) = 0$ if $t < 0$, $U(t) = 1$ if $t > 0$) is $(1/2\pi)\ \mathrm{sech}^{-1}(r/ct)$; it is clear from this result that it is reasonable to assume in the present problem that the velocity potential depends only on two variables $s\ (= r/t)$ and θ. This is the assumption of dynamic similarity. It may be added that the pressure corresponding to the above potential is identical with Hadamard's elementary solution (1923) of the wave equation in two dimensions.

Suppose now that some quantity $S(s,\theta)$ satisfies the wave equation in the variables (r,θ,t). Then since $s = r/t$ it follows that S must satisfy the equation

$$s^2\left(1-\frac{s^2}{c^2}\right)\frac{\partial^2 S}{\partial s^2}+s\left(1-\frac{2s^2}{c^2}\right)\frac{\partial S}{\partial s}+\frac{\partial^2 S}{\partial\theta^2}=0. \tag{2}$$

If $s > c$, the equation is hyperbolic. Put $s = c\sec u$, so that

$$\frac{\partial^2 S}{\partial\theta^2}-\frac{\partial^2 S}{\partial u^2}=0, \tag{3}$$

and

$$s = f(u-\theta)+g(u+\theta), \tag{4}$$

where f and g are arbitrary functions, and the lines on which $u+\theta$ and $u-\theta$ are constant are characteristic lines tangent to the circle $s = c$. If $s < c$, equation (2) is elliptic. Put $s = c\,\mathrm{sech}\,(-v)$, so that

$$\frac{\partial^2 S}{\partial\theta^2}+\frac{\partial^2 S}{\partial v^2}=0. \tag{5}$$

It follows from equation (5) that with the harmonic function S in the elliptic region we may introduce a conjugate $T(v,\theta)$, so that $W = S+iT$ is an analytic function, and such that

$$\frac{\partial S}{\partial v}=\frac{\partial T}{\partial\theta},\quad \frac{\partial S}{\partial\theta}=-\frac{\partial T}{\partial v}. \tag{6}$$

In §2 the detailed solution of the acoustic problem is given. In §5 we describe the change to be made to give the results relevant in the setting up of a charged line or of a line current.

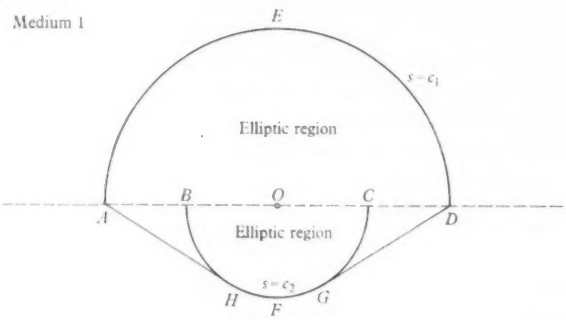

Figure 1. The elliptic regions in the (s,θ)-plane.

2. A line source of step function time dependence

In figure 1 we depict the physical situation in the (s,θ)-plane. The upper half of this plane, $0 < \theta < \pi$, represents the region occupied by a medium 1, and the lower half, $0 > \theta > -\pi$, that occupied by a medium 2. The respective density ρ and sound velocity c are distinguished by the suffix 1 or 2 where appropriate. We assume that $c_1 > c_2$. The semicircles $s = c_1$, $s = c_2$ separate the elliptic and the hyperbolic regions in each medium.

There are two requirements on the solution of our problem. The first is that the solution of the steady problem shall be approached in the limit as $s \to 0$ (i.e. as $t \to \infty$). The second is that at the interface both the pressure and the normal component of velocity shall be continuous.

Suppose that the quantity S and the velocity potential are related by the equation $\rho c^2 S = \phi$. From equations (1) it follows that the radial and transverse components (q_r, q_θ) of the velocity, and the pressure change p, satisfy the equations

$$\left.\begin{aligned} \frac{\partial S}{\partial s} &= -\frac{tq_r}{c^2} = -\frac{pt}{\rho c^2 s}, \\ \frac{\partial S}{\partial \theta} &= -\frac{rq_\theta}{c^2}. \end{aligned}\right\} \tag{7}$$

Putting $m = c_2/c_1$, $k = \rho_2/\rho_1$, then we may write the continuity conditions in the form

$$m^2 k \frac{\partial S_2}{\partial s} = \frac{\partial S_1}{\partial s}, \tag{8}$$

and

$$m^2 \frac{\partial S_2}{\partial \theta} = \frac{\partial^2 S_1}{\partial \theta}. \tag{9}$$

We may refer again to figure 1 to discuss some of the properties of the solution. In the hyperbolic region, it is clear that the value of S as $s \to \infty$ corresponds to the initial value of S. Hence S is uniformly zero at infinity for all values of θ, and from the nature of the solution (4) it follows that the value of S is everywhere zero outside the region $AFDE$. Within the triangle CDG the solution is necessarily of the form $S_2 = f(u-\theta)$, and in the triangle ABH the solution must be of the form $S_2 = g(u+\theta)$, where f and g are functions to be determined. The solution must be symmetric about the vertical axis in figure 1; hence we need only examine the field in the right-hand half of the (s, θ)-plane.

Consider the region $s \leqslant c_1$, $0 \leqslant \theta \leqslant \frac{1}{2}\pi$. In this region we have that (i) the line OE is a line of symmetry on which $\partial S_1/\partial \theta = 0$. The arc ED, which is the envelope of the characteristics in the hyperbolic region, is itself a characteristic. Across this arc the pressure and the radial velocity will be discontinuous. The tangential velocity component must be continuous, however, so that (ii) $\partial S_1/\partial \theta = 0$ on ED.

The continuity of pressure and of normal velocity across the interface CD implies that on CD

$$\frac{\partial S_1}{\partial s} = m^2 k \frac{\partial S_2}{\partial s} = m^2 k \frac{\partial S_2}{\partial u_2}\frac{\partial u_2}{\partial s} = -m^2 k \frac{\partial u_2}{\partial s}\frac{\partial S_2}{\partial \theta} = -k\frac{\partial u_2}{\partial s}\frac{\partial S_1}{\partial \theta} = k\frac{\partial u_2}{\partial s}\frac{\partial s}{\partial v_1}\frac{\partial T_1}{\partial s}.$$

Thus

$$\frac{\partial}{\partial s}\left(S_1 - kT_1\frac{\partial u_2}{\partial v_1}\right) = 0.$$

so that

$$\mathscr{R}\left(\frac{\partial W_1}{\partial s}\left(1 + ik\frac{\partial u_2}{\partial v_1}\right)\right) = 0. \tag{10}$$

On physical grounds we may expect singularities in W_1 only at the points O, C, D, E. The first quadrant in the circle in the (s, θ)-plane corresponds to a semi-infinite strip in the complex (v_1, θ)-plane and under the transformation

$$\zeta_1 = \xi_1 + i\eta_1 = \operatorname{sech}(v_1 + i\theta)$$

we may map this strip conformally into the upper half of the complex ζ_1-plane. The conditions just enumerated are that

(i) singularities are to be expected only at the points $\zeta_1 = 0$ m, 1 and ∞;

(ii) $\partial W_1/\partial\zeta_1$ is imaginary, for $\xi_1 = 0$ $\eta_1 > 0$;

(iii) $\partial W_1/\partial\zeta_1$ is imaginary, for $\eta_1 = 0$ $|\xi_1| > 1$; and

(iv) for $\eta_1 = 0$, $m < \xi_1 < 1$,

$$\frac{\partial W_1}{\partial \zeta_1} = R(\zeta_1)\left\{1 - \frac{i}{mk}\left(\frac{\zeta_1^2 - m^2}{1-\zeta_1^2}\right)^{\frac{1}{2}}\right\}^{-1},$$

where $R(\zeta_1)$ is a function which must take real values on this segment of the real axis. Since $s = c_1$, $\theta = \frac{1}{2}\pi$ is an ordinary point both for S and for $\partial S/\partial\theta$, it follows that as $|\zeta_1| \to \infty$,

(v) $\partial W_1/\partial\zeta_1 = O(\zeta_1^{-2-\delta})$ with $\delta > 0$. As $\zeta_1 \to 0$, the field must approach the steady state value, and therefore

(vi) $\partial W_1/\partial\zeta_1 = O(\zeta_1^{-1})$ for $\zeta_1 \to 0$.

Thus, after applying these conditions, we may write

$$\frac{\partial W_1}{\partial \zeta_1} = \frac{F(\zeta_1)}{\zeta_1[(1-\zeta_1^2)^{\frac{1}{2}} - (i/mk)(\zeta_1^2 - m^2)^{\frac{1}{2}}]}, \tag{11}$$

it being implied that $F(\zeta_1)$ is bounded as $|\zeta_1| \to \infty$, is real on the positive real axis for $\xi_1 > m$, and is real on the imaginary axis. This final condition implies that F must be an even function of ζ_1.

Whatever may be the formula for $F(\zeta_1)$ which we shall determine, we must, in setting up the solution for medium 2, satisfy the continuity conditions across OC. If in this elliptic region we use the conformal mapping $\zeta_2 = \xi_2 + i\eta_2 = \operatorname{sech}(v_2 + i\theta)$ to bring the region of interest, $s < c_2$, $0 > \theta > -\frac{1}{2}\pi$, into the fourth quadrant of the ζ_2-plane, then across OC, $\zeta_1 = m\zeta_2$, and the continuity conditions are

$$\left.\begin{aligned} m^2 k \frac{\partial S_2}{\partial \zeta_2} &= \frac{\partial S_1}{\partial \zeta_2}, \\ \text{and} \qquad m^2 k \frac{\partial T_2}{\partial \zeta_2} &= k\left(\frac{1-m^2\zeta_2^2}{1-\zeta_2^2}\right)^{\frac{1}{2}} \frac{\partial T_1}{\partial \zeta_2}. \end{aligned}\right\} \tag{12}$$

It is clear under the conditions imposed that $F(\zeta_1)$ must be real on the whole of the real axis. If $F(\zeta_1)$ is complex on the real axis for $0 < \xi_1 < m$, there must be branch points of F at the points $\xi_1 = 0$ and $\xi_1 = m$. Hence for this region we may write

$$F(\zeta_1) = A(\zeta_1) + iB(\zeta_1)\left(\frac{\zeta^2}{m^2 - \zeta^2}\right)^{\frac{1}{2}}, \tag{13}$$

where $A(\zeta_1)$ and $B(\zeta_1)$ are even functions of ζ_1 which are real on the whole of the real axis and which are bounded as $|\zeta_1| \to \infty$. The continuity conditions (12) lead to the equation

$$m^2 k \frac{\partial W_2}{\partial \zeta_2} = \frac{A(m\zeta_2) + ikB(m\zeta_2)\,[(1-m^2\zeta_2^2)\,\zeta_2^2/(1-\zeta_2^2)]^{\frac{1}{2}}}{\zeta_2\{(1-m^2\zeta_2^2)^{\frac{1}{2}} + k^{-1}(1-\zeta_2^2)^{\frac{1}{2}}\}}. \tag{14}$$

This result, derived for real values of ζ_2 with $0 < \zeta_2 < 1$, may be continued analytically into the whole of the fourth quadrant of the ζ_2-plane. If the function B exists, expression (14) has a simple pole at $\zeta_2 = 1$, so that W_2 has a discontinuity

at this point. At the corresponding point $\zeta_1 = m$, W_1 has no discontinuity (from equations (11) and (13)); the only way to avoid this inconsistency is to set $B \equiv 0$. It follows that $F(\zeta_1)$ is a regular function bounded at infinity and real on the real axis, so that it can only be a real constant A. The vanishing of B means that there is no normal velocity between the two subsonic regions. This section OC of the interface is a vortex sheet which is steadily lengthening.

We may now write the explicit results

$$\left.\begin{aligned} \frac{\partial W_1}{\partial \zeta_1} &= \frac{A}{\zeta_1\left\{(1-\zeta_1^2)^{\frac{1}{2}} - \dfrac{i}{mk}(\zeta_1^2-m^2)^{\frac{1}{2}}\right\}}, \\ \text{and} \qquad m^2k\frac{\partial W_2}{\partial \zeta_2} &= \frac{A}{\zeta_2\{(1-m^2\zeta_2^2)^{\frac{1}{2}} + k^{-1}(1-\zeta_2^2)^{\frac{1}{2}}}. \end{aligned}\right\} \tag{15}$$

The velocity components and the pressure, which are related to the derivatives of S as in equations (7), may now be found. Thus, for $s < c_1$ in medium 1, when $\zeta_1 = \operatorname{sech}(v_1 + i\theta)$ and $s = c_1 \operatorname{sech}(-v_1)$,

$$\left.\begin{aligned} \frac{\partial S_1}{\partial s} &= -\frac{A}{s\left(1-\dfrac{s^2}{c_1^2}\right)^{\frac{1}{2}}}\mathscr{R}\left\{\frac{1}{1-\dfrac{i}{mk}\left(\dfrac{\zeta_1^2-m^2}{1-\zeta_1^2}\right)^{\frac{1}{2}}}\right\}, \\ \frac{\partial S_1}{\partial \theta} &= A\mathscr{I}\left\{\frac{1}{1-\dfrac{i}{mk}\left(\dfrac{\zeta_1^2-m^2}{1-\zeta_1^2}\right)^{\frac{1}{2}}}\right\}, \end{aligned}\right\} \tag{16}$$

and for $s < c_2$ in medium 2, when $\zeta_2 = \operatorname{sech}(v_2 + i\theta)$ and $s = c_2 \operatorname{sech}(-v_2)$

$$\left.\begin{aligned} m^2k\frac{\partial S_2}{\partial s} &= -\frac{A}{s\left(1-\dfrac{s^2}{c_2^2}\right)^{\frac{1}{2}}}\mathscr{R}\left\{\frac{1}{\dfrac{1}{k}+\left(\dfrac{1-m^2\zeta_2^2}{1-\zeta_2^2}\right)^{\frac{1}{2}}}\right\}, \\ m^2k\frac{\partial S_2}{\partial \theta} &= A\mathscr{I}\left\{\frac{1}{\dfrac{1}{k}+\left(\dfrac{1-m^2\zeta_2^2}{1-\zeta_2^2}\right)^{\frac{1}{2}}}\right\}. \end{aligned}\right\} \tag{17}$$

The constant A is a measure of the volume of fluid produced by the line source; by considering the steady state in the limit $s \to 0$ or $\zeta \to 0$, we find that the volume created in each medium is $\pi k A c_1^2/(1+k)$ in medium 1 and $\pi A c_1^2/(1+k)$ in medium 2. Thus the strength, for $t > 0$, of the source is Ac_1^2; the fluid then produced is apportioned between the two media in the inverse ratio of the densities, so that the mass of fluid produced is the same in each medium.

To determine the velocity components and the pressure in the hyperbolic region CDG, we use the explicit results derived from equation (16) and (17) for points on the boundary CD, and we use the characteristic form of the solution in CDG to find the complete result. Thus in CDG $S_2 = f(u-\theta)$ where $s/c_2 = \sec u$; it follows that $\partial S_2/\partial\theta = -f'(u-\theta)$. For $c_2 < s < c_1$,

$$\begin{aligned} f'(u) = -\frac{1}{m^2}\left(\frac{\partial S_1}{\partial \theta}\right)_{\theta=0} &= -\frac{A}{m^3k}\left(\frac{s^2-c_2^2}{c_1^2-s^2}\right)^{\frac{1}{2}} \Bigg/ \left\{1+\frac{1}{m^2k^2}\left(\frac{s^2-c_2^2}{c_1^2-s^2}\right)^{\frac{1}{2}}\right\} \\ &= H(s), \text{ say.} \end{aligned} \tag{18}$$

It follows that in CDG,

$$\left.\begin{aligned} &\partial S_2/\partial\theta = -H(s^*), \\ \text{where}\quad &s^*/c_2 = \sec(u-\theta) = s/c_2\cos\theta + \sin\theta(s^2-c_2^2)^{\frac{1}{2}}. \end{aligned}\right\} \tag{19}$$

Similarly the derivative $\partial S_2/\partial s$ is given by the equation

$$\frac{\partial S_2}{\partial s} = \frac{H(s^*)}{s[(s^2/c_2^2)-1]^{\frac{1}{2}}}. \tag{20}$$

3. A line source with delta-function strength

As far as fluid motion is concerned the analysis of §2 is merely an exercise in setting up a quantity which has the property of dynamic similarity in a region with the properties given. By assuming uniform densities for two media, we are of course neglecting gravity, but it is not clear whether we can neglect the effect at the interface. Under the usual first-order approximations, given a small displacement $y = \eta$ in the position of the surface, the conditions of continuity of pressure and of normal velocity take the form

$$\rho_1\frac{\partial\phi_1}{\partial t} - \rho_2\frac{\partial\phi_2}{\partial t} = g(\rho_1-\rho_2)\,\eta + \ldots,$$

$$\frac{1}{\rho_1}\frac{\partial\phi_1}{\partial y} - \frac{1}{\rho_2}\frac{\partial\phi_2}{\partial y} = \frac{\partial\eta}{\partial t},$$

where y is the axis normal to the interface.

Although from these equations alone we may find only what sort of surface waves may exist on the interface by prescribing a form for the displacement, we shall eliminate the dispersive effects due to gravity by insisting that η be a function continuous in x and t, small in comparison with the quantities

$$[p_0+p_1]\,[g(\rho_1-\rho_2)]^{-1} \quad \text{and} \quad [p_0+p_2]\,[g(\rho_1-\rho_2)]^{-1},$$

where p_0 is the steady pressure at the interface. Then $\partial\eta/\partial t$ is also small. The assumption of an acoustic line source of infinitesimal amplitude and step function time-dependence in §2 in no way violates this assertion.

With these remarks in mind we can now state that the results for an (acoustic) source of delta-function time-dependence on the interface are obtained from the formulae in §2 simply by differentiating with respect to time throughout. Thus the known results for $\partial\phi/\partial t$ in §2 represent the values of the velocity potential in the impulse problem. These values are

$$\phi_1 = \frac{A\rho_1 c_1^2}{[t^2-(r^2/c_1^2)]^{\frac{1}{2}}}\,\mathscr{R}\left[1-\frac{i}{mk}\left(\frac{\zeta_1^2-m^2}{1-\zeta_1^2}\right)^{\frac{1}{2}}\right]^{-1} \quad \text{for} \quad r < c_1 t,$$

where
$$\zeta_1 = \frac{r}{c_1 t\cos\theta - i\sin\theta(c_1^2t^2-r^2)^{\frac{1}{2}}},$$

and
$$\phi_2 = \frac{A\rho_1 c_1^2}{[t^2-(r^2/c_2^2)]^{\frac{1}{2}}}\,\mathscr{R}\left[\frac{1}{k}+\left(\frac{1-m^2\zeta_2^2}{1-\zeta_2^2}\right)^{\frac{1}{2}}\right]^{-1}, \quad \text{for} \quad r < c_2 t,$$

where
$$\zeta_2 = \frac{r}{c_2 t\cos\theta - i\sin\theta(c_2^2t^2-r^2)^{\frac{1}{2}}}.$$

Also
$$\phi_2 = \frac{A\rho_1 c_1^2}{[(r^2/c^2)-t^2]^{\frac{1}{2}}}\left[\frac{1}{m}\left|\frac{c_0^2-c_2^2}{c_1^2-c_0^2}\right|^{\frac{1}{2}}\Big/\left\{1+\frac{1}{m^2k^2}\left(\frac{c_0^2-c_2^2}{c_1^2-c_0^2}\right)\right\}\right],$$

where
$$c_0 = \frac{rc_2}{c_2 t\cos\theta + \sin\theta(r^2-c_2^2t^2)^{\frac{1}{2}}}.$$

This final expression for ϕ is valid within the hyperbolic region GCD.

4. The supersonic source

The results given in § 2 are immediately applicable in the calculation of the fields which accompany a semi-infinite line source of uniform strength, which is moving lengthways on the interface between two fluids. This line singularity moves steadily with a velocity V which must be supersonic with respect to both media, and it lies on the z-axis.

The flow is conical, and the variable s is now of the form $s = rV/(Vt-z)$ for steady motion in the positive z-direction. The s- and θ-derivatives of the potential are then given by equations (17) to (20) if we replace c_1 by $c_1 V(V^2-c_1^2)^{-\frac{1}{2}}$ and c_2 by $c_2 V(V^2-c_2^2)^{-\frac{1}{2}}$, and if we modify the quantity m accordingly. The z-derivative, that is the quantity $\{s/(Vt-z)\}(\partial S/\partial s)$, then represents either the velocity component parallel to the line singularity, or the potential of a supersonic point source moving along the interface.

5. The electromagnetic problem

The results derived in the acoustic problem are applicable in the theory of electromagnetic pulses involved in the sudden setting-up of a current in an infinite line or of a charged line on the interface between two media. In the former case the vector potential has only one component $A_z = c^2 S(s,\theta)$, the constant k is the ratio of the magnetic permeabilities μ_2/μ_1, and m is the ratio c_2/c_1. The non-zero field components, derived from Maxwell's equations, are

$$B_r = \frac{\mu c^2}{r}\frac{\partial S}{\partial\theta}, \quad B_\theta = -\frac{\mu c^2}{t}\frac{\partial S}{\partial s} \quad \text{and} \quad E_z = -sB_\theta.$$

For the charged line we relate the quantity S to the scalar potential Φ through the equation $\Phi = c^2 S$. In this case k is the ratio of the dielectric constants ϵ_2/ϵ_1, and the non-zero field components are

$$E_r = -\frac{c^2}{t}\frac{\partial S}{\partial s}, \quad E_\theta = \frac{c^2}{t}\frac{\partial S}{\partial\theta} \quad \text{and} \quad B_z = \frac{1}{t}\frac{\partial S}{\partial\theta}.$$

The results given in equations (16), (17), (19) and (20) may be used directly to derive the field components.

6. Conclusion

The assumption of dynamic similarity is used to determine the velocity potential and pressure field of an impulsive line source which is suddenly set up on the plane which separates two media of different density and sound velocity.

The solution for the potential may be identified with Hadamard's elementary solution of the wave equation in the homogeneous case, when

$$\phi = \frac{c}{2\pi}(c^2t^2 - r^2)^{-\frac{1}{2}} \quad \text{if} \quad r < ct,$$

$$\phi = 0 \qquad\qquad\qquad\quad \text{if} \quad r > ct.$$

In the case of two media considered in this paper, there are similar algebraic singularities on the shock fronts $r = ct$ in medium 1 and $r = c_2 t$ in medium 2.

A feature of the solution is that since $\partial W/\partial\zeta$ is real on the section OC of the interface, there is no normal velocity between the two subsonic regions. This section of the interface is a contact discontinuity (i.e. OC is a steadily expanding vortex-sheet).

The author presented these results verbally at the spring (1959) meeting of the U.R.S.I. in Washington, D.C. A similar method has been used independently by Keller & Gardner (1959) to find the solution for a line dipole. This research has been sponsored in part by Air Force Cambridge Research Center under contract AF 19(604)–4561, and in part by the Office of Naval Research and the David W. Taylor Model Basin under contract Nonr-562(24).

REFERENCES

Craggs, J. W. 1956 *Proc. Roy. Soc.* A, **237**, 372.

Craggs, J. W. 1957 *J. Fluid Mech.* **3**, 176.

Friedlander, F. G. 1958 *Sound Pulses.* Cambridge University Press.

Hadamard, J. 1923 *Lectures on Cauchy's Problem.* Yale University Press.

Keller, J. B. & Gardner, C. S. 1959 U.R.S.I. Symposium on electromagnetic theory, Toronto (to be published).

Lamb, H. 1932 *Hydrodynamics*, 6th ed. Cambridge University Press.

Papadopoulos, V. M. 1959*a* *Proc. Roy. Soc.* A, **252**, 520.

Papadopoulos, V. M. 1959*b* U.R.S.I. Symposium on electromagnetic theory, Toronto (to be published).

Sound emission from jets at high subsonic velocities

By ERIK MOLLÖ-CHRISTENSEN
AND RODDAM NARASIMHA
Department of Aeronautics and Astronautics, Massachusetts Institute of Technology

(Received 16 September 1959)

Measurements of spectra of sound emission to the far field from jets at high subsonic velocities are presented. The similarity relations found in the experiments suggest a mechanism of sound generation and scattering where the latter is of dominant importance. A possible mechanism is described.

1. Introduction

This paper reports on some measurements performed at the California Institute of Technology during the past year. While many results of jet noise measurements were available in the literature, no single set of experiments was sufficiently complete to allow one to establish the similarity relations for the spectra of emitted sound.

The purpose of our experiments was to find these similarity relations. This can be attained only by performing the experiments under closely controlled circumstances which are difficult to obtain, as was soon discovered. Parasitic variables, involving the amplitude of sound from the air supply, the reflectivity of the surroundings and scattering from the microphone all presented serious problems. Only after months of attention to these details was it possible to obtain meaningful narrow band-pass data, which would yield the spectral definition required.

2. The air flow arrangement

The experimental arrangement is shown in figure 1. From the laboratory air supply the air passed through a water separator, a reducing valve and a throttling valve through a flexible hose to the settling chamber. The settling chamber was lined with 1 in. fibreglass mats, and contained twelve perforated disks, made up from plywood faced on both sides with fibreglass. The perforations consisted of eight 1 in. holes randomly arranged. The baffles were followed by three screens. The first contraction was made of plaster of Paris, and after a short straight run through a 2 in. smooth pipe, the air entered the final nozzle. The nozzles were made of brass, polished on the inside; they all ended in a straight run, three diameters long for each of two 'laminar' nozzles 0·375 and 0·201 in. diameter, and about forty-three diameters long for the turbulent nozzle, 0·375 in. diameter. The overall contraction ratio, based on area, varied from approximately 100 to 400.

The anechoic chamber, in which all the measurements were performed, was 8×8 ft. in cross-section, and was 10 ft. long. Its anechoic properties were judged

to be satisfactory after the jet noise measurements showed the existence of far-field similarity of spectra, within experimental accuracy. No far field can exist inside a reflecting enclosure.

Measurement of the sound level at the end of the first contraction at maximum mass flow showed it to have a root-mean-square amplitude of less than 1 dyne/cm^2;

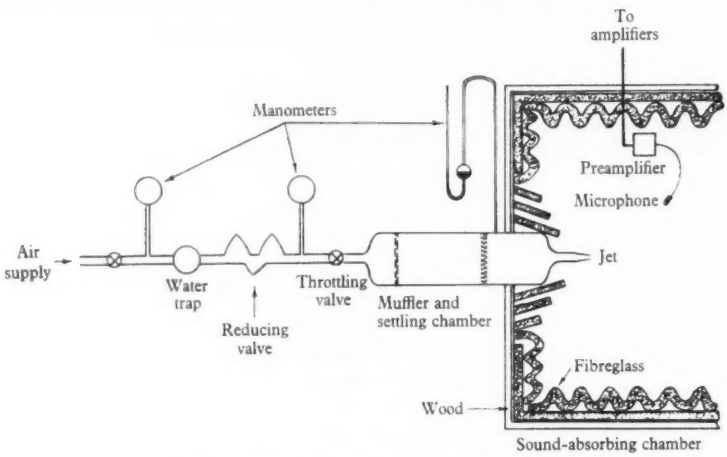

FIGURE 1. Experimental arrangement.

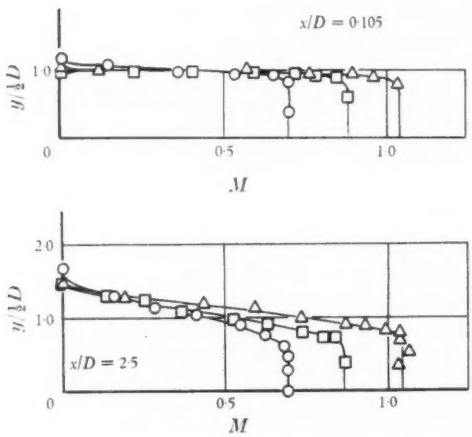

FIGURE 2. Mach number profiles for 0·201 in. diameter jet. ○, $M = 0{\cdot}70$; □, $M = 0{\cdot}88$; △, $M = 1{\cdot}04$.

most of this noise was outside the frequency band of the measurements. The use of small capillary tubing for transmitting the pressure in the stagnation chamber to the manometer effectively prevented cavity resonance in this tube.

Profiles of the Mach numbers of the resulting flow are shown in figures 2, 3 and 4 for several jet Mach numbers.

3. Method of sound measurement and recording

A barium titanate microphone of the type designed by Willmarth (1958) was used in all the measurements. The face diameter of the microphone was 0·25 in. A small shock tube was built and used for microphone calibration.

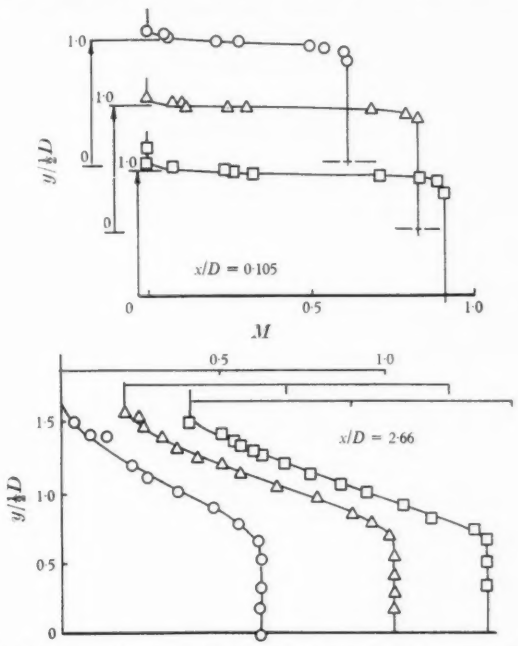

FIGURE 3. Mach number profiles for 0·375 in. diameter jet. ○, M = 0·61; △, M = 0·83; □, M = 0·91.

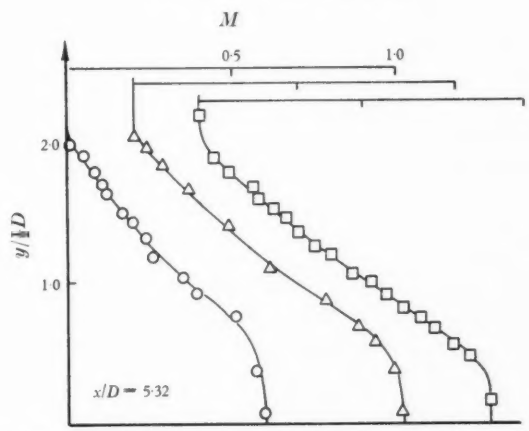

FIGURE 4. Mach number profiles for 0·375 in. diameter jet. ○, M = 0·61; △, M = 0·83; □, M = 0·91.

The amplifiers designed and built for the purpose gave a r.m.s. noise level of 1·7 mV at the input, or, in terms of pressure, 1 dyne/cm², over the band-width 500 c/s to 100 kc/s.

The signal from the amplifier was passed through a band-pass filter, cutting off at 500 and 100,000 c/s. The signal then went into a true r.m.s. meter, into an oscilloscope for monitoring against overloads and a Donner Model-21 wave-form analyser. The output from the wave-form analyser went to a low-pass filter, for averaging, and the filter output was recorded by a pen recorder.

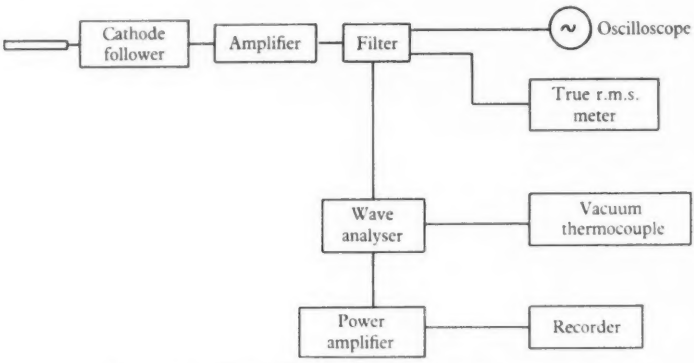

FIGURE 5. Block diagram of recording equipment.

The power band-width (Q_p) of the wave-form analyser was 45 c/s, a measure of the width of an equivalent rectangular spectral window.

The frequency dial of the wave-form analyser was driven by a clockmotor, and its position recorded by the other pen of the pen recorder. Taking account of the traversing speed of the frequency dial, the resulting spectra were thus averaged over a maximum of three band-widths.

In addition to this primary equipment, many pieces of secondary equipment were used from time to time in the development of a satisfactory experimental arrangement.

The microphone was supported on a thin wire, and was pointed at the jet nozzle to minimize scattering. In spite of this, scattering occurred at approximately 37,000 c/s, as could be seen in the spectra. No data were taken above this frequency.

A block diagram of the recording system is shown in figure 5.

4. Dimensional analysis and similarity of emitted sound

In the study of aerodynamically generated sound, the fluctuating pressure $p'(\mathbf{r}, t)$ is measured. Its statistical properties determine the structure of the sound field and its relation to the sound-producing flow.

The simplest and most important quantities to be measured are the mean square pressure $\overline{p'^2}$ and the power spectral density $\phi(f, \mathbf{r})$ with respect to frequency f (c/s). They are related by $\overline{p'^2} = \int \phi \, df$.

The sound-producing flow is described by a set of parameters which involve at least the following: density ρ, kinematic viscosity ν, velocity of sound a, velocity U and a characteristic length D. There will also be a number of other parasitic parameters, such as the sound and turbulence levels of the stream used, the microphone diameter, the cut-off frequencies of the recording equipment, the averaging time, etc.

Indeed, the decisive part of an experimental study of aerodynamic noise lies in the identification and elimination of parasitic parameters. This is obvious for any experiment; it is emphasized here for the case of aerodynamic noise because the nature of the problem, namely, the study of a random wave-field of small intensity without *a priori* knowledge of what to expect, often makes it very difficult to know whether one has succeeded in measuring what was intended or not.

If one assumes that all parasitic parameters have been eliminated, dimensional analysis yields for the form of $\overline{p'^2}$ and ϕ

$$\overline{p'^2} = \rho^2 U^4 F\left(\frac{\mathbf{r}}{D}, Re, M\right),$$

where $Re = UD/\nu$ and $M = U/a$ are Reynolds number and Mach number, respectively; and

$$\phi(f, \mathbf{r}) = \rho^2 U^4 \frac{D}{V} G\left(\frac{\mathbf{r}}{D}, \frac{fD}{V}, Re, M\right),$$

where V is some characteristic velocity.

If one adds some physical insight to the process of dimensional analysis, one may find that only certain combinations of the dimensionless variables occur. For example, one may apply the law of conservation of radiated energy in the far field of an emitter of limited size, from which one finds that the intensity must fall off as $1/r^2$. Thus,

$$\overline{p'^2} = \rho^2 U^4 \frac{D^2}{r^2} F_1(\theta; Re, M),$$

$$\phi = \rho^2 U^4 \frac{D^3}{Vr^2} G_1\left(\theta, \frac{fD}{V}; Re, M\right),$$

where r is the distance from the jet exit and θ the angle $\mathbf{r}$ makes with the jet axis.

To go beyond this stage, one must adopt a more detailed physical model. The choice of physical models will be suggested by the results of the experiments, this being a purpose of experiment.

From these similarity considerations it was decided to present the results in the following form, with $V = a = a_0$,

$$g\left(\frac{fD}{a}, Re, M, \theta\right) = \left\{\frac{r^2}{D^2} \frac{1}{p_A^2 M^4} \frac{a}{D} \frac{Re^n}{M^m} \phi\left(\frac{fD}{a}, r, \theta, Re, M\right)\right\}^{\frac{1}{2}}.$$

The reasons for the different terms are the following.

r^2/D^2 takes account of the far-field radiation law.

$\dfrac{1}{p_A^2 M^4} \sim \dfrac{1}{\rho^2 U^4}$ scales the pressure fluctuation by the jet dynamic pressure, or, alternatively, the spectral intensity or spectral sound energy flux through the jet nozzle, $\frac{1}{2}\rho U^3$ times the Mach number.

a/D establishes the time constant.

Re^n/M^m is a multiplying factor; the exponents are chosen such as to enable all the data to be plotted as closely on a single curve as possible.

5. Measured sound spectra

The measured far-field spectra are shown in figures 6–10. In each case, the similarity parameter Re^n/M^m was chosen such as to give the best possible fit. The spectra have been plotted on linear scales, as it was thought that this would be more revealing than the usual octave-decibel system.

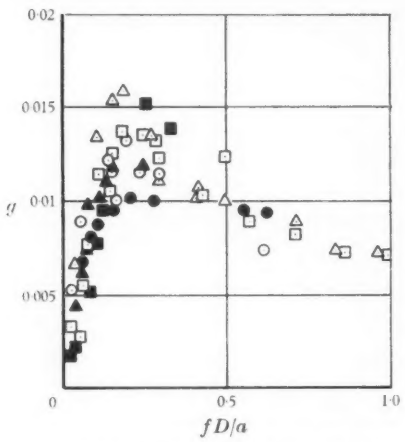

FIGURE 6. Similarity in spectra at $r = 20{\cdot}5$ in. and $\theta = 25°$.

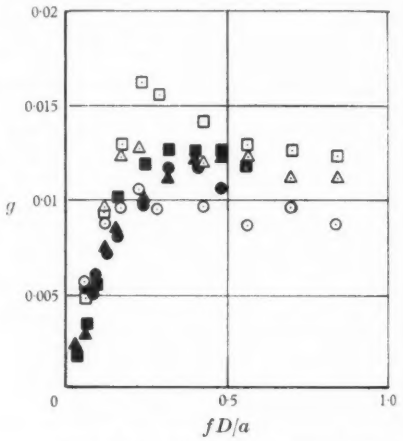

FIGURE 7. Similarity in spectra at $r = 20{\cdot}5$ in. and $\theta = 35°$.

In figures 6–10 the following notation is used:

$$g = \left[\frac{r^2}{D^2}\frac{a}{Q_p D}\frac{\overline{p'^2}}{\overline{p_A^2}}\frac{1}{M^{4+m}}\frac{R}{R_{\text{ref.}}}\right]^{\frac{1}{2}}.$$

M	$D = 0{\cdot}375$ in.	$D = 0{\cdot}201$ in.
0·70	⊙	●
0·88	△	▲
0·99	⊡	■

(Here $\overline{p'^2}/Q_p$ denotes power spectral density, $\overline{p'^2}$ being the mean-square pressure within the bandpass Q_p of the wave analyser.)

In figures 6 and 7, $m = 6$.

Some of the spread in the data is probably due to experimental inaccuracy, and some of it due to application of an inexact similarity parameter. For example, it should not be expected that for the entire spectrum at any given point there would be *no* relation between M and fD/a in the function g.

Considering the spectra as they have been presented, a few features are immediately apparent.

(1) Reynolds number appears to be an important similarity parameter as far as sound emission is concerned.

(2) In most regions, the spectra scale slightly better with fD/a than with fD/U.

(3) Spectra near the jet show a maximum intensity at a Strouhal number $fD/a = 0{\cdot}2$, but for $\theta = 35°$ there was no maximum in the frequency band in which measurements were made.

(4) The power of Mach number which gives the best similarity varies with θ from $m = 4$ at $\theta = 90°$ and $m = 6$ at 25°.

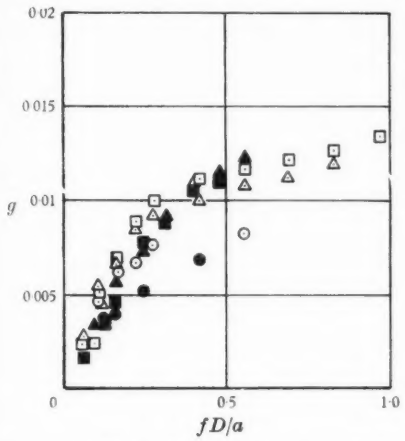

FIGURE 8. Similarity in spectra at $r = 20{\cdot}5$ in. and $\theta = 45°$. See figure 6 for notation; $m = 6$.

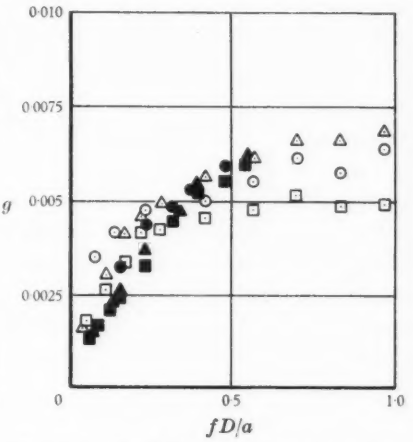

FIGURE 9. Similarity in spectra at $r = 20{\cdot}5$ in. and $\theta = 60°$. See figure 6 for notation; $m = 5$.

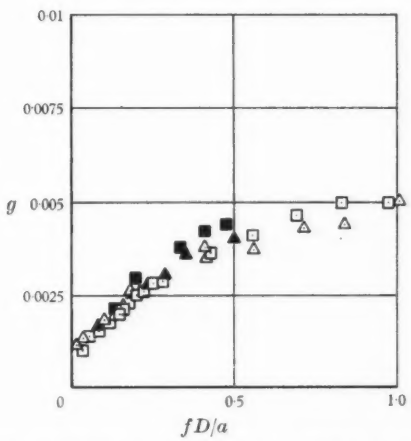

FIGURE 10. Similarity in spectra at $r = 20{\cdot}5$ in. and $\theta = 90°$. See figure 6 for notation; $m = 4$.

6. Outline of a working hypothesis of jet noise

The appearance of Reynolds number as a similarity parameter in the far-field noise suggests that the far-field noise is generated in a region of the jet where Reynolds number is an important parameter. The only such region is the region

of high mean shear immediately downstream of the nozzle. Here the thickness of the shear layer is determined by the thickness of the boundary layer on the nozzle wall at the exit, and this boundary-layer thickness depends strongly upon Reynolds number.

It appears that all the features of the observed far-field spectra can be explained in terms of a generator of sound in the early free-shear layer, and scattering of this sound by the mean flow of the jet. As will be shown, this scatter is coherent for long wavelengths, and partly omnidirectional for short wavelengths. The scatter is thus to some extent frequency selective; the most striking consequence of this is the appearance of a maximum at low frequencies in the spectra near the jet axis.

As will be discussed later, the sound emission from the early shear layer will be that of a dipole sheet, probably anticorrelated about a diameter. Further downstream, turbulence increases, and the turbulent sound sources in the turbulent mixing region possess space correlations of much higher order than the sound sources in the early shear layer, and therefore the radiation to the far field is negligible in comparison. In the near field, these pressure fluctuations with high-order correlation may be dominant, but they will radiate very little energy to the far field.

The lowest order sound emitter has thus been located. We proceed to examine the scattering of sound from the early shear layer by the flow in the jet. For sound of wavelengths of several jet diameters, such that the wavelength is large compared to the mean shear layer thickness, the scattering may be approximated by that of a discrete shear layer with uniform flow inside and still air outside. A sound wave travelling in the downstream direction will be moving with the velocity of sound with respect to the air in the jet, and with a Mach number of $M+1$ with respect to the air outside. The transmitted radiation will therefore be predominantly in the direction $\theta = \cos^{-1}[1/(1+M)]$. A sound wave moving obliquely to the jet axis will be transmitted and reflected from the shear layer. The reflected wave will be different in phase from the impinging wave (Ribner 1957) so that certain wavelengths longer than two jet diameters will resonate back and forth across the jet. This will cause an increase in the radiation of such wavelengths to angles of $\theta = \cos^{-1}[1/(1+M)]$. However, the waves which have bounced back and forth many times will by then have been carried far downstream into the fully turbulent region of the jet, where the mean Mach number has decreased, and will therefore be radiated to points nearer the jet axis than $\theta = \cos^{-1}[1/(1+M)]$.

This accounts for the low-frequency maximum in the spectra near the jet axis. The wavelength which gives maximum resonance across the jet appears to correspond to $fD/a \doteqdot 0{\cdot}2$, as can be seen from the measured spectra.

For shorter wavelengths the scales of turbulence must be considered in the scattering phenomenon. In addition to direct transmission of the primary wave to regions in the vicinity of $\theta = \cos^{-1}[1/(1+M)]$ as before, the waves of wavelength comparable with the scale of turbulence will experience a more or less omnidirectional scattering, and this omnidirectional scattering will be most intense for the very short wavelengths, which will be scattered omnidirectionally

from the early part of the mixing region, where turbulence is most intense. This high-frequency omnidirectional radiation is apparent in the spectra. In addition to the scattered radiation, there is direct outward radiation from the early shear layer. This direct outward radiation will be of dipole character, and the dipoles will probably move at half the jet velocity. The angular intensity distribution of this radiation will be as $\sin\theta/(1-\frac{1}{2}M\cos\theta)^2$.

It is, of course, possible to replace both the sound generation and scattering mechanisms by a source distribution on the jet axis and obtain a correct representation of the far field. The separation of sound generation and coherent and omnidirectional scattering of the sound emitted by the generators chosen here does have the advantage of being closer to the physical processes which cause the noise observed in the far field.

In general, this model gives results in qualitative agreement with experiment. In particular, it gives an explanation of the maximum at low frequencies observed in the spectra near the jet axis, which other models of jet noise have failed to do.

7. Similarity laws for noise generation in the high shear region

These similarity laws are best obtained by rewriting the equations of motion of a gas as a non-homogeneous wave equation, as Lighthill (1952) has done. From the continuity equation

$$\frac{\partial\rho}{\partial t}+\frac{\partial}{\partial x_i}(\rho v_i)=0 \tag{7.1}$$

and the momentum equation

$$\frac{\partial(\rho v_i)}{\partial t}+\frac{\partial}{\partial x_j}(\rho v_i v_j)=-\frac{\partial p}{\partial x_i}+\frac{\partial}{\partial x_j}\tau_{ij} \tag{7.2}$$

one obtains, by adding the divergence of (7.2) to $a_0^2\nabla^2\rho$ and using (7.1)

$$-\frac{\partial^2\rho}{\partial t^2}+a_0^2\nabla^2\rho=-\frac{\partial^2}{\partial x_i\partial x_j}(\rho v_i v_j-\tau_{ij})-\nabla^2(p-a_0^2\rho). \tag{7.3}$$

Assuming a perfect gas and making use of the relations

$$\left(\frac{\partial p}{\partial\rho}\right)_S=a^2=\gamma RT;\quad \left(\frac{\partial p}{\partial S}\right)_\rho=\frac{p}{c_p}$$

one may derive

$$\begin{aligned}-\frac{\partial^2\rho}{\partial t^2}+a_0^2\nabla^2\rho=&-\frac{\partial^2}{\partial x_i\partial x_j}(\rho v_i v_j-\tau_{ij})+(a_0^2-a^2)\nabla^2\rho\\&-\left\{+\frac{p}{c_p}\nabla^2 S+\gamma R\frac{\partial\rho}{\partial x_i}\frac{\partial T}{\partial x_i}+\frac{1}{c_p}\frac{\partial S}{\partial x_i}\frac{\partial p}{\partial x_i}\right\}.\end{aligned} \tag{7.4}$$

This, with some minor modifications, is the equation used by Lighthill. For low Mach numbers the right-hand side can, as a first approximation, be considered known and so treated as a source term. At higher Mach numbers, however, scattering and convection cannot be neglected, and the right-hand side would contain terms depending on the sound emitted, a physical emitter being by its nature also a scatterer.

Chu & Kovasznay (1958) have considered the conditions under which Lighthill's approximation is valid. The sufficient conditions they find restrict, in principle, the approximation to weak turbulence in almost uniform flow.

In the presence of large gradients in the mean flow it is advantageous to write each variable as the sum of its time average and a fluctuation about this average. Denoting them by a bar and prime, respectively, (7.4) becomes

$$\begin{aligned}-\frac{\partial^2\rho'}{\partial t^2}+a_0^2\nabla^2\rho' = -\frac{\partial^2}{\partial x_i\partial x_j}(&\overline{\rho v_i}v_j'+\overline{\rho v_j}v_i'+\rho'\overline{v_iv_j}\\ &+\rho'v_i'\overline{v_j}+\overline{\rho}v_i'v_j'+\rho'\overline{v}_iv_j'+\rho'v_i'v_j'-\tau_{ij}')\\ &-\Big\{\gamma R\Big(\frac{\partial\overline{\rho}}{\partial x_i}\frac{\partial T'}{\partial x_i}+\frac{\partial\rho'}{\partial x_i}\frac{\partial\overline{T}}{\partial x_i}\Big)+\frac{\overline{p}}{c_p}\nabla^2S'\\ &+\frac{p'}{c_p}\nabla^2\overline{S}+\frac{1}{c_p}\Big(\frac{\partial\overline{S}}{\partial x_i}\frac{\partial p'}{\partial x_i}+\frac{\partial S'}{\partial x_i}\frac{\partial\overline{p}}{\partial x_i}\Big)\Big\},\end{aligned}\tag{7.5}$$

where the steady terms on both sides have been cancelled and second-order terms in ρ', T' and S' have been neglected.

Now restrict the discussion to the flow near the nozzle where there is a very thin shear layer separating the uniform parallel flow from the quiescent air outside the jet. If n is distance measured normal to the shear layer, the gradient $\partial\overline{v_1}/\partial n$ is very large, and so the dominant terms on the right-hand side are the ones that involve this derivative. Neglecting entropy and temperature gradients in the flow, we get from (7.5)

$$-\frac{\partial^2\rho'}{\partial t^2}+a_0^2\nabla^2\rho'-\overline{v}_1^2\frac{\partial^2\rho'}{\partial x_1^2}-\frac{2\overline{\rho v_1}}{\overline{\rho}}\frac{\partial^2\rho'}{\partial x_1\partial t}\simeq-2\frac{\partial\overline{\rho v_1}}{\partial n}\frac{\partial v_n'}{\partial x_1}\tag{7.6}$$

for the field inside the jet, and

$$-\frac{\partial^2\rho'}{\partial t^2}+a_0^2\nabla^2\rho'\simeq-2\frac{\partial\overline{\rho v_1}}{\partial n}\frac{\partial v_n'}{\partial x_1}\tag{7.7}$$

outside the jet, the right-hand side being zero outside the jet in both cases.

Equations (7.6) and (7.7) show that the shear layer acts like a dipole-sheet emitter. The strength of the dipoles is not known *a priori*, but their total strength at any instant has to be zero if the efflux from the jet is steady. The net effect is that the shear layer will appear from the outside as a longitudinal-lateral quadrupole.

If the right-hand side in (7.7) *is* considered known, we can formally write down for the density fluctuation in the far field (as in (4))

$$\rho'(\mathbf{x},t)=-\frac{1}{2\pi a_0^3}\iiint_{\text{dipole volume}}\frac{\partial(\overline{\rho v_1}(\mathbf{y}))}{\partial n}\frac{(y_1-x_1)}{|\mathbf{y}-\mathbf{x}|^2}\frac{\partial}{\partial t}\Big\{v_n'\Big(\mathbf{y},t-\frac{|\mathbf{x}-\mathbf{y}|}{a_0}\Big)\Big\}\,dV_{\mathbf{y}}.$$

We can now find the similarity law as follows. The analysis is admittedly rather crude, and is really justified only by the agreement of the final results with experiment. If δ is the shear-layer thickness, we now assume that the thickness and length of the dipole region are each proportional to δ, also that

$$\partial\overline{\rho v_1}/\partial n\sim(\overline{\rho}U/\delta)\quad\text{and}\quad v_n'\sim U.$$

We also assume that the characteristic time of the fluctuations varies like D/U, so that

$$\partial v_n'/\partial t \sim U^2/D.$$

The peripheral distance around the sheet is proportional to D, so we get

$$\rho' \sim \frac{1}{a_0^3 r}\frac{\bar{\rho}U}{\delta}\frac{U^2}{D}D\delta^2 \sim \bar{\rho}M^3\frac{D}{r}\frac{\delta}{D}.$$

For geometrically similar nozzles we might take $\frac{D}{\delta} \sim \sqrt{\frac{UD}{\nu}} = \sqrt{Re}$, so that one finally obtains

$$\frac{\rho'}{\bar{\rho}} \sim M^3\frac{D}{r}\frac{1}{\sqrt{\mathrm{Re}}}.$$

This yields

$$\frac{\overline{p'^2}}{\bar{p}^2} \sim \frac{M^6}{Re}\left(\frac{D}{r}\right)^2$$

and shows the experimentally found dependence on Reynolds number. The power of the Mach number was in most cases somewhat higher, presumably due to the effects of scattering. The spectral density of p' is found to be

$$\phi\left(\frac{fD}{a}, r, \theta, M, Re\right) \sim \frac{D^3}{r^2 a_0}\overline{p'^2}\frac{M^6}{Re}G\left(\frac{fD}{a_0}, \theta\right).$$

8. Jets with turbulent flow at the nozzle exit

From the present understanding of the experimental results, one is strongly led to believe that the mechanism of sound emission to the far field from jets with turbulent flow in the nozzle is the same as that described above.

The spectra obtained with the turbulent pipe flow nozzle, in general, resembled those obtained with the shorter nozzles. A strict comparison between them is not very revealing on account of the very different Mach number profiles for the different nozzles.

9. Conclusions

From a consideration of the similarity relations obtained from experiments, it has been possible to outline a theory of noise emission from subsonic and low supersonic jets.

The sound is generated in the high shear region of the jet, the shear layer of which is considered a dipole sheet with the dipoles oriented along the jet axis. This radiation is emitted both outward and inward. The inwardly emitted radiation is subject to multiple scattering before emergence from the jet. One effect of scattering is the occurrence of a low-frequency peak in the spectrum of emitted sound at an oblique angle to the jet axis, another effect is the increase of energy radiated to $\theta = \cos^{-1}[1/(1+M)]$.

With this description of the mechanism for jet noise, some methods of silencing of jets suggest themselves. It would be beyond the scope of the present paper to discuss them. The apparently intimate connexion between jet stability and noise generation appears worthy of further investigation, as does the effect of sound scattering upon the mean flow in the jet.

The authors have benefited greatly from the experience and advice of Willmarth (1959) and Weyers (1959) in the design of experimental equipment. Also, the frequent discussions with H. W. Liepmann on both theory and experiment are gratefully acknowledged. The amplifiers used in the experiments were built by Richard Swartley. This work was partly supported by the NASA.

REFERENCES

Chu, B-T. & Kovasznay, L. S. G. 1958 Non-linear interactions in a heat-conducting compressible gas. *J. Fluid Mech.* **3**, 494.

Lighthill, M. J. 1951 On sound generated aerodynamically. I. General theory. *Proc. Roy. Soc.* A, **211**, 564.

Ribner, H. S. 1959 Reflection, transmission and amplification of sound by a moving medium. *J. Acoust. Soc. America*, **29**, 431.

Weyers, Paul F. R. 1959 The vibration and acoustic radiation of thin-walled cylinders caused by internal turbulent flow. *NASA Memo.* (to be published).

Willmarth, W. W. 1958 Small barium titanate transducer for aerodynamic or acoustic pressure measurements. *Rev. Sci. Instrum.* **29**, 218.

Willmarth, W. W. 1959 Space-time correlations and spectra of the wall pressure in a turbulent boundary layer. *NASA Memo.* no. 3–17–59 W.

Steady longitudinal motion of a cylinder in a conducting fluid

By HIDENORI HASIMOTO

Department of Aeronautics, The Johns Hopkins University*

(Received 4 September 1959)

The steady motion of an infinitely long solid cylinder parallel to its length in a conducting fluid in the presence of a uniform magnetic field is discussed. Due to Alfvén waves originating at the cylinder we find two opposite 'wakes' parallel to the applied magnetic field.

A formula which relates the total drag on the cylinder to the electric potential difference $\delta\Phi$ between the two undisturbed regions outside these two wakes is derived

$$D/|\delta\Phi| = 2\sqrt{\rho\nu\sigma},$$

where $\rho\nu$ is the viscosity and σ is the conductivity of the fluid.

The reduction to a classical boundary-value problem is made for the case of an insulating cylinder.

Exact solutions are obtained for the case of a perfectly conducting or an insulating flat strip of semi-infinite width. These give a clear picture of the fields, especially in the transition region near the edge of the strip.

The case of a strip of finite width is also discussed with special reference to the viscous and the magnetic drags, D_f and D_m. We find that $D_f + \frac{1}{2}D_m$, on a perfectly conducting strip, is equal to the viscous drag on an insulating strip for which D_m is zero. Precise values of these drags are given.

1. Introduction

There are only a few cases in magneto-hydrodynamics for which exact treatments are possible. A typical case is that of the rectilinear fluid flow in pipes under the uniform transverse magnetic field. The studies initiated by Hartmann (1937) for the flow between two walls have been extended by Shercliff (1953, 1956) to the case of the flow in a straight pipe. Resler & Sears (1958) studied the case of a compressible fluid, neglecting viscosity. Also we should mention the work of Bleviss (1958) on the Couette flow between parallel walls.

As far as the author is aware, problems in which there is an unlimited fluid flow outside a rigid cylinder, corresponding to the above cases, have remained untouched, except for the oscillating flow (Kakutani 1958) and Rayleigh's problem (Rossow 1957; Chang & Yen 1959) for an infinite flat plate. In a study of Rayleigh's problem by the present author it was found that an inhomogeneous stationary field remains near the plate after a long period of time. This field has a boundary-layer structure in which the velocity goes from the speed of the plate

* On leave of absence from Kyoto University, Japan.

to a definite fraction of the plate speed sufficiently far away. This represents residual stationary disturbances from the passage of Alfvén waves along the applied magnetic field, and suggests the existence of non-trivial steady solutions for the case of the longitudinal motion of a cylinder of finite cross-section, even though such solutions do not exist for the case of no magnetic field. In the magnetic case, there will also appear interesting transition regions (B) between the regions (C) influenced by Alfvén waves originating at the cylinder and the outer regions (A) which may not be influenced directly by these waves for large Hartmann number M (figure 1). We will also derive the viscous and the magnetic drags on the cylinder. This is motivated by problems of practical interest, relating to the flight of slender bodies in space.*

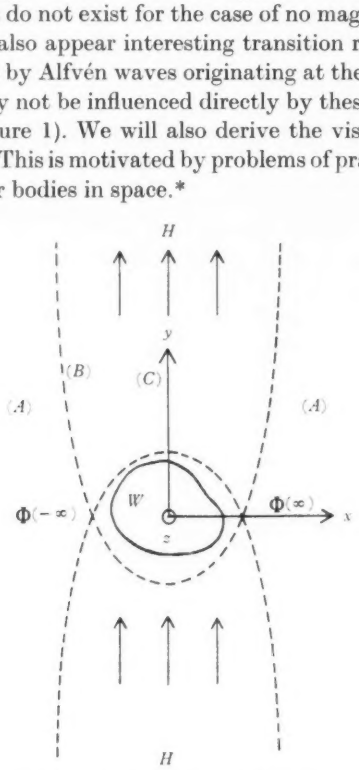

FIGURE 1. Cross-section of cylinder in a transverse magnetic field.

In § 2, we will write down the fundamental equations and the boundary conditions for our problem assuming that the magnetic permeability is the same in the fluid and the cylinder.

In § 3, general characteristics of the problem which allow two 'wakes' (C) in the positive and the negative directions of the applied field will be discussed. We derive a simple formula which relates the drag on the cylinder to the electric potential difference between two undisturbed regions (A) outside these wakes (figure 1). These two quantities are also related to the strength of the wakes at infinity.

We also show that the problem is simplified for the case of an insulating cylinder, since it reduces to a well-known boundary-value problem of mathematical physics.

* Our solutions are also considered to afford limiting fields around a huge annulus rotating slowly about its axis of symmetry, which is parallel to the strong applied magnetic field.

As an example, the problem for a flat strip is considered in §§ 4 and 5. We confine this study to the two cases of (I), insulating, and (II), perfectly conducting plates. In § 4, we reduce our problem to two standard boundary-value problems for the Helmholtz equation, and we give precise numerical values for the viscous and the magnetic drags on the plate.

In § 5, we give the exact solution of our problem for a strip of semi-infinite width. This solution affords a clear picture of the fields, especially in the boundary layer on the insulating plate and in the transition regions between the outer undisturbed region and the inner core region (which has almost the same velocity as the perfectly conducting plate and one-half the velocity of the insulating plate). Also we find the circuit of the induced electric current around this core.

This behaviour is considered to be the limiting behaviour of the field near a cylinder of given finite width, at sufficiently large Hartmann number. Some consideration is given to this configuration including the case of a thin flat plate with finite conductivity. Comparison with the final steady solutions in Rayleigh's problem with magnetic field for an infinite flat plate is made, and there is perfect agreement with a magnetic Prandtl number of 1.

2. Fundamental equations

We shall use m.k.s. units for the electromagnetic quantities and employ conventional notations. Then, the magneto-hydrodynamic equations for a steady incompressible fluid are

$$(\mathbf{V}.\nabla)\,\mathbf{V} = -\frac{1}{\rho}\nabla(p+\tfrac{1}{2}\mu\mathbf{H}^2)+\nu\nabla^2\mathbf{V}+\frac{\mu}{\rho}(\mathbf{H}.\nabla)\,\mathbf{H}, \tag{2.1}$$

$$\nabla.\mathbf{V} = 0, \tag{2.2}$$

$$(\mathbf{V}.\nabla)\,\mathbf{H} = \kappa\nabla^2\mathbf{H}+(\mathbf{H}.\nabla)\,\mathbf{V}, \quad \kappa = 1/(\mu\sigma), \tag{2.3}$$

$$\nabla.\mathbf{H} = 0, \tag{2.4}$$

$$\mathbf{E} = -\mu\mathbf{V}\wedge\mathbf{H}+\mathbf{J}/\sigma, \tag{2.5}$$

$$\mathbf{J} = \nabla\wedge\mathbf{H}, \tag{2.6}$$

in a Cartesian coordinate system (x, y, z), which is at rest with respect to the fluid at infinity.

Let us consider the steady flow due to the uniform longitudinal motion, with velocity W, of an infinitely long cylinder with its generators parallel to the z-axis, in the presence of a uniform magnetic field of strength H parallel to the y-axis. We assume that the magnetic permeability μ of the cylinder is the same as that of the fluid. The suffix i will be used to denote quantities in the cylinder (so that (2.1) and (2.2) should be replaced by $v_{ix} = 0$, $v_{iy} = 0$ and $v_{iz} = W$).

With similar assumptions to those in Shercliff's treatment, we have:

(1) all quantities are independent of z;

(2) the induced velocity and magnetic fields are parallel to the z-axis, i.e. $v_x = v_y = 0$, $H_x = 0$, $H_y = H$, and tend to zero at infinity. Then, (2.1)–(2.4) reduce to two-dimensional equations in the x–y plane

$$p = p_\infty - \tfrac{1}{2}\mu H_z^2, \tag{2.7}$$

$$\nabla^2 w + m(\partial h/\partial y) = 0, \tag{2.8}$$

$$\nabla^2 h + m(\partial w/\partial y) = 0, \tag{2.9}$$

where
$$w = v_z/W, \quad h = mH_z/(\sigma\mu HW), \tag{2.10}$$
$$m = \sqrt{(\mu H^2/\rho)}/\sqrt{\nu\kappa} = \sigma\mu\,|H|/\sqrt{(\rho\nu\sigma)}, \tag{2.11}$$
$$\nabla^2 = \partial^2/\partial x^2 + \partial^2/\partial y^2, \tag{2.12}$$

and p_∞ is the constant fluid pressure at infinity. The electric current density $\mathbf{J}$ and electric field $\mathbf{E}$ are also parallel to the (x, y)-plane

$$\mathbf{J} = (\sigma\mu HW/m)\,\mathbf{j} \tag{2.13}$$

and
$$E_x = \mu HW(w + j_x/m), \quad E_y = \mu HW j_y/m, \tag{2.14}$$

where
$$j_x = \partial h/\partial y, \quad j_y = -\partial h/\partial x. \tag{2.15}$$

Equations (2.8) and (2.9) must be solved with the boundary conditions

$$w \to 0, \quad h \to 0 \quad \text{at infinity}, \tag{2.16}$$
$$w = 1 \quad \text{on the surface of the cylinder } S, \tag{2.17}$$
$$h = h_i, \quad \partial h/\partial n = (\sigma/\sigma_i)\,\partial h_i/\partial n \quad \text{on } S, \tag{2.18}$$

where $\partial/\partial n$ is the outward normal derivative on the cylinder, and

$$h_i = mH_{iz}/(\sigma\mu HW) \tag{2.19}$$

is the magnetic field in the cylinder satisfying the induction equation (Maxwell's equation)
$$\nabla^2 h_i = 0, \tag{2.20}$$

derived from (2.9) by putting $w = 1$ and replacing h by h_i.

The condition (2.18) for h needs some elucidation. On the surface of the cylinder, we must satisfy the boundary conditions for the electromagnetic quantities

$$\mathbf{H} = \mathbf{H}_i, \quad \mathbf{E}_s = \mathbf{E}_{is}, \tag{2.21}$$

where the suffix s denotes the tangential component around S, and

$$E_{ix} = \mu HW + (\partial H_{iz}/\partial y)/\sigma_i, \quad E_{iy} = -(\partial H_{iz}/\partial x)/\sigma_i. \tag{2.22}$$

If we take into account (2.10), (2.19), (2.14), (2.17) and (2.22), we find that (2.21) is replaced by (2.18) or

$$\mathbf{J}_n = \mathbf{J}_{in} = \partial \mathbf{H}_z/\partial s, \quad \mathbf{E}'_{is} = \mathbf{J}_s/\sigma = \mathbf{J}_{is}/\sigma_i = (\partial \mathbf{H}_z/\partial n)/\sigma, \tag{2.23}$$

where
$$\mathbf{E}'_i = \mathbf{E}_i - \mu \mathbf{H} \wedge \mathbf{W} = \mathbf{J}_i/\sigma_i \tag{2.24}$$

is the electric field in the co-ordinate system moving with the cylinder. Equation (2.23) yields a kind of refraction relation for the electric current

$$\tan\alpha/\tan\alpha_i = \sigma/\sigma_i, \tag{2.25}$$

where α denotes the angle between the current and the normal to S.

Let us try to eliminate h_i from the problem by replacing (2.18) by a single condition for h. Let P and P_0 be two points on s and $N(P_0; P)$ be the Green function in the Neumann problem for the domain bounded by s. Then

$$h_i(P_0) = \frac{1}{s}\oint_S h_i(P)\,ds + \oint_S N(P_0; P)\,\frac{\partial h_i(P)}{\partial n}\,ds. \tag{2.26}$$

where s is the total length of S and ds is the line element of S at P. In the second integral of (2.26) we take the principal value. Also

$$\oint_S (\partial h_i(P)/\partial n)\, ds = 0, \tag{2.27}$$

because h_i is a harmonic function.

Introducing (2.18) into (2.26) and (2.27) we obtain

$$h(P_0) = \frac{1}{s}\oint_S h(P)\, ds + \frac{\sigma_i}{\sigma}\oint_S N(P_0; P)\frac{\partial h(P)}{\partial n}\, ds, \tag{2.28}$$

$$\oint_S (\partial h(P)/\partial n)\, ds = \oint_S j_s ds = 0. \tag{2.29}*$$

Equation (2.28), in conjunction with (2.29), is the boundary condition to be used instead of (2.18) for general values of σ_i/σ.

Taking into account the boundedness of h and $\partial h/\partial n$ for finite σ, we can reduce the above equations to a more simple form for the following two extreme cases.

(I) Perfectly conducting cylinder: $\sigma_i \to \infty$

$$\partial h/\partial n = 0 \quad (\text{or } j_s = 0) \quad \text{on } S. \tag{2.30}$$

This follows most readily from (2.23) because $\mathbf{E}' = 0$ in the cylinder. In this case the electric current in the fluid at the cylinder is perpendicular to S.

(II) Insulating cylinder: $\sigma_i \to 0$

$$h = h_i = \text{const.} \quad \text{in and on the cylinder} \tag{2.31}$$

with

$$\oint_S (\partial h/\partial n)\, ds = 0. \tag{2.32}$$

If the cylinder is symmetric with respect to some (x, z)-plane h_i is zero (see (3.23)). For the general asymmetric case, or if there is more than one cylinder, (2.32) seems to be necessary to determine h_i uniquely. The result (2·31) is evident when we remember that the electric current must be parallel to the cylinder and that h is the stream function of $\mathbf{j}$.

3. General properties of the fields

Before entering into specific boundary-value problems, we will discuss some properties of the solutions of (2·8) and (2·9), satisfying the conditions at infinity (2.16).

Eliminating w or h we obtain

$$(\nabla^2 - m\partial/\partial y)(\nabla^2 + m\partial/\partial y)(w \text{ or } h) = 0. \tag{3.1}$$

which yields

$$w = \phi_+ + \phi_-, \quad h = -\phi_+ + \phi_-, \tag{3.2}$$

where

$$(\nabla^2 \mp m\partial/\partial y)\,\phi_\pm = 0. \tag{3.3}$$

* (2.29) may be deduced more fundamentally from $\nabla \wedge \mathbf{E} = 0$, i.e. $\oint_S \mathbf{E}_s ds = 0$, if we use (2.14) and (2.17).

Introducing $$\phi_\pm = \phi_\pm \exp(\mp ky), \tag{3.4}$$

where $$k = \tfrac{1}{2}m, \tag{3.5}$$

we get $$(\nabla^2 - k^2)\phi_\pm = 0. \tag{3.6}$$

Equation (3.3) is well known as the Oseen equation (Lamb 1932), which suggests the existence of 'wakes' of vague parabolic shape along positive and negative y-axes at a great distance from the obstacle. This is shown by the general solution satisfying (2.16)

$$\phi_\pm = e^{\pm ky} \operatorname{Re} \sum_{n=0}^{\infty} A_{n\pm} K_n(kr)\, e^{in(\theta \mp \frac{1}{2}\pi)} \tag{3.7}$$

$$= B_\pm \sqrt{\frac{\pi}{2kr}}\, e^{-kr(1 \mp \sin\theta)} + O((kr)^{-\frac{3}{2}}) \quad \text{for} \quad kr \gg 1, \tag{3.7'}$$

with $$B_\pm = \operatorname{Re} \sum_{n=0}^{\infty} A_{n\pm}, \tag{3.8}$$

where K_n is the modified Bessel function of order n, and (r, θ) are the cylinder co-ordinates

$$x = r\cos\theta, \quad y = r\sin\theta. \tag{3.9}$$

Notice that $r(1 \pm \sin\theta) = \text{const.}$ are the parametric equations for a parabola.

These wakes represent residual stationary disturbances from the passage of Alfvén waves along the $\pm y$-axes ($\theta = \pm\frac{1}{2}\pi$) in the presence of the combined action of viscosity and conductivity of the fluid. In these two 'wakes', given by (3.7),

$$\phi_+ \gg \phi_- \quad \text{or} \quad \phi_+ \ll \phi_- \quad \text{according as} \quad ky \to \pm\infty, \tag{3.10}$$

so that $$\tfrac{1}{2}\mu \mathbf{H}_z^2 = (\nu/\kappa)\, \tfrac{1}{2}\rho \mathbf{V}^2, \tag{3.11}$$

i.e. there is a simple relation between the induced magnetic energy and the kinetic energy of the fluid, and the electric current flows along the lines $w = \text{const.}$

We now show a simple relation between the drag per unit length of the cylinder and the difference $\delta\Phi$ between the electric potential at $x = +\infty$ and $x = -\infty$ (for fixed y). Except for a constant, the electric potential Φ is a single-valued function of position

$$[\Phi]_c = -\oint_C \mathbf{E}_s\, ds = 0, \tag{3.12}$$

for an arbitrary contour which may go through the cylinder. In particular,

$$\delta\Phi = \Phi(-\infty, y) - \Phi(\infty, y) = -\lim_{r\to\infty} \int_0^{\pi} rE_\theta\, d\theta = -\lim_{r\to\infty} \int_0^{-\pi} rE_\theta\, d\theta, \tag{3.13}$$

where E_θ is a tangential component of $\mathbf{E}$ along a large circle $x^2 + y^2 = r^2$ given by

$$E_\theta/(\mu HW) = -w\sin\theta + j_\theta/m = -w\sin\theta - (\partial h/\partial r)/m, \tag{3.14}$$

according to (2.14) and (2.15). Introducing (3.2) and (3.7), we obtain

$$\frac{\delta\Phi}{\mu HW} = \lim_{r\to\infty} \int_0^{\pm\pi} r\phi_\pm\, d\theta = \frac{\pi}{k} B_\pm. \tag{3.15}$$

Since $\delta\Phi$ is single valued,

$$B_+ = B_- = B. \tag{3.16}$$

On the other hand, the drag D per unit length of the cylinder is obtained by integrating the mechanical stress τ_{nz} and the Maxwell stress T_{nz} along an arbitrary contour C around the cylinder, i.e.

$$\begin{aligned}\frac{D}{\rho\nu W} &= -\frac{1}{\rho\nu W}\oint_C (\tau_{nz}+T_{nz})\,ds \\ &= -\frac{1}{\rho\nu W}\oint_C \left[\rho\nu\frac{\partial v_z}{\partial n}+\mu H H_z\cos(n,y)\right]ds \\ &= -\oint_C (\partial w/\partial n)\,ds + m\oint_C h\,dx. \end{aligned} \tag{3.17}$$

Choosing as C the above-mentioned large circle, and making use of (3.2)–(3.7) and (3.15)–(3.16), we get

$$D/(\rho\nu W) = \lim_{r\to\infty} m\int_0^{2\pi} r(\phi_+ + \phi_-)\,d\theta = 4\pi B. \tag{3.18}$$

Comparison of (3.15) and (3.18) yields

$$D/(\rho\nu W) = 2m\delta\Phi/(\mu H W) = 4\pi B, \tag{3.19}$$

or

$$D = 2\sqrt{(\rho\nu\sigma)}\,\delta\Phi\times\operatorname{sgn} H. \tag{3.20}$$

This is the final result, the relationship between drag and electric potential difference.

Before concluding this section, we add some remarks on the case of the insulating cylinder. Here, we can simplify the analysis by defining functions $F_\pm$ by

$$\phi_\pm = \tfrac{1}{2}(1\mp h_i)\,F_\pm. \tag{3.21}$$

The functions $F_\pm$ are solutions of (3.3) with conditions

$$F_\pm = 1 \quad \text{on } S \quad \text{and} \quad F_\pm = 0 \quad \text{at infinity}, \tag{3.22}$$

and thus satisfy all conditions except (2.32). This remaining condition is easily satisfied by taking

$$h_i = (Q_+ - Q_-)/(Q_+ + Q_-), \tag{3.23}$$

where

$$Q_\pm = -\oint_S (\partial F_\pm/\partial n)\,ds. \tag{3.24}$$

Then the viscous drag per unit length $D_f = D$ (there is no magnetic drag in this case) is given by

$$D/(\rho\nu W) = -\oint_S (\partial w/\partial n)\,ds = 2Q_+Q_-/(Q_+ + Q_-). \tag{3.25}$$

In the case of the symmetric configuration mentioned at the end of § 2, in which S is symmetric with respect to a generator (as in the case of an elliptic cylinder), (3.23) shows that h_i is zero because Q_+ is equal to Q_-. Then (3.25) reduces to

$$D/(\rho\nu W) = Q = Q_+ = Q_-. \tag{3.26}$$

Thus, the problem for an insulator has been reduced to a more familiar boundary-value problem of the type (3.3) and (3.22), (or to (3.27) and (3.28) below), and these solutions are easily transferable to our problem.

For example, we consider the case of the flat plate $|x| < a, y = 0$. Putting $\tilde{\phi}_+ = \frac{1}{2}\phi$ in (3.6) (i.e. $h_i = 0, F_+ = \phi \exp(ky)$ in (3.21)), equation (3.3) yields a Helmholtz equation for ϕ

$$(\nabla^2 - k^2)\phi = 0. \tag{3.27}$$

This leads to the same boundary-value problem as in Rayleigh's problem (Hasimoto 1951) for a non-conducting fluid, since

$$\phi = \exp(-ky) = 1 \quad \text{for} \quad y = 0 \quad \text{and} \quad |x| \leqslant a, \tag{3.28}$$

and

$$\phi = O(e^{-kr}) \quad \text{as} \quad r \to \infty. \tag{3.29}$$

We will study this case and the case of a perfectly conducting plate at some length in the following sections.

4. Flat plate of finite width: $|x| \leqslant a, \quad y = 0$

Introducing ϕ, determined by (3.27)–(3.29), into (3.2) we get

$$w = \phi \cosh ky, \tag{4.1}$$

$$h = -\phi \sinh ky = -w \tanh ky, \tag{4.2}$$

where we have used the symmetry of ϕ with respect to $y = 0$

$$\phi(x, y) = \phi(x, -y), \quad \text{i.e.} \quad \tilde{\phi}_+ = \tilde{\phi}_-. \tag{4.3}$$

In particular, at $y = 0$,

$$w = \phi \quad (= 1 \quad \text{for} \quad |x| < a), \quad h = 0, \tag{4.4}$$

$$\omega = \partial w/\partial y = \partial\phi/\partial y \quad (= 0 \quad \text{for} \quad |x| > a), \tag{4.5}$$

$$j_x = \partial h/\partial y = -k\phi, \quad j_y = -\partial h/\partial x = 0. \tag{4.6}$$

Equations (4.6), (2.14) and (2.15) show that the electric current density and the electric field on both sides of the insulating plate are given by

$$J_x = -\tfrac{1}{2}\sigma\mu HW = -\sigma E_x = \sigma E'_x, \quad E_y = E'_y = 0 \tag{4.7}$$

exactly, since $w = \phi = 1$ on the plate. The negative sign of σE_x represents the electromotive action of the plate, and assures the satisfaction of the condition (3.12).

Let us proceed to the case of a perfectly conducting flat plate. We put

$$\phi_\pm = \tfrac{1}{2}(\phi \mp \psi)\exp(\pm ky), \tag{4.8}$$

where

$$(\nabla^2 - k^2)\psi = 0. \tag{4.9}$$

The function ψ is antisymmetric with respect to $y = 0$

$$\psi(x, y) = -\psi(x, -y). \tag{4.10}$$

Then, from (3.2),

$$w = \phi \cosh ky - \psi \sinh ky, \tag{4.11}$$

$$h = -\phi \sinh ky + \psi \cosh ky. \tag{4.12}$$

In particular

$$w(x, 0) = \phi(x, 0), \tag{4.13}$$

$$h(x, 0) = \psi(x, 0) \quad (= 0 \quad \text{for} \quad |x| > a). \tag{4.14}$$

According to (4.13) we may use the same function ϕ as that in the insulating case. Also, on the plane $y = 0$,

$$\omega = \partial w/\partial y = \partial\phi/\partial y - k\psi \quad (= 0 \quad \text{for} \quad |x| > a), \tag{4.15}$$

$$j_x = \partial h/\partial y = -k\phi + \partial\psi/\partial y, \tag{4.16}$$

$$j_y = -\partial h/\partial x = -\partial\psi/\partial x \quad (= 0 \quad \text{for} \quad |x| > a). \tag{4.17}$$

Taking into account (2.16), (2.17), (2.30) and (4.17), we get the boundary conditions for ψ

$$\partial\psi/\partial y = k \quad \text{for} \quad |x| < a, \quad y = 0 \tag{4.18}$$

$$\psi = O(e^{-kr}) \quad \text{as} \quad r \to \infty. \tag{4.19}$$

We have now reduced the two flat-plate problems to two kinds of standard boundary-value problems involving the Helmholtz equation for ϕ and ψ.

For the sake of simplicity, we shall consider two important quantities from the practical point of view, i.e. the skin frictional drag $D_f(x)$ and the magnetic drag $D_m(x)$ at a point of the plate, denoting by suffixes I and C corresponding quantities for the insulating and perfectly conducting cases, respectively. The total drag obtained by integrating these drags is intimately related to the induction potential difference $\delta\Phi$ or wake strength B according to (3.19).

We obtain from (4.5) and (4.4)

$$D_{fI}(x)/(\rho\nu W) = -2\omega(x, +0) = -2(\partial\phi/\partial y)_{y=+0} \tag{4.20}$$

and

$$D_{mI}(x) = 0, \tag{4.21}$$

applying (3.17) on the surface element of the plate at x. In the same manner

$$D_{fC}(x)/(\rho\nu W) = -2(\partial\phi/\partial y)_{y=+0} + m\psi(x, +0) \tag{4.22}$$

and

$$D_{mC}(x)/(\rho\nu W) = -2m\psi(x, +0) \tag{4.23}$$

from (4.15) and (4.14). The drag $D_{mC}(x)$ is simply the force acting on the electric current $h(x, +0) - h(x, -0)$ in the perfectly conducting plate. Equations (4.20)–(4.23) afford an exact relation between the two cases

$$D_{fI}(x) = D_{fC}(x) + \tfrac{1}{2}D_{mC}(x) \quad \text{or} \quad D_I(x) = D_C(x) - \tfrac{1}{2}D_{mC}(x). \tag{4.24}$$

The solutions of our two plate problems have been discussed by many authors in many branches of mathematical physics. The following expansion formulae for small and large values of M are obtained from their work

$$-\frac{\partial}{\partial y}\phi(a\cos\alpha, +0) = \frac{1}{\sin\alpha}\left[\frac{D_I}{2\pi\rho\nu W} - \frac{M^2}{16}\left(1 - \frac{1}{2\Omega}\right)\cos 2\alpha - \frac{M^4}{256}\left\{\left(\frac{1}{3} + \frac{1}{2\Omega}\right)\cos 2\alpha + \left(\frac{1}{24} - \frac{1}{32\Omega}\right)\cos 4\alpha\right\} + \frac{M^6}{4096}\left\{\left(\frac{\Omega}{8} + \frac{13}{64} + \frac{11}{16\Omega} - \frac{1}{16\Omega^2}\right)\cos 2\alpha - \left(\frac{1}{40} + \frac{1}{32\Omega}\right)\cos 4\alpha - \left(\frac{1}{960} - \frac{1}{1152\Omega}\right)\cos 6\alpha\right\} + O(M^8)\right], \tag{4.25}$$

$$\frac{D_I}{\rho\nu W} = 2\pi\left[\frac{1}{\Omega}\left(1 - \frac{M^2}{16}\right) + \frac{M^4}{1024}\left(1 + \frac{3}{4\Omega} - \frac{1}{2\Omega^2}\right) + \frac{M^6}{49152}\left(1 + \frac{29}{12\Omega} + \frac{3}{2\Omega^2}\right) + O(M^8)\right] \tag{4.26}$$

$$= 2M + 2 - \frac{4}{\pi}[K_{01}(M) - K_{02}(M)] + O(e^{-2M}), \tag{4.26'}$$

$$-\psi(a\cos\alpha,+0)=\frac{M}{4\sin\alpha}\left[\frac{2D_{mC}}{\pi M^2\rho\nu W}-\cos 2\alpha+\frac{M^2}{16}\{(\Omega+\tfrac{5}{6})\cos 2\alpha-\tfrac{1}{12}\cos 4\alpha\}\right.$$
$$\left.-\frac{M^4}{256}\{(\Omega^2+\tfrac{11}{8}\Omega+\tfrac{33}{64})\cos 2\alpha-(\tfrac{1}{8}\Omega+\tfrac{13}{160})\cos 4\alpha+\tfrac{1}{320}\cos 6\alpha\}+O(M^6)\right], \tag{4.27}$$

$$\frac{D_{mC}}{\rho\nu W}=2\pi\left[\frac{M^2}{4}-\frac{M^4}{64}(\Omega+\tfrac{3}{4})+\frac{M^6}{1024}(\Omega^2+\tfrac{5}{4}\Omega+\tfrac{7}{16})+O(M^8)\right]. \tag{4.28}$$

$$=4M-4+\frac{8}{\pi}[K_{01}(M)+K_{02}(M)]+O(e^{-2M}), \tag{4.28'}$$

where
$$M=ma=2ka=\sqrt{\{\sigma/(\rho\nu)\}}\,\mu\,|H|\,a, \tag{4.29}$$

$$\Omega=-\gamma-\log(M/8),\quad \gamma=0{\cdot}5772\ldots\text{(Euler's const.)}, \tag{4.30}$$

$$K_{01}(M)=\int_M^\infty K_0(x)\,dx\sim\sqrt{\frac{\pi}{2M}}\,e^{-M}\left(1-\frac{5}{8M}+\frac{129}{128M^2}-\ldots\right), \tag{4.31}$$

$$K_{02}(M)=\int_M^\infty K_{01}(x)\,dx=M[K_1(M)-K_{01}(M)]$$
$$\sim\sqrt{\frac{\pi}{2M}}\,e^{-M}\left(1-\frac{9}{8M}+\frac{345}{128M^2}-\ldots\right). \tag{4.32}$$

We have used a result by Hasimoto (1951) for (4.25), and transformed Levine's result (1957) for Rayleigh's problem into the convenient form (4.26′), where the first two terms have been obtained by Howarth (1950) and by the author (Hasimoto 1951). Equation (4.27) has been calculated by use of the integro-differential equation

$$\left(\frac{\partial\psi}{\partial y}\right)_{y=0}=\frac{1}{\pi}\left(\frac{d^2}{dx^2}-k^2\right)\int_{-a}^{a}K_0(k\,|x-x_0|)\,\psi(x_0)\,dx_0=k, \tag{4.33}$$

or an integral equation

$$\int_{-a}^{a}K_0(k\,|x-x_0|)\,\psi(x_0)\,dx_0=-(\pi/k)(1-A\cosh kx) \tag{4.34}$$

for $\psi(x,0)$ and an unknown constant A subject to the condition

$$\psi(\pm a,0)=0, \tag{4.35}$$

which is found to be essentially the same as that discussed in diffraction theory (Bowkamp 1954). Equation (4.28′) was derived by use of Levine's technique (1957), initially applied to (4.26′), although the first two terms of (4.26′) can be easily determined from the results in the next section, where we also give the form of $(\partial\phi/\partial y)_{y=0}$ and $\psi(x,0)$ for large M. Table 1 and figure 2 give the numerical values of D_f and D_m calculated by these formulae.

We notice the following points.

(1) The matching of the two types of approximate formulae, especially for D_f, is good for intermediate values of M.

(2) $D_{fI}>D_{fC}$, but
$$D_I=D_{fI}<(D_f+D_m)_C=D_C. \tag{4.36}$$

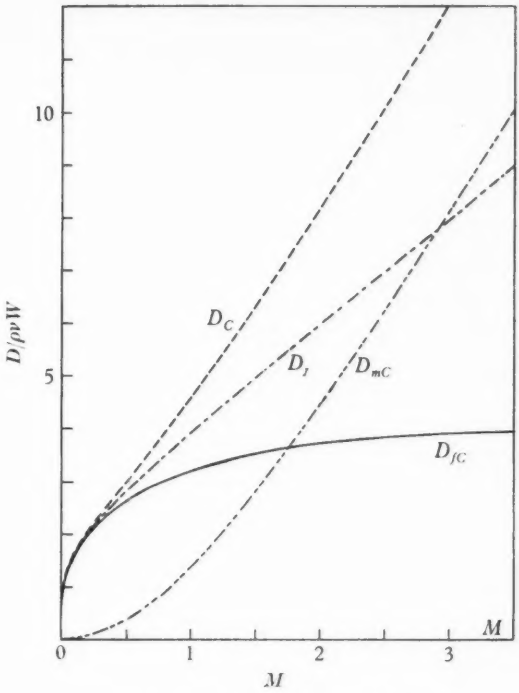

FIGURE 2. Total drag for the finite plate.

	Perfect conductor						Insulator	
	$D_f/(\rho\nu W)$		$D_m/(\rho\nu W)$		$D/(\rho\nu W)$		$D/(\rho\nu W)$	
M	Eqs. (4.28), (4.28′)						Eqs. (4.26), (4.26′)	
0·01	0·940	—	0·00016	—	0·940	—	0·940	—
0·05	1·395	—	0·00390	—	1·399	—	1·397	—
0·1	1·64	—	0·0167	—	1·66	—	1·65	—
0·2	1·98	—	0·062	—	2·04	—	2·01	—
0·4	2·45	—	0·24	—	2·69	—	2·57	—
0·6	2·79	—	0·53	—	3·32	—	3·05	—
0·8	3·04	—	0·91	—	3·96	—	3·50	—
1·0	3·24	—	1·38	—	4·62	—	3·93	3·93
1·2	3·39	$3·3_5$	$1·9_1$	$2·0_0$	5·30	$5·3_5$	4·35	4·35
1·4	$3·5_1$	$3·4_9$	$2·5_1$	$2·5_4$	$6·0_2$	$6·0_3$	4·76	4·76
1·6	$3·5_9$	$3·6_0$	$3·1_6$	$3·1_4$	$6·7_6$	$6·7_4$	5·17	5·17
1·8	$3·6_4$	$3·6_8$	$3·8_8$	$3·7_9$	$7·5_2$	$7·4_7$	5·58	5·58
2·0	$3·6_6$	$3·7_5$	—	$4·4_7$	—	$8·2_2$	5·99	5·99
2·4	—	3·84	—	5·89	—	9·74	—	6·79
2·8	—	3·90	—	7·39	—	11·29	—	7·60
3·0	—	3·92	—	8·15	—	12·07	—	8·00
3·2	—	3·95	—	8·92	—	12·86	—	8·39
3·6	—	3·96	—	10·48	—	14·44	—	9·20
4·0	—	3·97	—	12·05	—	16·03	—	10·00

TABLE 1. The total drag for a finite plate.

(3) For small M, D_{mC} is small since it is $O(M^2)$. In fact

$$D_{mC}/(\rho\nu W) = \tfrac{1}{2}\pi M^2 + O(M^4) \tag{4.37}$$

and, indeed, is so small that D_I and D_C are given by the same formula

$$D_I = D_C = 2\pi/\Omega + O(M^2). \tag{4.38}$$

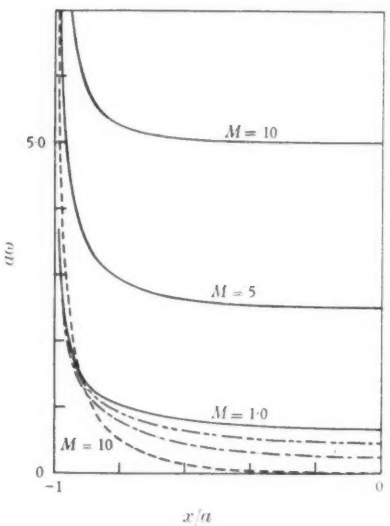

FIGURE 3. Non-dimensional vorticity distribution on the plate. —, Insulator. $a\omega_C$: — · · —, $M = 1$; — · —, $M = 5$; · · · · $M = 10$.

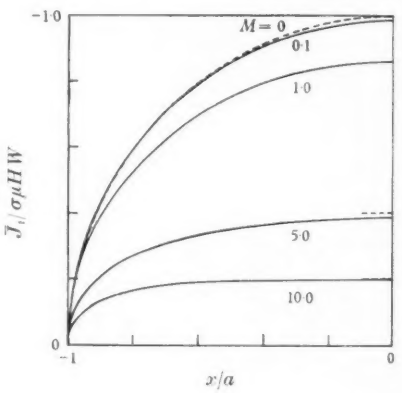

FIGURE 4. Electric current in the perfectly conducting plate.

This is explained by the fact that the current in the plate is so small that its effect on the field in the fluid is negligible.*

(4) For large M (e.g. $M > 3$), the following formulae give good approximations

$$D_I/(\rho\nu W) = 2M + 2, \tag{4.39}$$

$$D_{fC}/(\rho\nu W) = 4, \quad D_{mC}/(\rho\nu W) = 4M - 4. \tag{4.40}$$

Figures 3 and 4 show, respectively, the vorticity ω on the plate and the electric current $\bar{J}_i(x)$ in the perfectly conducting plate.

* We can easily show that (4.38) is valid for an arbitrary shape of cylinder cross-section and arbitrary ratio of σ_i/σ, if we take as $\frac{1}{2}a$ the electrostatic capacity c of this shape. The analogous results have been derived for Rayleigh's problem in non-conducting fluids, by Batchelor (1954) and by the author (1954). We note that ϕ_+ and ϕ_- are given by

$$2\phi_\pm = 1 - \tfrac{1}{2}\log(Z\bar{Z})/[-\gamma - \log(\tfrac{1}{4}mc)] + O(kr),$$

for small values of kr, where the domain outside of the cylinder is conformally mapped onto the region outside the unit circle $Z\bar{Z} = 1$ in the complex Z-plane, by use of the mapping function

$$x + iy = c\left(Z + \sum_{n=1}^{\infty} c_n Z^{-n}\right).$$

Then, (3.2) and (3.17) yield (4.38).

5. Flat plate of semi-infinite width

Let us consider the case of a flat plate of semi-infinite width at greater length, inasmuch as this case has simple exact solutions and affords an approximate, but clear, picture of the field for the finite plate at large M.

For convenience, we introduce the parabolic co-ordinates (ξ, η)

$$kx = \xi^2 - \eta^2, \quad ky = 2\xi\eta, \quad -\infty < \xi < \infty \quad (\eta \geqslant 0), \tag{5.1}$$

so that

$$kr = \xi^2 + \eta^2, \tag{5.2}$$

as suggested by Lamb's study (1932) of the sound diffraction problem. The coordinate η vanishes on the plate ($0 \leqslant x \leqslant \infty$, $y = 0$) and the coordinate ξ has opposite signs on the two opposite sides of the axis of x, and is zero on the negative x-axis (figure 5).

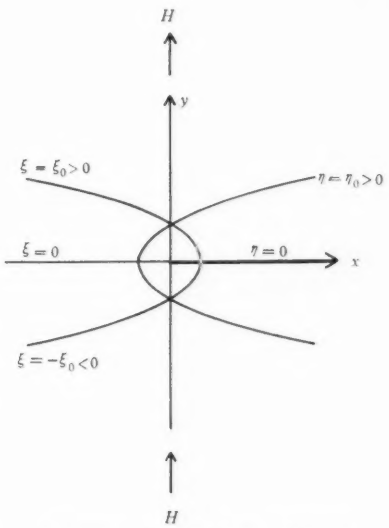

FIGURE 5. Parabolic co-ordinates.

Then (3.3) is transformed to

$$\left(\frac{\partial^2}{\partial\xi^2} + \frac{\partial^2}{\partial\eta^2} \mp 4\eta\frac{\partial}{\partial\xi} \mp 4\xi\frac{\partial}{\partial\eta}\right)\phi_\pm = 0 \tag{5.3}$$

which is satisfied by

$$\phi_\pm = E_0(\eta \mp \xi), \tag{5.4}$$

where E_0 is the complementary error function

$$E_0(\zeta) = \operatorname{erfc}\zeta = 1 - \operatorname{erf}\zeta = \frac{2}{\sqrt{\pi}}\int_\zeta^\infty e^{-\zeta^2}\,d\zeta. \tag{5.5}$$

We can construct from (5.4) two solutions of the Helmholtz equations which are symmetric and antisymmetric with respect to $y = 0$, taking into account (3.4), (3.6) and (5.1):

$$\left.\begin{matrix}\phi \\ \psi\end{matrix}\right\} = \tfrac{1}{2}[e^{ky}E_0(\eta + \xi) \pm e^{-ky}E_0(\eta - \xi)]. \tag{5.6}$$

Fortunately, these satisfy all the conditions required for ϕ and ψ in the previous section, if, by considering the infinite extent of the plate, we replace $|x| \leqslant a$ by $0 \leqslant x \leqslant \infty$ and $r \to \infty$ by $\eta \to \infty$ in (3.29) or (4.19). We can easily establish this solution by taking into account the symmetry of $E_0(\eta - \xi)$ and $E_0(\eta + \xi)$, and the results

$$E_0(-\xi) + E_0(\xi) = 2, \tag{5.7}$$

$$E_0(\zeta) \sim e^{-\xi^2}/(\sqrt{(\pi)}\,\zeta) \quad \text{or} \quad 2, \quad \text{as} \quad \zeta \to +\infty \quad \text{or} \quad -\infty, \tag{5.8}$$

$$\frac{\partial}{\partial y} E_0(\eta \pm \xi) = \frac{1}{2r}\left(\eta \frac{\partial}{\partial \xi} + \xi \frac{\partial}{\partial \eta}\right) E_0 \to -\sqrt{\frac{k}{\pi x}}\, e^{-\xi^2} \quad \text{as} \quad \eta \to 0. \tag{5.9}$$

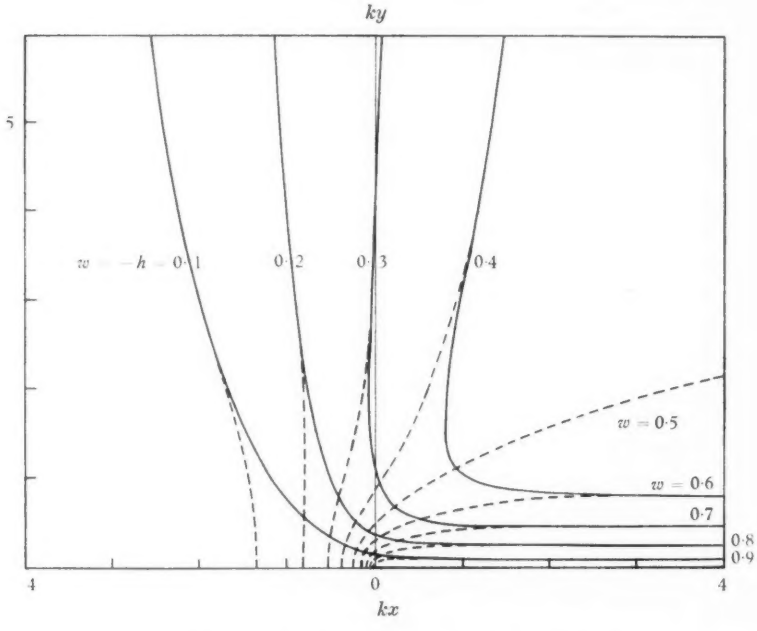

FIGURE 6. Field for the insulating semi-infinite plate.
- - - -, w = const.; —, h = const.

Let us proceed to the discussion of the exact solutions constructed in this way for the two extreme cases.

5.1. *The insulating plate*

From (4.1), (4.2) and (5.6) we get

$$\left.\begin{matrix} w \\ -h \end{matrix}\right\} = \frac{1}{2}\left\{\begin{matrix} \cosh ky \\ \sinh ky \end{matrix}\right\} [e^{ky} E_0(\eta + \xi) + e^{-ky} E_0(\eta - \xi)]. \tag{5.10}$$

Figure 6 shows the distribution of the isovels (w = const.) and electric current lines h = const. We have only to consider the positive y-plane since w is symmetric and h is antisymmetric with respect to $y = 0$.

From this analysis, the interesting points are as follows.

(1) There is a boundary layer on the plate, as shown by

$$\lim_{\xi\to\infty}\frac{w}{h} = \tfrac{1}{2}(e^{-m\eta}\pm 1) \tag{5.11}$$

for fixed positive values of η. It is interesting that the values of w and $-h$ tend to $\frac{1}{2}$ in a wide region outside this boundary layer.

(2) There is a transition region of vague parabolic shape for large ky between the above-mentioned region (core) and the undisturbed region represented by $\eta\to\infty$. This also is shown by (5.8) and

$$w = -h \to \phi_+ = \tfrac{1}{4}E_0(\zeta)+O(1/\sqrt{(kr)}) \quad \text{as} \quad \xi,\eta\to\infty, \tag{5.12}$$

where

$$\zeta = \eta-\xi, \quad y = \tfrac{1}{2}k[(x/\zeta)^2-(\zeta/k)^2]. \tag{5.13}$$

We note that the current lines coincide with isovels for large ky, where (3.10) is valid. On the line $x=0$ ($\xi=\eta$), we get

$$\left.\begin{matrix} w \\ -h \end{matrix}\right\} = \tfrac{1}{4}(1\pm e^{-m\eta})\,[1+e^{m\eta}\,E_0(2\sqrt{(ky)})] \sim \tfrac{1}{4}+O\left(\frac{1}{\sqrt{(ky)}}\right). \tag{5.14}$$

The value $\frac{1}{4}$ is the mean of their values; $\frac{1}{2}$ in the core, and zero in the undisturbed region. This region is rather narrow compared with the width of our plate and is shifted outward to the undisturbed region for moderate values of ky. We might call this region a shear layer.

(3) For $HW<0$, the main part of the electric current comes from $ky=\infty$, along isovels in the shear layer, and go into the other isovels in the plate boundary layer parallel to the plate for large kx. For $HW>0$, this direction is reversed.

(4) In the vicinity of the edge, isovels take parabolic shapes given by

$$1-w \sim 2\eta/\sqrt{\pi}. \tag{5.15}$$

Here, the electric current lines are almost parallel to the plate

$$h \sim -ky, \tag{5.16}$$

corresponding to (4.6), (4.7) and (5.11).

5.2. *The perfectly conducting plate*

Introducing (5.6) into (4.11) and (4.12) we get simple expressions

$$\left.\begin{matrix} w \\ -h \end{matrix}\right\} = \tfrac{1}{2}\,[E_0(\eta-\xi)\pm E_0(\eta+\xi)]. \tag{5.17}$$

This equation could have been constructed from (5.4) directly. Figure 7 shows the field in this case. We can notice the symmetry between w and $1-|h|$ with respect to the y-axis

$$w(x,y)+|h(-x,y)| = 1, \tag{5.18}$$

derived from (5.17), (5.7) and (5.1).

We may remark that:

(1) There is no boundary layer on the plate except near the edge $kx\ll 1$, and the fluid is moving with almost the same speed as the plate for a wide core region, as shown by

$$\lim_{\xi\to\infty} w \sim -\lim_{\xi\to\infty} h = 1 \quad \text{for fixed } \eta. \tag{5.19}$$

(2) The strengths of the vorticity and the current in the shear layer have values twice those of the insulating case, and the shear layer is more distinct than that case. This is shown by (5·8) and

$$w \sim -h \sim \tfrac{1}{2}E_0(\xi) \quad \text{for} \quad \xi, \eta \gg 1. \tag{5.20}$$

In the distinct centre of this layer ($x = 0$) w and $-h$ have values which are the mean of their values in the core and their values in the undisturbed region, i.e. $\frac{1}{2}$.

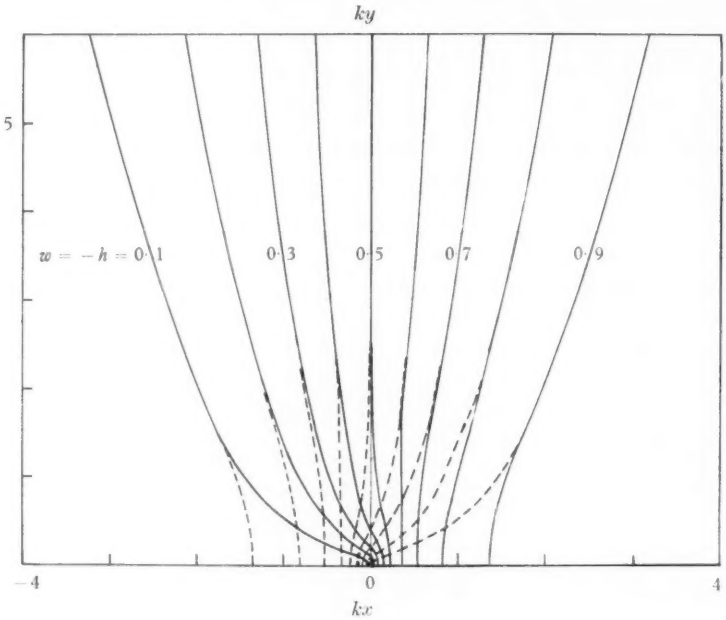

FIGURE 7. Field for the perfectly conducting semi-infinite plate.
- - - -, w = const.; —, h = const.

(3) The electric current from the shear layer enters the plate perpendicularly, almost at the edge of the plate, and flows in the plate to $kx = +\infty$, if HW is negative. This electric current and the induced magnetic field on the plate are given by

$$\left.\begin{aligned} j_y &= -\omega = \sqrt{\{k/(\pi x)\}}\exp(-kx), \\ -h &= 1 - E_0(\xi) = \operatorname{erf}(\sqrt{(kx)}). \end{aligned}\right\} \quad \text{for} \quad y = +0. \tag{5.21, 5.22}$$

Equations (2.13), (2.15) and (5.22) show that the total electric current $\bar{J}_i$ in the plate is given by

$$\bar{J}_i/(\sigma\mu HW) = m^{-1}[h(x, +0) - h(x, -0)] = -(2/m)\operatorname{erf}\sqrt{kx} \tag{5.23}$$

which grows from zero at $x = 0$ to $2\sqrt{(\rho\nu\sigma)}\,W$ at $kx = \infty$ gathering all the electric currents from the fluid (for $HW < 0$) (figure 4). $\sqrt{(\rho\nu\sigma)}\,W$ is equal to the total current in the upper shear layer $m^{-1}\sigma\mu HW[h_{(x=-\infty)} - h_{(x=+\infty)}]$.

(4) In the vicinity of the edge, isovels and current lines form orthogonal parabolic nets

$$1-w \sim 2\eta/\sqrt{\pi}, \quad h \sim -2\xi/\sqrt{\pi}, \tag{5.24}$$

which should be compared with (5.15) and (5.16).

6. Discussion for the cylinder of finite width at large Hartmann number

The quantities on the plate $y = 0$ derived from the previous section are simple expressions and are useful in the rest of the paper. They are given in table 2, wherein the lower sign of $\mp$ denotes the value for $y = -0$ (the under side of the plate). The following notation is also used in Table 2.

$$\left.\begin{aligned} E_n &= \int_\xi^\infty E_{n-1}(\xi)\,d\xi, \quad \xi = \sqrt{(k|x|)}, \\ E_1 &= \frac{1}{\sqrt{\pi}}e^{-\xi^2} - \xi E_0 \sim \begin{cases} 1/\sqrt{\pi} & \text{for} \quad \xi = 0, \\ \frac{1}{2}e^{-\xi^2}/(\sqrt{(\pi)}\,\xi^2) & \text{for} \quad \xi \gg 1, \end{cases} \\ E_2 &= \tfrac{1}{4}E_0 - \tfrac{1}{2}\xi E_1 \sim \begin{cases} \frac{1}{4} & \text{for} \quad \xi = 0, \\ \frac{1}{4}e^{-\xi^2}/(\sqrt{(\pi)}\,\xi^3). \end{cases} \end{aligned}\right\} \tag{6.1}$$

	(I) Insulator		(II) Perfect conductor	
	$x<0$	$x>0$	$x<0$	$x>0$
w	E_0	1	E_0	1
h	0	0	0	$\mp(1-E_0)$
ω	0	$\mp(k+\sqrt{(k/x)}\,E_1)$	0	$\mp\sqrt{\{k/(\pi x)\}}\,e^{-kx}$
j_x	$-kE_0$	$-k$	$-\sqrt{(k/\lvert\pi x\rvert)}\,e^{-k\lvert x\rvert}$	0
j_y	0	0	0	$-\omega$
$E_x/(\mu HW)$	$\frac{1}{2}E_0$	$\frac{1}{2}$	E_0+j_x/m	1
$E_y/(\mu HW)$	0	0	0	$-\omega/m$
$\dfrac{\Phi-\Phi(-\infty,0)}{\mu\mathcal{H}W}$	$\dfrac{1}{m}(2E_2-E_0)\leqslant 0$	$-\dfrac{1}{2m}(1+mx)$	$\dfrac{1}{m}(4E_2-E_0)\leqslant 0$	$-x$
$D_{fx}/(\rho\nu W)$	0	$1+mx-4E_2$	0	$2-2E_0$
$D_{mx}/(\rho\nu W)$	0	0	0	$2mx-2-(8E_2-4E_0)$

TABLE 2. Quantities on the semi-infinite plate.

Equations (6.1)–(6.3) are tabulated in the book of Carslaw & Jaeger (1947). D_{fx} is the total frictional drag on the plate between o and x, and D_{mx} is the corresponding magnetic drag

$$D_{fx} = -2\rho\nu W\int_0^x \omega\,dx, \tag{6.2}$$

$$D_{mx} = -2m\rho\nu W\int_0^x h\,dx. \tag{6.3}$$

Except for Φ and D we can separate the quantities on the plate into two terms: one which is constant everywhere (e.g. k in the ω term) and the other which is significant only at the edge and tends to zero rapidly as $kx \to \infty$ (e.g. $\sqrt{(k/x)}\,E_1$, in the ω term). If we limit our plate by another edge at $x = 2a$, and superpose the contribution due to this edge, we may obtain a picture of the field near the plate of finite width $2a$ at large Hartmann number $M = ma$. In the quantities D and Φ,

the integrals of ω, h and E_x, the contributions due to an edge appear as constants. For example, the total frictional drag and the total magnetic drag for the finite plate are

$$D_{fI}/(\rho\nu W) \sim 2M+1+1 = 2M+2, \quad D_{mI} = 0 \tag{6.4}$$

in the case of an insulator, and

$$D_{fC}/(\rho\nu W) \sim 2+2 = 4, \quad D_{mC}/(\rho\nu W) = 4M-2-2 = 4M-4 \tag{6.5}$$

for a perfect conductor, where we have added to $D_{f,2a}$ etc., as they appear in the table, the contributions due to the presence of another edge. We have neglected also small terms like E_n. Equations (6.4) and (6.5) are identical with (4.39) and (4.40). We can also show the validity of (3.20), (4.7), (4.24), etc., by the general theory, using Table 2 and the above argument for the edge correction. For example

$$\delta\Phi_I/(\mu HW) = a+1/m = D_I/(2m\rho\nu W), \tag{6.6}$$

$$\delta\Phi_C/(\mu HW) = 2a = D_C/(2m\rho\nu W) \tag{6.6'}$$

(compare this with (3.20)).

From these results and the results of the previous sections we may easily build up a picture of the field at large but finite M. In the following, we proceed to show that our picture is applicable generally to the field around a cylinder ($|x| \leqslant a, f_-(x) < y < f_+(x) f_\pm(x) = O(a)$) at extremely large $M = ma$, if we are not concerned with the fine structure of the field (e.g. at an edge $x = a$ on S). We may suppose, according to (2.11) that the fluid has low viscosity and high conductivity and that the applied field is strong. We also assume HW to be negative for convenience.

6.1. *Perfectly conducting cylinder*

In this case the cylinder carries magnetic lines of force frozen in it corresponding to the induction current in the x-direction accompanying its motion. This movement of magnetic lines will drag the fluid in the region $|x| < a, y < \infty$, (i.e. the core) with the same velocity as the cylinder, since the fluid is highly conducting. Then, putting $m = \infty$ in (2.14), we find that the electric field in this region is $E_x = \mu HW$, $E_y = 0$. Taking into account (3.13) and the fact that $E = 0$ in the undisturbed region $|x| > a$, we find that (6.6′) is valid in our general case. The viscous drag is also negligible.

We may note that this picture is perfectly consistent with the fundamental equations and boundary conditions (2.8), (2.9) and (2.30) in the limit of $m \to \infty$, except for the conditions at $y = \infty$ and $|x| = a$. By adding to this picture wakes ((3.7′), (3.15) and (3.16)) for $y \to \infty$, and shear layers of thickness $O(\sqrt{(ky)}/k) = O(\sqrt{(y/m)})$ (see (5.20)) due to the presence of the viscosity and the finite conductivity, we can satisfy all the conditions required. Taking into account (3.2), (3.10) and $w = 1$, valid in the core, we find that $h = 1$ in the upper core. According to this result, the electric current in the core is negligibly small compared with the current in the cylinder starting from an edge at $x = -a$ and goes into the other edge at $x = a$, owing to the assumption $\sigma_i/\sigma = \infty$. We find that this current forms a closed circuit around the core. This circuit consists of the cylinder (playing the role of a motor with terminals at $x = \pm a$), shear layers (across which h jumps from 0 to ∓ 1) and wakes at infinity (where current lines coincide with isovels elongated in the direction of the applied field).

6.2. *Insulating cylinder*

In this case there is no induction current in the cylinder itself. However, the electric current is induced in the fluid dragged by the cylinder through viscosity and confined in $|x| < a$ due to the strong magnetic field. This current will form surface currents of thickness $O(1/[m\cos(n,y)])$ (Shercliff 1953) from $x = -a$ to $x = a$ (figure 8). This surface current will retard the velocity of the fluid and will yield a boundary layer in which the velocity changes from the speed of the cylinder to a core speed which is a definite fraction of the cylinder speed. The field near the edge $|x| < a$ will be complicated in general, on account of the interaction of the boundary layer and shear layer, and will be inflated a little outwards. The general features of the field will be the same as those in the case of a perfect conductor (or the case of a plate in §§ 5 and 6), if we consider the boundary-current layer to be included in the cylinder.

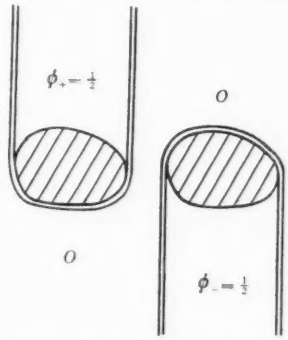

FIGURE 8. Field near the insulating cylinder for extremely large M.

We may show that these features are consistent with the fundamental equations as $m \to \infty$, if we take as the quantities in the core

$$w = \tfrac{1}{2}, \quad h = \mp\tfrac{1}{2}, \tag{6.7}$$

which yield also (6.6), if we neglect small terms $o(ma)$ and take into account (2.14) and (3.13). It is convenient to start from (3.3) and (3.22). Letting $m \to \infty$, we get

$$\phi_+ = \tfrac{1}{2}(1-h_i) \quad \text{for} \quad \infty > y \geqslant f_-(x) \quad \text{and} \quad |x| < a, \tag{6.8}$$

$$= 0 \quad \text{for} \quad y = \infty, \quad \text{or} \quad |x| > a \quad \text{or} \quad y < f_-(x) \tag{6.8'}$$

(approximation of geometrical optics). The field given by (6.7) (the field in the upper core region and on the cylinder) is connected with the outside undisturbed region given by (6.7) through the wake, the shear layers, and a boundary layer $\phi_+ = \frac{1}{2}(1-h_i)\exp[-mn\,|\cos(n,y)|]$ on the lower surface of the cylinder (figure 8). A similar solution is obtained for ϕ_- and yields, with ϕ_+, (6.7). By taking a rectangular circuit around the cylinder in equation (3.12), we find that h_i is $o(ma)$.

6.3. *A plate of small thickness* $2b$ ($kb \ll 1$) *and finite conductivity*

The fields in the core obtained so far seem to be independent of the finite width of the cylinder. The dependency on the finite conductivity is also not clear. As an illustration, we consider the region of the plate far from the edge, where every quantity will be independent of x. In this case $N(P_0; P)$ of (2.26) is given approximately by

$$N(P_0; P) \sim -\tfrac{1}{2}\delta(x_P - x_0)\,|\,y_P - y_0\,|. \tag{6.9}$$

Then

$$h(P_0) = \pm\,(\sigma_1 b/\sigma)\,(\partial h/\partial y)_{P_0}, \tag{6.10}$$

approximately, where the first integrals in (2.28) and (2.29) vanish by symmetry. Equation (6.10) can also be obtained from (2.18) and (2.20) by assuming a uniform current, i.e. constant $\partial h_i/\partial y$, in the plate and putting $h_i(P_0)$ equal to $b(\partial h_i/\partial y)$. We find that (4.11)–(4.17) and (4.24) are also valid in this case.

According to table 2, (6.10) is satisfied for large kx by taking a weighted mean of I and II (*c*)

$$(1+\beta)\,h = h_I + \beta h_{II}, \quad (1+\beta)\,w = w_I + \beta w_{II}, \tag{6.11}$$

where

$$\beta = \sigma_i kb/\sigma, \tag{6.12}$$

if we put the x-axis on the upper surface of the plate. Then,

$$\left.\begin{matrix} w \\ -h \end{matrix}\right\} = \frac{1}{2(1+\beta)}\left[1+2\beta \pm e^{-my}\right] \quad (mx \to \infty,\ y > 0). \tag{6.13}$$

which gives for the fields in the core

$$w_{\text{core}} = -h_{\text{core}} = \tfrac{1}{2}(1+2\beta)/(1+\beta). \tag{6.14}$$

Our perfectly conducting infinitely thin plate is the limiting case in which b is very small but σ_i/σ is extremely large (figure 9).

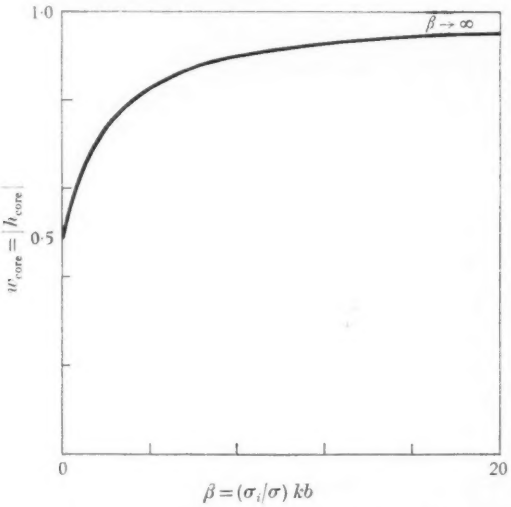

FIGURE 9. Core velocity w_{core} *vs* $(\sigma_i/\sigma)\,kb$.

Let us compare these solutions with the corresponding final stationary solutions in Rayleigh's problem for an infinite flat plate

$$Gw = 1+2\beta+\sqrt{(\kappa/\nu)}\,e^{-my}, \quad -G\sqrt{(\nu/\kappa)}\,h = 1+2\beta-e^{-my} \tag{6.15}$$

where

$$G = 1+\sqrt{(\kappa/\nu)}+2\beta, \quad (y > 0). \tag{6.16}$$

We find that:

(1) In general, the two results do not coincide with each other, although they do not contain the width of the plate explicitly. This discrepancy should be reduced to the existence of shear layers in our problem. These layers originate at the edges of the plate and yield finite jumps of field quantities. In the case of

Rayleigh's problem we have no such edges in space, although the time $t = 0$ might play the same role.

(2) It is a remarkable fact that these two results coincide, if the magnetic Prandtl number is 1, i.e. if $\nu = \kappa$. This is the case in which equipartition of the induced magnetic energy and the kinetic energy of the fluid is attained far from the plate (see (3.11)). This is the same feature as that of the wave of finite amplitude in the non-viscous and perfectly conducting fluid (Walén 1942).

In conclusion the author expresses his cordial thanks to Prof. F. H. Clauser and Prof. L. S. G. Kovasznay for their useful suggestions and encouragement, and also to Prof. R. R. Long for his kind help in the revision of the manuscript. The author has been supported by the International Cooperation Administration under the visiting research programme administered by the National Academy of Sciences of U.S.A.

REFERENCES

Batchelor, G. K. 1954 *Quart. J. Mech. Appl. Math.* **7**, 179.
Bleviss, Z. O. 1958 *J. Aero. Sci.* **25**, 601.
Bowkamp, C. J. 1954 *Rep. Prog. Phys.* **17**, 35.
Carslaw & Jaeger 1947 *Conduction of Heat in Solids.* Oxford University Press.
Chang, C. C. & Yen, J. T. 1959 *J. Phys. Fluid*, **2**, 393.
Hartmann, J. 1937 *Math.-Fys. Medd.* **15**, no. 6.
Hasimoto, H. 1951 *Proc. 1st Japan. Nat. Congress Appl. Mech.* (1951) p. 447.
Hasimoto, H. 1954 *J. Phys. Soc. Japan*, **9**, 611.
Howarth, L. 1950 *Proc. Camb. Phil. Soc.* **46**, 127.
Kakutani, T. 1958 *J. Phys. Soc. Japan*, **13**, 1504.
Lamb, H. 1932 *Hydrodynamics*, 6th ed. Cambridge University Press.
Levine, H. 1957 *J. Fluid Mech.* **2**, 145.
Resler, E. L. Jr. & Sears, W. R. 1958 *J. Aero. Sci.* **25**, 235.
Rossow, V. J. 1957 NACA, TN, 3971.
Shercliff, J. A. 1953 *Proc. Camb. Phil. Soc.* **49**, 136.
Shercliff, J. A. 1956 *J. Fluid Mech.* **1**, 644.
Walén, C. 1944 *Ark. Mat. Astr. Fys.* **30**A, 15.

On the motion of a non-conducting body through a perfectly conducting fluid

By K. STEWARTSON
Department of Mathematics, Durham University, Durham

(Received 24 September 1959)

The motion of bodies in a direction parallel to an applied magnetic field and through a perfectly conducting fluid is considered. It is shown that the perturbation in the state of the fluid cannot remain small except in the particular case when the velocity U of the body is much smaller than that of the Alfvén waves in the fluid. In this case, however, the perturbation is not confined to the neighbourhood of the body, and extends to infinity inside planes which touch the body and are parallel to the undisturbed magnetic field. In addition the body experiences a drag.

1. Introduction

In a previous paper (Stewartson 1956) the motion of a sphere through a conducting fluid in the presence of a strong magnetic field was considered, attention being focused on the ultimate flow pattern assuming that it is steady. It was found that the magnetic field is completely undisturbed but that the velocity field is cylindrical, being independent of the co-ordinate in the direction of the magnetic field. Further, the cylinder C circumscribing the sphere and having its generators parallel to the magnetic field separates two regions with different flow properties: for example, inside C the fluid moves with the sphere as if solid.

The chief assumptions in this theory are that the sphere is a perfect conductor, that the fluid velocity is small compared with the Alfvén velocity and that the magnetic Reynolds number is small. In particular the theory could not apply to a perfectly conducting fluid. The reason for this limitation is that if both the body and the fluid are perfect conductors there is nothing to prevent the build-up of current in the fluid until the magnetic field is seriously perturbed; accordingly, the implicit assumption of small disturbances in the magnetic field is invalidated.

If, however, the *body* is a non-conductor no such difficulty arises for it radiates Alfvén waves into the fluid which serve to control the build-up of current and, in all probability, to keep the disturbances small. It is possible therefore to apply the general method developed earlier to these problems, which are of interest at the present time.

In the present paper we shall make a start on this programme concentrating attention solely on two-dimensional flows in an aligned magnetic field, i.e. the direction of motion of the body relative to the fluid at infinity is parallel to the magnetic field at infinity. First, in § 2 the equations of motion of a perfectly conducting fluid are reduced to a single equation for the stream function ψ

of the motion but which contains two arbitrary functions of ψ. If these functions are constants, ψ satisfies Laplace's equation and a theory of thin aerofoils based on this equation has been developed by Sears & Resler (1959). This theory is discussed in the light of the present work in § 7.

In § 3 the boundary conditions are set out, particular attention being paid to the circumstances in which it is legitimate to require continuity of the tangential component of the magnetic field across the surface of the body. The general unsteady motion of the fluid around a thin aerofoil is analysed in § 4 on the assumption that the disturbances are small. It is shown that if ultimately the flow becomes steady and the perturbations from the undisturbed state are small, the effect of the body on the fluid is non-vanishing at infinity in general. However, on applying the general properties of the ultimate steady flow to determine the flow pattern round a thin aerofoil a contradiction is found because the magnetic field inside the body is seriously affected and with it the velocity field ahead and behind the body. Accordingly, we must conclude that the perturbations if ultimately steady cannot have remained small. There remains, however, one special case, that of a strong magnetic field in which the fluid velocity is in general much smaller than the Alfvén velocity. It turns out that the small perturbation theory can be applied here without contradiction because the fluid velocity and not merely its perturbation component may be assumed small. In § 6 this problem is considered and a full solution obtained for a circular cylinder; other bodies, including thin aerofoils, may be treated if desired. It is concluded that the magnetic field is only slightly disturbed except at two points, but that the magnetic field at infinity is no longer uniform. Further, the fluid inside the planes, which touch the cylinder and are parallel to the undisturbed magnetic field, moves with the cylinder as if solid; the fluid outside them is at rest. It is noted that many of the features of the motions described earlier (Stewartson 1956) are repeated here: the differences may be ascribed to the finite conductivity of the fluid in the earlier problem.

2. Equations of motion

The equations governing the motion of an incompressible fluid of density ρ, permeability unity, electrical conductivity σ and kinematic viscosity ν are

$$\operatorname{div} \mathbf{q} = 0, \tag{2.1}$$

$$\frac{\partial \mathbf{q}}{\partial t} - \mathbf{q} \wedge \operatorname{curl} \mathbf{q} = -\operatorname{grad}\left(\frac{p}{\rho} + \tfrac{1}{2}\mathbf{q}^2\right) + \frac{1}{4\pi\rho}(\operatorname{curl} \mathbf{H} \wedge \mathbf{H}) + \nu\nabla^2\mathbf{q}, \tag{2.2}$$

$$\frac{\partial \mathbf{H}}{\partial t} - \operatorname{curl}(\mathbf{q} \wedge \mathbf{H}) = \frac{1}{4\pi\sigma}\nabla^2\mathbf{H}, \tag{2.3}$$

where $\mathbf{q}$ is the velocity of the fluid, $\mathbf{H}$ the magnetic field and p the pressure. The units are Gaussian. In these equations it is assumed that the effects of the flow of charged particles and of the temporal variation of the displacement vector on the current are negligible. Once the initial uniform magnetic field has been set up, these assumptions can be justified in the types of flow considered here.

Consider the particular case of the steady two-dimensional flow of a perfectly conducting inviscid fluid. If, in addition, the velocity of the fluid and the

magnetic field are parallel at infinity, equations (2.1)–(2.3) may be formally simplified. For, using an orthogonal Cartesian triad $Oxyz$ as frame of reference and taking $\mathbf{q}$, $\mathbf{H}$ to be parallel to the plane $z = 0$, we may write, from (2.1),

$$u = \frac{\partial \psi}{\partial y}, \quad v = -\frac{\partial \psi}{\partial x}, \tag{2.4}$$

where $\mathbf{q} = (u, v, 0)$ and ψ is a stream function. Then from (2.3), since $\sigma = \infty$,

$$\mathbf{q} \wedge \mathbf{H} = A\mathbf{k},$$

where $\mathbf{k}$ is a unit vector parallel to the z-axis and A is a constant scalar. Further, since $\mathbf{q}$ is parallel to $\mathbf{H}$ at infinity, $A = 0$, whence

$$\mathbf{H} = \alpha \mathbf{q}. \tag{2.5}$$

Here α is a scalar function of position, which may be shown to be a function of ψ only by the use of the equation $\operatorname{div} \mathbf{H} = 0$. On substituting into (2.2) and setting $\nu = 0$, we obtain

$$-\mathbf{q} \wedge \operatorname{curl} \mathbf{q} = -\operatorname{grad}\left(\frac{p}{\rho} + \tfrac{1}{2}\mathbf{q}^2\right) + \frac{\alpha(\psi)}{4\pi\rho}\{\alpha(\psi) \operatorname{curl} \mathbf{q} - \alpha'(\psi)\, \mathbf{q} \wedge \operatorname{grad} \psi\} \wedge \mathbf{q},$$

i.e.

$$\left\{\left(1 - \frac{\alpha^2}{4\pi\rho}\right)\nabla^2\psi - \frac{\alpha\alpha'}{4\pi\rho}\mathbf{q}^2\right\} \operatorname{grad} \psi = \operatorname{grad}\left(\frac{p}{\rho} + \tfrac{1}{2}\mathbf{q}^2\right),$$

so that

$$\left(1 - \frac{\alpha^2}{4\pi\rho}\right)\nabla^2\psi = \frac{\alpha\alpha'}{4\pi\rho}(\operatorname{grad} \psi)^2 + \beta(\psi), \tag{2.6}$$

where $\beta(\psi)$, like $\alpha(\psi)$, is an arbitrary function of ψ which must be determined before (2.6) can be solved for ψ.

Suppose now that at infinity upstream the velocity is uniform with components $(U, 0, 0)$ and that the magnetic field is uniform with components $(H_\infty, 0, 0)$. Then

$$\alpha(\psi) = H_\infty / U, \quad \beta(\psi) = 0, \tag{2.7}$$

since $\psi \to Uy$ as $x \to \infty$, and hence

$$\nabla^2 \psi = 0 \tag{2.8}$$

on all streamlines starting from an infinite distance upstream. Then if we can be sure that no streamline in the flow is closed and that none starts and ends at an infinite distance downstream, we may conclude that the motion of the fluid is exactly the same as when the magnetic field is absent and that the magnetic lines of force coincide with the streamlines. In addition as may be seen from the next section, the boundary conditions on a fixed solid body, consisting of non-magnetic insulating material, are all satisfied because the magnetic field is tangential to it on its surface.

However, we have no guarantee that in any steady motion which can be set up from rest $\alpha(\psi)$ must be constant, nor can we be sure that every streamline in the flow field starts from an infinite distance upstream. If the fluid is set into motion with constant velocity $(U, 0, 0)$ at infinity and moves past a fixed obstacle, the velocity field at $t = 0+$ will certainly be irrotational. If in addition a uniform magnetic field $(H_\infty, 0, 0)$ has been applied, at infinity the magnetic

field will still be uniform at $t = 0+$. Hence, curl $(\mathbf{q} \wedge \mathbf{H}) \neq 0$ at $t = 0+$ so that $\mathbf{H}$ must begin to change. Part of this change is accounted for by the convection of the magnetic field by the fluid and part by the Alfvén waves set up to ensure that the new magnetic field satisfies the boundary conditions at the body. These waves start at the body and move relative to the fluid with a velocity

$$\frac{|\mathbf{H}|}{(4\pi\rho)^{\frac{1}{2}}}. \tag{2.9}$$

Accordingly downstream of the body these waves can be expected to reach infinity where, unless their strength has declined to infinitesimal proportions, they will modify the flow and disturb the values of α, β assumed in (2.7). It is conceivable, for example, that they could cause a reversed flow behind the body. A similar argument holds upstream of the body except that the absolute velocity of the Alfvén waves is reduced, since they are being propagated against the direction of motion of the fluid. If, however,

$$U < \frac{H_\infty}{(4\pi\rho)^{\frac{1}{2}}}, \tag{2.10}$$

we can expect them to reach infinity upstream and again they may distort the values of α, β leading to a rotational motion of the fluid everywhere. On the other hand, if

$$U > \frac{H_\infty}{(4\pi\rho)^{\frac{1}{2}}}, \tag{2.11}$$

Alfvén waves can only penetrate to infinity upstream by a more indirect process, since in the region where the flow is almost undisturbed their relative velocity is too small to permit any penetration in the upstream direction. Hence at any stage the velocity field ahead of the furthest point hitherto reached by the Alfvén wave must have been seriously weakened by the presence of the body before the waves can penetrate further. This requirement seems to be too stringent and it appears reasonable to conjecture that, on the streamlines which come from infinity upstream, (2.8) holds with (2.11). These streamlines need not cover the whole region outside the body, however, and the possibility of closed streamlines near the forward stagnation point and of reversed flow behind the body cannot be excluded.

In view of the doubts which have been expressed about the validity of using (2.8) to describe the whole field of flow, it is worth discussing in a particular case the way in which the motion develops as t increases and the ultimate motion which is produced as $t \to \infty$. Before doing this, however, we shall discuss the appropriate boundary conditions which are not all immediately obvious.

3. Boundary conditions

We consider the problem of a fixed body in a perfectly conducting inviscid fluid which at time $t = 0$ is given a velocity U at infinity in the direction of x increasing. At the same or earlier time a magnetic field of magnitude H_∞ is imposed in the same direction. The following boundary conditions can be written down at once. First, at $t = 0+$ the velocity field is the irrotational field which

would be appropriate to this problem if there were no magnetic field. The magnetic field is still uniform and of magnitude H_∞ at $t = 0+$. Secondly, at an infinite distance from the body

$$\mathbf{q} \to (U, 0, 0), \quad \mathbf{H} \to (H_\infty, 0, 0) \tag{3.1}$$

at any *finite* time t, since all disturbances start from the body. This does *not* imply that (3.1) holds at an infinite time.

In order to ascertain the correct boundary conditions at the body some care is needed. We shall suppose that the body is composed of a non-magnetic, non-conducting material so that it is not a source of magnetic field and in it $\sigma = 0$. Two conditions at the surface of the body, namely, that the normal components of the magnetic field and of the velocity must be continuous and zero, respectively, are clear either from the equation of continuity or on physical grounds. If the normal component of the magnetic field vanishes on the body then there is no restriction on the tangential components of the magnetic field, the reason being that surface currents cannot be dispersed. In general, however, we cannot assume that the normal component of the magnetic field is zero at the body and we shall obtain the conditions on the tangential components when it does not vanish.

If the boundary of a perfectly conducting fluid is free it has already been shown (Stewartson 1957) that the tangential component of the magnetic field must be continuous. An initial forced discontinuity is immediately dispersed, travelling into the fluid as an Alfvén wave. This result was proved by considering an inviscid fluid of large but finite conductivity σ and proceeding to the limit $\sigma \to \infty$. There was no need to assume that the fluid had a small coefficient of kinematic viscosity ν and to allow $\nu \to 0$ independently because viscous effects in this problem are of the second order. The reason is that the adjustment of the velocity field to preserve a continuous tangential component of stress at the boundary is vanishingly small as $\nu \to 0$. At a solid boundary, however, viscous effects may matter because the appropriate condition is that $\mathbf{q} = 0$ at the boundary. Hence as $\nu \to 0$ a boundary layer in $\mathbf{q}$ must develop which may have serious effects on the magnetic field. The mutual effects of the velocity and magnetic fields can be determined from the following problem of steady motion.

A fluid of conductivity σ and kinematic viscosity ν is in contact with a fixed solid insulator along the plane $x = 0$. In the solid, which occupies the region $x < 0$, the magnetic field is $(H_0, H_-, 0)$ and in the fluid the magnetic field is $(H_0, h, 0)$ and the velocity field is $(0, v, 0)$. In the fluid at large distances from the solid $v \to U$, $h \to H_+$. The motion is one-dimensional so that v, h are functions of x only; all other quantities being constant. The equations governing the motion of the fluid, (2.1)–(2.3), then reduce to

$$-H_0 \frac{\partial v}{\partial x} = \frac{1}{4\pi\sigma} \frac{\partial^2 h}{\partial x^2}, \quad -\frac{H_0}{4\pi\rho} \frac{\partial h}{\partial x} = \nu \frac{\partial^2 v}{\partial x^2}. \tag{3.2}$$

The appropriate boundary conditions are that

$$\left.\begin{aligned} v \to U, \quad h \to H_+ \quad &\text{as} \quad x \to \infty +, \\ v = 0, \quad h = H_- \quad &\text{as} \quad x \to 0, \end{aligned}\right\} \tag{3.3}$$

since for a fluid of *finite* conductivity all components of the magnetic field are continuous at its boundary. The solution of (3.2) subject to (3.3) is

$$\left.\begin{aligned} h &= H_+ + (H_- - H_+)\exp\left\{-H_0 x\left(\frac{\sigma}{\rho\nu}\right)^{\frac{1}{2}}\right\}, \\ v &= \frac{H_+ - H_-}{4\pi(\rho\nu\sigma)^{\frac{1}{2}}}\left[1-\exp\left\{-H_0 x\left(\frac{\sigma}{\rho\nu}\right)^{\frac{1}{2}}\right\}\right]. \end{aligned}\right\} \tag{3.4}$$

Hence

$$U = \frac{H_+ - H_-}{4\pi(\rho\nu\sigma)^{\frac{1}{2}}} \tag{3.5}$$

and is not arbitrary. Now if we let $\nu \to 0$, $\sigma \to \infty$ to obtain a perfectly conducting inviscid fluid it follows that

$$h = H_-, \quad v = 0 \quad \text{if} \quad x < 0;$$

$$h = H_+, \quad v = (H_+ - H_-)/4\pi(\rho\nu\sigma)^{\frac{1}{2}} \quad \text{if} \quad x > 0,$$

a magnetohydrodynamic boundary layer of a particularly simple kind being formed at $x = 0$. Thus in this specific problem it is not necessary that the tangential component of $\mathbf{q}$ should be zero at the boundary or that the tangential components of $\mathbf{H}$ must be continuous in the limit $\nu \to 0$, $\sigma \to \infty$. We must, however, have

$$[\mathbf{H}]_s = [\mathbf{q}]_s 4\pi(\rho\nu\sigma)^{\frac{1}{2}}, \tag{3.6}$$

where $[\ ]_s$ denotes 'the leap in the tangential component of'. The value of $\nu\sigma$ for a perfectly conducting inviscid fluid is indeterminate, but for a real fluid which is highly conducting and almost inviscid it can be worked out from the known physical properties. Actually in fluids of importance in terrestrial and interplanetary experiments $\nu\sigma$ is invariably very small and so in this paper we shall replace (3.6) by

$$[\mathbf{H}]_s = 0, \tag{3.7}$$

but there is no special difficulty about using (3.6).

Although (3.6) has been deduced for one specific and simple case the generalization to a curved wall and a general magnetohydrodynamic field is immediate. For, when σ is large and ν small the changes implied in (3.4) occur so rapidly in the x-direction that other changes due to wall curvature, etc., are negligible. The relevant equations governing the magnetohydrodynamic boundary layer at the wall are therefore identical with (3.2) and we conclude that (3.6) is a general condition on $\mathbf{q}$, $\mathbf{H}$ which must be satisfied at the boundary of a solid insulator with a perfectly conducting inviscid fluid.

If initially the motion is such that (3.6) is *not* satisfied then the manner in which the appropriate discontinuities are dispersed may easily be investigated and follows the same lines as when the boundary of the fluid is free. It will not be given here; it is merely pointed out that just as in the case of a free boundary the dispersion is immediate. The interested reader can readily work out the details for himself using the arguments of Stewartson (1957) and the corresponding equations allowing for viscosity. These equations have been discussed by Ludford (1959) in a related problem of magnetohydrodynamics.

4. Unsteady perturbations in a perfectly conducting fluid

In this section we consider the perturbation induced by a thin body placed along the x-axis, assuming that at time $t < 0$ the magnetic field is $(H_\infty, 0, 0)$, and that the fluid is set in motion at $t = 0$ with a velocity $(U, 0, 0)$ at infinity. Since the body is thin we can write

$$\mathbf{q} = (U+u, v, 0), \quad \mathbf{H} = (H_\infty + h_x,\ h_y,\ 0), \tag{4.1}$$

where u, v, h_x, h_y are all small. Neglecting squares and products of these small quantities and setting $\nu = 0$, $\sigma = \infty$, equations (2.1)–(2.3) reduce to

$$\frac{\partial h_x}{\partial x} + \frac{\partial h_y}{\partial y} = 0, \quad \frac{\partial u}{\partial x} + \frac{\partial v}{\partial y} = 0, \tag{4.2}$$

$$\left.\begin{aligned} \frac{\partial h_x}{\partial t} + U\frac{\partial h_x}{\partial x} = H_\infty \frac{\partial u}{\partial x}, \qquad & \frac{\partial h_y}{\partial t} + U\frac{\partial h_y}{\partial x} = H_\infty \frac{\partial v}{\partial x}, \\ \frac{\partial u}{\partial t} + U\frac{\partial u}{\partial x} = \frac{\partial P}{\partial x} + \frac{H_\infty}{4\pi\rho}\frac{\partial h_x}{\partial x}, \quad & \frac{\partial v}{\partial t} + U\frac{\partial v}{\partial x} = \frac{\partial P}{\partial y} + \frac{H_\infty}{4\pi\rho}\frac{\partial h_y}{\partial x}, \end{aligned}\right\} \tag{4.3}$$

where

$$P = -\frac{p}{\rho} - \frac{H_\infty^2}{4\pi\rho} + \text{const.} \tag{4.4}$$

These equations may be divided into two parts. First, there is a part which is directly due to P and which may easily be seen to be irrotational. Denoting its contributions to $\mathbf{q}$, $\mathbf{H}$ by a superscript (1) and writing

$$h_x^{(1)} = H_\infty \frac{\partial^2 \phi}{\partial x^2}, \quad h_y^{(1)} = H_\infty \frac{\partial^2 \phi}{\partial x \partial y}, \quad \text{where} \quad \frac{\partial^2 \phi}{\partial x^2} + \frac{\partial^2 \phi}{\partial y^2} = 0, \tag{4.5}$$

it follows that

$$u^{(1)} = \frac{\partial^2 \phi}{\partial t \partial x} + U\frac{\partial^2 \phi}{\partial x^2}, \quad v^{(1)} = \frac{\partial^2 \phi}{\partial t \partial y} + U\frac{\partial^2 \phi}{\partial x \partial y}, \tag{4.6}$$

$$P = \frac{\partial^2 \phi}{\partial t^2} + 2U\frac{\partial^2 \phi}{\partial t \partial x} + \left(U^2 - \frac{H_\infty^2}{4\pi\rho}\right)\frac{\partial^2 \phi}{\partial x^2}. \tag{4.7}$$

The second part is explicitly independent of P and is wave-like. Denoting its contributions to $\mathbf{q}$, $\mathbf{H}$ by a superscript (2)

$$\left(\frac{\partial}{\partial t} + U\frac{\partial}{\partial x}\right)^2 u^{(2)} = \frac{H_\infty^2}{4\pi\rho}\frac{\partial^2 u^{(2)}}{\partial x^2}, \quad \frac{H_\infty}{4\pi\rho}\frac{\partial h_x^{(2)}}{\partial x} = \frac{\partial u^{(2)}}{\partial t} + U\frac{\partial u^{(2)}}{\partial x} \tag{4.8}$$

with corresponding equations for $v^{(2)}$, $h_y^{(2)}$, the two pairs of functions being connected by (4.2). These solutions correspond to the Alfvén waves mentioned in § 2 and we see that in this small disturbance theory the irrotational and wave-like motions are additive.

The solution of (4.8) for $u^{(2)}$ is

$$\frac{u^{(2)}}{U} = f\left(t - \frac{mx}{(1+m)U}, y\right) + g\left(t + \frac{mx}{(1-m)U}, y\right), \tag{4.9}$$

where f, g are arbitrary functions and

$$H_\infty m = U(4\pi\rho)^{\frac{1}{2}},$$

m being the ratio of the velocity of the undisturbed fluid to the velocity of the Alfvén waves. All disturbances to the motion originate at the body, none come from infinity, and hence if $m < 1$

$$u^{(2)} = Uf\left\{t - \frac{mx}{(1+m)\,U}, y\right\}, \quad h_x^{(2)} = -mH_\infty f \quad \text{when} \quad x > 0, \tag{4.10}$$

$$u^{(2)} = Ug\left\{t + \frac{mx}{(1-m)\,U}, y\right\}, \quad h_x^{(2)} = mH_\infty g \quad \text{when} \quad x < 0, \tag{4.11}$$

while if $m > 1$

$$u^{(2)} = U(f+g), \quad h_x^{(2)} = mH_\infty(g-f) \quad \text{when} \quad x > 0, \tag{4.12}$$

$$u^{(2)} = h_x^{(2)} = 0 \quad \text{when} \quad x < 0, \tag{4.13}$$

from which $v^{(2)}$, $h_y^{(2)}$ may be written down.

In particular as $t \to \infty$ these functions become independent of t if, as we shall assume, the motion is ultimately steady. Hence writing

$$f(\infty, y) = f(y), \quad g(\infty, y) = g(y), \tag{4.14}$$

we have if $m < 1$

$$\left.\begin{aligned} u^{(2)} &= Uf(y), \quad h_x^{(2)} = -mH_\infty f(y), \quad v^{(2)} = h_y^{(2)} = 0 \quad (x > 0), \\ u^{(2)} &= Ug(y), \quad h_x^{(2)} = mH_\infty g(y), \quad\quad v^{(2)} = h_y^{(2)} = 0 \quad (x < 0), \end{aligned}\right\} \tag{4.15}$$

while if $m > 1$

$$\left.\begin{aligned} u^{(2)} = U\{f(y)+g(y)\}, \quad h_x^{(2)} = mH_\infty\{g(y)-f(y)\}, \quad v^{(2)} = h_y^{(2)} = 0, \quad \text{for} \quad x > 0, \\ u^{(2)} = v^{(2)} = h_x^{(2)} = h_y^{(2)} = 0 \quad \text{for} \quad x < 0. \end{aligned}\right\} \tag{4.16}$$

Hence, if the disturbances are always small, it is given, if the ultimate motion is steady, by the sum of (4.5), (4.6) and (4.15) or (4.16), viz.

$$\left.\begin{aligned} u &= U\left(\frac{\partial^2\phi}{\partial x^2} + f(y)\right), \quad v = U\frac{\partial^2\phi}{\partial x\,\partial y}, \\ h_x &= H_\infty\left(\frac{\partial^2\phi}{\partial x^2} - mf(y)\right), \quad h_y = H_\infty\frac{\partial^2\phi}{\partial x\,\partial y} \quad \text{for} \quad x > 0, \end{aligned}\right\} \tag{4.17}$$

$$\left.\begin{aligned} u &= U\left(\frac{\partial^2\phi}{\partial x^2} + g(y)\right), \quad v = U\frac{\partial^2\phi}{\partial x\,\partial y}, \\ h_x &= H_\infty\left(\frac{\partial^2\phi}{\partial x^2} + mg(y)\right), \quad h_y = H_\infty\frac{\partial^2\phi}{\partial x\,\partial y} \quad \text{for} \quad x < 0, \end{aligned}\right\} \tag{4.18}$$

if $m < 1$; and

$$\left.\begin{aligned} u &= U\left(\frac{\partial^2\phi}{\partial x^2} + f(y) + g(y)\right), \quad v = U\frac{\partial^2\phi}{\partial x\,\partial y}, \\ h_x &= H_\infty\left\{\frac{\partial^2\phi}{\partial x^2} + mg(y) - mf(y)\right\}, \quad h_y = H_\infty\frac{\partial^2\phi}{\partial x\,\partial y} \quad \text{for} \quad x > 0, \end{aligned}\right\} \tag{4.19}$$

$$u = U\frac{\partial^2\phi}{\partial x^2}, \quad v = U\frac{\partial^2\phi}{\partial x\,\partial y}, \quad h_x = H_\infty\frac{\partial^2\phi}{\partial x^2}, \quad h_y = H_\infty\frac{\partial^2\phi}{\partial x\,\partial y} \quad \text{for} \quad x < 0, \tag{4.20}$$

if $m > 1$, where ϕ is harmonic and f, g are arbitrary functions of y. Inside the body the magnetic field is harmonic since it is non-magnetic and an insulator. Hence we may write

$$h_x = H_\infty \frac{\partial^2 \psi}{\partial x^2}, \quad h_y = H_\infty \frac{\partial^2 \psi}{\partial y \partial x}, \tag{4.21}$$

where ψ is harmonic and analytic inside the body.

5. Thin aerofoils in steady motion

Let us now apply the theory of the previous section to the flow engendered by a slender convex aerofoil, symmetrically disposed with respect to the x-axis and whose surface is given by

$$|y| = \epsilon S(x) \quad (-b \leqslant x \leqslant a), \tag{5.1}$$

where ϵ is small and S is a function of x of order one, with a bounded derivative and vanishing at $x = -b, a$. Then the boundary conditions to be satisfied imply that on the aerofoil

$$v = \epsilon U S'(x) \operatorname{sgn} y, \tag{5.2}$$

whence, from (4.17)–(4.20),

$$\frac{\partial \phi}{\partial x} = \frac{\epsilon}{2\pi} \int_{-b}^{a} S'(x_1) \log \{(x - x_1)^2 + y^2\} \, dx_1 \tag{5.3}$$

since ϕ is harmonic, where a prime denotes differentiation. Further, in order to ensure that $\mathbf{q}$, $\mathbf{H}$ are continuous in the fluid the plane $x = 0$ must be chosen to pass through the aerofoil at its maximum cross-section, and then

$$f(y) = g(y) = 0$$

if $|y| > \epsilon S(0)$.

Since $U h_y = H_\infty v$ outside the aerofoil

$$h_y = \epsilon H_\infty S'(x) \operatorname{sgn} y \tag{5.4}$$

on the aerofoil; hence to a first approximation

$$h_y = \frac{H_\infty y S'(x)}{S(x)} \tag{5.5}$$

inside the aerofoil. Using the equation of continuity and (5.5) it follows that

$$h_x = H_\infty \log S(x) + \text{const.} \tag{5.6}$$

inside the aerofoil to a first approximation in ϵ. The additive constant is apparently indeterminate in slender wing theory. Thus although h_y is small in the aerofoil h_x is of the same order as H_∞ so that the field inside is seriously perturbed.*

Since

$$\frac{\partial^2 \phi}{\partial x^2} = \frac{\epsilon}{2\pi} \int_{-b}^{a} \frac{S'(x_1) \, dx_1}{x - x_1} \tag{5.7}$$

* In fact it has a logarithmic singularity at $S(x) = 0$ but it must be remembered that singularities at isolated points are often removable in aerofoil theory: if this were the only objection to the present argument it would be felt that the theory were substantially valid.

on the aerofoil, it follows that

$$mg(y) = -\frac{\epsilon}{2\pi}\int_{-b}^{a} \frac{S'(x_1)\,dx_1}{x-x_1} + \log S(x) + \text{const.} \quad (-b < x < 0). \tag{5.8}$$

where $y = \epsilon S(x)$, with a similar formula for $f(y)$. Thus if $m < 1$ the magnetic field and the velocity field are seriously distorted inside the planes $y = \pm \epsilon S(0)$, and since this region is the most vital part of the fluid the initial assumption that the disturbances remain small must be regarded as incorrect. If $m > 1$ the situation is even more serious for (5.6) contradicts (4.20) and so no solution is possible at all. A study of the initial motion of the fluid past the aerofoil from a state of rest shows that the motion in which the disturbances are small in fact breaks down straight away. The reason is that ahead of the body, according to small disturbance theory, no Alfvén waves can occur. Hence, on that part of the boundary for which $x < 0$ the continuity of h_x, h_y implies that the magnetic field inside the aerofoil is given by the analytic continuation of ϕ. But at $t = 0+$, ϕ is due to a source distribution in the aerofoil along the x-axis and hence so is the magnetic field. This is a contradiction, since the aerofoil is non-magnetic. It should be noted that the difficulties in the theory when $m > 1$ are due entirely to the linearization of the equations. When the full equations are used, Alfvén waves have no difficulty propagating into the fluid from the aerofoil. If the more general boundary condition (3.6) is used instead of (3.7) the theory also breaks down. The reason is that any restriction on the tangential component of $\mathbf{q}$ implies that the value of v at the boundary is not small in comparison with U.

The main conclusion to be drawn from the work of this section may be stated in the following way. Let a thin non-conducting aerofoil be set in motion, with uniform velocity $U \neq 0$ in a direction parallel to its length through a perfectly conducting fluid; then the perturbation in the state of the fluid caused by the motion of the aerofoil cannot ultimately become steady if it remains small.

There is one exception, however. If $m \ll 1$ it is possible to obtain a consistent linearized theory of the motion because the fluid velocity and not merely its perturbation component may be assumed small. The ultimate motion in this case is discussed in the next section.

6. The slow motion of a body in a perfectly conducting fluid

The equations which govern the state of the fluid in this limiting problem are the same as (4.2)–(4.4), provided we neglect the terms in them containing U as a multiplicative factor. It is assumed until proved otherwise that the disturbances remain small; it is worth noting, however, that it is no longer necessary to restrict the aerofoil to be thin. If the theory is valid at all it is valid for all bodies. The general solution of the equations is now

(*a*) For $x > 0$,

$$\left.\begin{aligned} h_x &= H_\infty \frac{\partial^2 \phi}{\partial x^2} - U(4\pi\rho)^{\frac{1}{2}} f\left(t - \frac{x}{V}, y\right), \\ u &= \frac{\partial^2 \phi}{\partial t\,\partial x} + Uf\left(t - \frac{x}{V}, y\right). \end{aligned}\right\} \tag{6.1}$$

(*b*) For $x < 0$,

$$\left.\begin{aligned} h_x &= H_\infty \frac{\partial^2 \phi}{\partial x^2} + U(4\pi\rho)^{\frac{1}{2}} g\left(t + \frac{x}{V}, y\right), \\ u &= \frac{\partial^2 \phi}{\partial t \partial x} + Ug\left(t + \frac{x}{V}, y\right), \end{aligned}\right\} \tag{6.2}$$

where ϕ is harmonic and of the same order as U, while

$$V = \frac{H_\infty}{(4\pi\rho)^{\frac{1}{2}}}. \tag{6.3}$$

From (6.1) and (6.2), v and h_y may be written down. In particular, if the motion of the fluid is ultimately steady we have, using (4 14),

$$u = Uf(y), \quad v = 0, \quad h_x = H_\infty \frac{\partial^2 \phi}{\partial x^2} - U(4\pi\rho)^{\frac{1}{2}} f(y), \quad h_y = H_\infty \frac{\partial^2 \phi}{\partial x \partial y} \tag{6.4}$$

if $x > 0$; and

$$u = Ug(y), \quad v = 0, \quad h_x = H_\infty \frac{\partial^2 \phi}{\partial x^2} + U(4\pi\rho)^{\frac{1}{2}} g(y), \quad h_y = H_\infty \frac{\partial^2 \phi}{\partial x \partial y} \tag{6.5}$$

if $x < 0$. Further

$$P = \text{const.} - \frac{H_\infty}{4\pi\rho}\left(h_x - H_\infty \frac{\partial^2 \phi}{\partial x^2}\right). \tag{6.6}$$

Suppose now that the body is convex and denote its boundary by S. Then the plane $x = 0$ must contain its maximum cross-section, and if further this cross-section lies between $y = \pm c$ it follows that

$$\left.\begin{aligned} g(y) = f(y) &= 1 \quad \text{for} \quad |y| < c, \\ g(y) = f(y) &= 0 \quad \text{for} \quad |y| > c, \end{aligned}\right\} \tag{6.7}$$

to satisfy the condition on the velocity at S. According to (6.7) the fluid contained within $|y| = c$ is completely at rest, while outside $|y| = c$ on the other hand it moves with uniform velocity U completely undisturbed by the presence of the body. In order to find the magnetic field, let it be given by

$$h_x = H_\infty \frac{\partial^2 \psi}{\partial x^2}, \quad h_y = H_\infty \frac{\partial^2 \psi}{\partial y^2} \tag{6.8}$$

inside S where ψ is harmonic and regular there. Since all components of **H** must be continuous at S, it follows that

$$\frac{\partial^2 \psi}{\partial x \partial y} = \frac{\partial^2 \phi}{\partial x \partial y} \quad \text{at } S, \tag{6.9}$$

$$\left.\begin{aligned} \frac{\partial^2 \psi}{\partial x^2} &= \frac{\partial^2 \phi}{\partial x^2} - \frac{U}{V} \quad \text{at } S, \quad \text{for} \quad x > 0, \\ \frac{\partial^2 \psi}{\partial x^2} &= \frac{\partial^2 \phi}{\partial x^2} + \frac{U}{V} \quad \text{at } S, \quad \text{for} \quad x < 0. \end{aligned}\right\} \tag{6.10}$$

The detailed properties of ψ, ϕ depend on the explicit form taken by S; as an example we shall now consider the case of a circular cylinder whose boundary is given by

$$r = c, \tag{6.11}$$

where $r\cos\theta = x$, $r\sin\theta = y$.

Let
$$\frac{\partial \phi}{\partial x} = \sum_{n=1}^{\infty} A_n \left(\frac{c}{r}\right)^n \frac{\cos n\theta}{n} - A_0 \log r, \tag{6.12}$$

$$\frac{\partial \psi}{\partial x} = \sum_{n=1}^{\infty} B_n \left(\frac{r}{c}\right)^n \frac{\cos n\theta}{n} + B_0, \tag{6.13}$$

where A_n, B_n are all constants to be found. From (6.9)

$$-\sum_{0}^{\infty} A_n \sin(n+1)\theta = -\sum_{2}^{\infty} B_n \sin(n-1)\theta,$$

i.e.
$$B_n = A_{n-2} \quad (n \geqslant 2), \tag{6.14}$$

whence from (6.10)

$$-2\sum_{n=0}^{\infty} A_n \cos(n+1)\theta - B_1 = \frac{U}{V}\operatorname{sgn}(\cos\theta) = \frac{4U}{\pi V}\sum_{s=0}^{\infty}\frac{(-)^s}{2s+1}\cos(2s+1)\theta.$$

i.e.
$$B_1 = 0, \quad A_{2s+1} = 0, \quad A_{2s} = \frac{2U(-)^{s+1}}{V\pi(2s+1)} \quad (s = 0, 1, 2, \ldots). \tag{6.15}$$

Using (6.15) in conjunction with (6.12), it is a straightforward matter to show that

$$\frac{\partial \phi}{\partial x} = \frac{U}{2\pi V}\Big[4c - 2x\tan^{-1}\frac{2cx}{r^2-c^2} + (y-c)\log\{x^2+(y-c)^2\} - (y+c)\log\{x^2+(y+c)^2\}\Big], \tag{6.16}$$

while $\partial\psi/\partial x$ differs from $\partial\phi/\partial x$ by a constant only. According to (6.16) the magnetic field has a logarithmic singularity at $x = 0$, $y = \pm c$ and so the assumption of small disturbances breaks down in the neighbourhood of these points. Since U is small the region in which the basic assumption of small disturbances is invalid is exponentially small, and in consequence it is unlikely that the correction when the full equations are used will be significant. In fact the breakdown of the small-disturbance theory in this problem would seem to be of negligible importance when compared with the breakdown in conventional thin aerofoil theory. It should be remembered, however, that that theory, unlike ours, has a solid corpus of exact solutions to support it.

At large distances from the circular cylinder the total magnetic field consists of two parts. First, there is a component in the x-direction equal to

$$H_\infty - U(4\pi\rho)^{\frac{1}{2}}\operatorname{sgn} x, \tag{6.17}$$

if $|y| < c$, and to H_∞ if $|y| > c$. This field does not of course tend to zero as $|x| \to \infty$. Secondly, there is a contribution due to an apparent magnetic pole at the origin of strength

$$\frac{2U}{\pi}(4\pi\rho)^{\frac{1}{2}}. \tag{6.18}$$

The pressure may be calculated from (6.6), and as $t \to \infty$ we find that

$$p \to p_0 - \left(\frac{\rho}{4\pi}\right)^{\frac{1}{2}} UH_\infty \operatorname{sgn} x \quad \text{for} \quad |y| < c,$$

$$p \to p_0 \quad \text{for} \quad |y| > c,$$

where p_0 is a constant. Hence the force on the circular cylinder tends to

$$2c\left(\frac{\rho}{\pi}\right)^{\frac{1}{2}} UH_\infty \text{ per unit thickness,} \tag{6.19}$$

in the direction of x increasing. This result is also true for all convex bodies, whatever their shape, provided only that their maximum thickness is $2c$.

A previous paper by the author (1956) was concerned with the motion of a perfectly conducting sphere through an imperfectly conducting fluid with conductivity σ. Although the conclusions as to the ultimate motion of the fluid were the same as those obtained here there are several important points of divergence. First, an important condition of the previous theory is that $\sigma U \ll 1$ so that it is not strictly applicable to a perfectly conducting fluid. Secondly, the condition on the magnetic field at the surface of the sphere is simply that the normal component of the perturbed field should vanish while the tangential component may be discontinuous. This condition can be satisfied without the necessity for any Alfvén waves and in fact as $\sigma \to \infty$ it was shown that the perturbed field increased indefinitely without changing the velocity field. Thus if the body is a perfect conductor, no matter how slowly it moves through a perfectly conducting fluid we can expect the magnetic field to be seriously perturbed ultimately. This is because there is nothing to prevent the build-up of current when U is small. In the present problem the build-up is controlled by the Alfvén waves radiated from the body. Finally, it should be noted that in the earlier problem the magnetic field was ultimately uniform and there was no force on the body.

7. Discussion

The steady motion of a non-conducting body through a perfectly conducting inviscid fluid in the presence of an aligned magnetic field has been shown to be a formidable problem. If one considers only the steady state it is found that the motion of the fluid is indeterminate depending on two arbitrary functions of the stream function ψ. If the conditions a long way upstream and downstream are uniform, then both of these functions can be found, but it must be expected that such a simple state of affairs will not exist in general.

These unknown functions can be found in any particular case by examining how the steady state is set up. For example, this may be done by setting the body in motion and tracing the behaviour of the fluid as $t \to \infty$. In such a method the fluid velocity and the magnetic field are uniquely determinate at all values of t including $t = \infty$, and so we can expect to obtain some information about the unknown functions of ψ by considering the unsteady equations of motion. This can be done fairly easily if the perturbations are small, and we have been able to find the properties of the ultimate flow assuming that the perturbations are small. On applying these properties to the motion of thin aerofoils, however, it is found that the ultimate motion is either not steady or not small, because otherwise large disturbances occur in the magnetic field in the body. One exceptional case, when the applied magnetic field is strong, can be successfully carried through and consistent results are found. Of these the most important is that the fluid inside

planes touching the body and parallel to the imposed magnetic field moves with the body as if solid. This result is true for all bodies and not only for thin aerofoils.

These conclusions may be compared with a theory of thin aerofoils in a perfectly conducting fluid recently developed by Sears & Resler (1959). In their paper two cases are considered according as the applied magnetic field is parallel or perpendicular to the direction of motion of the aerofoil, but we are concerned only with the first of these here. In the theory it is assumed that the conditions at infinity both upstream and downstream of the body are undisturbed, in which case the stream function is harmonic exactly as if there were no magnetic field, and the magnetic field is zero inside the body. All the requirements which can be derived from steady state equations and boundary conditions are satisfied. Attractive as this theory is, it is only one of an infinite number of equally self-consistent theories: further the assumption that conditions at infinity are undisturbed, while in accord with the corresponding theory in the absence of a magnetic field, is not in accord with the corresponding theory for a transverse magnetic field in which the effect of the aerofoil extends indefinitely in certain directions: again as $m \to 0$ and the speed of the aerofoil is reduced to zero, the magnetic field is not uniform everywhere since it must be zero inside the body.

None of these features implies that the theory is invalid but they do make it questionable whether it is realistic, i.e. can be produced in an experiment. Certainly if by some means the motion envisaged could be set up then there is absolutely no reason why it should not continue. On the other hand the same is true of an infinity of other solutions. The natural way of setting up a steady motion is to set up the field first and then start the relative motion of body and fluid. Accordingly the steady motion required is preceded by an unsteady motion in which disturbances from the uniform state are small if the body is thin, and so the work of the present paper is relevant to the correct description of the ultimate steady motion. The conclusions of the paper for all except small m do not absolutely contradict any of the features of the Sears & Resler theory but the way in which disturbances propagate to infinity in finite form make it unlikely to be realistic. The solution when m is small, however, contradicts the conclusions of their theory in so many ways, of which the most important are: (i) the conditions at infinity are disturbed, (ii) the fluid velocity is either reduced to rest relative to the body or is undisturbed, (iii) the magnetic field consists of a harmonic element and a piecewise constant element, (iv) the body experiences a drag, that when $m \ll 1$ their theory must be rejected for a steady motion which is set up by the unsteady process stated above. Further, in view of the doubts expressed above its relevance must be queried when m is not small and in particular when $m < 1$.

A very recent paper by Greenspan & Carrier (1959) provides some confirmation of this view. They consider the hydromagnetic boundary layer on a fixed semi-infinite flat plate defined by $x \geqslant 0$, $y = 0$; the fluid is highly conducting and almost inviscid and the conditions at infinity are exactly the same as in the present paper. Their main conclusion is that the boundary layer exists in its conventional form only if $m > 1$. If $m < 1$ it leads to a contradiction suggesting that the problem is incorrectly posed, which is in accord with our view that the flow at infinity upstream is disturbed by the presence of the plate.

We emphasize that these doubts refer to the description of the ultimate state of the motion of the fluid if it is either started from rest or, more generally, if the velocity of the fluid and the magnetic field are each almost uniform at some stage before the steady state is reached. For a steady state achieved without satisfying these conditions the objections do not apply.

REFERENCES

GREENSPAN, H. P. & CARRIER, G. F. 1959 *J. Fluid Mech.* **6**, 77.
LUDFORD, G. S. S. 1959 *Archive Rational Mech. Anal.* **3**, 14.
SEARS, W. R. & RESLER, E. L. 1959 *J. Fluid Mech.* **5**, 257.
STEWARTSON, K. 1956 *Proc. Camb. Phil. Soc.* **52**, 301.
STEWARTSON, K. 1957 *Proc. Camb. Phil. Soc.* **53**, 774.

The oscillating plate problem in magnetohydrodynamics

By W. I. AXFORD
Department of Mathematics, University of Manchester

(Received 30 July 1959)

The oscillating plate problem is investigated for the case of an incompressible, electrically conducting fluid in the presence of a magnetic field. The boundary conditions are examined in detail, and a solution is found with the aid of suitable approximations. The motion of the fluid is shown to consist mainly of magnetohydrodynamic waves, but there is also a viscous boundary layer in which the solution agrees with that given by other writers.

1. Introduction

Certain difficulties occur in the theory of magnetohydrodynamic boundary layers which may possibly be resolved by an examination of the corresponding linear problem in which the fluid motion is caused by an infinite flat plate moving in its own plane. Ludford (1959) has considered the Rayleigh problem (impulsive motion of the flat plate) including magnetohydrodynamic effects, and in the present note the related case is examined in which the plate executes simple harmonic motion and the flow is quasi-steady. There is an advantage in considering this case, since the mathematical difficulties encountered by Ludford are then avoided.

The case in which the kinematic viscosity is small compared with the magnetic diffusivity is examined in detail, since this is likely to be the situation in experimental work. The most interesting effect found is the production of magnetohydrodynamic waves which become diffused due to the finite electrical conductivity of the fluid. A viscous boundary layer occurs at the surface of the plate, and the solution in this region agrees exactly with that found by Ong & Nicholls (1959), using an approximate equation given by Rossow (1957). The reasons for this agreement and also the approximations involved in Ong & Nicholls' solution are discussed.

The implications of the assumption made by Ludford, that the boundary consists of material having infinite electrical conductivity, are examined in detail, and necessary conditions for its validity are given.

2. Equations and boundary conditions

The equations* describing plane laminar motion of an incompressible conducting fluid in the absence of a pressure gradient are

$$\left(\eta\frac{\partial^2}{\partial y^2}-\frac{\partial}{\partial t}\right)H+H_0\frac{\partial u}{\partial y}=0, \tag{1}$$

* M.K.S. units are used throughout. Since Ludford has given a neat form of the solution of the algebraic equation (11), his notation is used for convenience.

$$A_0^2 \frac{\partial H}{\partial y} + H_0 \left(\nu \frac{\partial^2}{\partial y^2} - \frac{\partial}{\partial t} \right) u = 0, \tag{2}$$

where the motion is in the x-direction, and the velocity $\mathbf{v}$, magnetic field $\mathbf{H}$, and current $\mathbf{j}$ are given by

$$\mathbf{v} = (u, 0, 0), \quad \mathbf{H} = (H, H_0, 0), \quad \mathbf{j} = (0, 0, j). \tag{3}$$

H_0 is a constant magnetic field perpendicular to the plane of motion, which is used to define an Alfvén velocity as follows:

$$A_0^2 = \mu H_0^2 / \rho. \tag{4}$$

There are two diffusivities involved in the equations, namely the kinematic viscosity ν, and the magnetic diffusivity, η, which is defined as

$$\eta = 1/\mu\sigma, \tag{5}$$

where μ is the permeability and σ the conductivity of the fluid. The equation for the pressure is

$$\frac{\partial}{\partial y} \left(p + \frac{\mu H^2}{2} \right) = 0, \tag{6}$$

and the current is given by

$$j = -\frac{\partial H}{\partial y}. \tag{7}$$

We shall consider a quasi-steady motion, neglecting transients, in which the time-dependent part of the solution is a factor $e^{i\omega t}$. Hence the operator $\partial/\partial t$ in equations (1) and (2) can be replaced by $i\omega$, and it is then easily shown that the general solution of the equations is

$$u = [A e^{my} + B e^{-my} + C e^{ny} + D e^{-ny}] e^{i\omega t}, \tag{8}$$

$$H = \frac{H_0}{A_0^2} \left[\left(\frac{i\omega}{m} - m\nu \right) A e^{my} + \ldots \right] e^{i\omega t}, \tag{9}$$

$$j = -\frac{H_0}{A_0^2} [(i\omega - \nu m^2) A e^{my} + \ldots] e^{i\omega t}, \tag{10}$$

where A, B, C and D are arbitrary constants and $r = \pm m, \pm n$, are the roots of the quartic

$$(\eta r^2 - i\omega)(\nu r^2 - i\omega) - A_0^2 r^2 = 0. \tag{11}$$

Ludford has shown that

$$m = (a + ib\omega)^{\frac{1}{2}} + (a + ic\omega)^{\frac{1}{2}}, \tag{12}$$

$$n = (a + ib\omega)^{\frac{1}{2}} - (a + ic\omega)^{\frac{1}{2}}, \tag{13}$$

where

$$a = \frac{A_0^2}{4\eta\nu}, \quad b = (\eta^{\frac{1}{2}} + \nu^{\frac{1}{2}})^2 / 4\eta\nu, \quad c = (\eta^{\frac{1}{2}} - \nu^{\frac{1}{2}})^2 / 4\eta\nu. \tag{14}$$

Under laboratory conditions it is usually found that $\eta \gg \nu$*, and in these circumstances, b and c are very nearly equal. Hence we can write

$$b = d(1 + \epsilon), \quad c = d(1 - \epsilon),$$

where

$$d = 1/4\nu, \quad \epsilon = 2(\nu/\eta)^{\frac{1}{2}},$$

and so

$$(a + ib\omega)^{\frac{1}{2}} = (a + id\omega)^{\frac{1}{2}} \left\{ 1 + \frac{i\omega d\epsilon}{2(a + id\omega)} + O(\epsilon^2) \right\},$$

$$(a + ic\omega)^{\frac{1}{2}} = (a + id\omega)^{\frac{1}{2}} \left\{ 1 - \frac{i\omega d\epsilon}{2(a + id\omega)} + O(\epsilon^2) \right\}.$$

* For instance, $\nu/\eta \approx 10^{-7}$ for mercury.

Substituting from (14), and neglecting all but the terms of lowest order in ϵ, equations (12) and (13) give

$$m \approx (A_0^2 + i\omega\eta)^{\frac{1}{2}}/\sqrt{(\eta\nu)}, \tag{15}$$

$$n \approx i\omega/(A_0^2 + i\omega\eta)^{\frac{1}{2}}. \tag{16}$$

Thus, in the general solution, the terms with exponent $(i\omega t \pm my)$ contain the combination $y/\nu^{\frac{1}{2}}$, showing that there is an ordinary viscous boundary layer outside of which the fluid is affected only by the oscillations of the magnetic field. The terms with exponent $(i\omega t \pm ny)$ are independent of ν and represent diffused Alfvén waves moving along the lines of force of the undisturbed field $(0, H_0, 0)$.

The simplest example of laminar periodic motion is that caused by a solid boundary at $y = 0$ which oscillates in the x-direction with velocity $Ue^{i\omega t}$. The fluid is assumed to extend to infinity in $y > 0$, and the space $y < 0$ is occupied by solid material of uniform composition. We shall use primes to denote quantities in the solid region, which contains a magnetic field of the form $(H', H_0', 0)$, where H_0' is constant and H' is an induced field satisfying the equation

$$\frac{\partial H'}{\partial t} = \eta' \frac{\partial^2 H'}{\partial y^2}. \tag{17}$$

The appropriate solution of this equation which vanishes for large negative values of y is

$$H' = F \exp\left[\left(\frac{\omega}{2\eta'}\right)^{\frac{1}{2}} y + i\left\{\omega t + \left(\frac{\omega}{2\eta'}\right)^{\frac{1}{2}} y\right\}\right], \tag{18}$$

where F is a further arbitrary constant.

The disturbance must vanish as y tends to infinity, and so A and C must be zero since the real parts of m and n are positive. We are therefore required to determine three constants, namely B, D and F, from the conditions at the boundary $y = 0$.

The first condition is that there should be no slip at the boundary, that is

$$u = u' = Ue^{i\omega t} \quad \text{on} \quad y = 0. \tag{19}$$

There are two conditions on the magnetic field, requiring that the normal component of $\mu\mathbf{H}$ and the tangential component of $\mathbf{H}$ should be continuous. Hence

$$\mu H_0 = \mu' H_0', \tag{20}$$

and

$$H = H' \quad \text{on} \quad y = 0. \tag{21}$$

The remaining condition is on the tangential component of the electric field, which must also be continuous. Thus

$$\frac{1}{\sigma}\frac{\partial H}{\partial y} + \mu u H_0 = \frac{1}{\sigma'}\frac{\partial H'}{\partial y} + \mu' u' H_0' \quad \text{on} \quad y = 0,$$

which reduces, on using (19) and (20), to

$$\frac{1}{\sigma}\frac{\partial H}{\partial y} = \frac{1}{\sigma'}\frac{\partial H'}{\partial y} \quad \text{on} \quad y = 0. \tag{22}$$

The three conditions (19), (21) and (22) are sufficient to determine the three constants B, D and F.

3. Simplifying approximations

A simplified form of these boundary conditions is possible under certain circumstances. First, it can be seen from (18) that the field in the solid is confined* to a layer near the surface with thickness of order $(\eta'/\omega)^{\frac{1}{2}}$. Similarly the field induced in the fluid is confined to a layer with thickness at least of order $(\eta/\omega)^{\frac{1}{2}}$. Thus if $\eta \gg \eta'$, the field induced in the solid can be neglected, and the current associated with this induced field can be assumed to form a current sheet on the boundary which allows a discontinuity in the field. In this case, F does not have to be calculated, and the two conditions required to find B and D are (19) and

$$\left(\frac{\partial H}{\partial y}\right)_{y=0} = \frac{\sigma}{\sigma'}\left(\frac{\omega}{2\eta'}\right)^{\frac{1}{2}} e^{i\pi/4} H(0). \tag{23}$$

The second possible simplification is found by considering the ratio $\left|\frac{L}{H}\frac{\partial H}{\partial y}\right|_{y=0}$, where L is some typical length. This is found to be of the order of $\left(\frac{\sigma\mu'}{\mu\sigma'}\right)^{\frac{1}{2}}$. Thus provided

$$\sigma/\sigma' \ll \mu/\mu', \tag{24}$$

the boundary condition (23) can be taken to be

$$\frac{\partial H}{\partial y} = 0 \quad \text{on} \quad y = 0, \tag{25}$$

which is the condition used by Ludford. In general μ and μ' will be approximately equal, unless the solid is of a ferromagnetic material, when μ' will be much larger than μ. Whatever the case, (24) is a sufficient condition for $\eta \gg \eta'$, and for the boundary conditions to be (19) and (25) with F zero. If (24) is not satisfied, but $\eta \gg \eta'$, then the boundary conditions are (19) and (23) with F zero. Finally, if η is not much greater than η', the boundary conditions must be (19), (22) and (23), and F is not zero.

We shall consider a case in which the condition (24) holds, and it is easily found from (19) and (25) that

$$B = (\nu n^2 - i\omega)\, U/\nu(n^2 - m^2),$$
$$D = (i\omega - \nu m^2)\, U/\nu(n^2 - m^2).$$

Hence

$$u = \frac{U e^{i\omega t}}{\nu(n^2 - m^2)}\left[(\nu n^2 - i\omega)\, e^{-my} - (\nu m^2 - i\omega)\, e^{-ny}\right], \tag{26}$$

$$H = U H_0 e^{i\omega t}\frac{(\nu n^2 - i\omega)(\nu m^2 - i\omega)}{A_0^2 \nu(n^2 - m^2)}\left[\frac{e^{-ny}}{n} - \frac{e^{-my}}{m}\right]. \tag{27}$$

When $\eta \gg \nu$, m and n are given by (15) and (16), and these solutions for u and H become

$$u = \frac{U e^{i\omega t}}{\left(1 + \frac{i\omega\eta}{A_0^2}\right)}\left[\exp\left\{-\frac{i\omega y}{(A_0^2 + i\omega\eta)^{\frac{1}{2}}}\right\} + \frac{i\omega\eta}{A_0^2}\exp\left\{-\frac{y(A_0^2 + i\omega\eta)^{\frac{1}{2}}}{\sqrt{(\eta\nu)}}\right\}\right], \tag{28}$$

$$H = \frac{U H_0 e^{i\omega t}}{A_0\left(1 + \frac{i\omega\eta}{A_0^2}\right)^{\frac{3}{2}}}\left[\left(1 + \frac{i\omega\eta}{A_0^2}\right)\exp\left\{-\frac{i\omega y}{(A_0^2 + i\omega\eta)^{\frac{1}{2}}}\right\} - \frac{i\omega\sqrt{(\eta\nu)}}{A_0^2}\exp\left\{-\frac{y(A_0^2 + i\omega\eta)^{\frac{1}{2}}}{\sqrt{(\eta\nu)}}\right\}\right]. \tag{29}$$

* The 'skin effect'.

The solutions in the viscous boundary layer are found by taking the limit as y and ν tend to zero while $y/\nu^{\frac{1}{2}}$ remains finite. These boundary layer solutions are

$$u = \frac{Ue^{i\omega t}}{\left(1+\frac{i\omega\eta}{A_0^2}\right)}\left[1+\frac{i\omega\eta}{A_0^2}\exp\left\{-\frac{y(A_0^2+i\omega\eta)^{\frac{1}{2}}}{\sqrt{(\eta\nu)}}\right\}\right], \tag{30}$$

$$H = \frac{UH_0e^{i\omega t}}{A_0\left(1+\frac{i\omega\eta}{A_0^2}\right)^{\frac{1}{2}}}. \tag{31}$$

This expression for u is exactly that found by Ong & Nicholls, using the equation

$$\frac{\partial u}{\partial t}+\frac{A_0^2}{\eta}(u-Ue^{i\omega t}) = \nu\frac{\partial^2 u}{\partial y^2}, \tag{32}$$

first given by Rossow. This confirms the result found by Ludford, that Rossow's equation gives the correct solution in the viscous boundary layer provided $\eta \gg \nu$. The truth of this can be found from an examination of equation (1), for

$$\frac{\partial H}{\partial t} \ll \eta\frac{\partial^2 H}{\partial y^2},$$

if

$$UL \ll \eta, \tag{33}$$

where L is a length typical of the region under consideration. For the viscous boundary layer, L is ν/U, and (33) is simply $\eta \gg \nu$. Neglecting the term $\frac{\partial H}{\partial t}$, equation (1) can be integrated to give

$$\eta\frac{\partial H}{dy} = H_0(Ue^{i\omega t}-u), \tag{34}$$

using the boundary condition (25), and substitution of this result into equation (2) yields (32). The chief drawbacks of Rossow's equation are that it cannot be used to give the solution for H, nor does it give any indication of the effect of the magnetic field on the motion of the fluid outside the viscous boundary layer. Because of this, Rossow's approach will fail in many cases in which the flow outside the viscous boundary layer is affected by the magnetic field, as it gives no indication of the correct condition at the outer edge of the boundary layer. There may also be some doubt about the validity of using (25) as a boundary condition in some circumstances.

The solution for the flow and field outside the boundary layer are found from (28) and (29) by allowing ν to tend to zero whilst y remains finite, giving

$$u = \frac{U}{\left(1+\frac{i\omega\eta}{A_0^2}\right)}\exp\left\{i\omega t-\frac{i\omega y}{(A_0^2+i\omega\eta)^{\frac{1}{2}}}\right\}, \tag{35}$$

$$H = \frac{UH_0}{A_0\left(1+\frac{i\omega\eta}{A_0^2}\right)^{\frac{1}{2}}}\exp\left\{i\omega t-\frac{i\omega y}{(A_0^2+i\omega\eta)^{\frac{1}{2}}}\right\} = \frac{H_0}{A_0}\left(1+\frac{i\omega\eta}{A_0^2}\right)^{\frac{1}{2}}u. \tag{36}$$

Thus the disturbance is a diffused Alfvén wave propagating in the direction of increasing y. This can be seen more readily if a low frequency ($\omega \ll A_0^2/\eta$) approximation is made, for the above equations then become

$$u = U \exp\left\{-\frac{\omega^2\eta}{2A_0^3}y + i\omega\left(t - \frac{y}{A_0}\right)\right\}, \tag{37}$$

$$H = \frac{UH_0}{A_0}\exp\left\{-\frac{\omega^2\eta}{2A_0^3}y + i\omega\left(t - \frac{y}{A_0}\right)\right\}, \tag{38}$$

showing that the fluid and field move together, and the disturbance is an Alfvén wave which is damped out over a distance of order $2A_0^3/\omega^2\eta$. This is the result obtained by Alfvén (1950, p. 82) in an investigation of the effect of finite conductivity of the fluid on plane magnetohydrodynamic waves.

I wish to extend my thanks to the New Zealand Scientific Defence Corps, my employers, for making my period of study in Manchester possible, and also to Professor M. J. Lighthill, F.R.S., for his encouragement of this work.

REFERENCES

Alfvén, H. 1950 *Cosmical Electrodynamics.* Oxford: Clarendon Press.
Ludford, G. S. S. 1959 *Arch. Rat. Mech. Anal.* **3**, 14–27.
Ong, R. S. & Nicholls, J. A. 1959 *J. Aero. Sci.* **26**, 313–14.
Rossow, V. J. 1957 *Nat. Adv. Comm. Aero. Wash., Tech. Note*, no. 3971.

A note on the breakdown of continuity in the motion of a compressible fluid

By D. C. PACK

Department of Mathematics, The Royal College of Science and Technology, Glasgow

(Received 1 August 1959)

By a consideration of the relationships holding along the characteristics in an unsteady motion involving plane, axially or spherically symmetrical flow of compressible inviscid fluid, it is shown that the existence of a region of compression anywhere in the flow must lead eventually to the breakdown of continuity. The paper generalizes and unites previous work on this topic, and discusses some recent numerical calculations in which the expected discontinuity was not found.

1. Introduction

The fact that a wave of compression, in one-dimensional unsteady flow of an inviscid non-heat-conducting gas always leads eventually to a breakdown in the continuity of the flow has been known for a century. Challis (1848) observed that Poisson's simple-wave solution (1808) of the differential equation of flow in an isothermal gas could not always be solved uniquely for the velocity, and it was Stokes (1848) who first attempted to insert a discontinuity of velocity into the flow in order to continue it beyond the point in (x, t)-space at which the mathematical solution broke down. Although it was many years before the exact nature of these discontinuities, or 'shock waves', was correctly worked out, it is now well understood that in the simple wave resulting from the positive acceleration of a piston into a (one-dimensional) gas at rest, a shock wave must occur (see, for example, Courant & Friedrichs 1948). It is not, however, immediately obvious that such a breakdown of continuity in a compressive wave must necessarily occur when the motion has cylindrical or spherical symmetry. In these cases, the rapid increase in the volume occupied by a gas during its expansion may cause the pressure gradients in the gas to fall in the initial stages. A calculation performed by Unwin (1941) on the expansion of a spherical mass of gas released suddenly from a state of rest did not reveal the occurrence of a discontinuity up to the t-coordinate (t being the time) at which he ended his computations. In a recent paper Fox & Ralston (1957) have reworked Unwin's example, and while disagreeing with his numerical results, have concluded, even more strongly than he did, that no shock wave will result from a continuation of their calculations. Roberts (1957), calculating the development of a stronger initial distribution of pressure, also reached these conclusions.

In contrast with these results, it was shown by Hantzsche & Wendt (1940), who examined the development of a wave moving irrotationally with a region of compression at its head into gas at rest, that ultimately the continuity would break

down. Kuo (1947) has discussed a similar type of flow and has also found some sufficient conditions for breakdown in the general case by a consideration of the flow in the hodograph plane.

Furthermore (although these authors seem not to have been aware of it) Burton showed, as long ago as 1893, that the continuity of an expanding spherical wave will eventually break down if there is at all times a region of compression, no matter how weak, somewhere within the wave. Burton obtained his results by intuitive arguments based upon inequalities.

In this note the problem is reconsidered in terms of the theory of characteristics, which enables Burton's arguments to be expressed in a more precise form and at the same time generalizes the results of Hantzsche & Wendt.

2. Equations of motion

Let us consider the characteristic surfaces of a gas motion, these surfaces being given by the equations

$$\frac{dr}{dt} = u \pm c,$$

where u is the particle velocity and c the local speed of sound at a point (r, t), r being distance from the centre, from the axis or from a fixed plane according as the motion is radially or cylindrically symmetrical or plane (one-dimensional). The conditions of compatibility, which have to be satisfied on these surfaces are, in differential form,

$$du \pm \frac{2dc}{\gamma - 1} \pm \frac{\epsilon uc}{r} dt - \frac{1}{\gamma} c^2 \frac{\partial \Sigma}{\partial r} dt = 0,$$

where γ is the (supposed constant) ratio of specific heats; $\epsilon = 2$, 1 or 0 according as we are considering radially or cylindrically symmetrical or plane flow; Σ is a function of the specific entropy S defined by $\Sigma(S) = \{2\gamma/(\gamma - 1)\} \log c - \log p$, p being the pressure; and where the alternative signs correspond respectively to those in the previous equation of the characteristics. We shall also suppose that the two families of characteristics in the (r, t)-plane are respectively designated in some way as the curves $\alpha = \text{const.}$ and $\beta = \text{const.}$ We then consider two points P and Q which are allowed to vary in such a way that, in (α, β)-space, their co-ordinates are (α_1, β) and (α_2, β), where β is a variable and α_1, α_2 are arbitrary constants (see figure 1).

Suppose that P is at radial distance r and Q at distance $r + \Delta r$. We shall investigate the change in Δr as the time increases and P, Q move along their α-characteristics. If at some time Δr becomes zero, the α-characteristics will intersect, an indication of the breakdown of the continuity of the motion.

If such a breakdown occurs in the early stages of the motion, there is nothing to prove. The important question is whether, if no discontinuity occurs before the disturbances become of small magnitude, the motion can avoid indefinitely the onset of such a discontinuity. We suppose, therefore, that P and Q lie on a β-characteristic which is sufficiently far from the origin for Δr to be small compared with r. Also, we suppose that the disturbances have decayed to such an extent that u is small compared with c; on the other hand, Δu and Δc (the symbol Δ represents the increment in the value of the following quantity from the point P

to the point Q), while small, may be of the same order of magnitude as u. Since both P and Q move on α-characteristics, it follows that

$$\frac{\partial}{\partial\beta}\left(\Delta u+\frac{2\Delta c}{\gamma-1}\right)+\epsilon\Delta\left(\frac{uc}{r}\frac{\partial t}{\partial\beta}\right)=\frac{1}{\gamma}\Delta\left(c^2\frac{\partial\Sigma}{\partial r}\frac{\partial t}{\partial\beta}\right).$$

When the disturbances are weak, $\Sigma(S)$ is of the order of magnitude of $(u/c)^3$ at most, the order of magnitude obtained when there is already a weak shock-wave ahead of the region under consideration; in homentropic flow, $\Sigma(S)$ is constant.

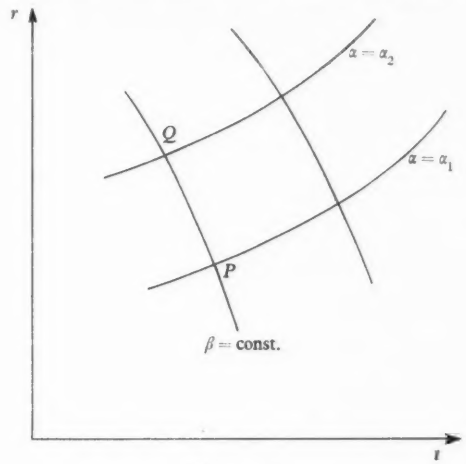

FIGURE 1.

Hence, when terms of second and higher orders of smallness are neglected in the above equation, we obtain

$$\frac{\partial}{\partial\beta}\left(\Delta u+\frac{2\Delta c}{\gamma-1}\right)+\epsilon c_0\Delta\left(\frac{u}{r}\frac{\partial t}{\partial\beta}\right)=0, \tag{1}$$

where c_0 is the speed of sound in the gas at rest.

Since P and Q lie on a β-characteristic, we have

$$\Delta u-\frac{2\Delta c}{\gamma-1}-\int_P^Q\frac{\epsilon uc}{r}\frac{dr}{u-c}=0,$$

the integral being taken along the characteristic and the entropy term being omitted for the same reason as in (1). An examination shows that the third term above may also be neglected, to the same order of approximation. This leads to the simple relation

$$\Delta u=2\Delta c/(\gamma-1). \tag{2}$$

If we use a suffix zero to denote the conditions at some time $t=T$ for which r is already sufficiently large (and equal to r_0), then we may replace r by $r_0+c_0(t-T)$ to a first approximation and rewrite the equation (1) above, with the aid of (2), as

$$\frac{\partial}{\partial\beta}(\Delta u)+\tfrac{1}{2}\epsilon c_0\left(\frac{1}{c_0 r}\frac{\partial r}{\partial\beta}\Delta u\right)=0.$$

This is immediately integrable and gives

$$\frac{\Delta u}{(\Delta u)_0} = \left(\frac{r_0}{r}\right)^{\frac{1}{2}\epsilon}.$$

Since, from the equation of the α-characteristic,

$$\begin{aligned}\frac{\partial}{\partial\beta}(\Delta r) &= \Delta\left[(u+c)\frac{\partial t}{\partial\beta}\right] \\ &= \frac{\gamma+1}{2c_0}\frac{\partial r}{\partial\beta}\Delta u \quad \text{(to the order of approximation adopted).} \\ &= \frac{\gamma+1}{2c_0}\frac{\partial r}{\partial\beta}(\Delta u)_0\left(\frac{r_0}{r}\right)^{\frac{1}{2}\epsilon},\end{aligned}$$

we have on integration:

$$\begin{aligned}&\text{for } \epsilon = 0, \quad \Delta r - (\Delta r)_0 = \tfrac{1}{2}(\gamma+1)(\Delta u)_0(r-r_0)/c_0; \\ &\text{for } \epsilon = 1, \quad \Delta r - (\Delta r)_0 = (\gamma+1)(\Delta u)_0(\sqrt{r_0}/c_0)(\sqrt{r}-\sqrt{r_0}); \\ &\text{for } \epsilon = 2, \quad \Delta r - (\Delta r)_0 = \tfrac{1}{2}(\gamma+1)(\Delta u)_0(r_0/c_0)\log(r/r_0).\end{aligned}$$

3. Breakdown of continuity

If the points P and Q are taken indefinitely close together we may write $(du/dr)_\beta$ in place of $\Delta u/\Delta r$, this being the derivative of u with respect to r along the characteristic $\beta = \text{const}$. This is equal to $\partial u/\partial r + (u-c)^{-1}\partial u/\partial t$. The previous results may now be rewritten in the form

$$(du/dr)_\beta = \begin{cases} -k/[1-(\gamma+1)k(r-r_0)/2c_0], & \text{for } \epsilon = 0, \\ -k\sqrt{(r_0/r)}/[1-(\gamma+1)kr_0^{\frac{1}{2}}(\sqrt{r}-\sqrt{r_0})/c_0], & \text{for } \epsilon = 1, \\ -k(r_0/r)/[1-(\gamma+1)kr_0\{\log(r/r_0)\}/2c_0], & \text{for } \epsilon = 2, \end{cases}$$

where $-k$ indicates the value of $(du/dr)_\beta$ at time $t = T$ on the positive characteristic through (r, t).

These results correspond exactly with those derived by Hantzsche & Wendt for the gradient at the head of a wave. The argument concerning the breakdown of continuity may now follow exactly as in their paper. The vanishing of Δr corresponds, as we should expect, to an infinite gradient of velocity, indicating the occurrence of a limit line. We observe that this is a possibility for $r > r_0$ only if $k > 0$. Positive values of k correspond to negative values of $(du/dr)_\beta$ at $t = T$, and there is therefore a region of compression moving across $r = r_0$ at that instant. We shall consider the behaviour of $(du/dr)_\beta$ as t increases, under the supposition that $k > 0$.

First we see that for plane waves ($\epsilon = 0$) the gradient of velocity in the β-direction increases with r and t along the α-characteristic. The gradient becomes infinite when the denominator vanishes. This occurs when

$$r - r_0 = 2c_0/(\gamma+1)k.$$

This result is identical with the well-known result for plane waves (Durand 1935). For cylindrical and spherical waves the circumstances differ in that the values of

$(du/dr)_\beta$ may at first diminish on account of the factors $r^{-\frac{1}{2}}$ and r^{-1} which occur in the right-hand sides of the formulae given above; only if k is sufficiently large will $(du/dr)_\beta$ increase continuously with time. In both cases, however, it is clear that the denominator vanishes eventually, for any $\gamma > -1$, so that an infinite gradient of velocity must appear on the characteristic. For spherically symmetrical motion, for example, it will occur not later than time t given by

$$t - T = (r_0/c_0)\,[\exp\,[2c_0/r_0 k(\gamma+1)]-1].$$

Hence, for any plane, cylindrically or spherically symmetrical gas motion the continuity must eventually break down along a characteristic on which the motion is compressive.*

When $\gamma = -1$, there is no shock wave. For plane waves $(du/dr)_\beta$ is constant in this case. This is in agreement with the known result that, for $\gamma = -1$, plane waves propagate without change of form.

4. Comparison with some computations

Fox & Ralston (1957) and Roberts (1957) have carried out numerical calculations for a gas initially at rest with a density distribution given by

$$\rho = \rho_0[1 + p\exp(-4r'^2)],$$

where $r' = r/a$ (a is some characteristic length, ρ_0 the undisturbed density of air) and $p = 2$ (Fox & Ralston, following Unwin, 1941), or $p = 5$ (Roberts). They did not find any evidence of a breakdown of continuity. The disturbances represented by these distributions quickly become small everywhere, and when the theory of the present paper is applied directly to them, with $T = 0$, it is found that a shock wave should begin at $t' = 0{\cdot}7$ and $t' = 0{\cdot}3$, where $t' = c_0 t/a$, corresponding to $r' = 1{\cdot}2$ and $r' = 0{\cdot}9$, respectively.

In discussing this difference between the theoretical conclusions and those found by calculation, it may be said that, for spherical waves, the shock intensities can be so small that they may be masked by the errors involved in numerical calculations when the partial differential equations are replaced by finite difference calculations. The tendency to form extremely weak shock-waves in spherical expansions was indicated by Taylor in (1946) and Lighthill showed analytically in 1948 that, in the flow resulting from the expansion of a spherical piston with Mach number 1/5, the leading shock wave was of order e^{-44} in strength, i.e. 'of an order of smallness rarely encountered in physical problems'. When one considers this in conjunction with the fact that Roberts's finite difference system introduced an artificial viscosity which would have the effect of smoothing out discontinuities (as he himself says), it may be correct to conclude that the discrepancy between the conclusions of this paper and the results of the calculations which Roberts carried out is more apparent than real; that shock waves of the strength likely to occur could not have been detected by the numerical method adopted.

* It may be noted that Burton pointed out in his original paper that the inevitability of a discontinuous motion would not apply to flow in dimensions greater than three.

Fox & Ralston computed the case $p = 2$ by means of a finite difference scheme for the characteristics and the equations of compatibility. They remark that 'any tendency for the characteristics to converge is quickly dispelled and so there is never any sign of the formation of a shock'. As the author (1948) has shown in a paper on the formation of shock waves in jets, the initial point of a shock wave may be found by constructing characteristics over a field sufficient to allow mutual intersections of several neighbouring characteristics of the same family, and by extrapolating back to find the point at which two infinitesimally separated characteristics first begin to form the envelope of their family. The point $r' = 1{\cdot}2$, $t' = 0{\cdot}7$ lies near to the boundary of the region computed by Fox & Ralston, so that here again, with a very weak shock, the breakdown could not be expected to reveal itself.

The author therefore believes that the computations so far carried out could not have revealed the shock wave which was sought.

REFERENCES

Burton, C. V. 1893 *Phil. Mag.* (5), **35**, 317.

Challis, J. 1848 *Phil. Mag.* (3), **32**, 494.

Courant, R. & Friedrichs, K. O. 1948 *Supersonic Flow and Shock Waves.* New York: Interscience Publishers.

Durand, W. F. (Ed.) 1935 *Aerodynamic Theory*, **3**, 216. Berlin: Springer.

Fox, P. & Ralston, A. 1957 *J. Maths. Phys.* **36**, 313.

Hantzsche, W. & Wendt, H. 1940 *Jb. dtsch. Luftfahrtf.*

Kuo, Y-H. 1947 *Quart. Appl. Maths.* **4**, 349.

Lighthill, M. J. 1948 *Quart. J. Math. Appl. Mech.* **1**, 309.

Pack, D. C. 1948 *Quart. J. Math. Appl. Mech.* **1**, 1.

Poisson, S. D. 1808 *J. Éc. polyt., Paris*, **7**, 319.

Roberts, L. 1957 *J. Maths. Phys.* **36**, 329.

Stokes, E. E. 1848 *Phil. Mag.* (3), **33**, 349.

Taylor, Sir Geoffrey 1946 *Proc. Roy. Soc.* A, **186**, 273.

Unwin, J. J. 1941 *Proc. Roy. Soc.* A, **178**, 153.

On a singular point in the Newtonian theory of hypersonic flow

By N. C. FREEMAN

National Physical Laboratory, Teddington, England*

(Received 15 October 1959)

An examination of the Newtonian inviscid theory of hypersonic flow past a sphere is made in the neighbourhood of the singular point which occurs at $\theta = 60°$. A uniformly valid theory is developed in this neighbourhood which exhibits the limiting detached 'free-layer' behaviour postulated by Hayes and Lighthill in the limit as $\gamma \to 1$. A complete solution is obtained which gives details of streamline and shock wave shape, pressure distribution, etc. for $\gamma - 1$ small.

Reasons are given why the empirical 'modified' Newtonian theory of Lees proves to be a good approximation to experimentally determined pressure distributions.

A novel check to the theory is provided by a simple power-law relation between the pressure on the sphere surface and the distance of the shock wave away from sphere at the same point.

1. Introduction

The Newtonian theory of hypersonic flow has been developed in the past few years from the original ideas of Busemann (1933). A review of this work is given by Hayes & Probstein (1959), to which the reader is referred for numerous references. A solution to the problem of flow of a hypersonic inviscid stream past a bluff body is achieved by an expansion procedure in powers of ρ_0/ρ_s, where ρ is the density and the suffices 0 and s denote values in the free stream and behind the bow shock wave, respectively. The free-stream Mach number is generally assumed infinite although this is not essential (e.g. Chester 1956). In the case of a perfect gas, the above ratio is simply $(\gamma-1)/(\gamma+1)$, where γ is the ratio of specific heats, and the expansion is then carried out in powers of $\epsilon = (\gamma-1)/(\gamma+1)$. No rigorous proof has been given that such an expansion will converge and close examination of the first few terms would seem to indicate that it is, at best, only slowly convergent. However, the solution obtained is the correct solution in the limit as $\epsilon \to 0$. For this reason, one might expect that it would give results which bear a resemblance to those for $\epsilon \neq 0$; but both numerical computations using the complete equations and experimental results would seem to indicate that this is not so. In particular, the pressure predicted on the surface of the body seems to bear little relationship to that observed in experiments. Lees (1955) has suggested that the correct form for reduction of experimental results on a sphere is given by

* This research was undertaken while the author was on leave of absence at Princeton University.

$C_p/C_{p_{\max}} = \cos^2\theta$, where C_p is the pressure coefficient, $C_{p_{\max}}$ its value at the stagnation point and θ is the angle measured from the stagnation point. This result would seem to indicate that, to obtain a theoretical justification, one need simply admit that the pressure is determined by a spherical shock wave with a suitable adjustment for the pressure at the stagnation point. Although this result has the virtue of simplicity, it adds little to our understanding of the theoretical problem. Moreover, the theoretical result as suggested by Busemann (1933) would require a more complicated expression for the pressure distribution, since the pressure is determined not only by the shock-pressure rise, but also by the centrifugal effect due to the curvature of the body. The resulting pressure distribution is then made up of a pressure rise at the shock wave followed by a pressure drop between the shock wave and body. The resulting form of the pressure variation on a sphere in the limit $\epsilon \to 0$ is then

$$C_p/C_{p_{\max}} = \sin 3\theta/3\sin\theta$$

or, alternatively,

$$C_p/C_{p_{\max}} = \cos^2\theta - \tfrac{1}{3}\sin^2\theta.$$

The final term is the contribution from the centrifugal pressure gradient between shock wave and body. It should be noticed that the pressure becomes zero for $\theta = 60°$ when the first and second terms above become equal. At this point, the assumptions of the Busemann theory are no longer valid and the solutions obtained from the theory have a singular behaviour. The author believes that it is at this point that the answer to the discrepancy between theory and experiment may be found. The non-uniformity of the convergence of the solution as $\epsilon \to 0$ near this point produces a singular behaviour which influences a large part of the flow field.

In this paper, we shall investigate the nature of the singularity near this point and postulate a solution which converges uniformly in this neighbourhood. Although it is impossible to state whether this solution is unique, it would seem to possess all the characteristics required of it. The problem, as it presents itself, is as follows: For $\theta < 60°$, we have a solution as determined by the Newtonian theory in which the pressure tends to zero like $(\frac{1}{3}\pi - \theta)$ and the distance of the shock wave away from the sphere (measured radially) becomes infinite like $(\frac{1}{3}\pi - \theta)^{-\frac{2}{3}}$. For $\theta > 60°$, it was originally suggested by Busemann that the flow 'separates'. This idea has led Lighthill (1957) and Hayes & Probstein (1959) to postulate that the fluid is flung away from the sphere at this point and proceeds as a 'free-layer', the pressure on the body surface becoming identically zero. If the assumption is then made that the fluid proceeds in a thin layer close to the shock wave, it is possible to obtain an analytic expression for the shape of the shock wave. The 'free-layer' solution of Lighthill (1957) and Hayes & Probstein (1959) has the limiting form for the shock shape

$$\tfrac{1}{6}(\theta - \tfrac{1}{3}\pi)^3$$

near $\theta = \frac{1}{3}\pi$. For the Newtonian solution, the shock layer thickness is proportional to ϵ, while for the free-layer solution it is independent of ϵ. Thus, we are required to find a solution to the problem which behaves like

$$\epsilon(\tfrac{1}{3}\pi - \theta)^{-\frac{2}{3}} \quad \text{for} \quad \theta < \tfrac{1}{3}\pi. \tag{1}$$

and like

$$(\theta - \tfrac{1}{3}\pi)^3 \quad \text{for} \quad \theta > \tfrac{1}{3}\pi. \tag{2}$$

The type of solution required is shown schematically in figure 1. If we consider an expanded system of co-ordinates and an expanded shock shape represented by a relationship of the form

$$\epsilon^{\alpha} Y[(\theta - \tfrac{1}{3}\pi)\,\epsilon^{\beta}], \tag{3}$$

these conditions require that

$$Y(z) \to z^3 \quad \text{as} \quad z \to +\infty \tag{4}$$

and

$$Y(z) \to (-z)^{-\frac{3}{8}} \quad \text{as} \quad z \to -\infty. \tag{5}$$

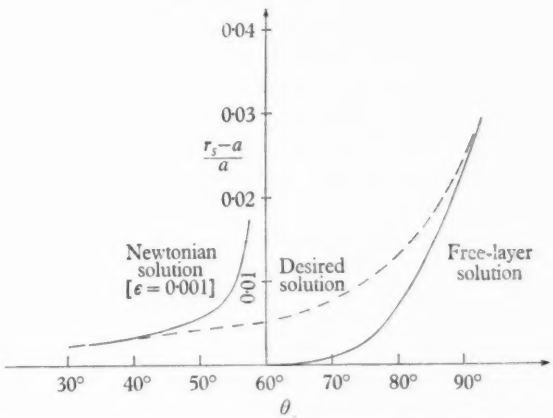

FIGURE 1. The desired form of solution for the shock shape.

In order that the dependence on ϵ be correct, we therefore require

$$\left.\begin{aligned} \alpha + 3\beta &= 0, \\ \alpha - (\tfrac{2}{3})\beta &= 1, \end{aligned}\right\} \tag{6}$$

by equating exponents of ϵ. Thus

$$\beta = -\tfrac{3}{11} \quad \text{and} \quad \alpha = \tfrac{9}{11}. \tag{7}$$

The shock shape is, therefore, given in the form

$$\epsilon^{\frac{9}{11}} Y(\{\theta - \tfrac{1}{3}\pi\}\,\epsilon^{-\frac{3}{11}}). \tag{8}$$

The limiting forms of the solution for Y are given by (4) and (5). It will be shown below that Y satisfies a non-linear second-order differential equation. It does not seem possible to obtain an analytic expression for Y. However, the equation can be integrated numerically and then we see from (8) that the solution is known for all ϵ. By the type of argument used above, it is possible to deduce the required behaviour of the shock shape with ϵ. It is possible to determine much more from the complete theory. The behaviour of the whole flow field can be determined in the neighbourhood of the singular point. The procedure used is to expand the variables, both dependent and independent, in series with coefficients

dependent upon powers of ϵ, in a similar fashion to that suggested by Lighthill (1949). In fact, we will only consider the first term in this expansion. This we will do mainly to reduce the complexity of the problem. It should also be necessary to examine the expansions at other points in the flow field if the higher order terms were required.

Most of the results obtained below were determined by the author in a previous paper (1958). The method used, however, relied primarily on arguments on the physical mechanism of the transition from a Newtonian theory to a detached free-layer solution. In that paper, it was argued that the most important effect to be taken into account at the singular point is that of curvature of streamlines relative to the body. This result is confirmed in the present paper. The fact that this is so is perhaps the most encouraging result of the work. It will be realized that the result of Lees (1955) already indicates that this might be the case. For if the pressure drop due to body curvature is to be nullified, some mechanism is required which will give an increased surface pressure. The most obvious one is that the streamline curvature relative to the body should become important. In fact, the theory shows that this curvature is of the same order as the body curvature at the singular point. As, in practice, the singular point behaviour influences the whole flow field (due to the fact that ϵ is not mathematically very small), the experimental predictions become more understandable.

The most disconcerting feature of the theory is, however, already obvious from the form of (8). It will be seen that near the singular point the dependence is on $\epsilon^{\frac{3}{2}}x$ rather than on ϵ. A more detailed study of the flow field shows that this is, indeed, the case. In practice, $\epsilon^{\frac{3}{2}}x$ is never small enough for the theory to hold. In other words, the transition from the Newtonian to the free-layer solution depends on $\epsilon^{\frac{3}{2}}x$ being small and the free-layer solution will only be achieved when this condition is satisfied.

The theory has been developed below for the case of a sphere; but the theory is not restricted only to the sphere. Similar results could be obtained for any two-dimensional or axially symmetric body. The dependence on ϵ would, however, be different although it would seem straightforward by arguments similar to those used above to determine the correct form.

More generally, the approach to the problem is that used by the author (1956) in his treatment of Newtonian theory. The shock layer is considered to be a narrow region in which rates of changes across the layer are much larger than those along it. By consideration of the orders of magnitude of the variables, it is then possible to simplify the equations of motion considerably. In the region near the singular point, however, the orders of magnitude of the variables change and we are required to modify the equations accordingly.

2. The equations of motion

By considering a particular body shape (the sphere) we are able to choose a co-ordinate system immediately simplifying the analysis considerably. We shall choose a spherical polar system of co-ordinates with r and θ measured from the centre of the sphere and the forward stagnation point, respectively, $r = a$ is the surface of the sphere.

The equations of continuity, momentum and energy can then be written in the form

$$\frac{\partial}{\partial r}(\rho u r^2 \sin\theta) + \frac{\partial}{\partial \theta}(\rho v r \sin\theta) = 0, \tag{2.1}$$

$$u\frac{\partial u}{\partial r} + \frac{v}{r}\frac{\partial u}{\partial \theta} - \frac{v^2}{r} + \frac{1}{\rho}\frac{\partial p}{\partial r} = 0, \tag{2.2}$$

$$u\frac{\partial v}{\partial r} + \frac{v}{r}\frac{\partial v}{\partial \theta} + \frac{uv}{r} + \frac{1}{\rho r}\frac{\partial p}{\partial \theta} = 0, \tag{2.3}$$

$$u\frac{\partial i}{\partial r} + \frac{v}{r}\frac{\partial i}{\partial \theta} = \frac{1}{\rho}\left[u\frac{\partial p}{\partial r} + \frac{v}{r}\frac{\partial p}{\partial \theta}\right], \tag{2.4}$$

where u, v are the velocities in the r and θ directions; ρ is the density; p the pressure; and i the enthalpy. If we assume a perfect gas with constant specific heats then

$$i = \frac{\gamma}{\gamma - 1}\frac{p}{\rho}. \tag{2.5}$$

Introduction of the Stokes' stream function, ψ, to satisfy equation (2.1), then gives the following set of equations:

$$\frac{\partial \psi}{\partial r} = \rho v r \sin\theta, \quad \frac{\partial \psi}{\partial \theta} = -\rho u r^2 \sin\theta, \tag{2.6}$$

$$\frac{\partial u}{\partial \theta} - v + \frac{\partial p}{\partial \psi} r^2 \sin\theta = 0, \tag{2.7}$$

$$v\frac{\partial v}{\partial \theta} + uv + \frac{1}{\rho}\left(\frac{\partial p}{\partial \theta} - \frac{\partial p}{\partial \psi}\rho u r^2 \sin\theta\right) = 0, \tag{2.8}$$

$$\frac{\partial i}{\partial \theta} = \frac{1}{\rho}\frac{\partial p}{\partial \theta}, \tag{2.9}$$

where θ and ψ are taken as the independent variables in equations (2.7) to (2.9).

The Newtonian theory may then be deduced by considering a new system of variables

$$\left.\begin{aligned} \rho' = \epsilon\frac{\rho}{\rho_\infty}, \quad p' = \frac{p}{\rho_\infty U_\infty^2}, \quad v' = \frac{v}{U_\infty}, \quad u' = \frac{u}{\epsilon U_\infty}, \\ \psi' = \frac{\psi}{\rho_\infty U_\infty a^2}, \quad r' = \frac{r-a}{a\epsilon}, \quad \theta' = \theta. \end{aligned}\right\} \tag{2.10}$$

All the dashed variables are then assumed of order unity. The equations (2.7) to (2.9) then reduce to

$$\frac{\partial p}{\partial \psi} = \frac{v}{a^2 \sin\theta}, \quad \frac{\partial v}{\partial \theta} = 0 \quad \text{and} \quad \frac{\partial i}{\partial \theta} = 0 \tag{2.11}$$

which together with (2.6) then give the Newtonian approximation. The shock layer is assumed thin and, hence, approximately spherical. Equations (2.11) can then be integrated to give

$$p = \frac{1}{a^2 \sin\theta}\int_{\psi_s}^{\psi} v(\psi)\, d\psi + p_s,$$

where s denotes values at the shock wave. Using the strong shock wave approximations we have

$$p = \left\{\frac{\sin 3\theta + \sin^3 \xi}{3 \sin \theta}\right\} \rho_\infty U_\infty^2, \tag{2.12}$$

where $$\psi = \tfrac{1}{2}\rho_\infty U_\infty a^2 \sin^2 \xi.$$

Equation (2.6) then gives

$$\frac{r-a}{a} = 3\epsilon \int_0^{\sin \xi} \frac{(1-s^2)\,ds}{\sin 3\theta + s^3}. \tag{2.13}$$

This is then the equation of the streamlines, $\xi = \text{const.}$, and $\xi = \theta$ is the equation of the shock wave.

	Order of magnitude	
Variable	Newtonian	Near singular point
$p/\rho_\infty U_\infty^2$	1	$\epsilon^{\frac{3}{11}}$
u/U_∞	ϵ	$\epsilon^{\frac{7}{11}}$
v/U_∞	1	$\epsilon^{\frac{1}{11}}$
ρ/ρ_∞	ϵ^{-1}	$\epsilon^{-\frac{8}{11}}$
$\psi/a^2\rho_\infty U_\infty$	1	$\epsilon^{\frac{3}{11}}$
$(r-a)/a$	ϵ	$\epsilon^{\frac{9}{11}}$
θ	1	—
$\frac{1}{3}\pi - \theta$	—	$\epsilon^{\frac{3}{11}}$

TABLE 1

From equation (2.13), it is clear that at $\theta = \frac{1}{3}\pi$, we have some kind of singular behaviour. In fact, we have

$$\frac{r-a}{a} \sim \frac{2\pi}{3^{\frac{7}{6}}} (\tfrac{1}{3}\pi - \theta)^{-\frac{3}{2}}, \tag{2.14}$$

provided that $$\lim_{\theta \to \frac{1}{3}\pi} [\sin \xi / (\sin 3\theta)^{\frac{1}{2}}] \to \infty.$$

Similarly, the pressure on the sphere surface ($\xi = 0$) tends to zero like

$$(2/\sqrt{3})\,(\tfrac{1}{3}\pi - \theta). \tag{2.15}$$

The breakdown of the theory is thus associated with the vanishingly small pressure at the sphere surface. When this occurs, it is no longer possible to assume orders of magnitude for the variables as in equation (2.10). Is it possible, though, to determine orders of magnitude for the variables in the neighbourhood of the singular point and, hence, obtain a uniformly valid solution in this region? In § 1, an argument was put forward which gives a uniformly valid form near $\theta = 60°$. This result indicates that near this point, the shock layer has a thickness which is order $a\epsilon^{\frac{9}{11}}$ and the rates of change along the shock layer are order $a\epsilon^{\frac{3}{11}}$. A close examination of the equations (2.1) to (2.4) then leads to the orders of magnitude shown in table 1, where they are also compared with the original orders of magni-

tude of the Newtonian theory. We therefore consider a new system of variables such that

$$\left.\begin{aligned} p &= \epsilon^{\frac{8}{11}}\rho_\infty U_\infty^2 P(z,\zeta),\\ u &= \epsilon^{\frac{7}{11}}U_\infty U(z,\zeta),\\ v &= \epsilon^{\frac{3}{11}}U_\infty V(z,\zeta),\\ \rho &= \epsilon^{-\frac{8}{11}}\rho_\infty \Omega(z,\zeta),\\ \psi &= \tfrac{1}{2}a^2\rho_\infty U_\infty \epsilon^{\frac{8}{11}}\zeta^2,\\ r-a &= \epsilon^{\frac{8}{11}}aR(z,\zeta), \end{aligned}\right\} \tag{2.16}$$

where
$$\theta-\tfrac{1}{3}\pi = \epsilon^{\frac{3}{11}}z \quad \text{and} \quad \sin\xi = \epsilon^{\frac{1}{11}}\zeta. \tag{2.17}$$

Substituting in equations (2.6) to (2.8), we obtain

$$\zeta\frac{\partial\zeta}{\partial R} = \Omega V\frac{\sqrt{3}}{2}, \quad \zeta\frac{\partial\zeta}{\partial z} = -\Omega U\frac{\sqrt{3}}{2} \tag{2.18}$$

$$\frac{\partial V}{\partial z} = O(\epsilon^{\frac{8}{11}}) \quad \text{and} \quad \frac{\partial}{\partial z}\left(\frac{P}{\Omega}\right) = O(\epsilon),$$

where terms of order $\epsilon^{\frac{3}{11}}$ have been neglected in the first two equations. These equations therefore remain essentially the same as for the 'Newtonian' theory. At first sight, it would appear that equation (2.9) does also, since this becomes

$$\frac{1}{\zeta}\frac{\partial P}{\partial\zeta}\frac{\sqrt{3}}{2} - V\left(1-\frac{z}{\sqrt{3}}\epsilon^{\frac{3}{11}}\right)+\epsilon^{\frac{3}{11}}\frac{\partial U}{\partial z} = 0. \tag{2.19}$$

However, the shock layer in the expanded co-ordinate system now extends from $\zeta = 0$ to $\zeta \sim \epsilon^{-\frac{1}{11}}$ and, hence, it is possible that the terms in $\epsilon^{\frac{3}{11}}$ can contribute.

Integrating equation (2.19), we obtain

$$P = \frac{2}{\sqrt{3}}\int_{\zeta_s}^{\zeta}\left\{V-\epsilon^{\frac{3}{11}}\left[\frac{Vz}{\sqrt{3}}+\frac{\partial U}{\partial z}\right]\right\}\zeta\,d\zeta + P_s, \tag{2.20}$$

where suffix s denotes values at the shock wave.

Now on the shock wave $V = U_\infty\cos\phi$, where Φ is the angle the shock wave makes with the free stream. Now $\phi = \frac{1}{2}\pi-\theta+O(\epsilon^{\frac{8}{11}})$ and, hence, $V = U_\infty\{\sin\theta+O(\epsilon^{\frac{8}{11}})\}$ on the shock wave. Also, since the value of ψ on the shock wave is related only to the slope of the shock wave, we have $\theta = \xi+O(\epsilon^{\frac{8}{11}})$ at the shock wave. Hence, using (2.16) and (2.18), we obtain

$$V = \zeta+O(\epsilon^{\frac{5}{11}}). \tag{2.21}$$

Similarly
$$\begin{aligned} p_s &= \rho_\infty U_\infty^2(1-\epsilon)\sin^2\phi\\ &= \rho_\infty U_\infty^2\{\cos^2\theta+O(\epsilon^{\frac{8}{11}})\}, \end{aligned}$$

and thus
$$P = \tfrac{1}{4}\epsilon^{-\frac{8}{11}}-\frac{\sqrt{3}}{2}z+O(\epsilon^{\frac{3}{11}}). \tag{2.22}$$

Again
$$\begin{aligned} \zeta = \zeta_s &= \epsilon^{\frac{1}{11}}\sin\theta\\ &= \epsilon^{-\frac{1}{11}}\frac{\sqrt{3}}{2}\left(1+\frac{\epsilon^{\frac{3}{11}}}{\sqrt{3}}z\right) \end{aligned} \tag{2.23}$$

on the shock wave.

Substituting in equation (2.20), we have

$$\begin{aligned} P &= \tfrac{1}{4}\epsilon^{-\frac{3}{11}} - \frac{\sqrt{3}}{2}z - \frac{2}{\sqrt{3}}\int_{\zeta}^{\zeta_s}\zeta^2\,d\zeta + \frac{2}{\sqrt{3}}\epsilon^{\frac{3}{11}}\int_{\zeta}^{\zeta_s}\zeta^2\,d\zeta \\ &\qquad + \frac{2}{\sqrt{3}}\epsilon^{\frac{3}{11}}\int_{\zeta}^{\zeta_s}\frac{\partial U}{\partial z}\,\zeta\,d\zeta + O(\epsilon^{\frac{3}{11}}) \\ &= -\frac{2}{\sqrt{3}}z + \frac{2}{\sqrt{3}}\frac{\zeta^3}{3} + \frac{2}{\sqrt{3}}\epsilon^{\frac{3}{11}}\int_{\zeta}^{\sqrt{\frac{3}{2}}\epsilon^{-1/11}}\frac{\partial U}{\partial z}\,\zeta\,d\zeta + O(\epsilon^{\frac{3}{11}}) \\ &= -\frac{2}{\sqrt{3}}z + \frac{2}{\sqrt{3}}\frac{\zeta^2}{3} + \frac{2}{\sqrt{3}}\int_{\zeta}^{\sqrt{\frac{3}{2}}\epsilon^{-1/11}}\frac{\partial}{\partial z}\left(\frac{U}{V}\right)\zeta^2\,d\zeta + O(\epsilon^{\frac{3}{11}}) \\ &= -\frac{2}{\sqrt{3}}z + \frac{2}{3\sqrt{3}}\zeta^3 + \frac{1}{4}\left\{\frac{\partial}{\partial z}\left(\frac{U}{V}\right)\right\}_{\zeta=\infty} + o(\epsilon^{\frac{3}{11}}). \end{aligned} \tag{2.24}$$

Now, from equation (2.18), we have

$$\frac{U}{V} = -\frac{\partial\zeta/\partial z}{\partial\zeta/\partial R} = \left(\frac{\partial R}{\partial z}\right)_{\zeta} \tag{2.25}$$

and, hence,

$$P = -\frac{2}{\sqrt{3}}z + \frac{2}{3\sqrt{3}}\zeta^3 + \frac{1}{4}\left(\frac{\partial^2 R}{\partial z^2}\right)_{\zeta=\infty} + o(\epsilon^{\frac{3}{11}}). \tag{2.26}$$

Thus, the pressure is modified from the Newtonian value which comprises the first two terms by a term which depends on the curvature of the streamlines at $\zeta = \infty$. In the expanded system of co-ordinates, $\zeta = \infty$ corresponds to the shock wave.

The distance of the streamlines away from the body is obtained from equations (2.18) as

$$R = \frac{2}{\sqrt{3}}\int_0^{\zeta}\frac{d\zeta}{\Omega}. \tag{2.27}$$

Since

$$\frac{P}{\Omega} = \frac{P_s}{\Omega_s} = 1 + O(\epsilon^{\frac{3}{11}}). \tag{2.28}$$

we obtain

$$\begin{aligned} R &= \frac{2}{\sqrt{3}}\int_0^{\zeta}\frac{d\zeta}{P} \\ &= \frac{2}{\sqrt{3}}\int_0^{\zeta}\frac{d\zeta}{\frac{\sqrt{3}}{4}(-z) + \frac{2}{3\sqrt{3}}\zeta^3 + \frac{1}{4}\left(\frac{\partial^2 R}{\partial z^2}\right)_{\zeta=\infty}}. \end{aligned} \tag{2.29}$$

If we let $R_1 = R(z, \infty)$, then

$$\begin{aligned} R_1 &= \frac{2^{\frac{2}{3}}}{\left\{\frac{2}{\sqrt{3}}(-z) + \frac{1}{4}\frac{d^2R_1}{dz^2}\right\}^{\frac{2}{3}}}\int_0^{\infty}\frac{d\eta}{1+\eta^3} \\ &= \frac{8\pi}{3\sqrt{3}}\left\{\frac{d^2R_1}{dz^2} + \frac{8}{\sqrt{3}}(-z)\right\}^{-\frac{3}{2}}. \end{aligned}$$

The equation of the shock wave is then given by

$$\frac{d^2R_1}{dz^2} - \frac{8}{\sqrt{3}}z = \left(\frac{8\pi}{3\sqrt{3}}\right)^{\frac{2}{3}}R_1^{-\frac{3}{2}}. \tag{2.30}$$

Near the sphere itself, where ζ is still small, the equations of the streamlines are given by

$$R = \frac{2}{\sqrt{3}} \int_0^{\zeta} \frac{d\zeta}{\frac{2}{\sqrt{3}}(-z) + \frac{1}{4}\frac{d^2R_1}{dz^2} + \frac{2}{3\sqrt{3}}\zeta^2}, \tag{2.31}$$

where R_1 is calculated from equation (2.30).

The pressure is obtained from equation (2.26); and, in particular, the pressure on the surface of the sphere is

$$P = \frac{2}{\sqrt{3}}(-z) + \frac{1}{4}\frac{d^2R_1}{dz^2}. \tag{2.32}$$

We have thus reduced the problem to solving equation (2.30). It does not seem possible to do this analytically; but since equation (2.30) only need be solved to give a complete solution, the numerical evaluation can be done once and for all. The boundary condition on equation (2.30) is given at $z = -\infty$, where R_1 must behave like the original Newtonian solution. The details of the types of solution of equation (2.30) and the method of solution are given in the Appendix.

In the original co-ordinate system, the shock wave shape is expressible in the form

$$\frac{r-a}{a} = \epsilon^{\frac{9}{11}} R_1[\epsilon^{-\frac{3}{11}}(\theta - \tfrac{1}{3}\pi)], \tag{2.33}$$

where R_1 is the solution of (2.30).

The surface pressure is given in the form

$$p = \rho_\infty U_\infty^2 \epsilon^{\frac{3}{11}} P_b[\epsilon^{-\frac{3}{11}}(\theta - \tfrac{1}{3}\pi)], \tag{2.34}$$

where

$$P_b(z) = \frac{2}{\sqrt{3}}(-z) + \frac{1}{4}\frac{d^2R_1}{dz^2},$$

and the streamlines by

$$\frac{r-a}{a} = \epsilon^{\frac{9}{11}} G[\epsilon^{-\frac{3}{11}}(\theta - \tfrac{1}{3}\pi),\ \epsilon^{-\frac{1}{11}} \sin\xi], \tag{2.35}$$

where

$$G(z,\zeta) = \frac{3}{F(z)^{\frac{8}{5}}} \int_0^{\zeta/[\{F(z)\}^{\frac{1}{5}}]} \frac{d\zeta}{1+\zeta^3}$$

and

$$F(z) = \frac{3\sqrt{3}}{2} P_b(z).$$

We see, therefore, that in the limit as $\epsilon \to 0$, the shock wave approaches the limiting forms of the solution at $\pm\infty$ depending on whether $\theta \gtrless \frac{1}{3}\pi$. The solution to equation (2.30) is such that

$$\begin{aligned} R_1 &\sim (-z)^{-\frac{3}{2}} && \text{as} \quad z \to -\infty \\ &\sim z^3 && \text{as} \quad z \to +\infty. \end{aligned}$$

In the limit of $\epsilon \to 0$, we have

$$\frac{r-a}{a} \sim \epsilon\,(\tfrac{1}{3}\pi - \theta)^{-\frac{3}{2}} \quad \text{for} \quad \theta < \tfrac{1}{3}\pi$$

and

$$\frac{r-a}{a} \sim (\theta - \tfrac{1}{3}\pi)^3 \quad \text{for} \quad \theta > \tfrac{1}{3}\pi.$$

We can also investigate the behaviour of the streamlines as $\epsilon \to 0$. For $\zeta = \infty$, the streamlines very close to the shock wave are identical with it. However, when ζ is not large the same limiting behaviour occurs when

$$\frac{2^{\frac{1}{3}} \sin \xi}{\sqrt{3}\, \epsilon^{\frac{1}{11}} \{P_b[\epsilon^{-\frac{3}{11}}(\theta - \tfrac{1}{3}\pi)]\}^{\frac{1}{3}}} \to \infty. \tag{2.36}$$

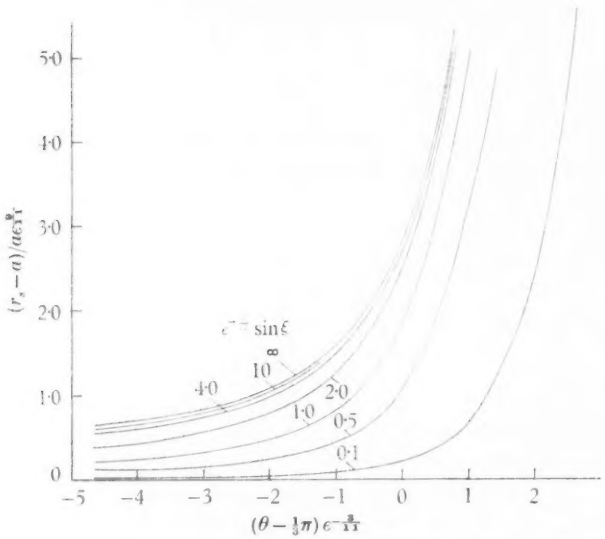

FIGURE 2. The shock shape ($\epsilon^{-\frac{1}{11}} \sin \xi = \infty$) and the streamlines ($\epsilon^{-\frac{1}{11}} \sin \xi = \text{const.}$) in the neighbourhood of the singular point ($\theta = 60°$).

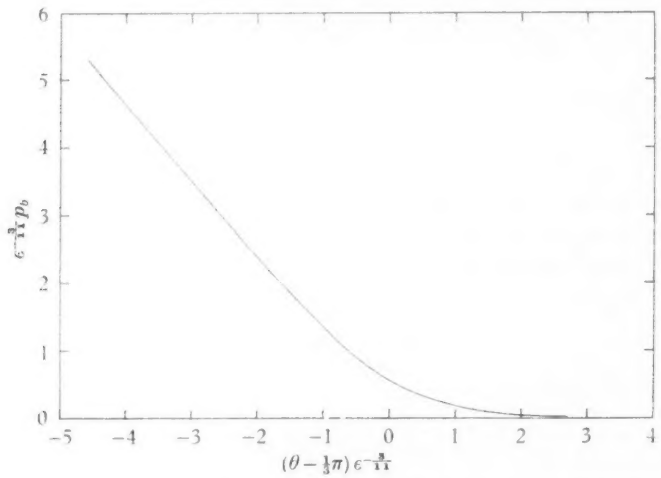

FIGURE 3. Pressure variation at the surface of the sphere in the neighbourhood of the singular point $\theta = 60°$.

For $\theta < \frac{1}{3}\pi$, this occurs when

$$\frac{\sin\xi}{(\frac{1}{3}\pi-\theta)^{\frac{1}{3}}} \to \infty,$$

and for $\theta > \frac{1}{3}\pi$, when $\quad \epsilon^{-\frac{1}{2}}(\theta-\frac{1}{3}\pi)^{\frac{3}{2}}\sin\xi \to \infty.$

Hence, for $\theta < \frac{1}{3}\pi$, the streamlines are distributed independently of ϵ, whereas for $\theta > \frac{1}{3}\pi$, the streamlines approach the shock wave at a rate proportional to $\epsilon^{-\frac{1}{2}}$ as ϵ tends to zero. Thus, we see from the equation for the shock wave shape that the region of transition from the Newtonian theory to the free-layer solution is of order $\epsilon^{\frac{3}{11}}$, but after separation, the free-layer solution is achieved comparatively rapidly like $\epsilon^{-\frac{1}{2}}$. The pressure along the body surface falls rapidly to zero like

$$\epsilon^{\frac{3}{2}}(\theta-\tfrac{1}{3}\pi)^{-\frac{9}{2}}.$$

The solution to equation (2.30) was calculated using the method outlined in the Appendix. The results are plotted in figure 2, together with the equations of the streamlines computed from equation (2.35). The rapidity of the transition to the free-layer solution is immediately evident although the scale of phenomena is proportional to $\epsilon^{\frac{3}{11}}$. The surface pressure is computed from equation (2.34) and is plotted in figure 3. In each case, the expanded co-ordinates are used to give universal curves for all ϵ.

3. Physical implications of the theory

As mentioned in § 1, it has been difficult in the past to try to compare directly the experimental and theoretical results, since the discrepancy between the two was inconsistent with the original Newtonian theory. It is clear, however, from the theory of § 2 that the modification necessary to correct the pressure distribution given by Newtonian theory is to take into account the curvature of the streamlines relative to the body. To a first approximation, this curvature may be taken equal to the curvature of the shock wave. This prediction may be checked in a rather interesting manner, for using (2.32) and (2.30) we see that

$$\frac{p_b}{\rho_\infty U_\infty^2} \propto \frac{\epsilon^{\frac{3}{2}}}{[(r_s-a)/a]^{\frac{3}{2}}}. \tag{3.1}$$

The pressure on the surface of the sphere p_b is, therefore, related to the distance of the shock from the sphere by an inverse three-halves power law. This result is plotted in figure 4 for two sets of experimental results: the first in air at $M_\infty = 5{\cdot}8$, due to Oliver (1956), and the second in helium at $M_\infty = 14{\cdot}0$, due to Vas, Bogdonoff & Hammitt (1958).

Direct comparison of the results with experiment is difficult, however, since ϵ is never small enough physically for the theory to hold. The transition region, discussed in the previous section, in practice spans the region from stagnation point to the shoulder of the sphere. Thus, the theory shows that the singular behaviour of the Newtonian result will tend in practice to influence the whole flow field. Comparison of the pressure with experimental results shows that the theoretical predictions are considerably larger than the experimental values for $\epsilon = \frac{1}{6}$ and $\frac{1}{4}$. This is due to the singular behaviour influencing the whole region including the stagnation region. Since the pressure is in the first approximation a linear function away from the singular point (as shown by the first term of (2.32)),

this would tend to over-emphasize the pressure in the stagnation region, where the Newtonian theory shows a nearly constant value. It should be noted, however, that equation (2.30) cannot be used right up to the stagnation point. For, it is clear that the factor multiplying d^2R/dz^2 in (2.30) is the momentum flow in the shock layer at $\theta = 60°$. It would be more correct, therefore, to reduce this as the

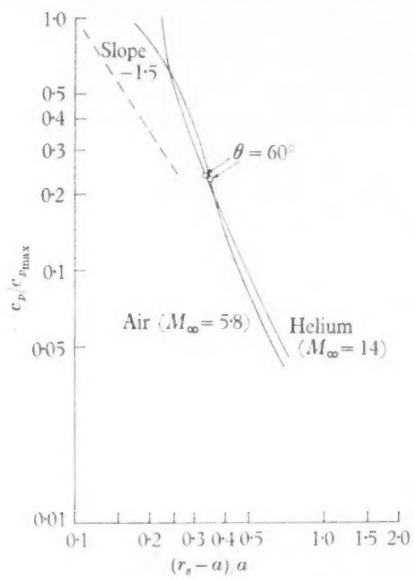

FIGURE 4. Experimental results of Oliver (1956) and Vas *et al.* (1958) plotted for comparison with equation (3.1).

stagnation point is approached to the correct value as given by the Newtonian theory at that value of θ. Integration of an equation using this correction and also the correct Newtonian pressure distribution shows that a distribution much closer to experiment can be obtained. In fact, for ϵ equal to $\frac{1}{6}$ or $\frac{1}{4}$ a further complication arises because the singular behaviour has influenced this linear variation even at the stagnation point. This effect is rather disconcerting, since the result obtained by using a much cruder equation for the pressure based on physical reasoning similar to the above gave a much closer agreement with experiment (cf. Freeman 1958). Of course, it is now clear that, mathematically, these additional refinements are unjustified within the uniformly valid approximation.

4. Conclusion

The theory outlined above shows the nature of the solution to the hypersonic inviscid flow past a sphere in the neighbourhood of the singular point obtained when $\epsilon \to 0$ for free-stream Mach number infinite. The result also indicates that the curvature of the streamlines relative to the body is the most important factor in this region. Although in practice ϵ is never so small that this part of the flow field is independent of the other parts, the limiting form of the solution is of

interest in showing how the transition from the initially attached Newtonian flow to the detached free-layer solution would occur.

It is clear from the results that the free-layer solution is reached fairly rapidly after the transition region (figure 2).

It would seem possible to develop similar theories for other bluff bodies, both two-dimensional and axially symmetric. The method would be essentially the same. A general formulation of the problem for any bluff body would seem to be rather complicated, however.

Perhaps a more interesting development from the above theory could be obtained by considering other Newtonian solutions and analyzing the solution in the neighbourhood of discontinuities of slope, curvature, etc. In this way, it would seem possible to develop a uniformly valid solution in the neighbourhood of such points.

It seems that the procedure developed in this paper is an extremely powerful one in obtaining solutions to the hypersonic bluff body problem. If one considers that the result obtained by the author in his previous paper (1956) to be the fundamental Newtonian solution, then the theory of the type developed above may be considered as the solution to a particular problem in a region where that solution does not have uniform validity. In a similar way, it is possible to obtain other Newtonian solutions by simply requiring that in other limiting processes a uniformly valid solution is required. The author has succeeded in obtaining the solution for a blunt body originally derived by Hayes (see Hayes & Probstein 1959, Chap. 5) and Serbin (1956).

The author would like to thank Prof. W. D. Hayes and Dr S. H. Lam of Princeton University for many valuable discussions on this subject.

The work was carried out at the Gas Dynamics Laboratory, Princeton University and is sponsored by the Office of Scientific Research, Air Research and Development Command, Fluid Mechanics Division, under Contract AF 49(638)-465.

Appendix

Solution to equation (2.30)

We require a solution to the equation

$$\frac{d^2R_1}{dz^2} - \frac{8}{\sqrt{3}}z = \left(\frac{8\pi}{3\sqrt{3}}\right)^{\frac{3}{4}} R_1^{-\frac{3}{4}}, \tag{A 1}$$

subject to the boundary condition that at $z = -\infty$ the solution is obtained by neglecting the d^2R_1/dz^2 term.

A change of variables

$$\left.\begin{aligned} y &= \frac{3^{\frac{33}{44}}}{8^{\frac{5}{11}}\pi^{\frac{9}{11}}} R_1, \\ \text{and} \quad x &= \frac{3^{\frac{8}{11}}2^{\frac{33}{44}}}{\pi^{\frac{8}{11}}} z \end{aligned}\right\} \tag{A 2}$$

reduces the equation to the form

$$\frac{d^2y}{dx^2} = x + \frac{1}{y^{\frac{3}{4}}}. \tag{A 3}$$

It does not seem possible to get an analytic solution to (A 3) and hence we must resort to numerical methods. The behaviour of the equation (A 3) near the point

$x = -\infty$ is somewhat complicated as can be seen from perturbing the known asymptotic form. For, putting

$$y = (-x)^{-\frac{3}{2}} + y_1,$$

we obtain

$$\frac{d^2y_1}{dx^2} + \tfrac{3}{2}(-x)^{\frac{5}{2}} y_1 = -\tfrac{10}{9}(-x)^{-\frac{5}{2}} \tag{A 4}$$

neglecting the higher order terms. We see that for x near $-\infty$ the above equation has complementary functions of the form

$$y_1 \sim \frac{1}{(-x)^{\frac{5}{12}}} \exp\left\{\pm i \tfrac{6}{11}\sqrt{\tfrac{3}{2}}(-x)^{\frac{11}{6}}\right\} \tag{A 5}$$

which tend to zero in an oscillatory manner with x but whose derivatives become infinite. The particular integral of (A 4) is the solution we require. It is clear, therefore, that we must use some procedure to get away from $x = -\infty$ before we use the normal integration procedure. We do this by using the asymptotic solution of (A 3) which is

$$y = (-x)^{-\frac{3}{2}} \sum_{n=0}^{\infty} b_n (-x)^{-\frac{11}{2}n}, \tag{A 6}$$

where b_0, b_1, b_2, ... are given in Table 2.

n	b_n
0	1·0
1	0·740741
2	12·0988
3	−602·554
4	60,999·4

TABLE 2

This solution is only slowly convergent but it was found possible to use the above expansion up to $x = -6$. The integration was then continued using the usual integration procedure up to $x = +6$, taking intervals of 0·25.

An asymptotic expansion can also be obtained for large x and fitted to the solution obtained by numerical integration.

REFERENCES

BUSEMANN, A. 1933 *Handworterbuch der Naturwissenschaften*, Auflage 2. Jena: Gustav Fischer.

CHESTER, W. 1956 *J. Fluid Mech.* **1**, 353.

FREEMAN, N. C. 1956 *J. Fluid Mech.* **1**, 366.

FREEMAN, N. C. 1958 *Aero. Res. Coun. Rep.* 19,871 (unpublished).

HAYES, W. D. & PROBSTEIN, R. F. 1959 *Hypersonic Flow Theory*, Chs. III–V. New York: Academic Press.

LEES, L. 1955 Hypersonic flow. *I.A.S. Preprint*, no. 554.

LIGHTHILL, M. J. 1949 *Phil. Mag.* 7th series, **40**, 1179.

LIGHTHILL, M. J. 1957 *J. Fluid Mech.* **2**, 1.

OLIVER, R. E. 1956 *J. Aero. Sci.* **23**, 177.

SERBIN, H. 1956 *Res. Memos.* RM 1713 and RM 1772. The Rand Corporation, Santa Monica, Calif.

VAS, I. E., BOGDONOFF, S. M. & HAMMITT, A. G. 1958 *Jet Propulsion*, **28**, 97.

The melting of ice in a hot humid stream of air

By DONALD L. TURCOTTE
U.S. Naval Postgraduate School, Monterey, California*

(Received 13 October 1959)

By use of appropriate approximations the incompressible stagnation-point ablation rate for ice is determined theoretically. The theory includes both melting and vaporization or condensation. To verify the theory hemispheres of ice were melted in a subsonic wind tunnel with controlled humidity. It is found that the effects of heat transfer and condensation are of equal importance in determining the melt rate. The agreement between theory and experiment is adequate.

1. Introduction

In order to understand the many mechanisms involved in ablation it seems appropriate to study some of the simpler problems in detail. It is the purpose of this paper to analyse the incompressible stagnation-point melting of ice from a hemisphere in hot, humid air. The convective heat transfer to the ice body will certainly melt it. However, vaporization or condensation of water can have an important effect on the melt rate. The problem considered here is illustrated in figure 1.

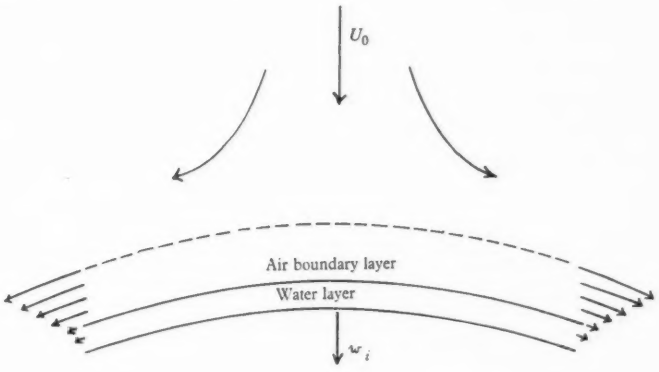

FIGURE 1. Illustration of stagnation-point ablation.

To obtain any solution to the problem many assumptions must be made. The work of Roberts (1958) provides an insight into what approximations are valid if mass transfer is neglected. In this paper these approximations are applied to the problem with diffusion effects included. The diffusion problem of mass transfer in boundary-layer flows has been discussed in detail by Lees (1958).

* Now at Cornell University, Ithaca, New York.

2. Theory

The solution of the incompressible boundary-layer equations for the stagnation region of a hemisphere is well known (Schlichting 1955, p. 162). The solution for a melting material which does not vaporize has been given by Roberts (1958). The results obtained by Roberts indicate what approximations may be valid in the present problem. A solution to the present problem will be obtained neglecting the presence of the water layer. This is equivalent to the following assumptions.

(i) The velocity at the air–water interface is small compared with the velocity at the outer edge of the air boundary layer.

(ii) The temperature increase across the water layer is small compared with the temperature increase in the air boundary layer.

(iii) The heat convected away in the water layer is small compared with the heat flux across the layer. Having obtained a solution utilizing this approximation, its validity will be checked.

With the presence of the water layer neglected, the boundary conditions at the water–ice interface may be applied at the air–water interface. Since it is assumed that the ice is at its melt temperature, the heat transfer $\dot{q}_W[l]$ on the liquid side of the air–water interface may be related directly to the melt rate w_i of the ice by the relation

$$\dot{q}_W[l] = \rho_i L_f w_i, \tag{1}$$

where L_f is the heat of fusion for water and ρ_i the density of ice.

The solution for the air boundary layer, including heat transfer and diffusion, may be obtained following the method of Lees (1958). For simplicity air will be denoted by the subscript A and water vapour by the subscript B. The enthalpy is then defined by $h = K_A h_A + K_B h_B$, where K_A and K_B are the concentrations by weight of air and water vapour ($K_A + K_B = 1$). Near the stagnation point of a hemisphere the appropriate boundary-layer equations for the conservation of mass, momentum, energy, and species concentration are

$$\frac{\partial(xu)}{\partial x} + \frac{\partial(xv)}{\partial y} = 0, \tag{2}$$

$$u\frac{\partial u}{\partial x} + v\frac{\partial u}{\partial y} = \frac{9}{4}\frac{U_0^2}{R^2}x + \nu\frac{\partial^2 u}{\partial y^2}, \tag{3}$$

$$u\frac{\partial h}{\partial x} + v\frac{\partial h}{\partial y} = \frac{\nu}{\sigma}\frac{\partial^2 h}{\partial y^2} + D_{AB}\left(1 - \frac{1}{\lambda}\right)\frac{\partial}{\partial y}\left[h_A\frac{\partial K_A}{\partial y} + h_B\frac{\partial K_B}{\partial y}\right], \tag{4}$$

$$u\frac{\partial K_B}{\partial x} + v\frac{\partial K_B}{\partial y} = \frac{\nu\lambda}{\sigma}\frac{\partial^2 K_B}{\partial y^2}, \tag{5}$$

where σ is the Prandtl number $\bar{C}_p\mu/\kappa$ and λ the Lewis number $\rho D_{AB}\bar{C}_p/\kappa$. For the diffusion of water vapour in air the binary diffusion coefficient D_{AB} has the value $0{\cdot}240 \times 10^{-3}$ ft.^{2}/sec. The corresponding value of the Lewis number is 1·20. In order to make the above set of equations amenable to analysis the remainder of the solution will be restricted to the case $\lambda = 1{\cdot}00$. The adequacy of this approximation may be deduced from comparison with experiment.

In order to reduce the above set of equations to their 'similarity' form the following set of dimensionless variables are introduced

$$\eta = \sqrt{\left(\frac{3}{2}\frac{U_0}{\nu R}\right)}\, y, \quad u = \frac{3}{2}\frac{U_0}{R} f'(\eta)\, x, \quad v = -2\sqrt{\left(\frac{3}{2}\frac{U_0 \nu}{R}\right)} f(\eta),$$

$$h = h_W - (h_W - h_0)\, g(\eta), \quad K_B = K_{BW} - (K_{BW} - K_{B0})\, n(\eta). \tag{6}$$

Assuming K_{BW} and h_W to be constant we may write equations (2–5) as a set of ordinary differential equations:

$$f'^2 - 2ff'' = 1 + f''', \tag{7}$$

$$g'' + 2\sigma f g' = 0, \tag{8}$$

$$n'' + 2\sigma f n' = 0. \tag{9}$$

The appropriate boundary conditions are:

$$\left.\begin{aligned} &\text{at} \quad \eta = 0, \quad f = f' = g = n = 0; \\ &\text{at} \quad \eta = \infty, \quad f' = g = n = 1. \end{aligned}\right\} \tag{10}$$

Actually vaporization corresponds to fluid injection so that $f(0) \neq 0$. But it will be assumed that $f(0) \ll 1$ so that the flow in the air boundary layer is unaffected. If this approximation is not adequate then an iteration procedure can be used to obtain a solution.

The numerical solution to (7) with the boundary conditions (10) is given by Schlichting (1955). The solutions to equations (8) and (9) have been obtained by Sibulkin (1952). The resultant values for the wall gradients of enthalpy and concentration are

$$\left.\frac{\partial h}{\partial y}\right|_W = 0{\cdot}812(h_0 - h_W)\sqrt{\frac{U_0}{R\nu}}, \tag{11}$$

$$\left.\frac{\partial K_B}{\partial y}\right|_W = 0{\cdot}812(K_{B0} - K_{BW})\sqrt{\frac{U_0}{R\nu}}. \tag{12}$$

where σ has been assumed to be 0·700. The differential of the enthalpy may be written $dh = \overline{C_p}\, dT + (h_A - h_B)\, dK_B$. Using this relation and the similarity between enthalpy and concentration gradients the temperature gradient at the wall may be written

$$\left.\frac{\partial T}{\partial y}\right|_W = 0{\cdot}812(T_0 - T_W)\sqrt{\frac{U_0}{R\nu}}. \tag{13}$$

To obtain the rate at which the ice melts, the gradients of temperature and concentration must be related to the rate at which heat is transferred through the water layer. A relation may be written for the conservation of water across the air–water interface. The balance of diffusion of water vapour against the normal current of water vapour above and water below the interface gives

$$(\rho v)_W = (\rho v)_W K_{BW} - \rho D_{AB} \left.\frac{\partial K_B}{\partial y}\right|_W. \tag{14}$$

This balance is illustrated in figure 2. In a similar manner the energy balance may be written. Equating the transport of heat by conduction and diffusion to the normal currents of energy in the air and water we obtain

$$\dot{q}_W[l] = \left[k\frac{\partial T}{\partial y} + \rho D_{AB}\left(h_A \frac{\partial K_A}{\partial y} + h_B \frac{\partial K_B}{\partial y}\right)\right]\Bigg|_W - (\rho v)_W h_W[g] + (\rho v)_W h_W[l]. \tag{15}$$

This balance is also illustrated in figure 2. Using the heat of vaporization for water defined by $L_v = h_{BW} - h_W[l]$ and (14) with the condition $\lambda = 1$, we may write (15) in the form

$$\dot{q}_W[l] = k\frac{\partial T}{\partial y}\bigg|_W + \rho D_{AB}\frac{L_v}{K_{AW}}\frac{\partial K_B}{\partial y}\bigg|_W. \tag{16}$$

Combination of (1), (11), (12) and (16) with the condition $\sigma = 0{\cdot}700$ then gives the stagnation melt rate for a hemisphere of ice in humid air,

$$w_i\sqrt{\frac{R}{U_0\nu}} = 1{\cdot}160\frac{\rho}{\rho_i}H, \tag{17}$$

where the dimensionless enthalpy transfer parameter H is defined by the equation

$$H = \frac{\overline{C_p}(T_0 - T_W)}{L_f} + \frac{L_v}{L_f}\left(\frac{K_{B0} - K_{BW}}{1 - K_{BW}}\right).$$

It should be emphasized that the numerical constant in (17) is valid only for $\sigma = 0{\cdot}700$. The only variable in the above result which needs further discussion is K_{BW}. The equilibrium value for K_{BW} would be the ratio of the density of saturated

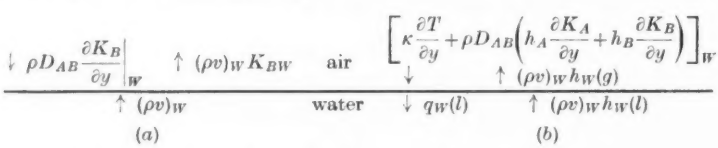

FIGURE 2. Mass and energy balances at the air–water interface. (*a*) balance of water mass; (*b*) energy balance.

water vapour at the melt temperature (T_W) to the local density. A theoretical determination of the departure from the equilibrium value requires a detailed analysis of the evaporation and adsorption processes such as that given by Bauer & Zlotnick (1958). In the present work it is assumed that the equilibrium value is applicable.

The above solution has been obtained by neglecting the presence of the water layer. To check this assumption an approximate solution for the flow and heat transfer in the water layer will be found. First, however, the requirement that $f(0) \ll 1$ will be considered. From (6), (12) and (14) with $\sigma = 0{\cdot}700$, it is found that

$$f(0) = 0{\cdot}472\frac{K_{B0} - K_{BW}}{1 - K_{BW}}. \tag{18}$$

If the velocity at the air–water interface is small compared with the velocity at the outer edge of the air boundary layer then $f'(0) \ll 0$. To determine this quantity the water layer is assumed to have a thickness δ_l independent of x and a velocity distribution linear in both x and y, $u = Gxy$. The validity of these choices has been discussed in some detail by Roberts (1958). Conservation of mass in the water layer gives

$$\rho_l G\delta_l^2 = \rho_i w_i - (\rho v)_W. \tag{19}$$

The continuity of stress at the air–water interface requires that

$$G = 2{\cdot}41\frac{\mu}{\mu_l}\frac{U_0}{R}\left(\frac{U_0}{\nu R}\right)^{\frac{1}{2}}. \tag{20}$$

In the present notation $u(0) = Gx\delta_l$, so combination of (6), (12), (14), (17), (19) and (20) gives, with the assumption $1+\dfrac{L_f}{Lv} \doteq 1$,

$$f'(0) = 1{\cdot}118\frac{\rho}{\rho_l}\left(\frac{\nu}{\nu_l}H\right)^{\frac{1}{2}}. \tag{21}$$

A similar method may be used to determine whether the temperature at the outer edge of the water layer is significantly larger than the melt temperature. If $g_T = (T-T_W)/(T_0-T_W)$, the required inequality is $g_T(0) \ll 1$. Assuming a linear temperature profile $T = Ay+T_W$ we obtain

$$k_l A = \dot{q}_W[l] \tag{22}$$

for the continuity of heat flux at the air–water interface. Then using (12), (13), (16), (19), (20) and (22), we find that

$$g_T(0) = 0{\cdot}565\frac{k}{k_l}\sqrt{\left(\frac{\nu_l}{\nu}\right)}\frac{L_f}{\overline{C_p}(T_0-T_W)}H^{\frac{1}{2}}. \tag{23}$$

To estimate the heat convected away in the water layer a quadratic temperature distribution is assumed for the water layer, $T = Ay+By^2+T_W$. The continuity of heat flux at the air–water interface gives

$$k_l(A+2B\delta_l) = \dot{q}_W[l]. \tag{24}$$

The difference in energy flux between the air–water interface and the ice–water interface is equated to the heat convected away in the water boundary layer to obtain the second required equation,

$$\dot{q}_W[l]-k_lA-(\rho v)_W c_l(A\delta_l+B\delta_l^2) = c_l(\rho_i w_i-(\rho v)_W)\left(\tfrac{2}{3}A+\tfrac{1}{2}B\delta_l\right)\delta_l, \tag{25}$$

where c_l is the specific heat of water. If a shielding parameter S is defined by $S = \{k_lA-q_W[l]\}/\{q_W[l]\}$, the convective losses in the water layer may be neglected if $S \ll 1$. The shielding parameter may be evaluated from (12), (13), (16), (17), (19), (20), (24) and (25). Thus

$$S = 0{\cdot}538\sigma_l\frac{\rho}{\rho_l}\sqrt{\left(\frac{\nu}{\nu_l}\right)}H^{\frac{1}{2}}. \tag{26}$$

The validity of the assumptions will be checked when specific experimental conditions are considered.

3. Experiments

The stagnation point ablation of a hemispheric model fabricated from ice was determined in a subsonic wind tunnel. The experiments were carried out in the 40×36 in. closed circuit subsonic wind tunnel at the U.S. Naval Postgraduate School, Monterey, California. The humidity of the air in the tunnel was controlled by a fine water spray. This method provided a constant moisture content at any

level above the atmospheric value. The water vapour content was measured with an Aminco–Dunmore electric hygrometer.

The ice models were cast in hemispherical moulds. Models with nominal radii of 2 and 4 in. were used. To obtain reproducible results ice was required which did not contain air bubbles. To accomplish this the standard commercial technique was utilized. While the model was freezing, air was bubbled through the distilled water. The agitation produced ice which was optically clear in the region melted during the experiments. For some time before it was used each model was stored at a temperature just below 32 °F.

When models which contained air bubbles were ablated deep erosions occurred. It is hypothesized that the irregularities in the ice induced transition in the external boundary-layer flow; this in turn increased the local heat transfer and rate of melting, causing deep cavities. Using ice free of air bubbles, steady ablation was observed over the full range of free-stream velocities available. The model remained hemispherical.

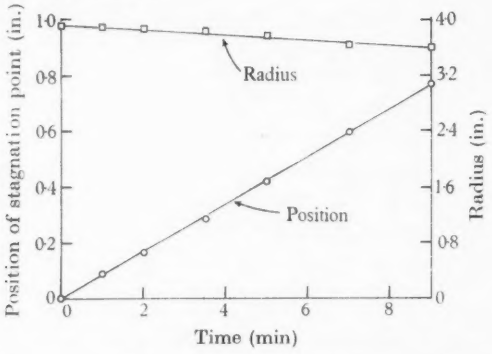

FIGURE 4. Dependence of the radius and stagnation point position on time; $U_0 = 237$ ft./sec, $T_0 = 84{\cdot}2$ °F, $\rho_{B0} = 1{\cdot}573 \times 10^{-3}$ lb./ft.^{3}, $w_i = 1{\cdot}066 \times 10^{-4}$ ft./sec.

Quantitative measurements of the rate of ablation at the stagnation point were obtained for fixed values of the free-stream velocity, temperature, and humidity. The range of free-stream velocities was from 40 to 250 ft./sec, the free-stream temperature was near 85 °F, the free-stream relative humidity ranged from 20 to 90%, and models with radii of 2 and 4 in. were used. During each run the model was photographed at regular intervals; a sequence of these photographs is shown in figure 3 (plate 1). The screen at the base of the hemisphere was used to control splashing during fabrication. From the photographs the position of the stagnation point was determined using an optical comparator. The radius of the hemisphere as a function of time was also determined from the photographs. These variables are plotted against time in figure 4 for the same run that is illustrated in figure 3. The constant slope of the position curve gives the rate of ablation at the stagnation point. From (17) this rate depends on the square root of the radius so that any change in slope should indeed be negligible.

For this representative run the validity of the approximations used in the analysis may be checked by using (18), (21), (23) and (26). The numerical values

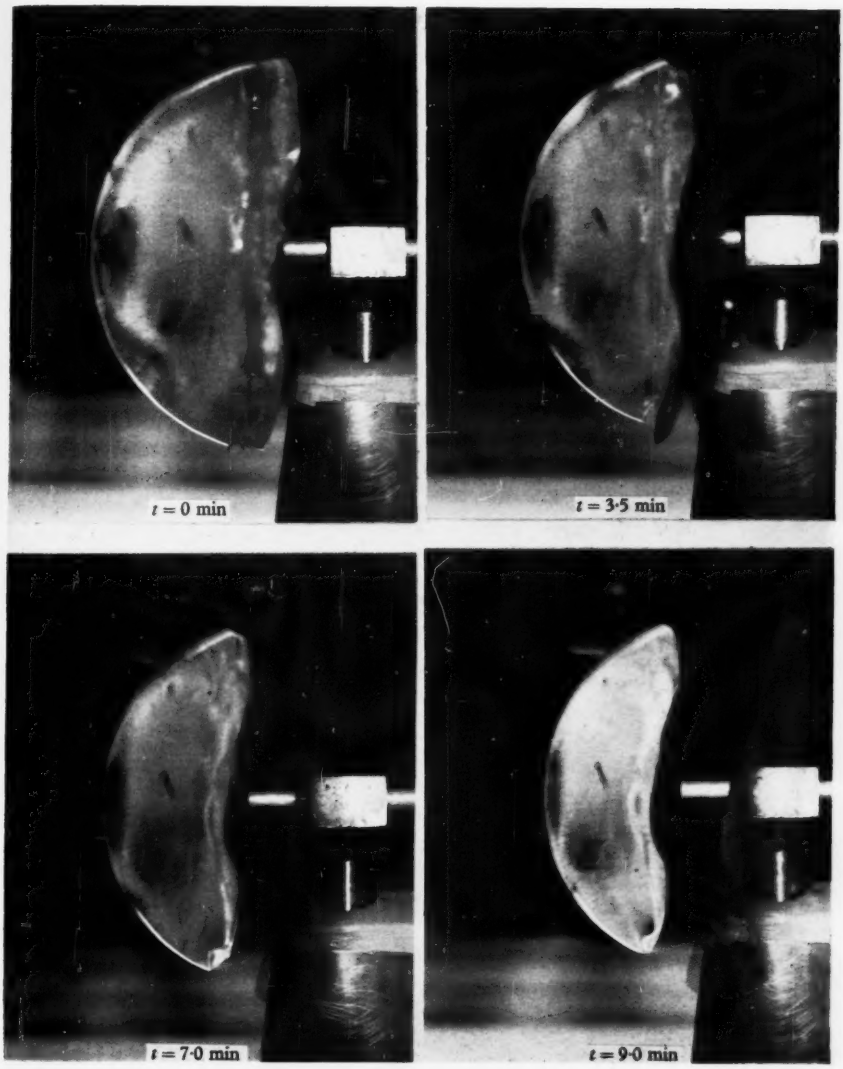

FIGURE 3 (plate 1). Photographs of an ablating hemisphere of ice; $U_0 = 237$ ft./sec., $T_0 = 84{\cdot}2$ °F, $\rho_{B0} = 1{\cdot}573 \times 10^{-3}$ lb./ft.^{3}.

(*Facing p.* 128)

obtained are $f(0) = 0{\cdot}845 \times 10^{-2}$, $f'(0) = 0{\cdot}182 \times 10^{-2}$, $g_T(0) = 1{\cdot}07 \times 10^{-2}$, and $S = 0{\cdot}135 \times 10^{-2}$. Since all values are considerably less than one the neglect of the water layer and the finite injection velocity at the air–water interface seems appropriate for the experimental conditions considered.

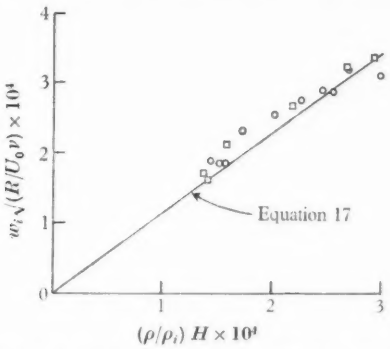

FIGURE 5. Dependence of the dimensionless melt rate on the enthalpy transfer parameter; $T_0 \doteq 85\,^\circ$F, $\rho_{B0} = 0{\cdot}55 - 1{\cdot}60 \times 10^{-3}$ lb./ft., $U_0 = 40$–250 ft./sec. □, $R = 2$ in.; ○, $R = 4$ in.

All measurements are plotted in figure 5 in terms of the dimensionless variables obtained from the theory. Equation (17) is plotted for comparison. The variation in the enthalpy transfer parameter was obtained by varying the free-stream moisture content. The value of K_{BW} was obtained from the density of saturated water vapour at 32 °F ($\rho_{BW} = 0{\cdot}303 \times 10^{-3}$ lb./ft.^{3}). For all cases considered the density of water vapour in the free stream was higher than the wall value so that moisture actually condensed at the air–water interface. It is interesting to note that this condensation caused from 30 to 70% of the ablation. This rather surprising result is due to the large heat of vaporization for water. The agreement between theory and experiment seems adequate.

REFERENCES

BAUER, E. & ZLOTNICK, M. 1958 *Physics of Fluids*, **4**, 355.

LEES, L. 1958 *Combustion and Propulsion*, p. 451. 3rd AGARD Colloquium. London: Pergamon Press.

ROBERTS, LEONARD 1958 *J. Fluid Mech.* **4**, 505.

SCHLICHTING, H. 1955 *Boundary Layer Theory*. New York: McGraw-Hill.

SIBULKIN, M. 1952 *J. Aero. Sci.* **19**, 570.

Stability of parallel flow in a parallel magnetic field at small magnetic Reynolds numbers

By P. G. DRAZIN
Department of Mathematics, Massachusetts Institute of Technology

(Received 1 September 1959)

The hydromagnetic stability of a basic two-dimensional parallel flow of an incompressible conducting fluid in a uniform magnetic field parallel to the flow is considered. By use of the generalization of the Orr–Sommerfeld equation for an electrically conducting fluid, it is shown that any given small wave disturbance can be stabilized by a sufficiently strong magnetic field if the Reynolds number is finite and the magnetic Reynolds number small.

Stability of velocity profiles with a point of inflexion at small magnetic Reynolds number and infinite Reynolds number is considered in detail. Perturbation methods are developed to find stability characteristics in two cases, when the magnetic field is weak, and when the disturbance is a long wave. These methods are applied to the jet and the half-jet, which are both found to be unstable to long-wave disturbances, however strong the magnetic field. Nonetheless, these two flows can be stabilized for any given harmonic disturbance of finite wavelength. The analysis of the jet reveals the surprising result that the magnetic field makes inviscid long-wave disturbances more *unstable*.

1. Introduction

Michael (1953) and Stuart (1954) were the first to consider the stability of a steady two-dimensional parallel flow of a viscous incompressible conducting fluid in a uniform magnetic field parallel to the flow. They supposed that the flow was bounded by perfectly conducting walls at $y = y_1, y_2$ (where y_1 and/or y_2 may be infinite if the flow is unbounded) and took a basic parallel flow with variable velocity

$$\mathbf{U} = (U(y), 0, 0) \quad (y_1 \leqslant y \leqslant y_2)$$

and a uniform parallel magnetic field

$$\mathbf{H}_0 = (H_0, 0, 0)$$

in cartesian components. Following the usual methods of hydrodynamic stability, they substituted the velocity and magnetic field of the basic flow together with a small disturbance (denoted by primes), say

$$\mathbf{u} = (u, v, w) = \mathbf{U} + \mathbf{u}'(\mathbf{x}, t) \tag{1.1}$$

and

$$\mathbf{H} = (H_x, H_y, H_z) = \mathbf{H}_0 + \mathbf{h}'(\mathbf{x}, t), \tag{1.2}$$

into the hydromagnetic equations for a homogeneous incompressible fluid of density ρ, kinematic viscosity ν, magnetic permeability μ, electrical conductivity

σ and magnetic diffusivity $\lambda = 1/4\pi\mu\sigma$. Then they linearized the equations by neglecting products of the primed quantities.

Squire's theorem that two-dimensional small disturbances of a parallel flow are the least stable is valid for a conducting fluid (Michael 1953; Stuart 1954). Therefore, in a proposed search for a sufficient condition for stability, only two-dimensional disturbances need be considered. Thus w, h'_z and $\partial/\partial z$ can be put equal to zero. Now the continuity equation $\nabla . \mathbf{u}' = 0$ and the Maxwell equation $\nabla . \mathbf{h}' = 0$ of the disturbance imply that there exist functions ψ', χ' such that

$$u' = -\partial\psi'/\partial y, \quad v' = \partial\psi'/\partial x, \tag{1.3}$$

and

$$h'_x = -\partial\chi'/\partial y, \quad h'_y = \partial\chi'/\partial x. \tag{1.4}$$

Assume that small disturbances can be resolved into dynamically independent wave-components by putting

$$\psi' = \phi(y)\exp\{i\alpha(x-ct)\}, \quad \chi' = \theta(y)\exp\{i\alpha(x-ct)\} \tag{1.5}$$

for some complex velocity $c = c_r + ic_i$ and positive wave-number α. This gives a wave with phase velocity c_r and logarithmic growth rate αc_i; so the motion is stable, neutrally stable or unstable according as c_i is respectively less than, equal to, or greater than zero.

If the velocity distribution $U(y)$ has velocity scale V and its space variation has length scale L, we can define dimensionless parameters for the flow, the first being the Reynolds number

$$R \equiv VL/\nu. \tag{1.6}$$

Analogously, we define the magnetic Reynolds number

$$R_M \equiv VL/\lambda. \tag{1.7}$$

This measures the ratio of terms representing convection and diffusion of the magnetic lines of force in the fluid. The ratio of magnetic to kinetic energy is measured by

$$S \equiv (\mu H_0^2/8\pi)/\tfrac{1}{2}\rho V^2; \tag{1.8}$$

S is also the square of the Alfvén velocity divided by V^2. It is useful to define a further dimensionless parameter

$$N \equiv SR_M = \mu H_0^2 L/4\pi\rho\lambda V. \tag{1.9}$$

By elimination of the hydrodynamic pressure, and by division of the appropriate dimensions out of the quantities y, U, c, α, ϕ and θ, it can be shown that the linearized hydromagnetic equations lead to

$$(U-c)\,\theta - \phi = -\frac{i}{\alpha R_M}(\theta'' - \alpha^2\theta) \tag{1.10}$$

and

$$(U-c)\,(\phi'' - \alpha^2\phi) - U''\phi - S(\theta'' - \alpha^2\theta) = -\frac{i}{\alpha R}(\phi^{\mathrm{iv}} - 2\alpha^2\phi'' + \alpha^4\phi), \tag{1.11}$$

where primes now denote differentiation with respect to y. These equations were

derived independently by Michael (1953) and Stuart (1954). On elimination of ϕ it at once follows that

$$\frac{i}{\alpha R_M}(D^2-\alpha^2)^3\theta+(U-c)(D^2-\alpha^2)^2\theta+4U'(D^2-\alpha^2)\theta'+2U''(D^2-\alpha^2)\theta+4U''\theta''+4U'''\theta'+U^{\mathrm{iv}}\theta$$
$$=-\frac{R}{R_M}\{(U-c)(D^2-\alpha^2)-U''\}(D^2-\alpha^2)\theta+i\alpha R\{(U-c)^2-S\}(D^2-\alpha^2)\theta+2i\alpha RU'(U-c)\theta', \quad (1.12)$$

where $$D\equiv d/dy.$$

The stability characteristics can be found by solving the sixth-order differential equation (1.12) subject to the six appropriate boundary conditions. These are

$$\alpha\phi=0=\phi' \quad (y=y_1,y_2), \quad (1.13)$$

which makes the velocity vanish at fixed walls, and

$$\alpha\theta=0 \quad (y=y_1,y_2), \quad (1.14)$$

which makes the normal component of the magnetic field vanish at perfectly conducting walls.

For given values of α, R, R_M and S we can (in principle) find the eigenvalue c. If $c_i<0$ we conclude that the disturbance of wave-number α is stable for the given R, R_M and S. In practice it is convenient to put $c_i=0$ and look for the resultant relation between α, R, R_M and S.

From equations (1.10) and (1.11) Stuart (1954) deduced the power equation of the disturbance

$$\frac{D}{Dt}\int\tfrac{1}{2}(\mathbf{u}'^2+S\mathbf{h}'^2)\,d\mathbf{x}=\int(-u'v'+Sh_x'h_y')\frac{dU}{dy}\,d\mathbf{x}-\frac{1}{R}\int(\nabla\times\mathbf{u}')^2\,d\mathbf{x}-\frac{S}{R_M}\int(\nabla\times\mathbf{h}')^2\,d\mathbf{x}. \quad (1.15)$$

This equation is a generalization of the Lorentz power equation for a non-conducting fluid. The first integral is the sum of the kinetic and magnetic energies of the disturbance, the second the rate of energy transfer *from* the basic parallel flow, the third the rate of viscous dissipation and the fourth the rate of ohmic dissipation of magnetic energy.

To see typical orders of magnitude of the dimensionless parameters, consider the following approximate values measured in a recent laboratory experiment (Murgatroyd 1953) on channel flow of mercury:

$$\lambda=8\times10^3\,\mathrm{cm^2/sec},\quad \nu=10^{-3}\,\mathrm{cm^2/sec},\quad \rho=14\,\mathrm{g/cm^3},$$
$$V=10\,\mathrm{cm/sec},\quad L=1\,\mathrm{cm},\quad H_0=10^3\,\mathrm{g}.$$

These give parameters

$$R\approx10^4,\quad R_M\approx10^{-3},\quad N\approx10^{-1}.$$

The value $R_M\approx10^{-3}$ suggests the approximation $R_M\ll1$ to simplify the formidable eigenvalue problem we are facing. Accordingly, let us balance the magnetic diffusion terms on the right-hand side of equation (1.10) with the

convection of the basic magnetic field by the disturbance, i.e. make the approximation

$$\theta'' - \alpha^2\theta = -i\alpha R_M \phi. \tag{1.16}$$

This is equivalent to taking the first term of a power series of the form

$$\theta = \sum_{n=1}^{\infty} R_M^n \theta_n(y; \alpha, R, N, c),$$

which is a regular expansion because R_M is the coefficient of terms other than the one of highest order in the differential equation (1.12). We shall suppose that N remains finite and non-zero as $R_M \to 0$, which requires $H_0 \to \infty$. Then θ can be eliminated from equation (1.11) by use of equation (1.16) to yield

$$(U-c)(\phi'' - \alpha^2\phi) - U''\phi + i\alpha N\phi = -\frac{i}{\alpha R}(\phi^{\mathrm{iv}} - 2\alpha^2\phi'' + \alpha^4\phi). \tag{1.17}$$

This equation was first derived by Stuart (1954). It reduces to the Orr–Sommerfeld equation in the absence of a magnetic field. The convection of the magnetic field of the disturbance by the basic flow being neglected, the magnetic and velocity fields of the disturbance have been separated, and it is only necessary to solve equation (1.17) subject to the boundary conditions (1.13) in order to find c. θ is of order R_M and need not be found from equation (1.16) after ϕ has been found. However, the basic magnetic field, being infinite as $R_M \to 0$, affects the velocity of the disturbance and requires the addition of the term $i\alpha N\phi$ in the Orr–Sommerfeld equation.

The assumption $R_M = \nu R/\lambda \ll 1$ also requires

$$R \ll \lambda/\nu \quad (= 6 \times 10^6 \quad \text{for} \quad Hg).$$

In spite of this limitation of the range of Reynolds number, we shall consider later the inviscid form of the Stuart equation (1.17), namely

$$(U-c)(\phi'' - \alpha^2\phi) - U''\phi + i\alpha N\phi = 0, \tag{1.18}$$

together with the inviscid boundary conditions

$$\alpha\phi = 0 \quad (y = y_1, y_2) \tag{1.19}$$

representing zero normal velocity at the walls. The justification is that the solution of the inviscid equation (1.18) will give an asymptotic solution to the Stuart equation (1.17) for large αR, as the Rayleigh equation gives one to the Orr–Sommerfeld equation. In many cases this asymptotic solution should not differ much from the viscous solution in the range of chief practical interest, where R is as large as 10^4. Our knowledge of equation (1.18) for $N = 0$ suggests that these cases occur when the velocity profile has a point of inflexion, i.e. when the inviscid flow as well as the viscous flow is unstable. Also Stuart (1954) adapted Lin's method combining the 'inviscid' and 'viscous' solutions of the Orr–Sommerfeld equation, so the study of inviscid hydromagnetic stability is at least an important preliminary to the viscous problem.

It is to be expected that the effect of the longitudinal primary magnetic field is generally stabilizing. This idea is made precise and it is shown (§ 2) that, for $R_M = 0$,

$$N^3 > 27R/\{256\,\alpha^2(\max.\, U')^4\}$$

is a sufficient condition for stability. After § 2 we continue to take $R_M = 0$, but take $R = \infty$ as well.

For velocity profiles with a point of inflexion there is a neutrally stable solution of the Rayleigh equation. It is of the form $\phi = \phi_s(y)$, $\alpha^2 = \alpha_s^2 \neq 0$, $c = U_s$, where U_s is the value of U at the point of inflexion. The perturbation for small N of this known solution for $N = 0$ is considered in § 3. A general equation of the tangent to the curve of neutral stability (i.e. the curve $c_i(\alpha^2, N) = 0$) at $(\alpha_s^2, 0)$ in the (α^2, N)-plane is found. The tangent is inclined downward, so the local effect of the magnetic field is stabilizing.

In § 4 an approach to the problem for small values of the wave-number is described.

The analysis of §§ 3, 4 gives a rough idea of the relation between α and N for each value of c_i, and for $c_i = 0$ in particular. This relation could be plotted as curves of constant c_i in the (α, N)-plane. We can find the values of c_i on the α-axis by solution of the Rayleigh equation. We can find the values near $(\alpha_s, 0)$ from § 3, and for small α from § 4. This may lead to our chief aim—to find if there is some critical value of N above which the flow is stable to disturbances of all wave-numbers. The solution for small α may show that this critical value does not exist, i.e. that for any value of N there exists some α for which the flow is unstable. If N has a critical value, it may be found by an explicit solution or by computation.

The ideas of §§ 3, 4 are applied in §§ 5, 6 to two important types of velocity profile with a point of inflexion and with $\nu = 0$. Helmholtz flow (unbounded uniform parallel flow with a single discontinuity of velocity) is found (§ 5) to be unstable for all values of the magnetic field at $R_M = 0$. Thus there is no critical value of N. However, the magnetic field makes the flow less unstable. Helmholtz flow is used to approximate the half-jet (with $U = \tanh y$, say), which is shown to be unstable similarly.

Also a broken-line velocity profile is used (§ 6) to approximate the jet (with $U = \operatorname{sech}^2 y$). This flow is unstable however large the magnetic field. For small wave-numbers it is found that the magnetic field *increases* the instability. This surprising result is discussed after the general conclusions of § 7.

2. Sufficient conditions for stability

Some fundamental stability characteristics of the viscous flow can be found by generalizing Synge's (1938) sufficient conditions for stability of parallel flow. We adapt this method for the Orr–Sommerfeld equation (see also Lessen 1952) to the Stuart equation. Thus the power equation (1.15) for $R_M = 0$ can be written, after use of (1.16), as

$$I_2^2 + 2\alpha^2 I_1^2 + \alpha^4 I_0^2 = -\tfrac{1}{2} i\alpha R(Q - Q^*) - \alpha R c_i (I_1^2 + \alpha^2 I_0^2) - \alpha^2 R N I_0^2. \tag{2.1}$$

where

$$I^2 \equiv \int_{y_1}^{y_2} |d^n\phi/dy^n|^2 \, dy \quad (n = 0, 1, 2), \tag{2.2}$$

$$Q \equiv \int_{y_1}^{y_2} \{U |\phi'|^2 + (\alpha^2 U + U'') |\phi|^2\} \, dy + \int_{y_1}^{y_2} U' \phi' \phi^* \, dy, \tag{2.3}$$

and an asterisk denotes a complex conjugate.

For inviscid fluid ($R = \infty$), this becomes

$$c_i(I_1^2+\alpha^2 I_0^2) = \int_{y_1}^{y_2} \tfrac{1}{2}iU'(\phi'\phi^* - \phi'^*\phi)\,dy - \alpha N I_0^2. \tag{2.4}$$

Therefore the flow is always stable if

$$\alpha N \geqslant \max.\left(\int_{y_1}^{y_2} \tfrac{1}{2}iU'(\phi'\phi^* - \phi'^*\phi)\,dy \Big/ \int_{y_1}^{y_2} |\phi|^2\,dy\right),$$

the maximum being with respect to any class of functions including the eigenfunctions of the inviscid equation (1.18). Unfortunately equation (1.18) has a singularity where $U = c$ and is not complex self-adjoint, and so does not appear to have a variational principle suitable for computation of eigenvalues.

Returning to Synge's method, we can deduce from equation (2.1) that a sufficient condition for stability ($c_i < 0$) is

$$q\alpha R < \min.\{(I_2^2 + 2\alpha^2 I_1^2 + \alpha^2(\alpha^2+RN)\,I_0^2)/I_0\,I_1\}, \tag{2.5}$$

where
$$q \equiv \max. U', \tag{2.6}$$

because
$$\tfrac{1}{2}|Q-Q^*| \leqslant qI_0 I_1$$

by Schwarz's inequality. To exploit inequality (2.5) further, Synge noted that

$$\int_{y_1}^{y_2}\left(\phi + \frac{2\tilde{\xi}}{y_2-y_1}y\phi' + \eta\phi''\right)\left(\phi^* + \frac{2\tilde{\xi}}{y_2-y_1}y\phi'^* + \eta\phi''^*\right)dy > 0 \tag{2.7}$$

for all real $\tilde{\xi}$, η. We must add the proviso that $y_2 - y_1 < \infty$. If one or both of the boundaries are at infinity, we can use the modifications of Lessen (1952), whose strongest result comes with $\tilde{\xi} = 0$. The cases of bounded and unbounded flow can be combined by putting $\xi = 2\tilde{\xi}/(y_2-y_1)$, which must be zero for unbounded flow. Therefore, on integration of the inequality (2.7) by parts and on further use of Schwarz's inequality,

$$\eta^2 I_2^2 > (\xi\eta - \xi^2 + 2\eta)\,I_1^2 + (\xi-1)\,I_0^2. \tag{2.8}$$

Combination of the inequalities (2.5) and (2.8) shows that the motion is stable provided

$$\eta^2\alpha R c_i(I_1^2+\alpha^2 I_0^2) < \eta^2 q\alpha R I_0 I_1 - I_1^2(2\alpha^2\eta^2 + \xi\eta - \xi^2 + 2\eta) - I_0^2(\eta^2\alpha^4 + \alpha^2\eta^2 RN + \xi - 1). \tag{2.9}$$

Stability is assured if the right-hand side is negative definite, i.e. if

$$(\eta^2 q\alpha R)^2 < 4(2\alpha^2\eta^2 + \xi\eta - \xi^2 + 2\eta)\,(\alpha^4\eta^2 + \alpha^2 RN\eta^2 + \xi - 1) \tag{2.10}$$

for all real ξ, η satisfying

$$2\alpha^2\eta^2 + \xi\eta - \xi^2 + 2\eta > 0, \quad \alpha^4\eta^2 + \alpha^2 RN\eta^2 + \xi - 1 > 0. \tag{2.11}$$

Note that the inequality (2.10) is weakened if we put $N = 0$.

For bounded flows we can get

$$(qR)^2 < 8(\alpha^2+1)\,(\alpha^2+RN) \tag{2.12}$$

when $\xi = 1 = \eta$, and

$$(qR)^2 < (2\alpha^2+1)\,(4\alpha^4 + 4\alpha^2 RN + 1)/\alpha^2 \tag{2.13}$$

when $\xi = 2 = \eta$. These two inequalities limit the region of possible instability in the (α, R)-plane for each value of N, inequality (2.12) showing that the flow is stable if $R < 8N/q^2$.

For bounded or unbounded flows we can put $\xi = 0, \eta = (3/RN)^{\frac{1}{2}}/\alpha$ in inequality (2.10) to get

$$N^3 > 27R/256\,\alpha^2 q^4. \tag{2.14}$$

Thus, given any finite R and $\alpha \neq 0$, we can find N such that the disturbance is stable.

3. Perturbation of the neutral solution of Rayleigh's equation

Rayleigh proved that, if the equation

$$\phi'' - \alpha^2\phi - \frac{U''}{U-c}\phi = 0 \tag{3.1}$$

has a neutral eigensolution (i.e. one with an eigenvalue $c_i = 0$), then

$$U''(y_s) = 0 \tag{3.2}$$

at some point y_s of the flow. Later Tollmien showed that when (3.2) is satisfied there exists an eigensolution

$$\phi = \phi_s, \quad c = U_s = U(y_s), \quad \alpha = \alpha_s > 0, \tag{3.3}$$

for certain functions $U(y)$, where ϕ_s is real. A perturbation of this neutral oscillation with non-zero wave-number (carried out first by Tollmien, and later by Lin) establishes the existence of amplified oscillations with slightly different wave-number. Lin (1955) has given the following formula, which we shall use:

$$(dc/d\alpha^2)_{\alpha=\alpha_s} = \left\{\int_{y_1}^{y_2} \phi_s^2\,dy\right\} \Big/ \left\{\mathfrak{P}\int_{y_1}^{y_2} \frac{K\phi_s^2}{U-U_s}\,dy + i\pi K(y_s)\,\phi_s^2(y_s)\right\}, \tag{3.4}$$

where $\mathfrak{P}$ denotes the principal value of the integral and

$$K \equiv -U''(y)/\{U(y) - U_s\}, \tag{3.5}$$

K being positive for the profiles under consideration. The sign of the imaginary term in (3.4) depends on taking the limit $c_i \to 0$ through positive values in order to get the correct inviscid limit of the viscous solution.

Our aim is to perturb the neutral solution (3.3) in order to find the stability when the magnetic field is weak. So use† the Taylor series

$$c = U_s + (\alpha^2 - \alpha_s^2)\frac{\partial c}{\partial \alpha^2} + \alpha N \frac{\partial c}{\partial(\alpha N)} + \frac{1}{2!}(\alpha^2 - \alpha_s^2)^2 \frac{\partial^2 c}{\partial(\alpha^2)^2} + \ldots, \tag{3.6}$$

the derivatives all being evaluated at $\alpha = \alpha_s$, $N = 0$. Then a neutral disturbance with $\alpha \neq \alpha_s$, $N \neq 0$ must be such that

$$\alpha_s N \sim -(\alpha^2 - \alpha_s^2)\left(\frac{\partial c_i/\partial \alpha^2}{\partial c_i/\partial(\alpha N)}\right)_{\alpha=\alpha_s,\, N=0} \quad \text{as} \quad \alpha \to \alpha_s. \tag{3.7}$$

We shall now find $\partial c/\partial(\alpha N)$ and combine it with the relation (3.4) for $\partial c/\partial \alpha^2_{\alpha=\alpha_s,\, N=0}$.

† This method is analogous to that for large Reynolds number used by Lessen & Fox (1955).

Subtract the product of ϕ_s and the equation

$$\phi'' - \alpha_s^2 \phi - \frac{U''}{U-c}\phi + \frac{i\alpha_s N}{U-c}\phi = 0 \tag{3.8}$$

from the product of ϕ and the equation

$$\phi_s'' - \alpha_s^2 \phi_s - \frac{U''}{U-U_s}\phi_s = 0. \tag{3.9}$$

Then, on integration between the boundaries, we obtain

$$i\alpha_s N \int_{y_1}^{y_2} \frac{\phi\phi_s}{U-c}\,dy = (c-U_s)\int_{y_1}^{y_2} \frac{U''\phi\phi_s}{(U-c)(U-U_s)}\,dy. \tag{3.10}$$

On taking the limit $c \to U_s$ such that $c_i \to 0$ through positive values, it can be shown that

$$\frac{\partial c}{\partial(\alpha N)_{\alpha=\alpha_s, N=0}} = -i\left\{\mathfrak{P}\int_{y_1}^{y_2} \frac{\phi_s^2}{U-U_s}\,dy + i\pi\phi_s^2(y_s)\right\} \div \left\{\mathfrak{P}\int_{y_1}^{y_2} \frac{K\phi_s^2}{U-U_s}\,dy + i\pi K(y_s)\,\phi_s^2(y_s)\right\}. \tag{3.11}$$

Combination of equations (3.4) and (3.11) with the limit (3.7) gives the tangent to the curve of neutral stability in the (α^2, N)-plane at the point $(\alpha_s^2, 0)$ as

$$N = \frac{\alpha_s^2 - \alpha^2}{\alpha_s}\left\{\pi K(y_s)\,\phi_s^2(y_s)\int_{y_1}^{y_2}\phi_s^2\,dy\right\} \div \left\{\mathfrak{P}\int_{y_1}^{y_2}\frac{\phi_s^2}{U-U_s}\,dy\,\mathfrak{P}\int_{y_1}^{y_2}\frac{K\phi_s^2}{U-U_s}\,dy + \pi^2 K(y_s)\,\phi_s^4(y_s)\right\}. \tag{3.12}$$

In cases of interest we shall find that these integrals are positive or zero, so that α^2 decreases from α_s^2 as N increases from zero. A disturbance with wave-number $\alpha < \alpha_s$ is unstable when $N = 0$ and, it now appears, is neutral for some $N > 0$; thus the effect of a small magnetic field is stabilizing.

4. Solution for small wave-numbers

When α is small the disturbance is a long wave, and the disturbance velocity is nearly parallel to the basic flow because

$$v' = i\alpha\phi \exp\{i\alpha(x-ct)\} \to 0 \quad \text{as} \quad \alpha \to 0.$$

On the large scale of a long wave the detailed structure of the velocity profile is unimportant in determining the stability characteristics. This property in the absence of a magnetic field is illustrated by a comparison, made by Carrier (cf. Esch 1957), of the stability properties of various forms of the velocity profile of the half-jet. He showed that the three unbounded profiles

$$U = y/|y|, \quad \begin{cases} y/|y| & (|y| > 1), \\ y & (|y| < 1), \end{cases} \quad 2\operatorname{erf} y - 1 \tag{4.1}$$

have the same inviscid eigenvalues ($c \to \pm i$) as $\alpha \to 0$. In fact the velocity profiles

$$U = \begin{cases} 0 & (|y| > 1), \\ 1 & (|y| < 1), \end{cases} \quad \begin{cases} 0 & (|y| > 1), \\ 1-|y| & (|y| < 1), \end{cases} \quad \operatorname{sech}^2 y \tag{4.2}$$

of a jet have similar stability characteristics ($c \sim \pm\alpha^{\frac{1}{3}}i$, $\pm(\alpha/3)^{\frac{1}{2}}i$, $\pm(2\alpha/3)^{\frac{1}{2}}i$, respectively) as $\alpha \to 0$.

The addition of the magnetic field does not affect any term involving a derivative of U in the inviscid equation (1.18). Therefore, in looking for the stability of the half-jet and jet to long-wave disturbances, we may use the simple first profiles of (4.1) and (4.2) rather than the complicated third profiles. Other flows can be approached in this way, as first demonstrated by Rayleigh (1945).

5. The half-jet

Consider the velocity profile

$$U = y/|y| \quad (\infty > y > -\infty) \tag{5.1}$$

as a limit of the smoothly varying profile of the half-jet. This case has been treated by Michael (1955) for $R_M = \infty$ and by Nisbet (1960) for a two-fluid model for all values of R_M.

There is a discontinuity of the solution at $y = 0$. As with ordinary Helmholtz instability (cf. Rayleigh 1945), the condition that a particle stays in the interface

$$y = Y_0 \exp\{i\alpha(x-ct)\}$$

is
$$Y_0 = -\{\phi/(U-c)\}_{y=0}$$

to first order of the small disturbance. Therefore $\phi/(U-c)$ is continuous at $y = 0$.

From equation (1.18)

$$[(U-c)\phi' - U'\phi]_{-\epsilon}^{\epsilon} = \int_{-\epsilon}^{\epsilon} \{\alpha^2(U-c) - i\alpha N\}\phi\, dy.$$

We are supposing that the smoothly varying profile tends to the broken-line profile (5.1), during which limit the integrand on the right-hand side is bounded. On letting $\epsilon \to 0$, it follows that $(U-c)\phi' - U'\phi$ is continuous at $y = 0$. This condition could be alternatively proved (cf. Rayleigh 1945) by the continuity of the hydrodynamic pressure across the interface.

For the velocity distribution (5.1)

$$(\pm 1 - c)(\phi'' - \alpha^2\phi) + i\alpha N\phi = 0 \quad (\pm y > 0). \tag{5.2}$$

Now
$$\alpha\phi \to 0 \quad \text{as} \quad y \to \pm\infty,$$

because the disturbance must die away at infinity. Therefore

$$Q = \begin{cases} A\exp\{-y[\alpha^2 - i\alpha N/(1-c)]^{\frac{1}{2}}\} & (y \to 0), \\ B\exp\{y[\alpha^2 + i\alpha N/(1+c)]^{\frac{1}{2}}\} & (y < 0), \end{cases} \tag{5.3}$$

where the square-roots are chosen to have positive real parts. The continuity of $\phi/(U-c)$ and $(U-c)\phi' - U'\phi$ at $y = 0$ implies that $(U-c)^2\phi'/\phi$ is continuous there; whence it can be seen from the solution (5.3) that the eigenvalue relation is

$$(1-c)^2[\alpha^2 - i\alpha N/(1-c)]^{\frac{1}{2}} + (1+c)^2[\alpha^2 + i\alpha N/(1+c)]^{\frac{1}{2}} = 0, \tag{5.4}$$

i.e.
$$f(c) \equiv -ic(1+c^2) + (N/4\alpha)(1+3c^2) = 0. \tag{5.5}$$

We can tabulate the key points of this cubic on the imaginary axis as follows

c/i	$-\infty$	-1	$-1/3^{\frac{1}{2}}$	0	$1/3^{\frac{1}{2}}$	1	$+\infty$
f	$+\infty$	$-N/2\alpha$	$-2/3^{\frac{3}{2}}$	$N/4\alpha$	$2/3^{\frac{3}{2}}$	$-N/2\alpha$	$-\infty$

It can be seen that all three roots c_1, c_2, c_3 are pure imaginary, with

$$-\infty < c_{i1} < -1, \quad -1/3^{\frac{1}{2}} < c_{i2} < 0, \quad 1/3^{\frac{1}{2}} < c_{i3} < 1.$$

If $N = 0$, $c_i = \pm 1$ or 0. The roots $c = \pm i$ are those found for Helmholtz instability with no magnetic field. The other root $c_2 = 0$ is inadmissible because it comes from implicitly using a square-root with negative real part after squaring equation (5.4).

If $\alpha/N \to 0$, then $c \to \pm i/3^{\frac{1}{2}}$ or $-3iN/4\alpha$. Discarding the root c_2, we get

$$c \sim i/3^{\frac{1}{2}} \quad \text{or} \quad -3iN/4\alpha. \tag{5.6}$$

In all cases the flow is unstable, because $c_{i3} > 0$. As N increases from zero to infinity, c_{i3} decreases from 1 to $3^{-\frac{1}{2}}$. Thus the magnetic field makes the flow less unstable.

We can take

$$U = \tanh y \quad (\infty > y > -\infty) \tag{5.7}$$

as a smoothly varying representation of the velocity profile of the half-jet. The neutral eigensolution of the Rayleigh equation is then (Curle 1956)

$$\phi_s = \operatorname{sech} y, \quad \alpha_s = 1, \quad c = 0. \tag{5.8}$$

Therefore $y_s = 0$, $\phi_s(y_s) = 1$, $K = 2\operatorname{sech}^2 y$ and the analysis of § 3 gives

$$N \sim 2(1-\alpha^2)/\pi \tag{5.9}$$

as $\alpha \to 1$ on the curve of neutral stability.

The result

$$c \to 3^{-\frac{1}{2}} i \quad \text{or} \quad -\tfrac{3}{4} iN/\alpha \quad \text{as} \quad \alpha \to 0 \tag{5.10}$$

for Helmholtz flow has been shown in § 4 to apply to the half-jet. This can be laboriously verified by use of the second velocity profile (4.1). In all cases (5.10) holds, showing that the half-jet is unstable, however strong the magnetic field.

6. The jet

The velocity of the broken-line jet

$$U = \begin{cases} 0 & (|y| > 1), \\ 1 & (|y| < 1), \end{cases} \tag{6.1}$$

is an even function of y. Therefore the even and odd parts of ϕ are separable in equation (1.18) and can satisfy the boundary conditions separately. We shall consider even ϕ (corresponding to an antisymmetric disturbance) only, because it can be shown (in the same way as for even ϕ) that odd ϕ give rise to weaker instability. Therefore, in looking for a sufficient condition for stability, we take the even solution of equation (1.18) which satisfies the boundary condition at infinity. This solution is defined by

$$\phi = \begin{cases} D\exp\{[\alpha^2 + i\alpha N/c]^{\frac{1}{2}}(1-y)\} & (y > 1), \\ E\cosh\{[\alpha^2 - i\alpha N/(1-c)]^{\frac{1}{2}} y\} & (1 > y \geqslant 0). \end{cases} \tag{6.2}$$

Also $(U-c)^2\phi'/\phi$ must be continuous at $y=1$, by the interfacial boundary conditions. Therefore

$$-c^2[\alpha^2+i\alpha N/c]^{\frac{1}{2}} = (1-c)^2[\alpha^2-i\alpha N/(1-c)]^{\frac{1}{2}}\tanh[\alpha^2-i\alpha N/(1-c)]. \quad (6.3)$$

If $N=0$, we get Rayleigh's solution with

$$c = 1/(1\pm i\coth^{\frac{1}{2}}\alpha) \quad (6.4)$$

and therefore instability for all α. If we fix $N\neq 0$ and let $\alpha\to 0$, it can be shown that

$$c/(\alpha N)^{\frac{1}{3}} \to i^{\frac{1}{3}} = \tfrac{1}{2}(3^{\frac{1}{2}}+i), \quad \tfrac{1}{2}(-3^{\frac{1}{2}}+i) \quad \text{or} \quad -i.$$

The second root is inadmissible because it corresponds to the square-root on the left-hand side of equation (6.3) with negative real part, i.e. to an exponentially increasing disturbance as $y\to\infty$. Therefore

$$c \sim -i(\alpha N)^{\frac{1}{3}} \quad \text{or} \quad \tfrac{1}{2}(3^{\frac{1}{2}}+i)(\alpha N)^{\frac{1}{3}} \quad \text{as} \quad \alpha\to 0. \quad (6.5)$$

The first root is stable ($c_i<0$) and must join up with the stable root $c=1/(1+i[\coth\alpha]^{\frac{1}{2}})$ of equation (6.4). But the second root is unstable and becomes *more* unstable as N increases. Thus we have found an unstable solution for all values of N, and the flow is therefore unstable. The strange circumstance that the magnetic field increases instability is discussed in § 7.

The continuous velocity profile of the jet (as found by Bickley—see Savic 1941) is

$$U = \operatorname{sech}^2 y \quad (\infty > y > -\infty), \quad (6.6)$$

and the neutral even eigensolution of the Rayleigh equation is

$$\phi_s = \operatorname{sech}^2 y, \quad \alpha_s = 2, \quad c = \tfrac{2}{3}. \quad (6.7)$$

After a little integration and computation, it can be shown that for this case equation (3.12) gives

$$\begin{aligned} N &= 6\pi(4-\alpha^2)/\{2\pi^2+81[1+3^{-\frac{1}{2}}\ln(2+3^{\frac{1}{2}})][2+3^{-\frac{1}{2}}\ln(2+3^{\frac{1}{2}})]\} \\ &= 0{\cdot}045(4-\alpha^2) \end{aligned} \quad (6.8)$$

for the tangent to the curve of neutral stability at $(4,0)$ in the (α^2, N)-plane. The steepness of the gradient of the line indicates a strong stabilizing influence of the magnetic field.

For small α we expect qualitative agreement with the limit (6.5) of c for the broken-line jet. That limit can be confirmed by use of the second profile (4.2).

7. Conclusions

The results of §§ 5, 6 can be pieced together to give a good picture of the inviscid stability characteristics of the half-jet and jet. The solution of the Rayleigh equation gives c_i on the α-axis in the (α, N)-plane, and, in particular, it gives $c_i=0$ at $(\alpha_s, 0)$. The analysis of § 3 has been used to give the curve of neutral stability near $(\alpha_s, 0)$. If the curve leaves this point and eventually passes through the origin or cuts the N-axis, there will be a critical value of N above which $c_i<0$ for all α. In fact this is not so for the half-jet or jet, since we have shown in §§ 5, 6 that these flows are unstable for small α, however large N is. Now the sufficient

condition (2.14) for stability implies that, for given finite R and non-zero α, the flow can be stabilized. Therefore, for given $\alpha \neq 0$, it can be stabilized at infinite Reynolds number by the argument of continuity. In this way it is deduced that the curves of neutral stability for the jet and half-jet have the form shown in figure 1, with no critical value of N.

Finite viscosity and magnetic diffusivity cannot be expected to stabilize long-wave disturbances, because the viscous and diffusion terms in the hydromagnetic equations involve second derivatives of the disturbance fields. However, there are alleviating circumstances that might give stability in practice. First, only long waves are unstable, and disturbances of great wavelength are not often excited by slight irregularities in an experiment. Secondly, the growth rate $\exp(\alpha c_i t)$ of the disturbance is small, because c_i is $O(\alpha^{\frac{1}{3}})$ for the jet and $O(1)$ for the half-jet as $\alpha \to 0$. Therefore unstable disturbances may be carried downstream before they have time to grow appreciably. These qualitative ideas indicate that jets may be stabilized in practice, the half-jet being more unstable than the jet.

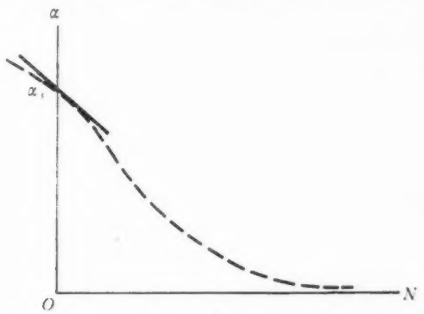

FIGURE 1. Conjectured form of the curve of neutral stability for the jet and half-jet.

It was found in § 6 that the jet was unstable, with $c_i \sim \frac{1}{2}(\alpha N)^{\frac{1}{3}}$ as $\alpha \to 0$, for $R_M = 0$, $R = \infty$ and finite $N \neq 0$. Therefore, if N is increased, c_i increases, i.e. the flow becomes more *unstable* to long-wave disturbances, contrary to our impression of the stabilizing tendency of magnetic fields. It should be remembered that this result is invalid if N is $O(\alpha)$ or $O(1/\alpha)$.

We should really be no more surprised at the creation of instability by the magnetic field than that by viscosity (the latter effect being known to occur under certain circumstances). In the complex dynamics of the flow, the magnetic field modifies the disturbance so that there is simultaneously magnetic energy dissipation and a different energy transfer from the basic flow to the disturbance by the Reynolds stress. Indeed, if the magnetic field were only a stabilizing agent, there should be an extremal principle for the energy as proof, contrary to the inconclusive power equation (2.4).

To verify this interpretation, we may use the power equation to give the rate of energy transfer from the basic flow per unit length in the z-direction as

$$P = \int_{-\infty}^{\infty} \tau \, (dU/dy) \, dy, \tag{7.1}$$

where the (dimensionless) Reynolds stress is

$$\tau \equiv -\overline{u'v'} \equiv -\frac{1}{2\pi}\int_0^{2\pi} u'v'\,dx$$
$$= \tfrac{1}{2}i\alpha\, e^{2\alpha c_i t}(\phi\phi'^* - \phi'\phi^*) \tag{7.2}$$

(we discount the magnetic Reynolds stress $S\overline{h_x' h_y'}$ because $|\mathbf{h}'| = O(R_M\phi)$ when R_M is small).

For the broken-line jet (6.1),

$$dU/dy = \delta(-1) - \delta(1)$$

in terms of the Dirac δ-functions; also the disturbance found in § 6 is anti-symmetric. Therefore

$$P = -2(\tau)_{y=1}. \tag{7.3}$$

Use of discontinuous profiles such as (6.1) leads to ambiguity (for flows with or without a magnetic field) because even though $\phi/(U-c)$ and $(U-c)\phi'$ are continuous, $(\phi\phi'^* - \phi'\phi^*)$ is discontinuous if $c_i \neq 0$. Thus use of discontinuous profiles cannot give precise information on the second-order quantity τ. However, we can find the trend for a smoothly varying profile of the jet $U = \operatorname{sech}^2 y$ by evaluating τ on both sides of the discontinuity of the known solution (6.2).

It can be shown from § 6 that

$$\alpha^{-1} e^{-2\alpha c_i t}(\tau)_{y\to 1} = -|D|^2 \operatorname{Im}\{[\alpha^2 + i\alpha N/c]^{\frac{1}{2}}\}$$

or

$$-|D|^2 \operatorname{Im}\left\{\frac{c(1-c^*)}{c^*(1-c)}[\alpha^2 + i\alpha N/c]^{\frac{1}{2}}\right\},$$

according as $y \to 1$ from above or below respectively, for the arbitrary constant D. If $\alpha \to 0$ for given $N \neq 0$, the unstable mode found in § 6 has $c \sim \frac{1}{2}(3^{\frac{1}{2}} + i)(\alpha N)^{\frac{1}{2}}$. Therefore

$$(\tau)_{y\to 1}/[(\alpha^4 N)^{\frac{1}{3}}|D|^2 \exp\{(\alpha^4 N)^{\frac{1}{3}} t\}] \to -\tfrac{1}{2} \quad \text{or} \quad -2.$$

On both sides τ is negative, so the tendency of the magnetic field is to increase the energy of the disturbance, as shown by equation (7.3).

I am very grateful to Prof. C. C. Lin for helpful advice and criticism throughout this work. It has been sponsored in part by the Office of Naval Research under contract Nonr 1841(12) with the Massachusetts Institute of Technology.

REFERENCES

Curle, N. 1956 *Aero. Res. Council, Lond., Unpublished Rep.* no. 18426.

Esch, R. E. 1957 *J. Fluid Mech.* **3**, 289.

Lessen, M. 1952 *Quart. Appl. Math.* **10**, 184.

Lessen, M. & Fox, J. A. 1955 50 *Jahre Grenzschichtforschung*, p. 122. Braunschweig: Friedr. Vieweg & Sohn.

Lin, C. C. 1955 *The Theory of Hydrodynamic Stability.* Cambridge University Press.

Michael, D. H. 1953 *Proc. Camb. Phil. Soc.* **49**, 166.

Michael, D. H. 1955 *Proc. Camb. Phil. Soc.* **51**, 528.

Murgatroyd, W. 1953 *Phil. Mag.* (7), **44**, 1348.

Nisbet, I. C. T. 1960 (to be published).

Rayleigh, J. W. S. 1945 *The Theory of Sound*, Vol. II, Chap. XXI. New York: Dover.

Savic, P. 1941 *Phil. Mag.* (7), **32**, 245.

Stuart, J. T. 1954 *Proc. Roy. Soc.* A, **221**, 189.

Synge, J. L. 1938 *Hydrodynamic Stability.* Semi-centennial publications of the Amer. Math. Soc. **2** (Addresses), 227.

The development of turbulent boundary layers with negligible wall stress

By A. A. TOWNSEND
Emmanuel College, Cambridge

(Received 25 September 1959)

In a recent paper, Stratford has described a turbulent boundary layer with continuously zero wall stress and has developed a theory to describe the flow based on two assumptions. The first is that the flow in the outer part of the layer is affected only by the original Reynolds stresses during the initial development, and the second is that flow in the equilibrium layer close to the wall is determined by the pressure gradient and is independent of upstream conditions. In this paper the same assumptions are used, but more careful consideration of their limitations has led to the elimination of some inconsistencies in the original work and to a theory that gives a better description of some of the experimental results. The principal results are: (i) a criterion for zero wall stress in an adverse pressure gradient of sufficient strength, (ii) the form of the pressure distribution for a self-preserving flow with zero stress, (iii) the mean velocity distribution in this flow, (iv) an estimate of the constant in the 'square-root' velocity distribution for flow near a wall with zero stress.

1. Introduction

The prediction of the course of development of a turbulent boundary layer in an arbitrary adverse pressure gradient is a problem of considerable practical importance in engineering, and a number of methods have been developed, some of which lead to reasonably accurate results. The more recent and successful methods take notice of the existence of a 'constant-stress' layer near the surface and approximate to the velocity profile by a combination of a logarithmic wall profile and an outer profile, but the combining of the two parts has been an arbitrary procedure justified only by results. Stratford (1959*a*), in a very interesting paper, points out that, in a boundary layer subjected to a severe pressure gradient over a short distance, the outer profile is determined by the initial profile and the pressure rise, and he goes on to develop a very simple criterion for zero stress by combining this observation with a deduction of the wall profile for zero stress. The significance of this work is not that it provides a more accurate prediction of pressure rise to separation than other methods (in fact, it is less accurate), but that it is founded on a physically acceptable model of the boundary-layer motion and that results derived from the model should have very wide validity if the nature of the underlying approximations is kept in mind. Although this work marks a step forward in the replacement of assumptions made for mathematical convenience by assumptions conforming to physical reality, the

assumptions that the initial profile has a power-law form, that the junction of the wall profile and the outer profile is necessarily smooth, and that the wall profile can extend to the outer edge of the layer, fall short in this respect and cause some inconsistency between the theory and the experimental results. This paper presents an alternative version of the theory that leads to a more consistent and complete description of the turbulent boundary layer with zero wall stress (Stratford 1959*b*) and that is consistent with present knowledge of self-preserving boundary layers. It is, in fact, a commentary on the original work of Stratford.

2. Notation

Turbulent boundary layers on a flat, smooth surface are considered using Cartesian co-ordinates to describe the flow. The axes are chosen so that $0x$ is in the surface and in the direction of mean flow (assumed two-dimensional) and $0y$ is at right angles to the surface. Then

U, V, 0 are the components of mean velocity

u, v, w are the components of the velocity fluctuation

P is the pressure at the wall $y = 0$

τ_0 is the shear stress at the wall

U_1 is the free-stream velocity

$\dfrac{dP}{dx} = -U_1\dfrac{dU_1}{dx}$ is the longitudinal pressure gradient

U_0 is the free-stream velocity at $x = x_0$, the beginning of the adverse pressure gradient

$c_f = 2\tau_0/v_0^2$ is the local friction coefficient, immediately upstream of x_0

$c_p = 1 - U_1^2/U_0^2$ is the pressure recovery coefficient

$\gamma = \tau_0^{\frac{1}{2}}/(KU_0)$ is the local friction parameter

K is the Kármán constant

K_0 is the constant in the velocity profile for zero stress

$R = [\tau_0(x)/\tau_0(x_0)]^{\frac{1}{2}}$

$\delta = \nu\tau_0^{-\frac{1}{2}}\exp(\gamma^{-1} - A)$ is the boundary-layer thickness at x_0

$\eta = y/\delta$ is a non-dimensional co-ordinate

ν_T is the effective eddy viscosity for the outer part of a self-preserving boundary layer

$R_\delta = \dfrac{1}{\nu_T}\displaystyle\int_0^\infty (U_1 - U)\,dy$ is a flow constant, equivalent to a Reynolds number based on the eddy viscosity

Validity of the boundary-layer approximation is assumed.

3. The two-layer model

It is well known that the turbulent flow very close to a solid boundary is very different in nature from the flow near the outer edge of a boundary layer, and that one reason for the difference is that the wall flow has a high rate of energy dissipation and so is nearly in a state of equilibrium determined by local conditions while the outer flow has a low rate of dissipation and its structure is dependent on conditions far upstream of the point of observation. In general, the

parts of the flow which have these properties in the purest forms can develop almost independently (e.g. entering upon a region of strong pressure gradient, modification of the wall flow is nearly instantaneous while the outer flow is modified at a much more gradual rate), and the first useful approximation for the description of a turbulent boundary layer is to represent it as the juxtaposition of an inner wall flow and an outer edge flow, neglecting the blending region within which the dissipation is neither large nor small. In the real flow, interaction between the two parts of the flow takes place in the neglected blending region, and this can be described in the model by imposing suitable conditions at the junction. If the layer is self-preserving, this distinction between the layers is expressed by assuming the velocity distribution in the outer layer to be that arising from constant eddy viscosity in the outer flow and a logarithmic distribution of velocity in the inner layer (Townsend 1956*a*; Clauser 1956), and this leads to satisfactory results if the junction is assumed smooth. If the layer is not self-preserving, the assumption of constant eddy viscosity must fail (in the outer layer, 'turbulent fluid' behaves like a visco-elastic fluid with a comparatively long relaxation time), and the junction conditions require special consideration.

Consider the changes in a turbulent boundary layer as it flows into a region of severe adverse pressure gradient after a period of development in favourable or zero gradient, and choose the origin so that x_0, the start of the pressure gradient, is equal to the distance from the leading edge at which a boundary layer developing in zero gradient would have the same friction coefficient. Initially, the stress gradients are of order τ_0/δ, and the criterion of severity is that accelerations due to the pressure gradient should be large compared with τ_0/δ, i.e.

$$c_f \ll \frac{\delta}{x_0}\left(x_0 \frac{dc_p}{dx}\right). \tag{3.1}$$

and, since δ/x_0 is of the order of $c_f^{\frac{1}{2}}$, this requirement is satisfied if

$$x_0 \frac{dc_p}{dx} \gg c_f^{\frac{1}{2}}. \tag{3.2}$$

In a flow satisfying (3.2), the total head is very nearly constant along streamlines except in regions where stress gradients have increased very considerably. This will happen first very near the wall, where the rate of dissipation of turbulent energy is so large that any reduction of the energy supply by retardation of the mean flow leads almost instantaneously to lower levels of turbulent intensity and to lower Reynolds stresses. Further from the wall, the rate of dissipation is less, and an appreciable change in Reynolds stress will take longer and the stress gradient will not become comparable with the pressure gradient so close to the start of the expansion. Sufficiently far downstream, supposing the layer to be still attached, the Reynolds stresses will be modified on all streamlines and will be determined more by the pressure distribution than by the initial values. These effects are illustrated in figure 1, which shows the variations of Reynolds stress with stream function at various distances from the beginning of the adverse gradient.

It is useful to distinguish three stages of development. In the *initial* stage, Reynolds stresses have been modified only in a thin layer close to the wall and this layer forms an equilibrium layer within which the flow is substantially determined by the local wall stress and pressure gradient. The remainder of the flow has been acted on only by the pressure field and, to a small extent, by the initial Reynolds stresses. Further retardation causes the region of modified Reynolds stress to form an appreciable part of the whole flow, and then only a part of the modified region is in a state of wall equilibrium and has a structure independent of upstream conditions. In the last stage of development, Reynolds stresses over the whole layer have been affected by the retardation, and it may happen that flow becomes *self-preserving* and independent of the initial flow. If this occurs, past experience suggests that Reynolds stress and mean velocity

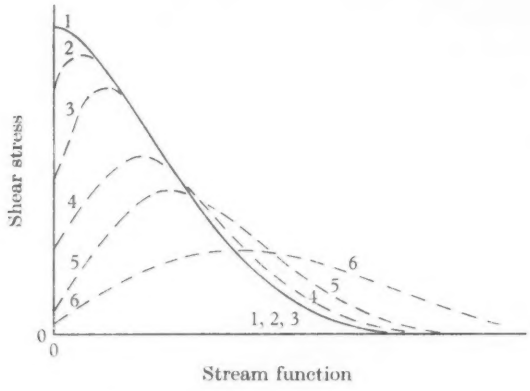

FIGURE 1. Distributions of shear stress in a boundary layer entering a region of strong adverse pressure gradient. (1) Initial distribution at $x = x_0$. (2) and (3) Initial stage of development. (4) and (5) Intermediate stage: modified stresses no longer confined to equilibrium layer. (6) Final stage: stresses modified everywhere.

gradient will be related through a coefficient of eddy viscosity in the outer layer. It follows that there are means of inferring the distributions of mean velocity both in the inner and outer layers if the layer is either in the initial stage of development or in a stage of self-preserving development, and a complete description is possible if the position and nature of the junction can be determined.

Two necessary conditions that must be satisfied at the junction are continuity of mean velocity and of Reynolds stress, as is easily seen by remembering that the neglected blending region has properties intermediate between those of the inner and outer layers. If mean velocity were discontinuous in the model, the mean velocity gradient in the blending region would be abnormally large, which would lead to abnormally high (or low) rates of production of turbulent energy and to abnormal Reynolds stresses. It follows that the inner and outer velocity distributions, when produced, intersect in the blending layer. Similarly, a discontinuity of Reynolds stress would lead to abnormal acceleration of the mean flow and the distributions of Reynolds stress must also intersect in the blending region and be

continuous in the two-layer model. In the initial stage of development, these two conditions are sufficient to determine the nature of the junction and any further condition is redundant, but a third condition must be imposed in the self-preserving stage of development. The reason for this is that stress gradients are then not negligible and, if the flow obeys the equation of mean motion, continuity of velocity implies continuity of stress. In the initial stage, Reynolds stress gradients are negelected in the equation of mean motion and, to this approximation, Reynolds stress and mean velocity are capable of independent variation. The third junction condition, applicable only to self-preserving flows, is usually taken to be continuity of mean velocity gradient, equivalent to continuity of effective eddy viscosity.

4. Wall equilibrium for zero wall stress

The concept of the equilibrium layer was first developed for the constant-stress layer, but it is capable of considerable extension to flow along any boundary on which the mean velocity is specified. Sufficiently close to any solid boundary, the convective terms in the averaged equations of motion are negligible compared with the stress terms, and the equations reduce to

$$\frac{\partial \overline{uv}}{\partial y} = -\frac{\partial P}{\partial x} + \nu \frac{\partial^2 U}{\partial y^2} \tag{4.1}$$

or, in integrated form,

$$\tau = -\overline{uv} + \nu \frac{\partial U}{\partial y} = \frac{\partial P}{\partial x} y + \tau_0. \tag{4.2}$$

So the distribution of shear stress depends only on the local parameters, τ_0 and $\partial P/\partial x$, and it may be inferred that the motion within a thin layer for which (4.2) is valid depends only on these parameters and on the fluid viscosity. The detailed justification of this assumption depends on the possibility of also neglecting convective terms in the equation for the turbulent kinetic energy, which implies that the turbulent motion is in a state of energy equilibrium. Within the fully turbulent part of such a layer, it is well known that

$$U = \frac{\tau_0^{\frac{1}{2}}}{K}\left[\log\left(\frac{\tau_0^{\frac{1}{2}} y}{\nu}\right) + A\right] \tag{4.3}$$

if $\tau_0 \gg (\partial P/\partial x)\, y$; but Stratford (1959*a*) has shown that, if $\tau_0 \ll (\partial P/\partial x)\, y$,

$$\frac{\partial U}{\partial y} = \frac{1}{K_0}\left(\frac{\partial P}{\partial x}\right)^{\frac{1}{2}} y^{\frac{1}{2}}, \tag{4.4}$$

and that, for zero wall stress

$$U = \frac{2}{K_0}\left(\frac{\partial P}{\partial x} y\right)^{\frac{1}{2}} + C\left(\nu \frac{dP}{dx}\right)^{\frac{1}{3}}. \tag{4.5}$$

(Here K_0 is an absolute constant, expected to be similar in magnitude to the Kármán constant K.) The condition that convective terms in the equation of mean motion are negligible is that

$$\left| \int_0^y \left(U \frac{\partial U}{\partial x} + V \frac{\partial U}{\partial y} \right) dy \right| \ll \frac{\partial P}{\partial x} y, \tag{4.6}$$

or, after substituting the equilibrium distribution,

$$y\frac{d}{dx}\left(\log\frac{\partial P}{\partial x}\right) \ll \tfrac{3}{2}K_0^2. \tag{4.7}$$

For the power-law variation of free-stream velocity, $U_1 \propto x^a$, this is

$$\frac{y}{x} \ll \frac{3}{2}\frac{K_0^2}{1-2a}. \tag{4.8}$$

5. Initial stage of development

In the initial stage of development in a strong adverse pressure gradient, the outer layer behaves nearly as an inviscid fluid and the inner layer is an equilibrium layer whose motion is determined by the local pressure gradient and the wall stress. The mean velocity distribution at the beginning of the adverse pressure gradient may be written in the form

$$U = U_1(x_0)\,[1-\gamma f(\eta)], \tag{5.1}$$

where $\gamma = \tau_0^{\frac{1}{2}}(x_0)/(KU_1(x_0))$, $\eta = y/\delta$, $\delta = \{\nu/KU_1(x_0)\}\exp(\gamma^{-1}-A)$.

Within the equilibrium (constant-stress) layer,

$$f(\eta) = -\log\eta. \tag{5.2}$$

In the outer layer, total head remains constant along streamlines, and

$$P(x_0)+\tfrac{1}{2}U_0^2[1-\gamma f(\eta)]^2 = P(x)+\tfrac{1}{2}U^2(x,y) \tag{5.3}$$

if $(x_0, \eta\delta)$ and (x, y) are on the same streamline. Within the inner layer,

$$U = \frac{\tau_0^{\frac{1}{2}}}{K}\left[\log\left(\frac{\tau_0^{\frac{1}{2}}y}{\nu}\right)+A\right] \tag{5.4}$$

if $\tau_0 \gg (dP/dx)\,y$, and* $$U = \frac{2}{K_0}\left(\frac{dP}{dx}y\right)^{\frac{1}{2}} \tag{5.5}$$

if $\tau_0 \ll (dP/dx)\,y$. Consider now the streamline which at x divides the inner, equilibrium layer from the outer layer. Since the inner layer is an equilibrium layer, its distance from the wall must be small compared with the layer thickness at x and therefore also at x_0. This dividing streamline lies in the constant-stress layer at x_0, and so we may use equation (5.2) for the velocity distribution function $f(\eta)$.

The condition that $(x_0, \eta_0\delta)$ and (x, y_1) lie on the dividing streamline is

$$U_0\eta_0\delta(1-\gamma+\gamma\log\eta_0) = RU_0y_1\left(1-\gamma+\gamma\log R\frac{y_1}{\delta}\right) \tag{5.6}$$

or $$= \frac{4}{3K_0}\left(\frac{dP}{dx}\right)^{\frac{1}{2}}y_1^{\frac{3}{2}}. \tag{5.7}$$

* The additive term $c(\nu\,dP/dx)^{\frac{1}{2}}$ in equation (4.5) is of order $U_1(U_1x/\nu)^{-\frac{1}{2}}$ and is negligible at Reynolds numbers over 10^6.

The first joining condition is continuity of mean velocity, i.e. that the mean velocity given by (5.4) or by (5.5) satisfies equation (5.3):

$$P_0+\tfrac{1}{2}U_0^2(1+\gamma\log\eta_0)^2 = P+\tfrac{1}{2}R^2U_0^2\left[1+\gamma\log\left(R\frac{y_1}{\delta}\right)\right]^2 \tag{5.8}$$

or

$$= P+\frac{2}{K_0^2}\frac{dP}{dx}y_1. \tag{5.9}$$

The second joining condition is continuity of shear stress, and is, to a good approximation, that

$$K^2\gamma^2U_0^2 = R^2K^2\gamma^2U_1^2+\frac{dP}{dx}y_1. \tag{5.10}$$

The two sets of equations (5.6), (5.8), (5.10) and (5.7), (5.9), (5.10) describe respectively the initial development and the condition for attainment of zero wall stress. The second set may be solved explicitly, and this produces*

$$\exp\left[\frac{(c_p+2\beta^2\gamma^2)^{\frac{1}{2}}-1}{\gamma}\right]\times\left[\frac{(c_p+2\beta^2\gamma^2)^{\frac{1}{2}}}{\gamma}-1\right]x_0\frac{dc_p}{dx}$$

$$=\frac{8}{3}\frac{K^3}{K_0}\gamma^2\frac{x_0}{\delta} = \tfrac{8}{3}\beta K^3R_0\gamma^2\exp(A-\gamma^{-1}), \tag{5.11}$$

where $R_0 = (U_0x_0/\nu)$. If the origin of x is so chosen that the boundary layer at x_0 has the same local friction coefficient as a constant-pressure layer that has developed for a distance x_0 (Townsend 1956*a*), we have

$$R_0 = [I_1-(2I_1+I_2)\gamma+2(I_1+I_2)\gamma^2]K^{-3}\gamma^{-2}\exp(\gamma^{-1}-A), \tag{5.12}$$

and then

$$\exp\left[\frac{(c_p+2\beta^2\gamma^2)^{\frac{1}{2}}-1}{\gamma}\right]\times\left[\frac{(c_p+2\beta^2\gamma^2)^{\frac{1}{2}}}{\gamma}-1\right]x_0\frac{dc_p}{dx}$$

$$=\tfrac{8}{3}\beta\gamma[I_1-(2I_1+I_2)\gamma+2(I_1+I_2)\gamma^2] = B. \tag{5.13}$$

This may be compared with Stratford's result, based on use of a power law for the initial velocity profile and use of continuity of velocity gradient as the second joining condition†

$$(2c_p)^{\frac{1}{4}(n-2)}\left(x\frac{dc_p}{dx}\right)^{\frac{1}{2}} = 1{\cdot}06\beta^{-1}(10^{-6}R_0)^{\frac{1}{16}}, \tag{5.14}$$

where $n = \log_{10}R_0$.

Stratford points out that a relation of this sort defines a pressure distribution in which a layer develops with continuously zero wall stress but without separa-

* Equations (5.2) and (5.10) are good approximations only if $\log\eta_0 < -3$, and the analysis is only valid if

$$c_p = (1+\gamma\log\eta_0)^2-2\beta^2\gamma^2 < (1-3\gamma)^2-2\beta^2\gamma^2.$$

For a Reynolds number of 10^6, $\gamma \doteqdot 0{\cdot}1$ and the pressure recovery coefficient may not exceed 0·47.

† Stratford also makes an allowance for the effect of Reynolds stresses on the outer flow by assuming them to be unaffected by the pressure gradient. This refinement has been omitted in the derivation of (5.13).

tion, and he has succeeded in producing such a zero-stress layer by slight modification of the pressure distribution defined by equation (5.14) (Stratford 1959*b*). The theory of this paper gives the relation between pressure and distance as

$$\exp\left[\frac{(c_p+2\beta^2\gamma^2)^{\frac{1}{2}}-1}{\gamma}\right]\times\left\{\left[\frac{(c_p+2\beta^2\gamma^2)^{\frac{1}{2}}}{\gamma}-1{\cdot}5\right]^2+0{\cdot}75\right\}=\tfrac{1}{2}B\gamma^{-2}\frac{x-x_0}{x_0}. \quad (5.15)$$

and in figure 2 this pressure distribution is compared with Stratford's theoretical distribution which is an adequate representation of the experimental distribution over the expected range of validity of the theory. It is clear that both theories

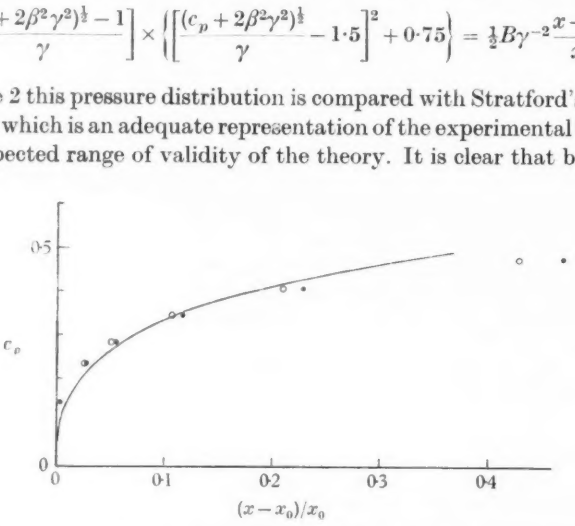

FIGURE 2. Comparison of predicted pressure distributions for development with continuously zero wall stress. Full line, Stratford ($K_0 = 0{\cdot}27$); ●, logarithmic theory ($K_0 = 0{\cdot}55$); ○, logarithmic theory ($K_0 = 0{\cdot}50$). $R_0 = 10^6$, $\gamma = 0{\cdot}10$.

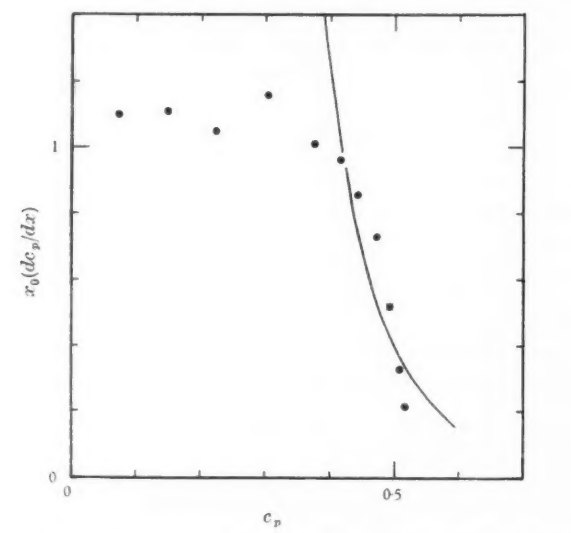

FIGURE 3. Comparison of the theoretical criterion for zero wall stress with measurements by Schubauer & Klebanoff (1951). (●, Experimental; full line, theory. $R_0 = 14{\cdot}3\times10^6$, $\gamma = 0{\cdot}075$, $K_0 = 0{\cdot}50$.)

are capable of describing the measurements for $c_p < 0{\cdot}40$ if a free choice of the value of the constant K_0 is allowed. Stratford used $K_0 = 0{\cdot}27$ compared with the values of 0·50 and 0·55 used in figure 2.

Equation (5.13) may be used to predict pressure-recovery coefficients at boundary-layer separation, i.e. zero wall stress, supposing the pressure distribution to be known and the adverse gradient to be so large that the approximations of the theory are valid. Of the available published material, only the layer studied by Schubauer & Klebanoff (1951) has an acceptably rapid rise of pressure, and this is compared with the rapid expansion theory in figure 3 by plotting c_p against $x_0(dc_p/dx)$, as given by equation (5.13) and as observed. Zero stress is predicted at $c_p = 0{\cdot}42$, compared with observed separation at $c_p = 0{\cdot}50$, but the nature of the experimental pressure distribution is such that a comparatively small amount of interaction between the inner and outer layers would lead to a considerable delay in attaining zero wall stress. In its present form it is unlikely that equation (5.13) would provide accurate predictions of separation in practical problems, but the author believes that the theoretical basis is sound and that it should give accurate estimates of effects due to change of Reynolds number or initial boundary-layer characteristics.

6. The self-preserving flow with zero wall stress

It has been pointed out that, after a sufficient period of development, the structure of the whole layer will be modified by the pressure gradient, and then a simple description is possible only if the flow is self-preserving. Clauser (1956) has given details of self-preserving flows in adverse pressure gradients with finite wall stress, but Stratford has suggested that the flow with continuously zero wall stress, defined by equations (5.13) or (5.14), becomes self-preserving with a distribution of mean velocity

$$U = \frac{1}{2K_0}\left(\frac{dP}{dx}y\right)^{\frac{1}{2}} \quad \text{for} \quad y < \frac{4K_0^2U_1^2}{dP/dx} \tag{6.1}$$

and a distribution of free-stream velocity

$$U_1 \propto (x-x_1)^{-0{\cdot}25}. \tag{6.2}$$

His experimental results suggest that this is a very rough description of the real behaviour, and a better one is easily obtained by using the theory of self-preserving boundary layers (Townsend 1956*b*). A turbulent flow is self-preserving if the distributions of mean velocity and of Reynolds stress may be expressed consistently in the forms

$$U = U_1 - u_0 f(y/l_0), \quad \overline{uv} = u_0^2 g(y/l_0), \tag{6.3}$$

where f and g are universal functions independent of x, and the scales u_0 and l_0 are functions only of x. The consistency may be tested by substitution in the averaged equations of motion, which leads to

$$-\frac{d(u_0U_1)}{dx}f + \frac{u_0}{l_0}\frac{d(U_1l_0)}{dx}\eta f' + u_0\frac{du_0}{dx}f^2 - \frac{u_0}{l_0}\frac{d(u_0l_0)}{dx}f'\int_0^\eta f(s)\,ds + \frac{u_0^2}{l_0}g' = 0. \tag{6.4}$$

neglecting the viscous terms and terms involving normal Reynolds stresses. This is of self-preserving form if

$$u_0 \propto U_1, \quad \frac{dl_0}{dx} = \text{const.}, \quad \frac{l_0}{U_1}\frac{dU_1}{dx} = \text{const.},$$

and the scales may be defined as

$$u_0 = U_1, \quad l_0 = x \tag{6.5}$$

by choosing a suitable origin for x. It has been shown (Townsend 1956*a*) that exactly self-preserving flow with finite wall stress is possible only if $U_1 \propto (x_1 - x)^{-1}$, but another type of self-preserving flow is possible if the wall stress is zero. The reason for this is that the velocity distribution in the equilibrium layer may be written as

$$\frac{U}{U_1} = \frac{2}{K_0}\left(-\frac{x}{U_1}\frac{dU_1}{dx}\right)^{\frac{1}{2}}\left(\frac{y}{x}\right)^{\frac{1}{2}} + C\left(-\frac{\nu}{U_1^2}\frac{dU_1}{dx}\right)^{\frac{1}{3}}, \tag{6.6}$$

which is a self-preserving form if $U_1 \propto (x - x_1)^a$ and if the additive term is negligibly small. The exponent a is necessarily negative and depends on the shape of the velocity profile. A simple application of the equation for the momentum integral shows that

$$-a = \frac{I_a - I_b}{3I_a - 2I_b}, \tag{6.7}$$

where

$$I_a = \int_0^\infty f(\eta)\,d\eta, \quad I_b = \int_0^\infty [f(\eta)]^2\,d\eta.$$

Experience with other self-preserving boundary layers has shown that an adequate approximation to the function $f(\eta)$ is obtained by assuming a sharp distinction between an inner equilibrium layer and an outer layer within which the effective eddy viscosity, $\nu_T = -\overline{uv}/(\partial U/\partial y)$, is independent of distance from the wall. Clauser (1956) has shown that the value of the eddy viscosity is such that

$$\frac{1}{\nu_T}\int_0^\infty (U_1 - U)\,dy = R_s, \tag{6.8}$$

where R_s is nearly independent of pressure gradient (see also, Townsend 1956*b*). Assuming this, the mean velocity in the outer layer ($\eta > \eta_1$) is determined by the non-dimensional equation for $f(\eta)$

$$-2af + (a+1)\eta f' + af^2 - (a+1)f'\int_0^\eta f(s)\,ds + \frac{I_a}{R_s}f'' = 0, \tag{6.9}$$

and, in the inner layer, by

$$f(\eta) = 1 - \frac{2}{K_0}(-a\eta)^{\frac{1}{2}}. \tag{6.10}$$

Equation (6.9) is a form of the Falkner–Skan equation, and solutions are required with the boundary conditions

$$f(0) = A, \quad f'(0) = 0, \quad f''(0) = \frac{R_s}{I_a}aA(2 - A), \tag{6.11}$$

where I_a and a depend on the form of $f(\eta)$. An approximate solution of (6.9) is

$$f(\eta) = A\,e^{-\frac{1}{4}a^2\eta^2}. \tag{6.12}$$

which satisfies the boundary conditions if

$$-\frac{\alpha^2 I_a}{aR_s} = 2 - A. \tag{6.13}$$

To make the problem determinate, the joining of the velocity distributions in the inner and outer layers must be specified by two independent conditions. Continuity of velocity requires that

$$A\, e^{-\frac{1}{2}\alpha^2\eta_1^2} = 1 - \frac{2}{K_0}(-a\eta_1)^{\frac{1}{2}}, \tag{6.14}$$

but, since the stress must satisfy equation (6.4), continuity of stress is assured for any value of η_1. In self-preserving layers developing in no pressure gradient, the junction is very nearly smooth, and so there is some justification in requiring continuity of velocity gradient, i.e. that

$$\alpha^2 A\eta_1\, e^{-\frac{1}{2}\alpha^2\eta_1^2} = \frac{1}{K_0}\left(\frac{-a}{\eta_1}\right)^{\frac{1}{2}}. \tag{6.15}$$

If the values of I_a and I_b are approximated by assuming that the outer velocity distribution (6.12) extends all the way to $\eta = 0$, then

$$I_a = \left(\frac{\pi}{2}\right)^{\frac{1}{2}}\frac{A}{\alpha}, \quad I_b = \frac{\pi^{\frac{1}{2}}}{2}\frac{A}{\alpha}, \tag{6.16}$$

and equations (6.7), (6.13), (6.14), (6.15) can be solved to give values of A, a, $\alpha\eta_1$, αK_0^2 as functions of $K_0 R_s^{\frac{1}{2}}$. These quantities are tabulated in table 1.

$K_0 R_s^{\frac{1}{2}}$	A	$-a$	$\alpha\eta_1$	αK_0^2
3·02	0·696	0·252	0·6	3·46
3·70	0·756	0·241	0·5	4·32
4·19	0·787	0·235	0·45	5·08
4·32	0·795	0·234	0·44	5·26
4·87	0·821	0·228	0·4	6·19
7·16	0·886	0·214	0·3	11·02

TABLE 1

These predictions are compared with the experimental results of Stratford in figure 4, assuming a virtual origin for the self-preserving flow at $x/x_0 = 0{\cdot}94$. It is evident that the velocity distributions for $c_p = 0{\cdot}489$, 0·624, 0·682 are nearly of the same shape and that the layer thickness is increasing nearly linearly with distance from the effective origin. The actual velocity distributions are represented fairly well by the composite distribution for

$$A = 0{\cdot}795, \quad -a = 0{\cdot}234, \quad K_0 = 0{\cdot}50, \quad R_s = 74{\cdot}2,$$

except near the edges of the flow. The assumption of constant eddy viscosity always leads to the prediction of a velocity distribution that approaches the free-stream velocity less rapidly than the real one, and the discrepancy near the edge of the flow is not unexpected. The value of the exponent a is less than the value suggested by Stratford ($-0{\cdot}25$), but it is in good agreement with the observed distribution of free-stream velocity (figure 5).

Two universal constants of uncertain magnitude appear in these results. The first is the flow constant R_s which describes the moving equilibrium attained in the outer flow. The application of the theory to the experimental results gives $R_s = 74 \pm 4$, which is larger than the mean of the experimental values of Clauser.

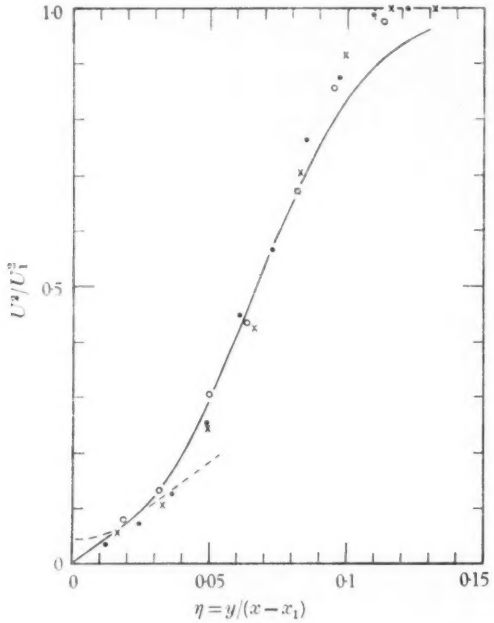

FIGURE 4. Mean velocity distributions for self-preserving flow with zero wall stress. (Full line, composite distribution for $K_0 = 0{\cdot}50$, $R_s = 74$; experimental points from Stratford (1959*b*) with $x/x_1 = 0{\cdot}94$.) ●, $c_p = 0{\cdot}682$; ×, $c_p = 0{\cdot}624$; ○, $c_p = 0{\cdot}489$.

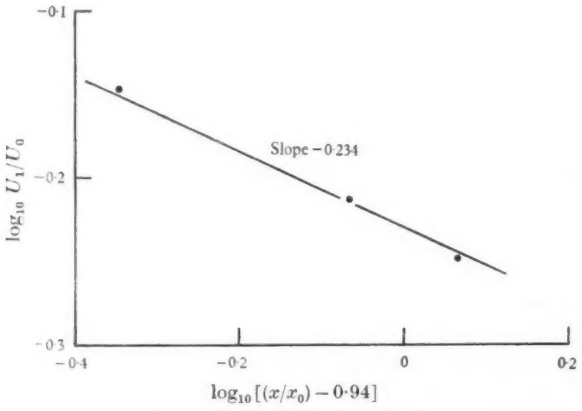

FIGURE 5. Comparison of observed variation of free-stream velocity with power-law variation inferred from the mean velocity distribution.

It is, however, close to the value deduced by a similar analysis of the constant-pressure boundary layer. The second constant is definitely rather larger than the Kármán constant, which is to be expected from a consideration of the effect of lateral transfer of turbulent energy on the level of turbulent intensity. The same value of K_0 will describe both the initial development and the self-preserving stage of the zero-stress layer. The conclusion is that $K_0 = 0{\cdot}50 \pm 0{\cdot}05$.

REFERENCES

Clauser, F. H. 1956 *Advances in Applied Mechanics*, **4**, 1.

Schubauer, G. B. & Klebanoff, P. S. 1951 *Nat. Adv. Comm. Aero., Wash., Rep.* no. 1030.

Stratford, B. S. 1959*a* *J. Fluid Mech.* **5**, 1.

Stratford, B. S. 1959*b* *J. Fluid Mech.* **5**, 17.

Townsend, A. A. 1956*a* *The Structure of Turbulent Shear Flow.* Cambridge University Press.

Townsend, A. A. 1956*b* *J. Fluid Mech.* **1**, 561.

REVIEWS

Advanced Mechanics of Fluids. Edited by HUNTER ROUSE. New York: John Wiley, 1959. 444 pp. $9.75 or £3. 18*s*.

Prof. Hunter Rouse's *Elementary Mechanics of Fluids*, which was published in 1946, has become firmly established as one of the best text-books on fluid mechanics suitable for engineering students at the undergraduate level. With the special merits of this earlier volume in mind, one is quite likely to be disappointed with the present book, which stands as its sequel by providing, for the graduate student with some basic knowledge of the subject, a fairly comprehensive introductory survey of the theory of incompressible flow. It would have been gratifying to have found that the 'advanced' mathematical aspects covered in this book were presented in the discerning and concise manner familiar from Prof. Rouse's elementary text; but these aspects seem largely to have eluded, perhaps inevitably, the model treatment he could give when dealing with the basic physical principles of fluid motion and their engineering applications. To dwell on this comparison would be unfair, however, in view of the much wider scope of the present book. Another difference is that the book is a joint enterprise shared by eight present or past colleagues of Prof. Rouse at the Iowa Institute of Hydraulic Research: these are Drs D. W. Appel, P. G. Hubbard, L. Landweber, E. M. Laursen, J. S. McNown, T. T. Siao, A. Toch and C. S. Yih, each of whom contributed a chapter on a topic in which he had specialized, though evidently all collaborated on the preparation of the final draft. Prof. Rouse directed the project and contributed an introductory chapter including an account of dimensional analysis.

The result of this intricate undertaking is a volume which, despite its shortcomings, is written in a remarkably consistent and attractive style—really an editorial triumph. This is especially creditable considering its wide coverage, which is seen at once from the titles of its eight chapters: Introduction to research in fluid motion (26 pp.), Fundamental concepts and equations (35 pp.), Principles of irrotational flow (69 pp.), Conformal representation of two-dimensional flow (53 pp.), Laminar motion (59 pp.), Turbulence (40 pp.), Boundary layers (51 pp.), Free-turbulence shear flow (44 pp.). Compressible flow, water waves and heat transfer are not covered, though the last two subjects are touched upon briefly.

To blame a book for falling short of its publisher's extravagant claims is always rather unjust; but the subtitle, 'A thorough treatment of the latest developments and research techniques in the field', which appears on the wrapper is so misleading as to be definitely harmful. Although the later chapters naturally make a good number of references to recent work, the book is essentially a primer in the miscellaneous mathematical procedures which have been applied to fluid mechanics, most of them long ago; and though it goes a long way towards filling in the necessary background, it will scarcely by itself equip a student for original research. For instance, 122 pages are devoted to perfect-fluid theory, though

covering only the basic material which can be found in a great many of the older text-books; the approach here is indeed more rudimentary than in some of these other books, since much of the space is given to preparatory accounts of elementary potential theory, general methods for solving Laplace's equation, Cauchy's theorem, and other incidental mathematical topics. Thus, the main purpose served by the book is to instruct the student in the relevant analytical methods, the development of his powers of physical reasoning being only a secondary objective.

It is very doubtful, however, that this is a satisfactory line of approach to the training of graduate students for research; and on this score the book will be found inadequate by some readers. Physical understanding is a more important requisite for creative work in modern fluid mechanics than sheer analytical ability; and in any case the latter is probably best gained in the first place by study of mathematical texts, rather than of *ad hoc* developments of theory in the context of particular hydrodynamical problems. A really helpful introduction to theoretical fluid mechanics would emphasize the essential physical explanations of flow phenomena to a far greater extent than in the present book and would present a more concise and utilitarian account of the analytical methods, relying on the many existing sources for much of the mathematical detail.

There are of course parts of the book which deal squarely with the realities of the subject, particularly in the chapters on turbulent flow where appeal to the observed facts becomes a continual necessity. But other parts seem unduly formal and sometimes remote from real problems, and it is the over-all emphasis that is under criticism. In the chapter on conformal representation, for example, a good outline of Kutta-Joukowsky wing theory depends on the statement of the basic hypothesis that 'the circulation on a two-dimensional foil adjusts itself so that the velocity at the trailing edge is finite'. An intelligent student will naturally inquire why this should be so; and even a brief explanation of the physical mechanism whereby the circulation develops to this extent would be of greater potential value to him than a large measure of complex-variable theory. But none is given anywhere in the book. In the chapter on laminar flow, a brief account of hydrodynamic stability concentrates on presenting a few items from perturbation theory, e.g. derivations of the Orr-Sommerfeld equation and Synge's sufficient stability conditions, and Squire's theorem—generalized by Yih—concerning the relative effects of two- and three-dimensional disturbances. This is all well done as far as it goes. But in the small space allowed it might have been more generally useful to concentrate on some of the interesting considerations that relate to the physical mechanism of instability, perhaps discussing the evidence that an inflexion in the primary velocity profile has a strong destabilizing effect, and perhaps repeating Prandtl's illuminating explanation of the role of viscosity in causing instability of boundary-layer flows.

Aside from this general criticism, it must be recognized that a very wide variety of material has been presented accurately and lucidly. There are very few omissions of any importance within the range suggested by the chapter headings and the introductory character of the book, although the absence of a mention of the Kármán vortex street seems one unfortunate case. That no

chapter stands out for special praise is testimony to the uniformly high standard of presentation; but chapter 2, on fundamental concepts, may be mentioned as being an attractive alternative to the various well-known presentations of the basic kinematical and dynamical equations. To note a further point in favour, which to some extent excuses the main criticism made above, the preface remarks that the volume as a whole has been planned for use in formal classes; obviously in these circumstances the deficiency of physical interpretations of the theory may not be so important, since the instructor may develop this side of the subject.

On the whole the text is attractively laid out, the diagrams are well done, and the mathematical printing is of high standard. A minor irritation is that the equations are unpunctuated. A valuable feature is the large number of problems set for the student. Many of these are remarkably searching and realistic, and they go a long way towards correcting the balance of the book. It is likely that very few of the problems could be solved by an average student without further help, although they all provide excellent examples for class instruction.

This can be recommended as a useful text-book to supplement a lecture course on incompressible flow, during which the lecturer could concentrate on presenting a well-balanced over-all account of the subject, referring to the book for many of the mathematical details and in particular clarifying the physical aspects. Thus, the book seems most appropriate to the American method of graduate training, which relies largely on formal lecture courses. Prof. Rouse in fact writes in his preface that the material has been taught as a two-semester course at the Iowa Institute. For the more casual British method, however, where the student has to depend more on private reading, the book is far less suitable; nevertheless, it might still be recommended if read in conjunction with books, such as Prandtl's *The Essentials of Fluid Dynamics*, which show clearly the status of the theory in relation to physical problems. Taking into account the specific purpose for which this book was written, it cannot be denied that Prof. Rouse and his co-authors have achieved it fairly successfully; and in any case they deserve to be congratulated on a most attractively written account.

T. Brooke Benjamin

Aerodynamik des Flugzeuges. Band I. By H. Schlichting and E. Truckenbrodt. Berlin: Springer-Verlag, 1959. 455 pp. DM. 52.50.

This first of two volumes on *Aerodynamics of the Airplane* contains the complete part A dealing with 'Fundamentals of fluid mechanics', and two chapters of part B on 'Aerodynamics of wings'. Part B will be completed in the second volume, which is to be published soon, and the review of part B can be postponed until then.

In part A, which is based on lectures by Dr Schlichting, the authors attempt the task of writing on almost the whole field of fluid mechanics, which is rather unusual in these days of the monograph. Their aim, however, is restricted and clearly stated in the foreword: they intend to given an introduction to fluid mechanics for the student of aeronautical engineering which is up-to-date.

There is certainly a need for such a book; the main problem, in view of the burgeoning knowledge accumulated in each field, is to know where to stop with the introduction. The authors are eminently successful in solving this problem; they have a sound and sober judgement of what has to be known by the student of the general field and what can be left out and relegated to special studies (which are encouraged and helped by a good bibliography).

The material is presented in four chapters: 'Introduction to the physical properties of the atmosphere,' 'Incompressible inviscid flow', 'Compressible inviscid flow' and 'Viscous flow'. Throughout, the authors favour simplicity and directness of the presentation over lengthy analysis. This does not mean a sacrifice in rigour, as every incompleteness of proof is clearly stated. The authors intend primarily to show what important results can be obtained by simple means (like momentum methods) and experience has shown that the gain in simplicity and clarity benefits not only the engineering student, but also those who later turn to the theoretical study of fluid mechanics. A large number of excellent illustrations enhance the value of the book, particularly for the beginner.

The modernized superstructure of the book is actually built on well-proven traditional foundations. In the chapter on incompressible inviscid flow, the presentation is made to fit the usual engineering curriculum by using first the real potential in plane flow; the paragraphs on complex potential are written without presupposing any knowledge of the theory of functions. The paragraph on the momentum theorem is a good example of the strong side of the book, as it contains material on over-all momentum balances which is often omitted by authors with purely theoretical interests.

The chapter on compressible flow does not appear to be as polished and well-balanced as the rest of the book. In particular, this reviewer found the presentation of the Prandtl–Glauert rule to be old-fashioned, even obsolete. A pure theoretician will consider all formulations of the Prandtl–Glauert rule as different only in trivial respects. Some modern text-books adopt this point of view, and the whole subject is dismissed by a one-line formula, which is all that is needed in principle. But an amazing number of papers (by distinguished authors!) containing erroneous results are to be found in the older literature on this subject; this should serve as a warning against considering the problem as completely trivial, particularly in books written for engineers.

Schlichting and Truckenbrodt choose to follow the historical presentation and give a derivation of the Prandtl–Glauert rule, in two 'different' formulations, for plane flow; the general three-dimensional (Göthert) rule is promised for the second volume. The derivation also contains the traditional mistake, an error of omission only, but nevertheless the same error which caused the confusion of the earlier writers; it is not pointed out that the results in two dimensions hinge on the proportionality between the potential and the body thickness in plane flow. This reviewer thinks that the exclusive use of the general and foolproof procedure given by B. Göthert would have been preferable.

The chapter on viscious flow appears to be essentially a condensed version of Dr Schlichting's own well-known book on boundary-layer theory, and is far

superior to the usual treatment of this subject in books on airplane aerodynamics.

Although the authors have clearly stated a restricted aim, it will be inevitable that their work will be criticized from the viewpoint of the present and future trends in the education of engineers in fluid mechanics. Many students to-day would like to be well prepared for work on missile aerodynamics in addition to aeronautical engineering, and for this purpose the introduction offered by Schlichting and Truckenbrodt is not adequate. In particular, an elementary presentation of the kinetic theory of gases in parallel with the foundations of continuum mechanics would be useful. A special chapter on hypersonics is a second requirement, although perhaps it is not important to find this section under the same cover with the rest. But the possibility of a schism between aeronautical and missile engineering is indicated by these omissions, which is regrettable. In the past the unified teaching of fluid mechanics for all engineering applications has not been achieved in most universities, and the outlook is that future developments will probably increase the division. This means that there may be students specializing from the beginning in traditional aeronautical engineering. For them, the use of Schlichting and Truckenbrodt's 'Fundamentals' is an excellent choice.

N. ROTT

Journal of Nuclear Energy. Part C: Plasma Physics—Accelerators—Thermonuclear Research. London: Pergamon Press Ltd. £7 or $20 per volume.

This journal has been set up to help cope with the prevailing spate of work on plasma physics, with Dr J. V. Dunworth as Editor-in-chief, a number of executive editors in U.K. and U.S.A., five general editors, and an imposing list of names on an editorial advisory board. The first part appeared in October 1959 and subsequent parts are to appear quarterly. Half of the eight papers in the first part are from the Atomic Energy Research Establishment at Harwell, although the editorial list suggests that later papers will be more diverse in origin. The emphasis appears to be on the field of applied nuclear energy, and there is unlikely to be any overlap with journals concerned with fluid mechanics, space flight or astrophysics. The inclusion of 'accelerators' within the journal's scope seems to be sensible. As well as original papers, the journal is apparently to contain two useful regular features, viz. translations of selected papers from the Russian journal *Atomnaya Energiya*, and a list of authors, titles and sources of recent papers published elsewhere on plasma physics, accelerators and thermonuclear research. The printing of the first part is of reasonable quality, but there is need for more care in the general editorial work; for instance, the address of the Editor-in-chief should be made known to intending authors.

So far as can be inferred from the information on the back cover, two volumes will be published each year. Evidently two parts like the one available for review (labelled 'Numbers 1/2' and containing 104 pages) will comprise a volume. £7 or $20 for a volume of about 208 pages is quite a price.

JOURNAL OF FLUID MECHANICS

Volume 8, Part 1 May 1960

CONTENTS

Unsteady flow through an underdrained earth dam
by ROGER J. M. DE WIEST *page* 1

Forced mixing in boundary layers
by G. B. SCHUBAUER and W. G. SPANGENBERG 10

A note on the velocity profile and longitudinal mixing in a broad open channel
by T. H. ELLISON 33

A line source on an interface between two media
by V. M. PAPADOPOULOS 41

Sound emission from jets at high subsonic velocities
by ERIK MOLLÖ-CHRISTENSEN and RODDAM NARASIMHA 49

Steady longitudinal motion of a cylinder in a conducting fluid
by HIDENORI HASIMOTO 61

On the motion of a non-conducting body through a perfectly conducting fluid
by K. STEWARTSON 82

The oscillating plate problem in magnetohydrodynamics
by W. I. AXFORD 97

A note on the breakdown of continuity in the motion of a compressible fluid
by D. C. PACK 103

On a singular point in the Newtonian theory of hypersonic flow
by N. C. FREEMAN 109

The melting of ice in a hot humid stream of air
by DONALD L. TURCOTTE 123

Stability of parallel flow in a parallel magnetic field at small magnetic Reynolds numbers
by P. G. DRAZIN 130

The development of turbulent boundary layers with negligible wall stress
by A. A. TOWNSEND 143

REVIEWS

Advanced Mechanics of Fluids 156

Aerodynamik des Flugzeuges. Band I 158

Journal of Nuclear Energy. Part C: Plasma Physics—Accelerators—Thermonuclear Research 160

Printed in Great Britain at the University Press, Cambridge
(Brooke Crutchley, University Printer)